The Electrophysiology of Mental Fatigue and Sleepiness

From Fundamental and Clinical Markers to Real-Life Exploration



Arthur Le Coz

Thèse de Doctorat Université Paris Cité
École doctorale FIRE (474)
Institut du Cerveau (ICM) UMR 7225
Dream Team

L'électrophysiologie de la Fatigue Mentale et de la Somnolence : des Marqueurs Fondamentaux et Cliniques vers une Exploration en Vie Réelle

Arthur LE COZ

Thèse de doctorat de Sciences Cognitives, Psychologie, Linguistique, Philosophie de la pensée.
Dirigée par Thomas Andrillon et Delphine Oudiette
Défendue publiquement le 2 Octobre 2025

Composition du Jury :

Laure Peter Derex	Université de Lyon	Rapporteur
Jérôme Sackur	EHESS	Rapporteur
Athena Demertzi	Université de Lièges	Examinateur
Arnaud Rabat	IRBA	Examinateur
Thomas Andrillon	Sorbonne Université	Directeur
Delphine Oudiette	Sorbonne Université	Directrice

Doctoral Thesis Université Paris Cité
Doctoral School FIRE (474)
Paris Brain Institute (ICM) UMR 7225
Dream Team

The Electrophysiology of Mental Fatigue and Sleepiness: From Fundamental and Clinical Markers to Real Life Exploration

Arthur LE COZ
PhD Thesis in Cognitive Science, Psychology, Linguistics, and Philosophy of Mind
Directed by Thomas Andrillon and Delphine Oudiette
Publicly defended on the 2nd of October 2025

Jury Composition:

Laure Peter Derex	Université de Lyon	Referee
Jérôme Sackur	EHESS	Referee
Athena Demertzi	Université de Lièges	Examiner
Arnaud Rabat	IRBA	Examiner
Thomas Andrillon	Sorbonne Université	Director
Delphine Oudiette	Sorbonne Université	Director

À Simone,
que je reverrai ailleurs si je ne la vois pas ici.

Our life is what our thoughts make it.

Marc Aurèle

Contents

CONTENTS **10**
RESUME **12**
SUMMARY **14**
LIST OF PUBLICATIONS **16**
KEYWORDS AND ACRONYMS **17**
ACKNOWLEDGEMENTS **20**
RESUME SUBSTANTIEL **25**
GENERAL INTRODUCTION **32**
I. MENTAL FATIGUE **33**
1. WHAT IS FATIGUE AND HOW TO STUDY IT? 33
2. COGNITIVE CONSEQUENCES 35
3. PHYSIOLOGICAL CORRELATES 37
4. EXCESSIVE FATIGUE IN CLINICAL POPULATIONS 38
II. SLEEPINESS **40**
1. WHAT IS SLEEPINESS AND HOW TO STUDY IT? 40
2. COGNITIVE CONSEQUENCES 42
3. PHYSIOLOGICAL CORRELATES 43
4. EXCESSIVE SLEEPINESS IN CLINICAL POPULATIONS 44
III. FROM GLOBAL TO LOCAL SLEEP **45**
1. WHAT IS LOCAL SLEEP? 45
2. PREDICTING INTERNAL STATES AND BEHAVIOR 46
3. IMPLICATIONS IN CLINICAL POPULATIONS 47
IV. BEYOND LABORATORY SETTINGS **50**
1. WHY? 50
2. HOW? 51
3. SO WHAT? 53
EXPERIMENTAL RESULTS **54**
STUDY 1 DISTINCT ELECTROPHYSIOLOGICAL SIGNATURES OF FATIGUE STATE AND CHOICE BIAS FOLLOWING DAYLONG COGNITIVE WORK **55**
1. 1. DIGEST **56**
1. 2. STUDY **57**
ABSTRACT 57
INTRODUCTION 58
RESULTS 60
DISCUSSION 66
MATERIALS AND METHODS 68
ACKNOWLEDGMENTS 75
SUPPLEMENTARY FIGURES 76
STUDY 2 EEG SIGNATURE OF IDIOPATHIC HYPERSOMNIA: INSIGHTS FROM SLEEP MICROARCHITECTURE AND HYPNODENSITY METRICS **79**
2. 1. DIGEST **80**
2. 2. STUDY **81**
ABSTRACT 81
INTRODUCTION 82
METHODS 84
DATA AVAILABILITY 91
RESULTS 92
DISCUSSION 99
ACKNOWLEDGEMENTS 103
SUPPLEMENTARY FIGURES 104

STUDY 3 NEITHER HERE NOR THERE: CAPTURING HALLUCINATORY STATES IN NARCOLEPSY TYPE 1 111
3. 1. DIGEST 112
3. 2. STUDY 113
ABSTRACT 113
INTRODUCTION 114
METHODS 116
RESULTS 122
DISCUSSION 127
ACKNOWLEDGEMENTS 130
3. 3 APPENDIX 131
APPENDIX OF STUDY 3 132
STUDY 4 SPONTANEOUS THOUGHTS FROM LABORATORY SETTINGS TO REAL LIFE 135
4. 1. DIGEST 136
4. 2. STUDY 137
ABSTRACT 137
INTRODUCTION 139
METHODS 141
STATISTICS 148
RESULTS 149
DISCUSSION 151
GENERAL DISCUSSION 156
I. SLEEP-LIKE SLOW WAVES, A UNIFYING SIGNATURE OF FATIGUE 157
II. BROADENING THE DEFINITION OF LOCAL SLEEP 162
III. HOW TO APPLY THESE FINDINGS TO REAL LIFE 166
CONCLUDING REMARKS 172
REFERENCES 173
SUPPLEMENTARY APPENDIX 190
NOTE ON CONTRIBUTION: 190
SUPPLEMENTARY APPENDIX 1: MIND THE BLANK: BEHAVIORAL, EXPERIENTIAL, AND PHYSIOLOGICAL SIGNATURES OF ABSENT-MINDEDNESS 191
SUPPLEMENTARY APPENDIX 2: WHEN YOUR HEART ISN'T IN IT ANYMORE: CARDIAC CORRELATES OF TASK DISENGAGEMENT 192
SUPPLEMENTARY APPENDIX 3: TALKING TO SLEEPWALKERS? RESPONSE TO COMMUNICATION EFFORTS IN DISORDERS OF AROUSALS 193

Résumé

La fatigue est une expérience universelle. Elle s'installe insidieusement après un effort prolongé, se fait sentir lorsque la vigilance décline, ou persiste pendant des mois, voire des années, dans certaines maladies chroniques. Elle nous ralentit, altère nos décisions, ou laisse notre esprit dériver loin de la tâche en cours. Pourtant, elle nous échappe souvent : difficile à définir, mal capturée par les questionnaires, elle reste un phénomène aux contours flous. Cette thèse explore l'hypothèse que ces différentes formes de fatigue ; en réponse à l'effort, au temps qui passe, ou chronique, reposent sur une même origine physiologique.

À travers quatre études complémentaires, je montre que la fatigue pourrait correspondre à une déstabilisation progressive de l'éveil, durant laquelle certaines régions du cortex cérébral basculeraient transitoirement dans un état proche du sommeil. Ces épisodes, repérables grâce à l'émergence d'ondes lentes dans l'activité cérébrale, constitueraient un marqueur objectif et sensible de la fatigue, là où les ressentis ou les performances cognitives ne suffisent pas toujours à la révéler.

La **première étude** s'intéresse à la fatigue aiguë provoquée par un effort mental soutenu. Les ondes lentes deviennent plus fréquentes sur les régions frontales et centrales, et prédisent un biais vers des décisions plus rapides et moins coûteuses, indépendamment des déclarations subjectives des participants.

La **deuxième étude** explore l'hypersomnie idiopathique, un trouble marqué par un sommeil profond mais non réparateur. Les analyses montrent une abondance d'ondes lentes et de fuseaux de sommeil plus nombreux et regroupés, suggérant qu'un excès de stabilité du sommeil pourrait paradoxalement accentuer l'inertie au réveil.

La **troisième étude** examine la narcolepsie de type 1, où la fatigue s'accompagne d'hallucinations à l'endormissement et au réveil. Des bouffées d'oscillations thêta proches de l'activité REM, apparaissent alors dans les régions pariéto-occipitales, révélant une nouvelle forme d'intrusion du sommeil dans l'éveil.

Enfin, la **quatrième étude** transpose ces investigations à la vie quotidienne. Grâce à l'EEG portable et à l'échantillonnage d'expériences en situation réelle (travail, réunions, cours), je montre qu'il est possible de suivre les ondes lentes et les baisses de vigilance hors du laboratoire, et que le contexte influence fortement la fréquence et le contenu des pensées spontanées.

Ces travaux proposent une vision unifiée de la fatigue comme un processus d'intrusions locales de sommeil, reliant conditions normales et pathologiques. Comprendre ces mécanismes ouvre la voie

à une nouvelle physiologie de la vigilance et, à terme, à des outils permettant de mieux détecter, comprendre et gérer nos limites d'éveil.

Mots Clés

Fatigue, Sommeil, Attention, Électroencéphalographie, Ondes Lentes, Hypersomnie, Narcolepsie, Hallucinations, Vie-réelle

Summary

Fatigue is a universal experience. It builds up silently after prolonged effort, settles in as vigilance wanes, or persists for months and years in certain clinical conditions. It slows us down, makes us impulsive, or leaves our mind to wander. Yet fatigue often escapes our awareness, defying subjective measures and eluding precise definitions. This thesis asks whether these diverse forms of fatigue (e.g., use-dependent, time-dependent, and chronic) might share a common physiological origin.

Across four complementary studies, I show that fatigue reflects a gradual destabilization of wakefulness, during which local regions of the cortex slip into transient and local sleep-like states. These events, indexed by the emergence of slow waves in the cortical activity, provide a sensitive marker of fatigue that captures fluctuations in cortical dynamics even when self-reports or performance do not.

In **Study 1**, I investigate acute fatigue induced by sustained mental effort and time on task. As participants tire, slow waves become more frequent over frontal and central areas and predict a shift toward low-cost, immediate decisions, revealing changes in neural processing not captured by subjective fatigue ratings.

Study 2 focuses on idiopathic hypersomnia, a chronic hypersomnolence disorder with unrefreshing sleep and difficulty waking. Analyses of sleep microstructure reveal a higher number of slow waves, and more numerous and clustered sleep spindles during nocturnal sleep in idiopathic hypersomnia compared to controls. These results suggest that increased sleep stability could paradoxically deepen sleep inertia. Chronic fatigue here may not stem from lack of restorative sleep, but from an abnormal balance between sleep depth and wakefulness stability.

In **Study 3**, I examine narcolepsy type 1, where chronic fatigue is accompanied by vivid hallucinations around sleep onset and awakening. I identify parieto-occipital theta bursts during these hallucinatory episodes, a possible REM-like signature unseen in controls. This finding could broaden the concept of local sleep, pointing to sleep intrusions beyond NREM-like activity that intrudes into wakefulness, disrupting intention and increasing behavioral errors.

Finally, **Study 4** takes these investigations into everyday life. Using portable EEG and experience sampling during natural activities (work, meetings, lectures), I show that slow waves and attention lapses can be tracked outside the lab, and that environmental context strongly shapes the occurrence and content of spontaneous thoughts. This demonstrates the feasibility of real-life neurophysiological monitoring of fatigue.

Together, these studies support a unified view of fatigue as a process of local sleep intrusions, bridging healthy and pathological conditions. Slow waves, and REM-like theta bursts in some cases, link neural dynamics to cognitive lapses, beyond subjective experience. This framework opens several avenues for future research: understanding the molecular and synaptic triggers of slow waves, clarifying their functional role in cortical regulation, expanding the taxonomy of local sleep intrusions, and developing unobtrusive, personalized tools for fatigue monitoring in real life.

By revealing how the brain gradually surrenders to sleep in fragments rather than all at once, this work brings us closer to understanding the limits of wakefulness, and how we could one day better live with them.

Keywords

Fatigue, Sleep, Attention, Electroencephalography, Slow Waves, Hypersomnia, Narcolepsy, Hallucinations, Real Life

List of Publications

Peer Reviewed Publications

Talking to sleepwalkers? Response to communication efforts in disorders of arousals
Y. Idir, R. Lopez, A. Barbier, S. Saint-Auret, E. Morain, R. Vollhardt, I. Ben Haj Kacem, A. Le Coz, A. Gales, P. Dodet, S. Leu-Semenescu, Y. Dauvilliers, I. Arnulf, D. Oudiette

Submitted or Under-Review

***EEG Signature of Idiopathic Hypersomnia: Insights from Sleep Microarchitecture and Hypnodensity Metrics**
A. Le Coz[#], R. Vollhardt[#], P. Champetier, R. Herzog, S. Leu-Semenescu, P. Dodet, V. Attali, A. Gales, D. Oudiette, I. Arnulf, T. Andrillon

When your heart isn't in it anymore: Cardiac correlates of task disengagement
A. W Corcoran, A. Le Coz, J. Hohwy, T. Andrillon

Mind the blank: behavioral, experiential, and physiological signatures of absent-mindedness
E. Munoz-Musat, A. Le Coz, A. W. Corcoran, L. Belloli, Naccache, T. Andrillon

REM sleep favors the restructuring of problem-related semantic associations
T. Bieth, N. Decat, Y. N. Kenett, M. Scuccimarra, M. Ovando-Tellez, A. Lopez-Persem, C. Lacaux, S. Ben Younes, A. Le Coz, S. Moreno-Rodriguez, I. Arnulf, E. Volle, D. Oudiette

In Preparation

***Distinct electrophysiological signatures of fatigue state and choice bias following daylong cognitive work**
S. Naik[#], A. Le Coz[#], F. Lachat, A Wiehler, T. Andrillon, M. Pessiglione

***Neither Here Nor There: Capturing Hallucinatory States in Narcolepsy Type 1**
A. Le Coz, M. Degrave, R. Vollhardt, S. Leu-Semenescu, P. Dodet, A. Gales, D. Oudiette, I. Arnulf, T. Andrillon

***Spontaneous Thoughts from Laboratory Settings to Real Life**
A. Le Coz, G. Oiry, J. De Los Santos, C. Lee Shatto, A. Spagna, T. Andrillon

What Crosses Your Mind when You Fall Asleep? Data-driven Classification of Conscious Experiences During the Sleep Onset Period
N. Decat, J. Sénéchal, I. Scellier-Dekens, H. de Verville, A. Le Coz, R. Herzog, T. Bieth, I. Arnulf, E. Volle, T. Andrillon, D. Oudiette

Sleep-like Slow Waves Predict the Severity and Recovery of Disorders of Consciousness
A. Ruyant Belabbas, A. Le Coz, J. Sitt, L. Naccache, B. Rohaut, T. Andrillon

[#] These authors have contributed equally to this work.

* These papers are the one mentioned in the manuscript. The others are work I contributed to during my PhD.

Keywords and Acronyms

AUC: Area Under the Curve

CAP: Cyclic Alternating Pattern

CSD: Current Source Density

CTL: Controls

DFT: Dynamic Framework of Thought

DKL: Kullback-Leibler divergence

EDS: Excessive Daytime Sleepiness

EEG: Électroencéphalogramme

EMG: Électromyographie

EOG: Électrooculogramme

ERP: Event-related potential

ESS: Epworth Sleepiness Scale

FDR: False Discovery Rate

FFT: Fast Fourier Transform

FG: Forgot

fMRI: Functional Magnetic Resonance Imaging

HA: Hallucination/Illusion

HI: Hypersomnie Idiopathique

ICA: Independent Component Analysis

IQR: Interquartile Range

KSS: Karolinska Sleepiness Scale

LME: Linear Mixed-Effects Models

lPFC: Lateral Prefrontal Cortex

MB: Mind Blanking

MSLT: Multiple Sleep Latency Test

MW: Mind Wandering

MWT: Maintenance of Wakefulness Test

NREM: Non-Rapid Eye Movement

NT1: Narcolepsie de Type 1

ON: On-Task

PGO: Ponto-geniculo-occipital

PSG: Polysomnographie

PSD: Power Spectral Density

PTP: Peak-to-Peak

PVT: Psychomotor Vigilance Task

REM: Rapid Eye Movement

RMSE: Root-Mean-Square Error

RS: Resting State

RT: Response Time

SART: Sustained Attention to Response Task

SE: Spontaneous Experience

SEM: Standard Error of the Mean

SOREMP: Sleep-Onset REM Period

SW: Slow Waves

TRT: Task-Related Thoughts

TUT: Task-Unrelated Thoughts

Acknowledgements

It is a particular feeling to write this. The journey that has been my PhD thesis was above all a journey of encounter. Along the way, I have met the most brilliant minds and kindest people I know. If there's one thing I am most grateful for, it is the privilege of being surrounded by great humans being and brilliant researcher.

I would like to start by thanking **Thomas**, my supervisor and mentor. I owe it to luck that you happened to be coming to Paris when I was looking for an M2 internship. That was 4.5 years ago, and since then, I have grown and worked harder than ever before. You always had the vision, the ideas, the metaphors to push the work to a different dimension. Thanks to you, I had the chance to meet and collaborate with exceptional scientist. We travelled for conferences where our discussions took a different turn than they did in Paris. I am deeply grateful to you for allowing me to walk on a path I am truly passionate about, and to continue working with you.

The reason I met you, Thomas, is **Delphine**. Delphine, you might hate this paragraph, as you don't like sugar-coated thank yous, but here it goes anyway: thank you. You opened the doors of the Dream Team and the ICM to me. You are an outstanding mentor, both humanly and scientifically. Always grounded in the reality, "all of this is interesting guys, but concretely…". You brought pragmatism and your sharpness to every discussion, long live the *Method Oudiette*! Besides being a scientifically an inspiring scientist, I found a drinking buddy and a friend. As the saying goes; "Always the same 3" (shout-out to Yannis). Leaving lab troubles behind, always ready for the best laughs. Thank you for the guidance, the patience, the friendship, and the touch of craziness and kindness we so badly need in the world of research.

Through you, I met **Yannis**. Man, I consider you a mentor and a brother, thank you for everything. You are one of the most peaceful souls I've met on this planet. I will forever cherish our late-night discussion after a day of struggle and debugging in the lab. Grabbing a beer, staying out until our brains were screaming for rest. Thank you for always pushing my thinking, showing me that there were no limits. Thanks for introducing me to philosophy, Diego and Maxence. I owe you guys a thank you too for the friendship and those eye-opening nights listening to that wild philosophy teacher.

When I started as an M2 intern with Thomas, there was another curly head starting as a M1: **Alessia**. I remember vividly the moment we met with Thomas on the ground floor of the ICM, sharing a cookie you were clearly not thrilled about. I will always be grateful to have met you. You are an inspiration, showing how far we can push our work beyond perfection. We were Thomas' very first students in the Dream Team and having you as a sidekick throughout this journey has been a blessing. Thanks for the long evening of analyses and fried chicken at the ICM. Always happy to meet and work on the weekends too. Always ready to have a conversation, whatever the topic,

whatever the duration. Methodology on ERPs? A deep dive in the slow waves? Tea spilling? Let's have it. Thank you for being a pillar during my PhD. Your honesty and altruism will be engraved in me.

As the saying goes, *jamais deux sans trois.* Along with Alessia there was our other blond head always with us, right **Nico**? The **trio**, always ready to hang out. Nico, my brother, thank you for everything. I remember the first time we met when you arrived at Eole, heading straight to the rooftop for a pot and stealing all the snacks. It was a pleasure sharing a desk at Eole and later at the ICM. We kind of missed it when we finally got space, didn't we? Though I'm glad we can work side by side without our feet constantly bumping. Man, we grew up. I remember both of us having the dreamiest vision on academia. Thank you for being "brutally honest", for sharing who you are with your heart and listening with it as well. Thanks for the sharp feedback on every idea, always pushing my work toward a better version. Thanks for being ready to get the job done, whenever and wherever. Thank you so much for taking the time to hear and make me the beautiful covers of my manuscript. Thanks for that perfect mix of craziness and calm we synced on whenever we shared a room during conferences. Thanks for opening new views on the world, and for introducing me to your LPI crew – Arve, Elena, Esra, Saatvik. Huge thanks to these guys – meeting you in Annecy was unforgettable. You are a bubble of fresh air every time I see you. In the years to come, we need to make our own retreat happen.

Julissa and **Guillaume**, you hold a special place in my heart because I had the luck to work with you during your internship. Thank you, Julissa, for impatiently correcting my English pronunciation after hearing me repeat words a dozen times, and for helping me showing the possibilities of portable EEG. Thank you, Guillaume, for lending a hand in recording the brain activity of just about everyone around us (people still hate the SART here!). And thank you for staying on board until the very end of the project.

This real-life project also gave me the chance to meet two incredible researchers from the other side of the Atlantic, **Alfredo** and **Connor**. You both believed in the vision, and without your trust and support, this project could never have come to life. I am truly grateful to you both.

On my path, I had the chance to meet **Borjan** (**Boki**). Thanks for the wisdom, the time and the brotherhood. Thanks for sharing my love for pepperoni and fried chicken. You are a truly remarkable human being, and I am grateful that our paths crossed.

Another incredible person, **Ruben** came straight from Chile! *Guapacito*, thanks for your knowledge, your patience, your love for plants, and your humanity. I can't wait to come visit your lab, to meet the team you are now building, congratulations, my friend!

Petit **Pierre**, I heard so much about you before you came back to the Dream Team. I enjoyed all the *tunnels* we shared. You are a formidable human and researcher. I loved our long discussion on slow waves, and sleep spindles, exchanging expertise and pushing each other's ideas further.

Little **Ilo**, thanks for your patience, your sunshine, your kindness. Thank you for believing in the people around you, and for giving so much attention and care to everyone.

The list is long! Every single person in the Dream Team has brought something valuable to me. I learned from every one of you who passed through. Thank you, Emma, for being the first to show me the struggles of MATLAB. Thank you, Célia, for stressing out when nobody else was talking. Thank you, Alexandrine and Céleste, for sharing the internship adventure with me. Thank you, Estef, for your spirit. Thank you, Sony, for your never-ending sentences and for losing so proudly at FIFA. Thanks Manu, Mini-Thomas, Amélie, Raphaël, Sophia, Jade, Mamie Imane, Claudia, Hermione, and Margaud. And thanks to all those I may have forgotten to mention here, but who will always have a place in my heart and mind. And beyond the Dream Team, in the Pic Nic crew: thank you, Romain, for your spontaneity. Thank you, Manon, for being your whole self and for your kindness. Thank you, Ivan, for the craziness and the hype for portable EEG. Thank you, Dragana, for the fascinating discussions on cycles of attention and mediation analyses.

A special thank you to **Athena**, **Laure**, **Arnaud**, **and Jérôme** for accepting to be part of my PhD jury. Jérôme, I was lucky to benefit from your sharp advice and your kindness during my thesis advisory committee meetings. Arnaud, I feel truly honored to have met you and Brice, and to have shared those discussions on fatigue and mind-wandering while debugging at Hôtel Dieu.

Alongside Jérôme, **Mélanie** and **Claire** were also part of my thesis advisory committee. Thank you for your invaluable guidance and for looking out for me throughout these four years.

I am deeply grateful to **Mathias** and **Shruti**, without whom the very first study of my PhD would not have come to life. Shruti, heartfelt thanks for your guidance throughout this project. I cannot count how much I've learned from our collaboration. Mathias, thank you for the countless hours of meetings, where the glutamate piled up as we pushed this project to new heights.

Thanks to **Isabelle** for opening the doors of the sleep pathology unit and sharing the richness of idiopathic hypersomnia and narcolepsy cases. Thanks to **Smaranda** for your patience while signing all those consent forms! Thank you, **Pauline**, for the caipirinhas in Rio, and for your lightness and kindness. **Stéphane**, I'll never forget the "deeper-than-black" coffee that my heart still remembers. And a tremendous thank you to the **paramedical team** of Eole, who saw me early mornings and late nights, always finding the words to make me smile and laugh.

I can't mention the caipirinhas without my dear friends, **Mickael**, **Nico**, and **Felipe**! I am forever grateful to have met you. I can't wait to bring the fUS into the world of sleep and fatigue, and I can't wait for the next conference we'll attend together. Sincere thanks to you Micka, *mon ami Breton*, for the guidance and honesty.

I wouldn't have made it through this journey without the people who surrounded me in my daily life. **Thomas**, **Justine**, **Marie**, thank you for your kindness, friendship, and patience. It has been a true pleasure to share a home with you throughout these years. I needed our inspiring discussions, the craziness, and your different perspectives on everything. I'm honored to call you friends and grateful to have grown alongside you.

Les mots ne suffiront jamais, mais **merci Maman**, **merci Papa**. Merci de m'avoir toujours laissé expérimenter, d'avoir été curieux et enthousiastes tout au long de cette épopée, de toujours croire en moi et pour votre amour inconditionnel. Merci pour chaque bouffée d'air frais qui m'a aidé à me remettre les idées en place ; à l'Alhambra ou pendant les triathlons ! Merci **Anaïs**, ma grande sœur, d'avoir toujours veillé sur ton petit frère. Et merci à toi **Laura**, personne fantastique que tu es, d'être ma colonne de Corinthe depuis le début de ce chemin. Merci pour toutes les attentions que tu as, et merci de toujours croire en moi, et d'être le soleil que tu es, d'être là qu'il pleuve, vente, neige ou grand beau temps.

Résumé Substantiel

La fatigue est une expérience universelle qui traverse aussi bien la vie quotidienne que les contextes cliniques. Elle peut être physique ou cognitive ; c'est cette dernière, souvent qualifiée de fatigue mentale, que j'ai étudiée dans ce manuscrit. À ses côtés se trouve fréquemment la somnolence, qui traduit une propension accrue à s'endormir. Cliniquement, la fatigue mentale se manifeste par une diminution des performances, généralement réversible après un repos suffisant, tandis que la somnolence exprime un besoin physiologique de sommeil. Dans ce travail, j'emploie le terme générique de fatigue pour décrire ces deux états, car ils partagent de nombreuses conséquences : ralentissement des réactions, augmentation des erreurs, dérives attentionnelles et altérations de la vigilance. Cette fatigue, au sens large, a un impact sociétal majeur : elle contribue à la survenue d'accidents de la route, altère les performances professionnelles et détériore la qualité de vie dans de nombreuses pathologies chroniques. Malgré son importance, la fatigue demeure difficile à définir et à mesurer. Les questionnaires manquent souvent de sensibilité, l'auto-évaluation subjective est sujette à biais, et les corrélats comportementaux restent variables et débattus. Sur le plan neurophysiologique, ses bases sont encore mal élucidées, ce qui complique la mise en place de marqueurs fiables et reproductibles.

L'objectif principal de cette thèse a été de trouver un marqueur commun à diverses formes de fatigues : après un effort cognitif soutenu (aiguë), après une veille prolongée (dépendante du temps), ou au sein de pathologies du sommeil (chronique). L'hypothèse directrice repose sur l'idée que la fatigue correspond à une déstabilisation progressive de l'éveil, marquée par des intrusions locales de sommeil dans le cerveau éveillé. Ces évènements sont caractérisés par l'émergence d'ondes lentes au niveau de l'activité cérébrale. Elles pourraient constituer un marqueur objectif et sensible de la fatigue, plus fiable que les mesures subjectives.

Afin de mettre à l'épreuve cette hypothèse, ma thèse s'articule autour de quatre études complémentaires : (i) l'induction de la fatigue mentale aiguë par une journée de travail cognitif soutenu, (ii) l'exploration de la microarchitecture du sommeil dans l'hypersomnie idiopathique, (iii) l'analyse des épisodes hallucinatoires dans la narcolepsie de type 1, (iv) et enfin la transposition de ces recherches dans la vie réelle. Ce parcours allant du laboratoire à la vie quotidienne en passant par la clinique vise à définir une physiologie intégrée de la fatigue.

La première étude visait à caractériser la fatigue mentale générée par une journée entière de travail mental. Deux groupes de participants ont réalisé une tâche cognitive plus ou moins exigeante pendant plusieurs heures suivies de décisions économiques. Cela a permis de suivre l'évolution de la fatigue au fil du temps et en fonction de la difficulté de la tâche. La performance comportementale globale ainsi que les rapports subjectifs de fatigue sont restés comparables entre les groupes. Cette observation illustre les limites des mesures de précision et subjectives pour capturer la fatigue. En revanche, les participants réalisant la tâche cognitive plus difficile ont

eu tendance à basculer vers des choix plus impulsifs, favorisant les décisions immédiates et peu coûteuses au détriment d'options plus avantageuses mais différées.

Au niveau de l'activité cérébrale, nous avons observé une modulation de l'amplitude de l'activité cérébrale juste avant ce biais dans la prise de décision. De plus, nous avons aussi observé une accumulation croissante d'ondes lentes au niveau frontal et central, présentes pendant la tâche cognitive ainsi que lors des prises de décision. Ces ondes lentes se sont avérées prédictives du biais décisionnel. Cette étude démontre que la fatigue ne se traduit pas nécessairement par une baisse de performance mesurable, mais par des modifications plus fines du traitement de l'information et de la régulation des choix.

Ces résultats apportent deux contributions majeures : d'une part, ils confirment que les ondes lentes locales constituent un marqueur objectif et sensible de la fatigue mentale, indépendant des ressentis déclarés par les participants ; d'autre part, ils réaffirment que la fatigue modifie la balance coût-bénéfice dans la prise de décision, révélant une vulnérabilité cognitive susceptible d'avoir des conséquences en situations réelles où des choix rapides et optimaux sont cruciaux (conduite, aviation, médecine).

La deuxième étude s'est intéressée à l'hypersomnie idiopathique, un trouble rare caractérisé par un sommeil long mais non réparateur, et une somnolence diurne excessive persistante. Ces patients décrivent une forme de fatigue chronique, difficile à soulager même après de longues périodes de sommeil, ainsi qu'une inertie au réveil particulièrement marquée. Cette condition offre donc un modèle privilégié pour explorer les bases neurophysiologiques de la fatigue chronique et ses liens avec l'architecture du sommeil.

L'analyse détaillée de la microstructure du sommeil a révélé deux résultats majeurs. D'une part, les patients présentaient un nombre accru d'ondes lentes pendant le sommeil profond. D'autre part, leurs fuseaux de sommeil étaient plus nombreux, souvent regroupés en séquences rapprochées. Ce profil contraste avec l'idée d'un sommeil appauvri ou instable : au contraire, l'hypersomnie idiopathique semble marquée par une stabilité du sommeil.

Ces observations suggèrent un paradoxe : loin d'expliquer la fatigue par un déficit de sommeil réparateur, l'hypersomnie idiopathique pourrait résulter d'un déséquilibre entre un sommeil trop profond et une difficulté à maintenir l'éveil. Ainsi, l'excès de stabilité nocturne favoriserait l'inertie matinale et la somnolence chronique, contribuant à une fatigue qui persiste malgré des nuits prolongées. Ce mécanisme enrichit la compréhension des troubles hypersomniaques et souligne que la qualité fonctionnelle de l'éveil ne se résume pas à la quantité ou la continuité du sommeil nocturne.

La troisième étude a porté sur la narcolepsie de type 1, une maladie du sommeil liée à la perte de neurones producteurs d'hypocrétine. La narcolepsie de type 1 est caractérisée par une somnolence diurne sévère, un sommeil fragmenté, des attaques de cataplexie et des hallucinations hypnagogiques et hypnopompiques. Ces expériences hallucinatoires, souvent vives et immersives, représentent un exemple extrême de perturbation de la frontière entre veille et sommeil, et en font un modèle clinique idéal pour étudier les intrusions du sommeil dans l'éveil.

En combinant enregistrements EEG et échantillonnage d'expérience pendant une tâche d'attention soutenue, nous avons capturé des épisodes hallucinatoires rapportés par les patients NT1, ce qui n'est pas le cas des contrôles. Ces hallucinations chez les patients narcoleptiques de type 1 sont accompagnées d'un profil comportemental plus déconnecté de l'environnement, avec une augmentation du taux d'erreurs et une somnolence subjective plus élevée. Électrophysiologiquement, ces hallucinations chez les patients atteints de narcolepsie de type 1 sont associées à une augmentation de puissance périodique en thêta (4-8Hz) et une diminution de beta (12-30Hz) au niveau occipital. Dans le but de trouver un marqueur temporel et spatial plus fin de ces hallucinations, nous avons détecté des bouffées de thêta. Ces bouffées de thêta étaient présentes au niveau frontal chez les contrôles et les patients avec narcolepsie de type 1, et au niveau pariétal seulement chez les patients. Comparé aux états mentaux traditionnels, les rapports d'hallucinations chez les patients avec narcolepsie de type 1 étaient accompagnés par une augmentation de densité de ces bouffées de thêta au niveau occipital.

Ces signatures rappellent les oscillations caractéristiques du sommeil paradoxal (REM), bien distinctes des ondes lentes associées au sommeil lent (NREM). Ces résultats étendent le concept de sommeil local en suggérant qu'il ne se limite pas à l'intrusion d'éléments NREM, mais peut aussi inclure des événements REM locaux dans le cerveau éveillé. De tels épisodes pourraient jouer un rôle déterminant dans la genèse des hallucinations, en perturbant la continuité de l'expérience consciente et en augmentant le risque d'erreurs comportementales. Ainsi, la NT1 illustre une forme pathologique où les intrusions de sommeil prennent une nouvelle dimension, offrant un éclairage unique sur les limites de la stabilité de l'éveil.

Ces trois premières études ont été réalisées dans les **conditions contrôlées de laboratoire**, au sein duquel les états mentaux et les corrélats neurophysiologiques sont contrôlés et provoqués. Mais qu'en est-il de l'irruption des expériences spontanées dans des conditions de vie réelle ? Pouvons-nous capturer ces ondes lentes ? Peuvent-elles nous permettre de prédire les fluctuations d'attention dans différents contextes de vie réelle ? Pour essayer de répondre à ces questions, nous avons combiné l'utilisation de casques EEG portables avec des sondes de pensées dans la **quatrième étude**. Ces derniers étaient utilisés durant divers contextes comme le travail, les réunions ou les cours magistraux et la tâche attentionnelle soutenue explorée en laboratoire.

Cette approche permettait de suivre en continu l'état cérébral et subjectif des participants dans des environnements riches et écologiquement valides, contrastant avec les contextes hautement contrôlés mais artificiels du laboratoire.

Le contenu mental s'est révélé modulé par le contexte. Les participants en condition de travail étaient plus concentrés que les participants en salle de classe ou ceux en train de réaliser la tâche attentionnelle explorée dans l'étude 3. Les participants avaient aussi plus tendance à penser à autre chose en salle de classe et durant la tâche que lorsqu'ils travaillaient. De plus, les participants rapportaient des états d'esprit moins volontaires ainsi qu'une somnolence plus importante lors de la tâche cognitive de laboratoire. L'acquisition de signal en vie réelle s'est révélée très bruitée pour utiliser les méthodes de traitement du signal traditionnel. Les quantités de signal exploitables se sont révélées limitées pour tirer des conclusions. En revanche, les analyses de signal préliminaires sont encourageantes et la détection d'ondes lentes est possible dans les conditions de vie réelle.

Cette étude démontre non seulement la faisabilité technique du suivi neurophysiologique de la vigilance en dehors du laboratoire, mais elle souligne aussi l'importance de prendre en compte l'environnement dans la compréhension des états mentaux. Elle ouvre la voie au développement d'outils de monitoring de la fatigue utilisables dans des conditions écologiques, avec un potentiel d'application directe dans les domaines professionnels et cliniques.

L'ensemble de ces travaux propose une vision unifiée de la fatigue comme un processus de désintégration progressive de l'éveil, se traduisant par des intrusions locales de sommeil dans le cerveau éveillé. Ces intrusions prennent la forme d'ondes lentes, signatures du sommeil lent, ou, dans certains contextes pathologiques, d'événements transitoires plus proches du sommeil paradoxal. Elles constituent un marqueur objectif et sensible, capable de relier les fluctuations cérébrales aux conséquences cognitives et phénoménologiques de la fatigue, au-delà de ce que les mesures subjectives ou les performances globales peuvent révéler.

Cette approche éclaire également la diversité des expressions de la fatigue. Dans le cadre expérimental de la fatigue aiguë, les ondes lentes frontales et centrales expliquent le biais vers des décisions rapides et impulsives. Dans la narcolepsie de type 1, l'excès d'ondes lentes durant l'éveil témoigne de la fatigue chronique durant l'éveil. De plus, la détection de bouffées thêta pariéto-occipitales pendant les hallucinations révèle l'existence d'intrusions REM localisées, qui perturbent la continuité de l'expérience consciente. Ces résultats montrent que les mécanismes de fatigue, bien qu'hétérogènes en apparence, les mécanismes de fatigue s'inscrivent dans un **continuum commun d'intrusions de sommeil**.

Au-delà des apports fondamentaux, ces travaux ouvrent la voie à de nombreuses applications translationnelles. Le suivi des ondes lentes et des intrusions de sommeil local, qu'elles soient de

type NREM ou REM, offre un marqueur objectif de la fatigue qui pourrait être utilisé dans des contextes variés : sécurité routière, aviation, médecine ou encore environnements de travail à forte demande cognitive. Les développements récents de l'électroencéphalographie portable, associés à d'autres mesures physiologiques (activité cardiaque, pupillométrie, analyse vocale), rendent envisageable un monitoring en temps réel, discret et personnalisé. À terme, de tels outils pourraient non seulement détecter les baisses de vigilance, mais aussi proposer des stratégies de gestion adaptées (pause, sieste, changement de tâche).

Sur le plan scientifique, plusieurs pistes se dessinent. Il reste à identifier les mécanismes moléculaires et synaptiques qui déclenchent les intrusions de sommeil local, et à préciser leur rôle fonctionnel dans la régulation corticale. Une meilleure cartographie des signatures électrophysiologiques permettra d'élargir la taxonomie des états intermédiaires entre veille et sommeil, en intégrant la diversité des expériences subjectives (vagabondage mental, blanc mental, hallucinations). Enfin, l'intégration de ces approches dans la vie réelle représente un défi majeur : développer des protocoles écologiques, capables de capturer la dynamique de la vigilance sans perturber l'activité quotidienne.

Finalement, en explorant la fatigue dans ses différentes formes : aiguë, chronique, clinique et quotidienne, cette thèse met en lumière un mécanisme commun : **les intrusions de sommeil dans l'éveil**. Ces intrusions, qu'elles se traduisent par des ondes lentes ou par des bouffées thêta d'allure REM, relient la physiologie cérébrale aux fluctuations cognitives et conscientes qui marquent les limites de l'éveil. En ce sens, la fatigue apparaît non plus comme un simple symptôme diffus, mais comme un processus neurophysiologique identifiable et mesurable.

Mon travail contribue à bâtir une physiologie intégrée de la vigilance, au croisement du sommeil et de l'éveil. Il ouvre des perspectives pour mieux comprendre nos fragilités cognitives, mais aussi pour développer des outils capables d'aider chacun à détecter, anticiper et gérer ses propres fluctuations de fatigue et d'attention. En révélant que le cerveau éveillé cède, parfois, au sommeil par fragments avant de sombrer totalement, mon travail éclaire les frontières mouvantes de notre rapport à l'éveil. Il suggère qu'apprendre à reconnaître ces frontières est une étape essentielle pour mieux vivre avec elles.

General Introduction

I. Mental Fatigue

1. What is fatigue and how to study it?

Fatigue ˈfəˈtiːg

Noun – Extreme tiredness resulting from mental or physical exertion or illness.

Tiredness ˈtʌɪədnəs

Noun – The state of wishing for sleep or rest, resulting from mental or physical exertion or illness.

Fatigue is a universal phenomenon. Its definition, as seen above, is rather broad, reflecting a complex and multi-faceted phenomenon (Balkin et al., 2023; Pessiglione et al., 2025). First, fatigue can be mental or physical. I will focus here exclusively on mental fatigue. Second, fatigue can be acute (resulting from an extended period of wakefulness for example or from cognitive effort) or chronic (patients diagnosed with chronic fatigue syndrome report severe and persistent mental and/or physical fatigue). Third, mental fatigue encompasses various subjective dimensions, and one of which is sleepiness. All these definitions of fatigue share a common endpoint of impaired functioning. They also all have the same solution: fatigue dissipates totally or partially with sleep or rest, which suggests that fatigue underlies a physiological need for rest or a drive to sleep. This so-called homeostatic regulation of fatigue stresses its deep connection with sleep and its restorative functions (Andrillon and Oudiette, 2023).

Yet, fatigue and sleepiness are not interchangeable. One can be mentally exhausted while feeling awake, struggling to maintain attention despite no urge to sleep. Conversely, one can feel sleepy without reporting fatigue, especially in low-stimulation contexts.

In this thesis, I focus on different facets of this broader construct. In **Study 1**, I investigated how **acute mental fatigue** emerges from the passing of time as well as sustained mental effort and its impact on attention, decision-making, and motivation. In particular, I examined whether sleep intrusions could account for the phenomenon of acute mental fatigue, its fluctuations in response to time and cognitive effort, and its consequences on cognition. In **Study 2,** I examined whether sleep disruptions could characterize individuals diagnosed with idiopathic hypersomnia, a clinical population that reports excessive daytime sleepiness and **chronic mental fatigue** (Boulanger et al., 2024). In **Study 3**, I investigated whether sleep intrusions could represent a plausible neurophysiological mechanism to account for **sleepiness** and its cognitive consequences, in individuals with Type-1 Narcolepsy. We focused on hallucinations, which are reported in extreme cases of mental fatigue. Altogether, these studies allowed me to explore the neural bases of mental fatigue, its cognitive consequences and its intersection with sleepiness and the mechanisms and

functions of sleep. This work may bring the study of fatigue and sleepiness closer together by framing them within a general neurophysiological model.

Perhaps, the most direct way to investigate mental fatigue is to examine how it emerges from an accumulation of cognitive demands, influenced by factors such as task difficulty (Blain et al., 2016), time spent on task (Mackworth, 1948), or duration of prior wakefulness (Humphrey et al., 1994). These determinants reflect how mental fatigue is not a discrete switch but a dynamic process, modulated by sustained cognitive effort and motivation. To capture this dynamic process, researchers have developed experimental paradigms that aim to either **induce**, **observe**, or **compare** fatigue-related states. In this thesis, I adopt all three approaches to explore different facets of mental fatigue and its interplay with cognitive and physiological processes.

First, **induction** paradigms involve sustained engagement in effortful cognitive tasks designed to tax specific brain regions such as the left prefrontal cortex (Blain et al., 2016; Wiehler et al., 2022; Pessiglione et al., 2025). These tasks are followed by assessments of decision-making. In this context, fatigue is revealed in the decision-making, which relies on the brain regions fatigued during the task. This methodology allows researchers to go beyond the study of behavioral performances and self-report measures, which often yield inconclusive results (Pessiglione et al., 2025).

Second, **observation** paradigms capture the spontaneous emergence of fatigue during monotonous or under-stimulating tasks. A typical example is the Sustained Attention to Response Task (SART), in which participants perform a repetitive Go/NoGo task with minimal external demand (Robertson et al., 1997). This context often elicits performance lapses, increased sleepiness, and a rich variety of spontaneous thoughts (Andrillon et al., 2021). Such paradigms allow for a dynamic exploration of how fatigue relates to attention, vigilance, and ongoing mental experience.

Third, clinical **comparisons** offer a complementary insight into fatigue by examining its pathological expressions. In this thesis, I contrast healthy controls with individuals diagnosed with narcolepsy type 1 (NT1) and idiopathic hypersomnia (IH). These two rare sleep-wake disorders are characterized by chronic feelings of exhaustion, reduced alertness, and altered subjective experiences during wakefulness (Sateia, 2014). These clinical populations provide valuable insights into the functional distinctions between mental fatigue, sleepiness, and arousal dysregulation.

Together, these three complementary approaches provide a comprehensive framework for investigating fatigue as both a transient state and a symptom. They enable us to examine how fatigue emerges, how it is experienced, and how it manifests across experimental and clinical

contexts. But beyond how fatigue is defined or measured, a central question remains: how does it impact cognition?

2. Cognitive consequences

The impact of mental fatigue on cognition can be illustrated by an historic event: the defeat of chess grandmaster Garry Kasparov by IBM's Deep Blue in 1997. After losing the final game of the match, Kasparov attributed his failure not to a tactical error, but to a profound state of mental exhaustion. The machine could compute indefinitely, but unlike it, humans face biological limits. Sustained cognitive effort inevitably leads to a decline in performance, even in highly trained individuals.

Mental fatigue can have serious cognitive consequences in real life, affecting activities where sustained attention and decision-making are critical. In aviation or road safety, for example, fatigue increases the risk of accidents as driving time increases (Lal and Craig, 2002; Goode, 2003). In sports such as soccer, it impairs physical performance and alters tactical decision-making, even when physiological load is controlled (Smith et al., 2016). In military contexts, fatigue can lead to physical and mental lapses, potentially determining the success or failure of critical missions (Rabat et al., 2025).

To do so, experimental paradigms have attempted to reproduce some of these dynamics in controlled settings. Time-on-task protocols have consistently shown that prolonged cognitive effort leads to slower reaction times, increased error rates, and reduced sustained attention (Boksem et al., 2006, 2005; Faber et al., 2012; Lorist et al., 2000). When mental fatigue sets in, behavioral performance often oscillates between **sluggishness** and **impulsivity**. Such variability complicates interpretation and can be further modulated by motivation, disengagement, or boredom.

Mental fatigue can also be expressed at the subjective level with decreased motivation, increased irritability, boredom or exhaustion. Accordingly, mental fatigue could be tightly linked to the phenomenon of mind wandering (MW), i.e., the tendency to not pay attention to the task at hand but to think about things that are both task-unrelated and stimulus-unrelated (i.e., not related to the direct environment, Smallwood and Schooler, 2015; Van den Driessche et al., 2025). Mind wandering is an emerging topic of investigation. Previous research has shown that mind wandering increases with time spent on task (Andrillon et al., 2021), sleep deprivation (Poh et al., 2016) or poor motivation (Unsworth and McMillan, 2013). The research on mind wandering stresses the importance of tracking the subjective experience of individuals when performing a long and straining task. In some cases, individuals can even report abnormal sensations or

experiences such as a presence or visual hallucinations (Waters et al., 2018), which can represent a good index of extreme fatigue.

Since mental fatigue can have both many causes and consequences, its scientific investigation can be extremely complex. To better operationalize the phenomenon of fatigue and isolate its neurophysiological mechanisms, researchers have focused on the fatigue resulting from the exertion of cognitive effort. Indeed, this approach allows for carefully designed paradigms in which the difficulty of the task is parametrically manipulated over an extended period (Blain et al., 2016; Wiehler et al., 2022; Pessiglione et al., 2025). By contrasting different levels of cognitive effort, these paradigms enable the experimental manipulation and induction of fatigue, eliminating possible confounding factors.

Another challenge in the investigation of mental fatigue is its measure. Subjective assessments of fatigue are notoriously noisy (Facque et al., 2022; Pessiglione et al., 2025), probably because fatigue also interferes with metacognition and the self-assessment of fatigue itself. To better titrate fatigue, measurements of cognitive performance can be used. Given the varied consequences of fatigue, it is important to track not only errors associated with a default of responsiveness but also inhibition (Andrillon et al., 2019). A reliable way to measure fatigue is to track economic decision-making involving trade-offs between immediate and delayed rewards (Blain et al., 2016; Wiehler et al., 2022; Pessiglione et al., 2025).

A study published in 2022 by the team of Mathias Pessiglione (Wiehler et al., 2022) illustrates well the advantage of this approach. In this study, two groups of healthy individuals were instructed to perform a cognitive task for a long period of time (entire day). One group was asked to perform a difficult version of the task, and the other an easy version of the task. With this paradigm, both groups reported similar subjective fatigue and find the task equally boring. Performance remained high across conditions (e.g. above 90% of hits), and there were no significant group differences. Yet, participants in the hard task group made significantly more impulsive choices at the end of the session. They preferred low-effort, immediate rewards over larger delayed ones (Blain et al., 2016; Wiehler et al., 2022). These results suggest that the behavioral consequences of mental fatigue may not be fully captured by performance accuracy or subjective experience alone. With fatigue, more subtle changes in decision-making strategies appear, we tend to be biased toward low-cost options. Could physiological correlates help uncover the mechanisms underlying the dual expression of fatigue, oscillating between sluggishness and impulsivity?

3. Physiological correlates

Identifying reliable physiological correlates of mental fatigue has been a long-standing objective in cognitive neuroscience. Various modalities have been explored, ranging from autonomic markers (e.g., heart rate, pupil size) to brain activity measures (e.g., EEG, fMRI, MRS).

The eye and the heart have been studied to explore how mental fatigue impairs the autonomic nervous system. A dilation of pupil size has been observed with time-on-task (van der Wel and van Steenbergen, 2018). Within the induce-and-reveal paradigm, pupil-size did not change during the cognitive task. Yet, the pupil dilated during economic choices (Wiehler et al., 2022). Regarding heart measures, researchers observed an increase in heart-rate variability along with mental fatigue (Zhao et al., 2012). Meanwhile others described a strong cardiovascular response (Wright et al., 2008). These mixed results reflect the variety of strategies one can use under mental fatigue. Either one can decide to rest and zone out, or to increase effort. While these measures offer valuable insight into arousal and effort regulation, they are sensitive to context-specific confounds (e.g., stress, motivation, drowsiness).

Studies using fMRI captured a reduced activation in prefrontal regions involved in cognitive control (notably the lateral prefrontal cortex, lPFC) (Blain et al., 2016), along with increased default mode network activity over time-on-task (Asplund and Chee, 2013; Esposito et al., 2014). These findings suggest a functional reconfiguration of brain networks as mental fatigue sets in, prioritizing disengagement over sustained effort. More recently, magnetic resonance spectroscopy (MRS) has provided a window into neurochemical changes associated with mental fatigue, revealing an increased glutamate diffusion in the lPFC following prolonged cognitive exertion (Wiehler et al., 2022). This metabolic shift has been interpreted as a sign of synaptic accumulation of glutamate, which could interfere with signal transmission. But it also could be interpreted as intracellular depletion. Importantly, these changes correlated with a greater tendency to make impulsive choices, linking metabolic changes, regional deactivation, and behavioral signatures of fatigue (Wiehler et al., 2022).

These fMRI and MRS findings were paralleled with the use of EEG to further investigate the temporal dynamics of mental fatigue-related brain activity. EEG offers a better temporal resolution and can be implemented in more flexible and ecologically valid settings. Currently, the main candidate as a marker of mental fatigue has been an increase in central theta and alpha over more posterior areas (Tran et al., 2020). But increase in both frequency bands has also been associated with other phenomena. Theta in healthy subjects has been observed in sleep deprived participants (Snipes et al., 2022) and is also a sign of sleep onset (Santamaria and Chiappa, 1987). An increase in theta could therefore turn out to be ambiguous, at times reflecting a broader

process of cognitive control regulation (Cavanagh and Frank, 2014; Helfrich and Knight, 2016), and at other times reflecting a drop in vigilance (Snipes et al., 2022). Likewise, modulations of the alpha-band have been linked to attentional lapses and task-unrelated thoughts. Yet the direction of this change differs from one study to another. An increase in alpha has been found to correlate with a shift away from goal-directed processing (Arnau et al., 2020; Compton et al., 2019). Yet, both increase and decrease of alpha power have been observed when contrasting lapses of attention (e.g., MW) with task-focused states (Andrillon et al., 2021, 2019). These mixed results raise concern about specificity of the current EEG markers of fatigue.

In summary, one emerging hypothesis is that mental fatigue, resulting from sustained cognitive effort, triggers a succession of events in the brain. Notably an accumulation of glutamate in the lPFC (Wiehler et al., 2022), a region particularly sensitive to cognitive load. This accumulation may interfere with synaptic transmission or reflect a depletion of intracellular resources, ultimately leading to regional hypoactivation (Blain et al., 2016; Wiehler et al., 2022). Such changes in prefrontal dynamics may underlie the behavioral manifestations of fatigue, particularly the shift toward impulsive or low-effort choices. Most importantly, the nature of the changes could represent a shift toward sleep-like activity. Focusing on unambiguous EEG markers of sleepiness such as delta waves could help better capture the relationship between mental fatigue, vigilance, and brain dynamics. In **Study 1**, I examined how new EEG measures can help us further characterize this state.

4. Excessive fatigue in clinical populations

While this chapter has primarily explored fatigue through the lens of experimental paradigms and behavioral impairments in healthy individuals whose fatigue is either spontaneous or induced, it is equally important to consider how fatigue manifests in clinical contexts. Fatigue is not only a product of exertion or cognitive load. Fatigue can also emerge as a persistent and debilitating symptom across a wide range of clinical conditions. In such contexts, fatigue is not only harder to control, but also more likely to interfere with quality of life and functional independence.

Fatigue is a core symptom in neurological and psychiatric disorders, often reported as one of the most disabling aspects of the condition (Nierenberg et al., 1999; Friedman et al., 2007; Braley and Chervin, 2010; Kluger et al., 2016). In multiple sclerosis, up to 75% of patients report fatigue at some point, with many describing it as more debilitating than pain or motor symptoms (Braley and Chervin, 2010). In Parkinson's disease, fatigue affects nearly half of patients (Friedman et al., 2007; Kluger et al., 2016). Importantly, fatigue affects patients often early in the disease course and is cited as the most limiting symptom by a third of patients (Friedman et al., 2007; Kluger et al., 2016). In major depressive disorder, fatigue is both a frequent persistent symptom and a residual

complaint even after treatment response (Nierenberg et al., 1999), affecting up to 90% of patients despite antidepressant use (Ferentinos et al., 2010). Beyond these, chronic fatigue syndrome represents a paradigmatic case where fatigue is the defining symptom, lasting over six months without any clear somatic explanation (Sapra and Bhandari, 2025).

These examples highlight the need to consider fatigue from both fundamental and clinical perspectives. Despite its omnipresence and impact, fatigue remains difficult to quantify and predict. This motivates the development of physiologically informed, ecologically valid tools to monitor fatigue over time and anticipate clinical deterioration. My working hypothesis is the existence of common neurophysiological mechanisms between the spontaneous or induced acute fatigue observed in healthy individuals and the chronic fatigue observed in clinical populations. I propose that these common mechanisms could include the intrusions of sleep-like activity within wakefulness, a hypothesis I will develop in the next section. It is worth noting that clinical populations in which fatigue is a core or frequent symptom are also associated with sleep disturbances. Given that sleep is under a strong homeostatic regulation (a poor sleep quantity or quality during the night increases sleep pressure during the day), it is thus possible that these sleep disruptions could increase sleep pressure during the day, leading to the pattern of fatigue and inattention that are commonly observed or reported in these populations.

II. Sleepiness

1. What is sleepiness and how to study it?

Sleepy ˈsliːpi

Adjective – Needing or ready for sleep

Sleepiness refers to a physiological urge to fall asleep, reflecting a reduced ability to maintain wakefulness. It is often confused with mental fatigue, but the two are dissociable at least at the subjective level. After a large meal or during a circadian dip, one can feel sleepy without feeling mentally fatigued. During a stressful exam or while managing multiple decisions under pressure, one may experience mental exhaustion without any desire to sleep. Nevertheless, sleepiness and mental fatigue often co-occur, especially under conditions of sustained effort or extended wakefulness. Moreover, as I have mentioned in the previous section, subjective self-assessments of fatigue can be noisy and indirect behavioral indexes of fatigue appear more sensitive (Facque et al., 2022). Likewise, self-assessment of sleepiness can fail to reflect objective behavioral (such as an increase in lapses of attention) or physiological changes associated with an increase in sleep pressure (Baiardi and Mondini, 2020; Curcio et al., 2001). The dissociation between sleepiness and fatigue at the subjective level could thus be partially explained by a lack of precision in our introspective feelings.

Beyond subjective self-assessment, sleepiness can be objectively measured using behavioral and EEG indexes. The root cause of sleepiness stems from the nature of sleep as a vital and necessary phenomenon: humans and animals alike, we all need to sleep (Cirelli and Tononi, 2008) and the more we stay awake, the more the pressure for sleep builds up. In fact, sleepiness emerges from the interplay of two core regulatory processes: a homeostatic drive (Process S), which builds up with time spent awake and dissipates with sleep, and a circadian rhythm (Process C), which modulates arousal levels over the 24-hour cycle (Borbély and Achermann, 1992). Under normal conditions, these processes jointly determine the timing and intensity of sleepiness across the day. For example, sleep pressure increases with prolonged wakefulness but is counteracted by the circadian arousal signal during the day, before both converge to promote sleep at night (Borbély and Achermann, 1992).

Studying sleepiness requires a diverse set of tools, ranging from subjective reports and clinical tests to behavioral paradigms. Self-report questionnaires remain the most accessible approach. For example, the Epworth Sleepiness Scale (ESS) measures a person's general tendency to fall asleep in everyday situations, making it a useful screening tool for excessive daytime sleepiness

(EDS) (Johns, 1991). In contrast, the Karolinska Sleepiness Scale (KSS) is designed to capture moment-to-moment fluctuations in alertness and can be administered repeatedly within a task to track the build-up of sleep pressure (Shahid et al., 2012). However, these subjective self-assessments (for example of the self-estimated propensity of falling asleep in the ESS) have been criticized for their poor correlation with more objective indexes of sleepiness such as the actual propensity to fall asleep measured by standardized protocols such as the Multiple Sleep Latency Test (MSLT) (Murray, 2017). In practice, the MSLT, quantifies how quickly a person falls asleep across several nap opportunities during the day. This technique is often used in the diagnosis of pathologies characterized by EDS, such as hypersomnias. Conversely, the maintenance of wakefulness test evaluates the ability to stay awake in a non-stimulating environment, often used to assess treatment efficacy and assess if patients can drive.

Beyond these tools, researchers have used behavioral tasks to probe how sleepiness affects sustained attention and vigilance. The Psychomotor Vigilance Task (PVT) (Dinges and Powell, 1985) and the SART (Robertson et al., 1997) are two widely used paradigms. Both are cognitively undemanding, which makes them particularly sensitive to the gradual onset of sleepiness. More recently, these paradigms have been enriched with experience sampling probes, allowing researchers to combine behavioral performance with subjective reports of mental states and sleepiness. This integrated approach provides additional information on how drowsiness unfolds during wakefulness and what are the consequences on spontaneous experience (SE). It is the method I adopted in **Study 3 and 4**.

SE refer to the subjective mental content that arise spontaneously. Historically, this field has been dominated by the study of MW. MW is the tendency for attention to drift away from the present task toward internally generated thoughts (Smallwood and Schooler, 2006). We spend from a third to half of our awake life MW (Kane et al., 2017, 2007; Killingsworth and Gilbert, 2010). These episodes often involve autobiographical memories, future planning (Smallwood and Schooler, 2015). More recently, researchers have described a distinct form of spontaneous experience known as mind blanking (MB) (A. F. Ward and Wegner, 2013). MB corresponds to the absence of identifiable mental content or access to such content (Andrillon et al., 2025; Van den Driessche et al., 2017). These two phenomena illustrate the range of spontaneous cognition, from richly immersive inner narratives to moments of mental silence. It has been further proposed that MW itself could represent a family of loosely connected phenomena (Seli et al., 2018). The concept of MW can be refined further by distinguishing task-related thoughts (TRT) from task-unrelated thoughts (TUT) (Smallwood et al., 2003). TRT remain anchored to the current activity while TUT drift away from external goals. Another important distinction is the difference between mind wandering with and without intention (Seli et al., 2016). SE are intimately linked to fluctuations of

vigilance as mind wandering typically track subjective assessment of sleepiness (Andrillon et al., 2021), increase with sleep deprivation (Anderson and Horne, 2006; Poh et al., 2016), and are modulated by the circadian cycle (Likar et al., 2023). In some cases, SE may take on atypical or pathological characteristics. This is the case of hallucinations and illusions, which respectively refer to the perception of something as present when in fact absent or the perception of an object in the environment as something else. Hallucinations and illusions are rare in healthy individuals but increase in extreme cases of sleep deprivation (Waters et al., 2018). They are also a very clear diagnostic cue for pathologies associated with strong sleep disturbances such as narcolepsy (Leu-Semenescu et al., 2011) or Parkinson's Disease (Arnulf et al., 2000). This literature thus stresses the importance of considering and describing SE in the context of heightened sleepiness. In this thesis, I use the term SE as an umbrella for these subjective states (TRT, TUT, MW, MB) and explore how they unfold across varying levels of fatigue, both in controlled settings and in daily life. Yet, adopting a recently proposed classification of mental states (Van den Driessche et al., 2025), I will also focus on these important distinctions within SW.

These different approaches range from subjective assessments to behavioral and clinical tools. They allow the investigation of sleepiness as both a state and a trait. They allow us to capture its fluctuations, its functional impact, and its role in sleep disorders. But to fully understand its relevance, we must now ask: how does sleepiness affect cognition and behavior?

2. Cognitive consequences

Sleepiness is a universal human experience. Most of the time, feeling sleepy is harmless yet can turn dangerous in everyday life. A striking example lies in road safety: more than 1 in 5 traffic accidents are attributable to sleepiness (Garbarino et al., 2001). Sleepiness can creep in silently, without the individual's awareness, impairing vigilance, slowing responses, and reducing the capacity for inhibitory control. It is precisely this duality of sluggishness combined with impulsivity in decision-making and response execution that makes drowsy driving so perilous.

These behavioral consequences are not only visible in real-world outcomes but can be systematically studied in controlled environments. In the PVT and the SART, drowsiness induces behavioral consequences: increased reaction times, higher variability, frequent attentional lapses, and a rise in both omissions and false alarms (Andrillon et al., 2021; Drummond et al., 2005). These patterns reflect not just a general slowing, but also a breakdown in the stability and consistency of cognitive control. Declining vigilance produces a fluctuating behavioral profile, combining delayed reactions with increased disinhibition.

Beyond performance metrics, sleepiness also influences SE. As arousal decreases, individuals are more likely to report experiencing MW or MB (Andrillon et al., 2021). These spontaneous mental

states correlate with distinct patterns of behavioral impairment. MW is a more impulsive state, associated with an increase in false alarms and reaction time (Andrillon et al., 2021). Whereas MB is more sluggish, associated with increased sleepiness, individuals miss more, and reaction time is longer (Andrillon et al., 2021). Importantly, they also provide a window into the transitional stages between wakefulness and sleep, where conscious access becomes unstable. As such, sleepiness offers a unique opportunity to study how fluctuations in arousal shape both cognition and conscious experience.

But what underlies these behavioral and experiential shifts? In the next section, we examine the physiological correlates that accompany the onset of sleepiness.

3. Physiological correlates

Sleepiness is not only reflected in behavior: it is also associated with distinct brain correlates. Functional neuroimaging studies have shown that sleep deprivation reduces activation in the DMN and disrupts thalamocortical connectivity, particularly with sensory and motor regions (Drummond et al., 2005; Killgore et al., 2015). These changes are interpreted as a gradual disengagement from the external environment (Killgore et al., 2015). Interestingly, they overlap with the changes associated with fatigue presented in the previous section.

Electrophysiological markers such as the P300 provide time-resolved insights into cognitive processing. The P300 is a component of the event-related potential (ERP), a signal extracted from EEG recordings by averaging brain responses to repeated stimuli. It reflects the brain's evaluation of salient events and is commonly used to assess attention (Fabiani et al., 1987) and conscious access of external stimuli (Dehaene et al., 2003). With increasing sleepiness, the P300 is attenuated and delayed, indicating a reduced capacity to allocate cognitive resources to external information and/or to consciously access external inputs (Koshino et al., 1993; Morris et al., 1992).

EEG spectral analyses provide further insight into the physiological impact of sleepiness. In real-life settings such as studies conducted with train drivers, sleepiness is accompanied by increased alpha activity and a modest rise in lower frequency (e.g., theta and delta, Torsvall and åAkerstedt, 1987). In laboratory settings, in sleep-deprived individuals, an increase in theta and delta power has been observed (Bernardi et al., 2015a; Hung et al., 2013; Snipes et al., 2022). Intriguingly, this increase in low-frequency activity is region-specific: it emerges preferentially in cortical areas engaged by the task at hand (Bernardi et al., 2015; Hung et al., 2013).

These low-frequency bands, typically associated with reduced vigilance, raise intriguing parallels with the patterns observed during sleep. Interestingly, the low-frequency activity that emerges with sleepiness corresponds to the most present oscillatory regimes in non-rapid eye movement

(NREM) sleep. Theta activity is typically associated with the transition from wake to sleep (NREM 1) (Santamaria and Chiappa, 1987). Whereas delta slow waves (SW) progressively increase in amplitude and density to reach their peak during NREM 3. As I will discuss in the next section, these results fit perfectly with the notion that sleepiness is associated with a shift of cortical activity toward sleep-like dynamics (Andrillon and Oudiette, 2023).

Together, these findings suggest that sleepiness involves a progressive disengagement from the external world, characterized by altered large-scale connectivity, diminished responsiveness to salient events, and the emergence of sleep-like activity in task-relevant cortical regions.

4. Excessive sleepiness in clinical populations

While sleepiness is a ubiquitous human experience, some individuals suffer from a pathological form known as EDS. EDS is a persistent and overwhelming tendency to fall asleep in passive or low-stimulation contexts. EDS is typically expected in cases of insufficient or poor-quality sleep, yet in some clinical conditions it persists despite seemingly adequate sleep duration and structure, challenging current operational definitions of what constitutes "restorative" sleep.

This paradox is particularly evident in two clinical conditions: NT1 and IH. NT1 is associated with a well-documented loss of hypocretin-producing neurons, leading to instability in the regulation of sleep and wakefulness (Sateia, 2014). Patients experience fragmented nocturnal sleep, sudden sleep attacks, and frequent transitions into REM sleep. Many also report hypnagogic hallucinations defined as vivid, dream-like experiences at sleep onset. IH presents a different clinical profile. Patients often report unrelenting sleepiness despite normal, or even prolonged sleep (Sateia, 2014). In **Study 2**, I will dive deeper in the sleep microarchitecture of IH to try to unravel the origin of the EDS in this population. Unlike NT1, IH is not characterized by REM dysregulation, and hallucinations are less common.

These two syndromes, though clinically distinct, both challenge the simplistic view that sleep quantity and quality are the solution to get rid of sleepiness. NT1 reveals how a discrete neurochemical deficit can destabilize vigilance and distort SE (Leu-Semenescu et al., 2011; Sateia, 2014). IH, by contrast, invites us to reconsider what defines “functional wakefulness” in the absence of major sleep disruption (Boulanger et al., 2024). Both disorders represent unique windows to study the boundaries of wakefulness, the role of sleep regulation mechanisms, and their phenomenological consequences.

These findings call for a finer-grained understanding of how sleep-related activity manifests not only globally, but also locally, within an awake brain. The next chapter explores the emerging concept of **local sleep**, and its implications for understanding vigilance lapses and internal states.

III. From Global to Local Sleep

1. What is local sleep?

Sleep has long been conceptualized as a global brain state, sharply distinct from wakefulness. Classically, the transition into sleep is marked by widespread cortical changes. EEG signals slow down, become more synchronized, and exhibit characteristic features such as SW: large-amplitude, low-frequency (<1–4 Hz) oscillations most prominent in NREM sleep (Andrillon and Oudiette, 2023). These SW are associated with alternating periods of neuronal activity (ON-periods) and neuronal silence (OFF-periods), reflecting the bistable states of cortical networks (Vyazovskiy and Harris, 2013).

However, this binary view of sleep and wakefulness has been increasingly challenged. Several studies have shown that sleep activity can be observed in awake animals, such as rodents (Krueger et al., 2019) or primates (Pigarev et al., 1997). More recently, a study in sleep-deprived rodents revealed the presence of SW during wakefulness, strikingly similar to those observed during NREM sleep. These events were characterized by transient neuronal OFF periods (e.g. brief silences in population firing, Vyazovskiy et al., 2011). These SW were homeostatically regulated, increasing in rodents with time spent awake. Crucially, these events were local rather than global. While some cortical areas exhibited clear SWs and neuronal silencing, other simultaneously recorded regions remained active (Vyazovskiy et al., 2011). This regional dissociation suggested that sleep-related processes could intrude into local brain areas during wakefulness, without triggering a full transition into sleep.

In humans, direct recordings of neuronal activity are typically limited to rare clinical contexts. One such opportunity arises in patients with epilepsy, who undergo intracranial monitoring. Thanks to this window into the human brain, researchers detected SW akin to those observed in sleep-deprived rodents. These events involved underlying neuronal populations entering brief OFF periods (Sheybani et al., 2023).

Beyond clinical populations, converging evidence from sleep-deprived healthy participants also points to the presence of SW. Here as well, SW appear to be regulated homeostatically: the longer participants remain awake, the more SW density increases. After recovery sleep, these densities return to baseline levels (Bernardi et al., 2015a; Hung et al., 2013). In addition, these SW do not emerge uniformly across the cortex. They tend to appear in regions most heavily engaged by the ongoing task, highlighting a form of region-specific vulnerability (Bernardi et al., 2015a; Hung et al., 2013). This dynamic suggests that sleep pressure can build locally over time.

Interestingly, SW are not restricted to states of extreme sleep pressure and were detected in well-rested individuals (Andrillon et al., 2021). These events share the same waveform and spectral characteristics as the SW observed during NREM sleep (Andrillon et al., 2021). This suggests that local sleep may reflect a general mechanism of vigilance regulation, operating continuously during wakefulness.

Could SW be related to cognitive lapses? If that's the case, they could indicate when the brain is more vulnerable to distraction, error, or disengagement. Understanding this predictive role could provide key insights into the moment-to-moment dynamics of wakefulness.

2. Predicting internal states and behavior

Local SW during wakefulness have been associated with transient impairments in behavioral performance. In sleep-deprived rats, the occurrence of OFF periods in the frontal cortex before a motor response predicted failures in a reward-reaching task (Vyazovskiy et al., 2011). This effect was not observed when SW occurred in the parietal cortex, suggesting that SW could act as a functional switch, perturbing normal information processing in specific neural circuits and leading to circuit-dependent impairments (Vyazovskiy et al., 2011). These observation in animal models were also replicated in sleep-deprived humans. Increases in the number of individual SW were associated with slower reaction times and more attentional lapses (Hung et al., 2013). These behavioral impairments followed the same time course as theta activity, increasing over time and returning to normal after recovery sleep (Hung et al., 2013). Not long after this study, SW were shown to be more likely to co-occur with commission errors in a Go/NoGo task than with correct withholds or responses (Bernardi et al., 2015a). This effect was strongest in medial frontal electrodes, suggesting an impact of local SW on impulse control mechanisms (Bernardi et al., 2015a). However, no such association was found between theta waves and performance in a visuomotor tracking task (Bernardi et al., 2015a). In patients with intracranial recordings, the rate of SW during memory retrieval predicted slower reaction times, even after excluding incorrect responses or periods of low vigilance (Sheybani et al., 2023). These findings converge to show that local SW can modulate or predict performance across tasks, especially when they occur in task-relevant regions. Yet, all errors aren't preceded by SW, and their effects vary by region, timing, and cognitive demand.

Beyond behavior, SW during wakefulness have been linked to changes in subjective mental states (Andrillon et al., 2021). Increases in SW density, amplitude, and slope over the 20 seconds preceding a probe were associated with lower self-reported vigilance (Andrillon et al., 2021). These properties were also negatively correlated with pupil size, an objective marker of arousal (Andrillon et al., 2021). Moreover, the spatial distribution of SW predicted the type of mental state

reported. MW was preceded by more SW over frontal and fronto-central electrodes. MB, in contrast, was predicted by SW over centro-parietal areas (Andrillon et al., 2021). In addition, SW predicted behavior on a trial-by-trial basis. Frontal SW co-occurred with faster responses and more false alarms, while posterior SW predicted slower responses and more omissions (Andrillon et al., 2021). Together, these results suggest that local SW are not just passive signatures of sleep pressure. They reflect, and potentially shape, the content and dynamics of SE.

In summary, SW during wakefulness have been linked to both behavioral impairments and changes in subjective experience (Andrillon et al., 2021; Bernardi et al., 2015a; Hung et al., 2013; Sheybani et al., 2023; Vyazovskiy et al., 2011). Their occurrence is not random: they tend to emerge in task-relevant cortical regions, where they transiently disrupt local processing (Andrillon et al., 2021; Bernardi et al., 2015a; Hung et al., 2013; Sheybani et al., 2023; Vyazovskiy et al., 2011). This regional specificity helps explain the diversity of their effects. Frontal SW are linked to impulsive errors, while posterior SW are associated with omissions and sluggishness (Andrillon et al., 2021). In parallel, SW topography also predicts the content of spontaneous experience, with frontal SW preceding mind-wandering and posterior SW preceding mind-blanking (Andrillon et al., 2021). Together, these findings suggest that local SW are not merely epiphenomenal markers of fatigue. SW reflect region-specific intrusions of sleep-like activity that influence both behavior and conscious experience.

3. Implications in clinical populations

So far, sleep intrusions with wakefulness have been mostly studied in healthy populations, either following a protocol of sleep deprivation or during long and strenuous tasks. These studies have helped characterize the physiological signatures of sleep intrusions, as well as their relationship with homeostatic regulation of sleep and use-dependent processes. They also have allowed the identification of their links with cognitive impairment or subjective experience. Comparatively, there has been far less work on the relevance of these local sleep intrusions in clinical populations.

In individuals experiencing EDS for example, past research focused on the processus of falling asleep, either when allowed to do so (as in the MSLT) or when asked to fight sleep (as in the WMT). Another common EEG index is the phenomenon of micro-sleep, defined as a period of global sleep (eyes closed, reduced alpha oscillations) lasting more than 3 s and less than 15 s (Cori et al., 2019). Arguably, sleep onset and micro-sleep represent the very end of the sleep onset period (De Gennaro et al., 2001) and could fail to capture earlier signs of sleepiness and their cognitive consequences. Local sleep intrusions represent an interesting candidate to capture lapses of attention before sleep onset (Andrillon et al., 2019).

I will test the relevance of the local sleep framework for sleep medicine in the context of hypersomnia. First, I will investigate IH, a sleep disorder marked by strong EDS. Individuals with IH report unrefreshing, prolonged sleep yet experience persistent daytime sleepiness (Sateia, 2014). While the underlying mechanisms remain debated, one could hypothesize that local intrusions of NREM-like activity may be more frequent in these individuals. Preliminary results on the topic will be shown in the **Appendix of Study 3**.

Clinical populations could also represent an opportunity to enrich the concept of sleep intrusions. Local sleep during wakefulness has primarily been associated with local intrusions of SW, a graphoelement of NREM sleep. However, the possibility that elements of REM sleep might also intrude locally into wakefulness has received comparatively less attention (Arnulf et al., 2000; Leu-Semenescu et al., 2011). This question is particularly relevant in narcolepsy type 1 (NT1), a disorder characterized by abnormal REM dynamics, including sleep-onset REM periods and vivid hallucinatory experiences. These hallucinations often occur at sleep-wake transitions, but a third of NT1 report them during wakefulness (Leu-Semenescu et al., 2011). These events are multi-sensory, immersive, and dream-like, which suggests a possible link with REM-related mechanisms.

Interestingly, in animal models, REM sleep is marked by specific phasic activity such as ponto-geniculo-occipital (PGO) waves, which have been associated with the generation of dream content (Jouvet et al., 1960). In humans, there is no history of recording of PGO waves. Among the rare activity characteristic of REM sleep, we find sawtooth waves and increased theta activity (Frauscher et al., 2020; Hutchison and Rathore, 2015; Jouvet et al., 1960). If REM-like activity were to intrude locally into the waking brain, one might expect transient and spatially restricted signatures resembling these oscillatory patterns. Given the association between PGO waves and Rapid Eye Movements (REMs) in sleep, the association between REMs and brain activity in areas associated with visual or mnesic processing (Andrillon et al., 2015; Miyauchi et al., 2009), it has been proposed that PGO waves and their cortical correlates could participate to the emergence of oneiric content (Gott et al., 2017; Hobson and Friston, 2012). Thus, their intrusion during wakefulness could potentially explain dream-like experiences such as hallucinations reported in NT1 and Parkinsonian patients (Arnulf et al., 2000). The fact that administering LSD (lysergic acid diethylamide), known for its powerful hallucinogenic effects in humans, to awake cats increase the amount of PGO waves (Brooks, 1975) provides further evidence for this hypothesis.

There is therefore the possibility that REM sleep-like events could emerge during locally and transiently during wakefulness. Whether such events occur in healthy individuals or only in populations with REM dysregulation remains an open question. NT1 provides a unique model to investigate this possibility. This hypothesis will be explored further in **Study 3**, which examines

hallucinatory experiences in individuals with NT1 and investigates their potential links with transient, sleep-like electrophysiological events during wakefulness.

SW are present in healthy individuals and increase with sleep pressure (Andrillon et al., 2021). However, their expression and consequences may differ substantially in clinical populations. Local sleep provides a new perspective for investigating the mechanisms underlying disorders with altered vigilance and/or increased fatigue.

IV. Beyond laboratory settings

1. Why?

In this manuscript, I illustrated the cases of fatigue and sleepiness through real-life examples. These situations raise questions and hypotheses that are later tested in the laboratory. There, we dissect the specific aspect of a phenomenon (e.g., fatigue, sleepiness, MW), explore their potential consequences, and examine associated physiological correlates. This forms the foundation upon which experimental knowledge is built, brick by brick. After decades of research, the field has matured to a point where laboratory findings can now be tested and extended in real life.

Researchers have long recognized the limitations of controlled paradigms in capturing the full complexity of fatigue. As early as 1900, researchers observed that performance decrements observed over a school day were more likely due to motivational decline than reduced cognitive capacity (Thorndike, 1900). Similarly, in 1921, researchers reported that dactylography performance was more affected by physical discomfort (e.g., muscle soreness) than by fatigue from time-on-task (Muscio, 1921). These results highlighted the influence of context, motivation, and subjective factors on fatigue. It is also worth noting that most laboratory tasks are, to varying degrees, monotonous—a factor that may amplify fatigue-related effects.

A more recent comparison between real and simulated driving contexts underscored that environment matters. While fatigue effects were detected in both settings, reaction times and subjective sleepiness were more affected in the simulator (Philip et al., 2005). Ecological setups offer a pragmatic compromise, allowing the use of laboratory-grade equipment in semi-naturalistic settings. Yet, they fall short of capturing the complexity and variability of real-life cognitive demands.

MW and MB have been thoroughly studied in highly constrained paradigms (e.g., SART, reading tasks). Yet, real-life offers a broader and less predictable set of demands. In laboratory settings, the distinction between voluntary and unvoluntary MW has been detailed (Seli et al., 2016). In real-life, voluntary MW has been shown to be associated with short-term academic cost (Wammes et al., 2016). In contrast, involuntary MW was associated with poorer long-term academic performance (Wammes et al., 2016). In addition to intention, the way thoughts relate to the task further complicates the phenomenology. In everyday activity, capturing the heterogeneity of SE is a challenge, but it is essential for a deeper understanding of spontaneous thoughts. Real-life contexts are often marked by fluctuating stress levels, which have been shown to significantly modulate the frequency and nature of spontaneous thoughts (Linz et al., 2021). Distractions triggered by the environment are also more prevalent in real life compared to lab settings,

suggesting a greater role of exogenous factors in shaping SE outside the lab (Varao-Sousa et al., 2018). Furthermore, the link between executive control and MW observed in laboratory tasks does not consistently replicate in real-world contexts (Kane et al., 2017).

These examples highlight both the value and the challenges of studying cognition outside the lab. Throughout this section, I have already hinted at some of the methods that enable such exploration. Let us now take a closer look at the concrete tools and strategies that make real-life cognitive neuroscience possible.

2. How?

Self-reported experience remains a cornerstone for assessing mental fatigue and spontaneous thoughts in daily life. Early studies on fatigue already emphasized the discrepancy between objective and subjective manifestations.

To explore spontaneous experiences, such as MW and MB, researchers increasingly rely on experience sampling methods (ESM) conducted in real-world contexts. These methods use momentary, in-situ self-reports (e.g., via smartphones) to reduce retrospective bias and improve ecological validity (Kane et al., 2017; Kawashima et al., 2023; Killingsworth and Gilbert, 2010; Linz et al., 2021). Studies consistently report high rates of MW, ranging from a third to half of sampled moments (Kane et al., 2017; Kawashima et al., 2023; Killingsworth and Gilbert, 2010; Linz et al., 2021). In everyday life, these episodes often involve prospective, self-related, or social thoughts and are triggered by both internal and external cues (Linz et al., 2021; Song and Wang, 2012).

However, spontaneous cognition in real-life settings does not always mirror lab-based findings. The overall rate of MW does not correlate robustly between laboratory and natural environments (Kane et al., 2017; Linz et al., 2021; Varao-Sousa et al., 2018), and real-world settings are associated with greater environmental distraction rather than purely endogenous thought (Varao-Sousa et al., 2018). Moreover, methodological factors such as probe frequency, study duration, and device type can introduce reactivity and bias reported rates (Kawashima et al., 2023). These findings underscore the need for careful study design and context-sensitive interpretation when measuring internal states in daily life. Laboratory-based conclusions do not automatically generalize to the richness and variability of everyday experience (Kane et al., 2017; Kawashima et al., 2023; Linz et al., 2021).

Beyond self-report, physiological monitoring tools have been increasingly applied to assess fatigue in real-life or semi-ecological settings. Typing speed and accuracy have been used to track fatigue as a function of time-on-task and time of day (Jong et al., 2020, 2018; Pimenta et al., 2014). EEG studies conducted during typewriting confirmed that these performance changes co-occur with

modulations in P3 ERP components, suggesting altered attentional processing (Jong et al., 2020). Reading has also been widely used as a paradigm to investigate attention and mind wandering (Giambra and Grodsky, 1989). Mindless reading refers reading automatically, with eye movements focusing on the words of a sentence one after the other but without the reader actually processing the meaning of that sentence. Mindless reading can be objectively measured by studying the fine details of the pattern of eye movements. Driving is another example of everyday activity where drivers frequently engage in mind wandering or drive in impaired conditions, for example due to fatigue or sleepiness (Walker and Trick, 2018; Williamson et al., 2011). In driving simulators, an increase in theta and alpha relative to beta power was predictive of subjective and behavioral fatigue (Wang et al., 2018). Reduced P300 amplitude and heart-rate variability were also markers of fatigue. In real-life driving, increased alpha power has been observed, linked with attentional withdrawal (Wascher et al., 2016). Moreover, reduced frontal theta has been observed, suggesting diminished cognitive controls (Wascher et al., 2016).

By contrast, physiological studies of spontaneous thought in real-life settings remain scarce. Paradoxically, with the progress in neuroimaging, the diversity of approach to study mind wandering and SE has decreased to favor more standardized tests. Most findings still stem from constrained lab environments or pseudo-ecological tasks. For instance, during an e-learning video, increased delta, theta, and alpha activity during self-reported MW episodes, along with reduced P2 ERP amplitudes were observed (Conrad and Newman, 2021). Participants with higher MW frequency also showed poorer learning outcomes. While informative, these results remain tied to structured settings. Re-focusing the study of fatigue, sleepiness and its associated phenomena of inattention or mind-wandering to more ecological situations like driving (Walker and Trick, 2018), endurance sports or activities (Mauvieux et al., 2022; Rabat et al., 2025), or games (Guillard et al., 2025; Sauvain et al., 2024), represent a very exciting and fruitful line of research on which I plan to focus in the near future.

These methodological advances provide an opportunity to revisit long-standing theoretical questions in the context of everyday life (Balkin et al., 2023). Can SW described in Chapter III also be detected in more naturalistic environments (e.g., during work or meetings)? How does SW evolve with the build-up of fatigue in daily life? These questions remain largely unanswered and addressing them requires extending the framework of local sleep beyond the lab. **Study 4** of this thesis aims to do explore these questions, by combining subjective reports and physiological signals to track internal states across everyday contexts.

3. So what?

Bridging laboratory precision with real-world complexity is no longer a speculative ambition. It is happening, and it will continue to do so in the future. I argue that to understand how internal states such as fatigue, sleepiness, and spontaneous thoughts unfold in daily life, we must study them where they naturally occur. These are the environments that challenge our vigilance, structure our attention, and shape our experiences. This transition invites a shift in both methodology and mindset. It calls for longitudinal designs that capture fluctuations across days, for multi-dimensional monitoring that aligns physiological signals with subjective experience, and for an openness to the noise and nuance of natural cognition.

As neurotechnologies become more portable and self-tracking tools more ubiquitous, the boundaries between lab and life are disappearing. This convergence opens new paths to study how sleep-related processes like local SW interact with cognition in complex, dynamic environments. The aim is not only to detect when the brain struggles, but to map how it negotiates the demands of modern life.

The studies that follow embrace this transition. Each contributes a piece of the puzzle. I will first consolidate the foundations by probing the neurophysiology of mental fatigue and pathological sleepiness. Then I will test the ecological validity of portable EEG and traditional EEG markers of MW in everyday settings. Together, they aim to reframe our understanding of vigilance. It is not a stable, global state, but a locally regulated continuum. Fatigue, sleepiness, and spontaneous thought are not isolated symptoms, but manifestations of this dynamic balance between brain, body, and context.

Experimental Results

Study 1
Distinct Electrophysiological Signatures of Fatigue State and Choice Bias Following Daylong Cognitive Work

In Preparation

Shruti Naik[1,2,#], **Arthur Le Coz**[1,3,#], Fanny Lachat[1], Antonius Wiehler[1], Thomas Andrillon[1,3,*], Mathias Pessiglione[1,2,*]

[1] Sorbonne University, Inserm U1127, CNRS U7225

[2] Motivation, Brain and Behavior team, Paris Brain Institute, Pitié-Salpêtrière Hospital, Paris, France

[3] Dream Team, Paris Brain Institute, Pitié-Salpêtrière Hospital, Paris, France

# These authors have contributed equally to this work.

* Corresponding Authors

1. 1. Digest

Mental fatigue is a common yet elusive phenomenon, difficult to define, measure, and distinguish from related states such as sleepiness or boredom. In this chapter, I aimed to characterize cognitive fatigue as a specific neurophysiological state emerging from sustained engagement in cognitively demanding tasks. This study builds on previous behavioral, fMRI, and MRS findings showing hypoactivation and a local accumulation of metabolites in the left prefrontal cortex. Here, I tested whether this state could be tracked using EEG, a more portable and temporally precise technique. Can impulsive decision-making, the behavioral consequences of fatigue, be predicted by EEG correlates? Specifically, could local SW be correlated with increasing mental fatigue?

1. 2. Study

Abstract

The quest for objective markers of cognitive fatigue was launched more than a century ago but still represents a scientific challenge nowadays. Because behavioral manifestations of cognitive fatigue (such as drops in performance) have proven elusive, researchers turned to measures of brain activity. A critical issue is the distinction between brain activity signaling the fatigue state and brain activity related to changes in cognitive processes driving the behavior. Here, we induced fatigue in healthy volunteers via the performance of cognitive control tasks for the duration of a short workday, with two difficulty levels assigned to two different groups. Following the duration-by-difficulty interaction, cognitive fatigue was expressed in economic decisions as a preference shift across the day toward low-cost options (small rewards obtainable at short delay with little effort). This shift was quantified as an increased choice bias in computational analyses. In high-density EEG recordings, the neural underpinnings of the preference shift were identified as a reduction of choice-evoked late negative potential over left frontal electrodes. The duration-by-difficulty interaction that induced cognitive fatigue was reflected in the density of sleep-like slow waves expressed by fronto-central electrodes, not only during choices but also during tasks. The pattern of results is therefore compatible with a scenario in which the fatigue state 1) continuously generates slow waves in a global cognitive control network and 2) impairs the activation of a specific cognitive control region when a decision must be made, which makes choices more impulsive.

Introduction

Scientific investigation of mental fatigue is as old as experimental psychology, with pioneering studies published more than a century ago (Ellis, 1917; Thorndike, 1900). Yet we still poorly understand how fatigue emerges and affects behavioral control. Even the mere identification of fatigue in experimental conditions has proven elusive (Ackerman, 2011; Hockey, 2011). Indeed, traditional measures of fatigue, such as self-reports and performance drops, have shown inconsistencies related to confusions between different types of fatigue (acute versus chronic fatigue, exhaustion versus drowsiness, etc.) and confounds with other phenomena (such as demotivation, boredom, frustration, etc.).

To overcome these limitations, we previously suggested a notion of cognitive fatigue (Pessiglione et al., 2025) defined as a work-induced neurophysiological state in which people avoid effort and seek rest. The type of work that generates cognitive fatigue includes all tasks that require the exertion of cognitive control (i.e., tasks for which automatic routines are not available or not appropriate, given the stimuli, responses and goals). The intensity of cognitive fatigue scales with the amount of cognitive control exerted, hence with task difficulty and duration. The experimental protocol that we used to induce such cognitive fatigue involved two groups of participants performing the same tasks (N-back and N-switch) for the same duration (a short workday) but with different difficulty levels. At the behavioral level, the best marker of cognitive fatigue was a preference shift, expressed in economic decisions, toward choice options that offer rewards at low cost, meaning with limited delay and effort (Blain et al., 2016; Wiehler et al., 2022). At the neurophysiological level, best markers were observed during choice deliberation, with both reduced pupil dilation and diminished fMRI activity in the left lateral prefrontal cortex (lPFC). Together, these results strengthen the idea that excessive solicitation of the cognitive control brain system makes it harder to mobilize for making decisions.

Importantly, these results only provide neural markers for the behavioral consequence of cognitive fatigue (the bias in economic decisions), not for the state of fatigue itself. Most research targeting neural markers of fatigue have used EEG, a portable recording technique with good temporal resolution but poor spatial resolution. According to meta-analyses (Tran et al., 2020), a consistent finding is a change in fronto-central low-frequency oscillations. However, the location, the frequency range and even the direction of this change differs across studies (Arnau et al., 2021; Snipes et al., 2022), possibly because fatigue can lead to either compensation or disengagement of cognitive control. Thus, the inconsistent observations could reflect an overlap between fronto-central low-frequency EEG activity related to the exertion of cognitive control, and the occurrence of sleep-like slow waves (SW) related to the emergence of cognitive fatigue (Siclari

and Tononi, 2017). Indeed, the density of SW might signal a dysfunction of neural networks and hence a need for rest (Andrillon et al., 2021), which would make it a promising marker for the fatigue state. It remains unclear yet whether SW affect the brain globally or just the brain regions mobilized by the fatigue-inducing task. Also, because of the analogy with sleep, SW may be taken as indicators of drowsiness (possibly due to boredom) more than use-dependent cognitive fatigue (Hung et al., 2013).

The aim of the present study was twofold. The first objective was to identify using a time-resolved technique (EEG) the neural underpinnings of the fatigue-induced preference shift toward low-cost options, which we previously associated with a reduced contribution of the left lPFC to economic decisions. The second objective was to test whether SW density in EEG recordings could represent a marker of the cognitive fatigue state, irrespective of its impact on economic choices.

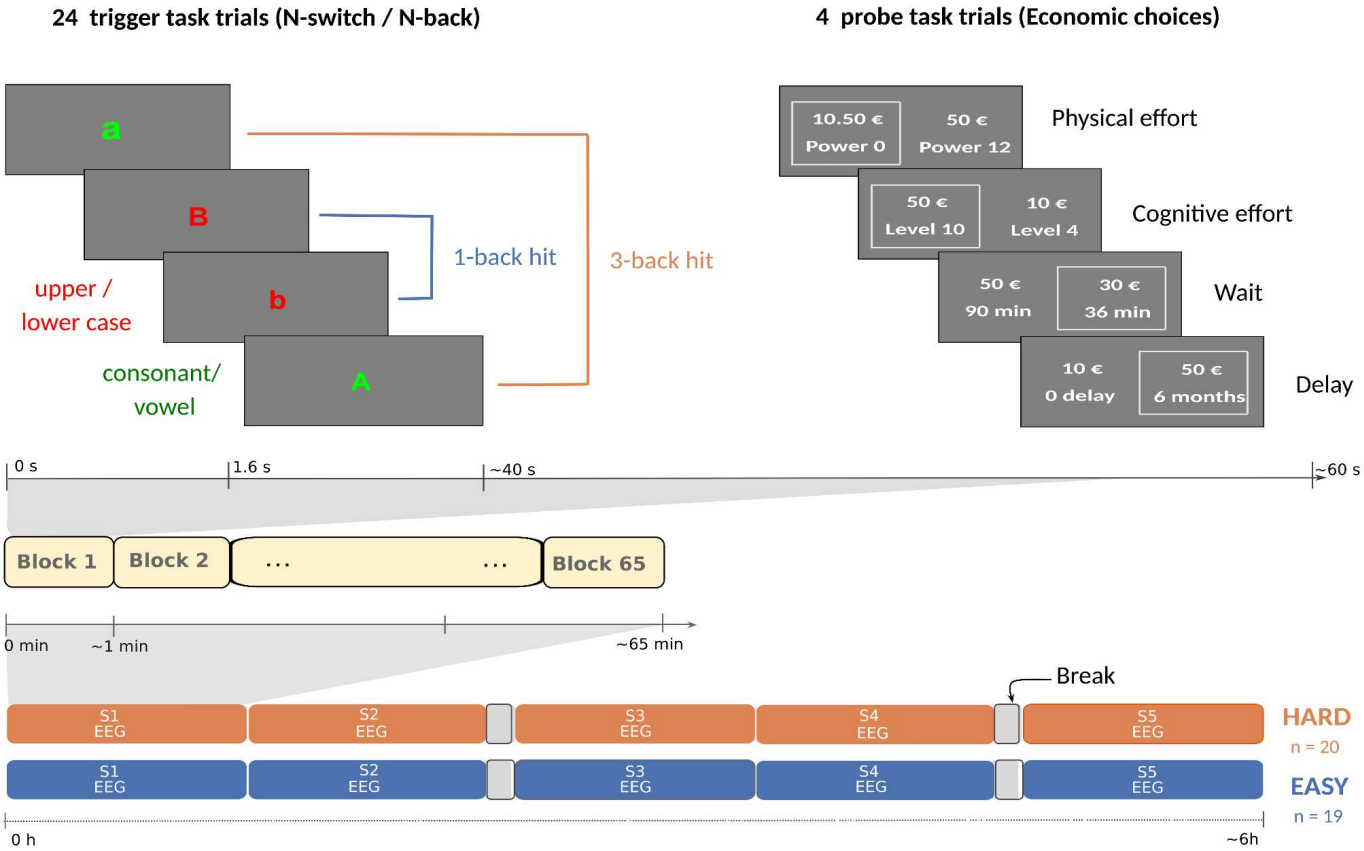

Figure 1.1. Experimental design: From top to bottom, the protocol is shown with diminishing time resolution. During training sessions preceding the testing day (not shown), participants learned to perform the cognitive control tasks until reaching a predefined threshold (90% of correct response) and practiced the economic choices to reveal their indifference points. On the test day, participants performed 5 sessions of 65 blocks with two short breaks, for a total duration close to 6 hours, while EEG signals were continuously recorded. Each block included 24 cognitive control task trials (N-switch and N-back) followed by 4 economic choice trials (physical effort, cognitive effort, wait, delay). Participants were randomly assigned to either the HARD group (n = 20, in orange), doing high-demand versions of the cognitive tasks (3-back and 12-switch) or the EASY group (n = 19, in blue), doing low-demand versions (1-back and 1-switch).

Results

In order to induce cognitive fatigue, we employed an experimental protocol (**Figure 1.1**) that was previously validated (Blain et al., 2016; Wiehler et al., 2022). Two groups of healthy participants performed either low-demand (easy group, n=19) or high-demand (hard group, n=20) versions of cognitive control tasks (N-back and N-switch), for almost 6 hours divided into 5 sessions. To probe fatigue, economic choices were inserted at the end of each 1-min block. Choice options were always a small financial reward obtainable at low cost versus a fixed bigger reward (50€) obtainable at higher cost. Cost domains were physical effort (power of a home-biking 30-min session), cognitive effort (difficulty of an additional 30-min session of N-switch task), wait (duration of stay in the lab before leaving) and delay (date of reward delivery).

Behavioral measures

Behavioral markers of fatigue should be sensitive to both difficulty and duration of cognitive control tasks, so all measures were regressed against a group-by-session linear mixed-effects model (**Figure 1.2**).

We started with self-reports, which were provided on analogous rating scales before and after each session. There was a significant effect of session ($\beta = 0.413$, $p < 0.001$), showing an increase of subjective fatigue with task duration. The interaction with task difficulty was modest but significant ($\beta = -0.105$, $p = 0.042$), yet in the opposite direction (with a greater increase in the easy group), possibly because fatigue was confused with the boredom induced by low-demand tasks. We also collected ratings of motivation, which declined with time in both groups (no significant interaction), ratings of stress, which remained stable throughout the day in both groups, and ratings of hunger, which peaked before lunch and plummeted after lunch, as could be expected (**Figure S1.1**). Thus, none of the self-report measures showed the expected group-by-session interaction.

Another classical measure of cognitive fatigue is task performance, which remained elevated (>80%) in all sessions and tasks for both groups. Here again, as observed in our previous studies, there was no group-by-session interaction ($\beta = -0.003$, $p = 0.64$), showing the robustness of the extensive training that participants received before the experiment, and/or the motivational impact of incentives for performance (each point above 80% being paid 3€).

We then turned to our more reliable marker of cognitive fatigue – the preference for low-cost options (small rewards involving little wait or effort). Based on the calibration session implemented before the experiment, options were distributed around indifference points for each participant, such that the choice rate was set to 50% in the first session. Pooling all domains together (**Figure**

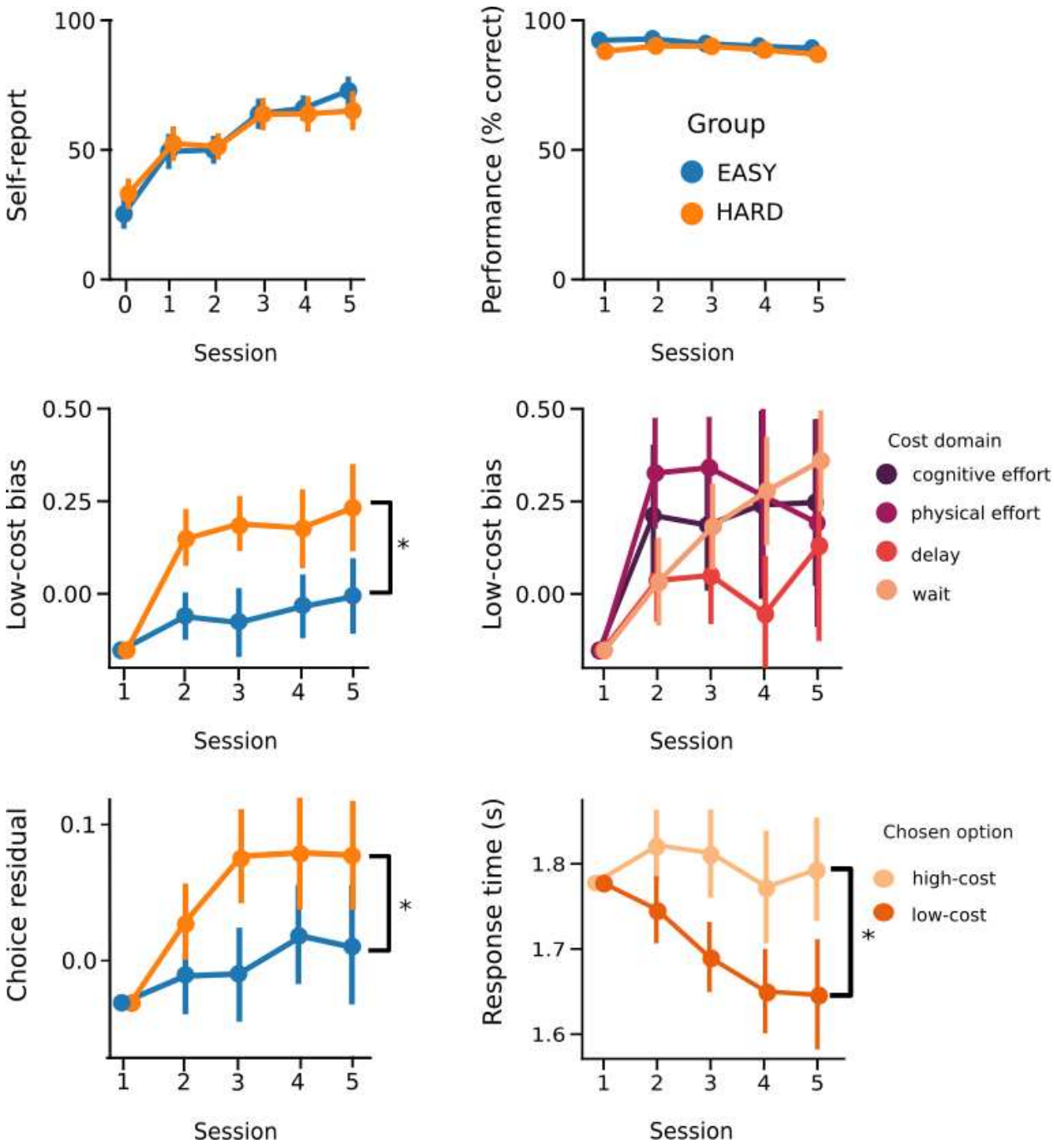

Figure 1.2. Behavioral Measures: All panels show how potential measures of cognitive fatigue vary across sessions in the 'EASY' and 'HARD' groups. Self-report is the subjective rating of fatigue on a visual analogue scale between 0 (I'm in top form') and 100 (I'm totally exhausted'). Performance is the percentage of correct responses averaged over the N-back and N-switch tasks. Low-cost bias is a free parameter of the choice model that captures an additive bonus for the low-cost option. Fitted bias parameters are plotted either separately for the two groups (left panel) or for the four cost domains (right panel) in the hard group. Choice residual is the trial-wise signed difference between observed choice and predicted choice (so greater residuals mean higher rates for low-cost options). Predictions were derived from a computational model fitted to low-cost choices, pooling the 5 sessions together but keeping the two groups apart. Median choice response time (RT) is shown separately for trials in which low-cost and high-cost options were selected, by the hard group. Bias parameters, choice residuals and choice RT were normalized to the grand mean of the first session. Error bars represent inter-participant Standard Error of the Mean (SEM). Stars (*) indicate significant interactions between group and session ($p < 0.05$).

S1.2), we observed an increase across sessions to ~62% in the hard group (β = 2.71, p<0.001), and relative stability in the easy group (β = 1.69, p = 0.052).

To gain further insight into fatigue effects on decision-making, we fitted a previously validated computational model (Heerema and Pessiglione, 2025; Wiehler et al., 2022) to choice behavior, separately for each session and participant. This model includes a discount function specific to each cost domain, which generates the subjective value of the two options, and a choice function that generates low-cost option selection probability from the decision value (difference between option values). Free parameters are the discount rate (weight on cost), the inverse temperature (weight on decision value) and the choice bias (bonus added to the decision value in favor of the low-cost option). Replicating our previous results, we observed a significant group-by-session interaction for the low-cost bias (β = 1.06, p = 0.03), but not for the discount rate (p = 0.95), nor for the inverse temperature (p = 0.62). Because delay and effort emerged as the two costs being sensitive to fatigue effect in our previous studies (Wiehler et al., 2022), the risk domain (for which there was no fatigue effect) was replaced here by the wait domain. We thus examined fatigue effects in the hard group, separately for the four types of costs, using a post-hoc repeated-measures ANOVA. The low-cost bias numerically increased in all cases, with a significant main effect of session ($F(4,76) = 4.06$, $p = 0.005$) and no significant domain-by-session interaction ($F(12,228) = 0.78$, $p = 0.67$).

The increase in the choice bias suggests that with fatigue, the low-cost option is more and more selected, irrespective of reward and cost levels, as if it became a default option. To examine this idea, we tested for a session-by-choice interaction on response time (RT). We found a significant interaction in the hard group (β = -0.036, p = 0.027), but not in the easy group (β = -0.022, p = 0.18), meaning that with fatigue, participants were not only more likely but also faster to select the low-cost option.

To get a trial-wise measure of fatigue effects, we calculated choice residual, defined as the (signed) difference between observed choice and choice probability generated by the computational model, using parameters estimated by fitting all sessions together (i.e., without accounting for fatigue effect on choice bias). Consistent with previous analyses, choice residual showed a significant interaction between group and session (β = 0.016, p = 0.016). This analysis confirms the preference shift towards low-cost options with time on task, which was more pronounced in the hard group (ß = 0.027, p < 0.001) than in the easy group (ß = 0.012, p = 0.003).

Event-related potentials

To identify neural underpinnings of the preference shift, we took an agnostic approach, searching for EEG markers across all channels and time points (during choice deliberation). For each channel

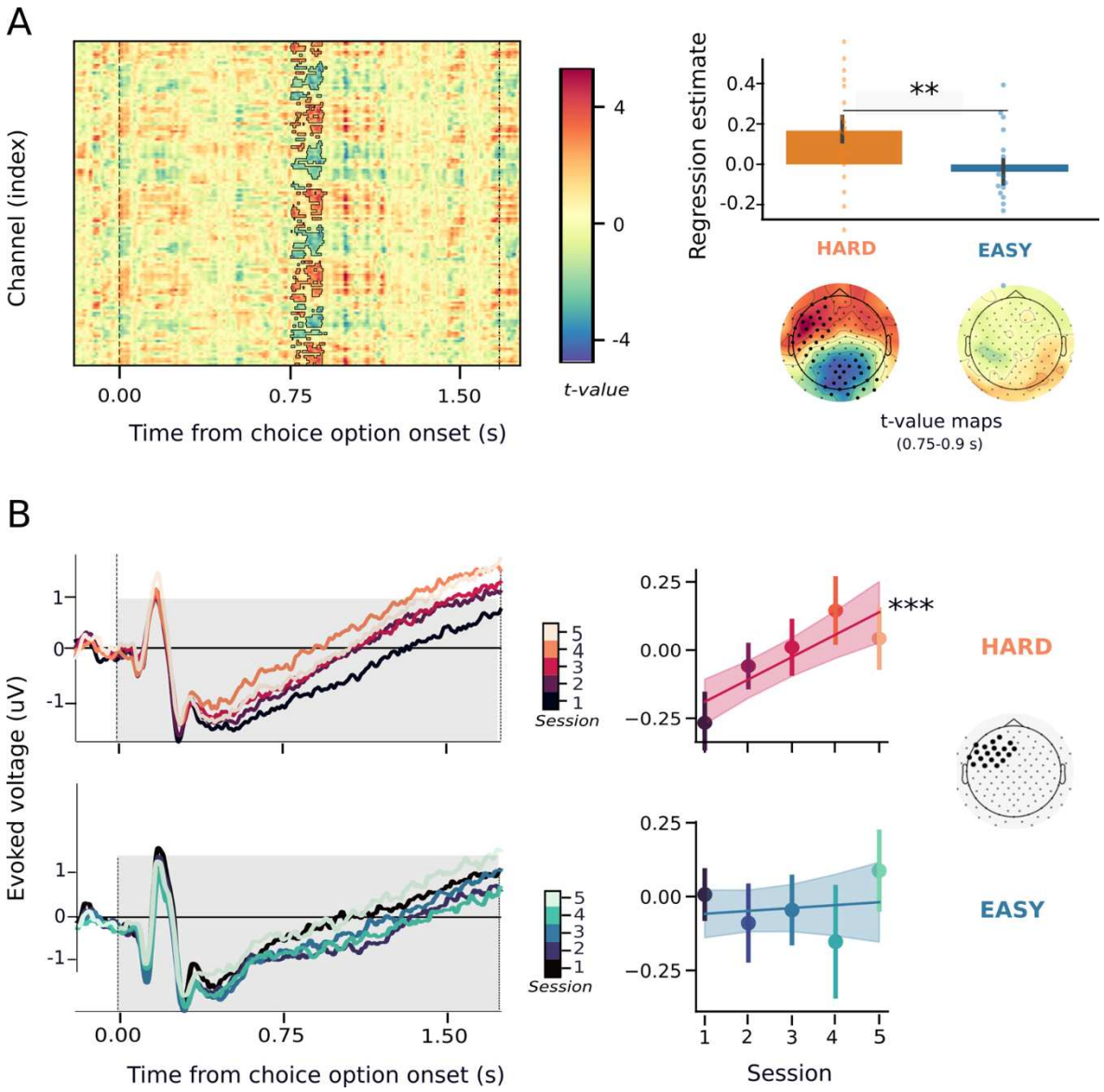

Figure 1.3: Choice-evoked potentials. A Regression of choice-evoked potentials against choice residuals. Time-series of voltage recording were locked on option display (vertical line at t = 0) and cut at mean choice response time (vertical line at t = 1.75s), pooling all choice trials together. Choice residuals are trial-wise differences between observed and modeled choices (positive difference meaning bias for low-cost option). Regressions of recorded voltage against choice residual was conducted across trials, at each time point between 0 and mean RT, separately for each channel of every participant. Significant spatio-temporal clusters (surviving corrections for multiple comparisons) at the group level (left graph) were confined to positive correlations observed in one time window (0.75-0.9s) and to two sets of channels (left frontal and right posterior). Whole-brain topographic maps show the mean t-value and the two significant clusters (black dots) in the easy and hard groups separately. There was no cluster surviving the corrected significance threshold in the easy group. Individual regression estimates were extracted from the left frontal cluster and compared between the easy and hard groups (right graph). Stars indicate significant differences between groups ($p<0.01$). **B Time course of choice-evoked potentials.** Voltage recorded from left frontal channels shown on scalp topography was locked on option display (t = 0), cut at mean choice RT (t = 1.75s), and averaged separately per group and session. Left graphs show the entire time course and right graphs the mean within the choice time-window (0-1.75s). Error bars indicate inter-participant Standard Error of the Mean (SEM), and shaded areas the SEM of linear regression fit. Stars indicate significant slope ($p<0.005$) across sessions.

and time point (between option display and average choice RT), recorded voltage was regressed against our best trial-wise marker of cognitive fatigue, namely choice residual. Regression estimates were calculated at the individual level and then taken to a group-level one-sample cluster permutation t-test (providing correction for multiple comparisons). Two significant spatio-temporal clusters were identified in the hard group (**Figure 1.3A**), with positive regression estimates over left frontal channels ($p = 0.04$), and negative regression estimates over right posterior channels ($p < 0.05$), both within a 0.75-0.9s time-window. In the following, we focus on the left frontal channels because they match with our a priori region of interest based on previous studies showing deactivation of left lPFC with cognitive fatigue (Blain et al., 2019, 2016). There was no spatio-temporal cluster showing significant regression estimates in the easy group. A post-hoc comparison of regression estimates extracted from left-frontal channels showed a significant difference between groups ($\beta = -0.05$ vs. $\beta = 0.16$, $p = 0.015$).

We then checked that choice event related potential (ERP) varied across sessions as expected (**Figure 1.3B**). To avoid double dipping, we extracted the mean ERP within the entire choice time window (from option display to button press). A linear regression fit showed that, indeed, mean ERP increased across sessions in the hard group ($\beta = 0.082$, $p = 0.001$), but not in the easy group ($\beta = 0.01$, $p = 0.79$). These results together provide evidence for an effect of cognitive fatigue on choice-evoked EEG activity recorded from left-frontal channels in the hard group. Note that the increase of choice-related activity was due to the negative deflection becoming less negative across sessions, which would denote a decrease in global field power (GFP). This reduced late negativity could reflect a disengagement of decision-related cognitive processes, compatible with the fMRI deactivation previously observed in the left lPFC.

Background slow waves

We then examined whether SW density could underlie cognitive fatigue, following the group-by-session interaction. SW events were automatically detected in EEG traces recorded from each channel (**Figure 1.4A and S1.3**). The SW average waveform showed a pronounced negative peak (**Figure 1.4B**), reminiscent of the sleep SW down-state, but overlapped with faster alpha oscillations confirming the participants were awake (e.g. Andrillon et al., 2021). Linear mixed-effects cluster analyses showed that SW density increased over the course of the day (**Figure 1.4C**), with a significant group-by-session interaction over fronto-central channel, during both choice trials ($t = 59.46$, $p < 0.001$) and task trials ($t = 84.27$, $p < 0.001$). Interestingly, plotting the average SW density over significant channels (**Figure 1.4D**) revealed that the increase across sessions was not following the same pattern as observed with the preference shift (indexed by low-cost bias or choice residual in **Figure 1.2**), with a reduction of SW density after lunch (between sessions 2 and 3).

We finally tested whether choice residual was still tethered to SW density when removing the common experimental factors. For this analysis, the effects of time and difficulty, and their interaction, were regressed out of both measures (see Methods). The correlation between corrected measures was significant for both choice and task trials ($t = 32.69$, $p < 0.01$), with a topography that overlapped with the interaction clusters (**Figure S1.3**). Thus, the fronto-central channels showed both a significant interaction (steeper increase with sessions in the hard group) and a link with choice residual that persisted above and beyond this interaction.

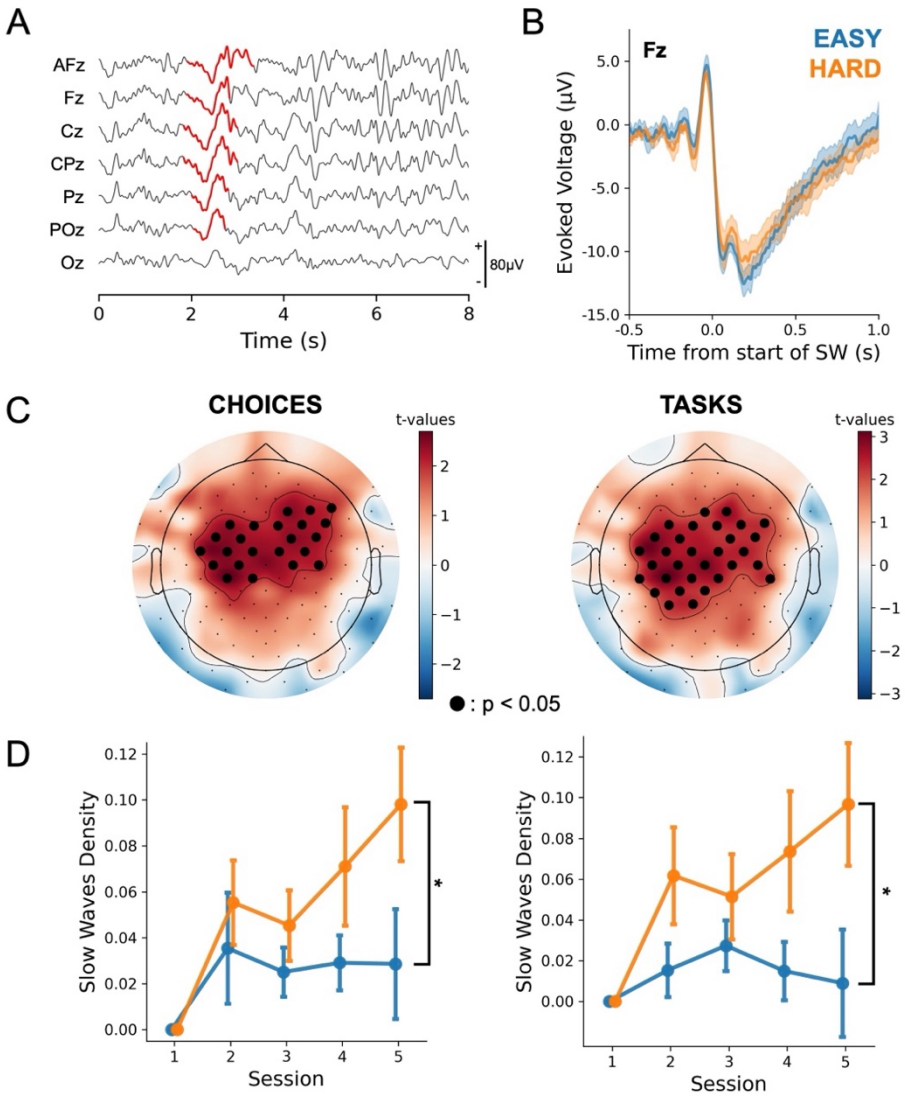

Figure 1.4: Fatigue-related slow wave density. A Slow wave detection in EEG traces. Example EEG traces were recorded from channels AFz–Oz in one participant. Detected slow waves are highlighted in red. **B Mean waveform**. Event-related potentials were recorded from channel Fz, time-locked to slow-wave onset, separately for easy (blue) and hard (orange) groups. **C Group-by-session interaction on slow wave density**. Scalp topographies show t-values for the interaction tested during choice trials (left) and task trials (right). Large black dots mark channels surviving cluster-based correction ($p < 0.05$). **D Variations of slow wave density across sessions.** Slow wave density (number of events per second) is averaged over the significant channels identified in scalp topographies, during choice trials (left) and task trials (right), separately for the easy (blue) and hard (orange) groups. Error bars indicate inter-participant Standard Error of the Mean (SEM).

Discussion

Regarding our first aim, we confirmed previous conclusions (Blain et al., 2016; Wiehler et al., 2022) that the fatigue related to duration and difficulty of cognitive control tasks manifests as a preference shift towards low-cost options (immediate and effortless rewards), underpinned by a reduction of left lPFC activity.

As expected, economic choices of participants performing difficult tasks drifted throughout the day from the predictions of a computational model that was blind to fatigue effects. This drift across sessions was best accounted for by an increase in a bias parameter providing a bonus for low-cost options. Because of this bonus, low-cost options were turned into default options, being chosen more frequently and more rapidly. Our results are in line with a literature that specified the behavioral changes due to cognitive fatigue as manifestations of choice impulsivity, which also affect other domains such as aggressivity in choices made during social interactions (Ordali et al., 2024).

Contrary to economic choices, more classical measures of fatigue such as self-reports and task performance did not show the expected duration-by-difficulty interaction. In line with previous considerations (Ackerman, 2011; Hockey, 2011), self-reports may not be reliable markers of cognitive fatigue, possibly because insight into fatigue is limited, because true fatigue is easily confused with other feelings (such as drowsiness and boredom), or because idiosyncrasies in the use of rating scales blur the comparison of fatigue levels between participants. Performance may not be a reliable marker either, because fatigue effects can be compensated when it matters, for instance when correct performance leads to financial reward, as implemented in our protocol. The motivational control of performance would accord well with theories that consider cognitive fatigue not as a loss of capacity, but as a shift in a cost-benefit tradeoff (Boksem and Tops, 2008; Inzlicht et al., 2014; Kurzban et al., 2013). In our own theory (Pessiglione et al., 2025), this shift is specified as an increase in the cost of cognitive control, due to metabolic changes in underlying brain regions (including the lPFC).

When looking for neural correlates of the preference shift toward low-cost options, we found a progressive reduction of choice-evoked potentials over left frontal and right occipital clusters. The absence of MR anatomical scans, the imprecise localization of the EEG electrodes on the skull and the poor spatial resolution of EEG recordings precludes an accurate source reconstruction of the scalp activity. Yet the distribution of significant electrodes is compatible with a source in the left lPFC region where we previously observed reduction of activity using fMRI (Blain et al., 2016), and accumulation of glutamate using MR spectroscopy (Wiehler et al., 2022), with the preference shift induced by the same experimental protocol. These previous observations are extended here

with a less expensive and more portable technique that would enable the detection of cognitive fatigue expressed when making economic decisions. Leveraging the temporal resolution of EEG recordings, we also specify that the diminution of lPFC activity precisely occurs during choice deliberation. A direct interpretation is that reduced lPFC activity reflects a diminished exertion of cognitive control, which would turn low-cost options into default options, being automatically chosen without further deliberation.

Regarding our second aim, we identified neural markers of the fatigue state, establishing links with the literature on low-frequency fronto-central oscillations observed in EEG activity (Borghini et al., 2014; Lal and Craig, 2002; Tran et al., 2020). The duration-by-difficulty interaction was indeed observed in SW density around a large fronto-central cluster. We take this increase in SW density as a marker of the fatigue state because it was not related to any particular event, being equally expressed during economic choices and during cognitive control tasks. The fronto-central location is consistent with previous reports of low-frequency EEG activity increasing during performance of cognitive control tasks (Bernardi et al., 2015a; Ordali et al., 2024). Because SW are reminiscent of EEG activity recorded during sleep, they are typically interpreted as a form of cortical bi-stability (Massimini et al., 2024) that spread with time spent awake across the entire brain, but even more so in the brain regions solicited by cognitive tasks (Andrillon and Oudiette, 2024). Here, the increase in SW density affected a large portion of channels that might reflect a broad shift of cortical dynamics within the cognitive control network. Because SW increased in the hard group more than in the easy group, we conclude that they reflect fatigue more than sleepiness, which is typically high during low-demand tasks (Andrillon et al., 2021).

We acknowledge that assigning our two neural markers (choice ERP and SW density) to distinct cognitive contructs (choice bias and fatigue state) is not providing a full mechanistic picture. A simple mechanism would be a causal chain: time and duration of cognitive work triggers the emergence of SW, which in turn alters brain activity during decision-making, reducing ERP and hence favoring impulsive choice. This scenario is consistent with the results that both ERP and SW are sensitive to the fatigue induction and linked to the choice bias. However, this scenario in which SW are causally responsible for choice ERP and bias is incompatible with several observations: SW were predominant in a different cluster of channels (fronto-central vs. left frontal), were expressed in different phases of the protocol (during tasks as well as during choices) and were following different dynamics (steady increase with transitory reduction around lunch vs. monotonic log-like shape). These observations call for a more complex mechanism following a causal fork, with time and difficulty of cognitive work inducing a state of fatigue, which on one side generate SW (irrespective of the behavior) and on the other side choice ERP (only when making decisions) and the associated choice bias.

If this more complex scenario is correct, the fatigue state remains to be specified. Following on our previous proposal (Pessiglione et al., 2025), we suggest that the fatigue state arises from metabolic alterations within the widespread cognitive control neural network. The accumulation of glutamate that we previously reported was observed in a left lPFC region, but it might also occur in the other cognitive control brain regions, which were not sampled in our MR spectroscopy study (Wiehler et al., 2022). Then, the accumulation of potentially toxic substances could impair the exertion of cognitive control, either by disabling the system directly or via some down-regulation loop preserving brain functions. Thus, less cognitive control would be exerted over decisions, leading to reduced ERP and choice impulsivity. Irrespective of the task, metabolic alterations that form the fatigue state could generate SW that would spread all over the brain. It has been reported, for instance, that elevated levels of glutamate can trigger the release of cytokines (e.g., TNF-α), which are associated with the generation of SW (Krueger et al., 2019). Thus, metabolic alteration could underlie both neural markers related locally to the preference shift and globally to the fatigue state. Testing this complex scenario would require further experiments with simultaneous metabolic and electrophysiological recordings.

In any case, fronto-central SW density might be a good candidate marker to detect cognitive fatigue in the workplace. Although it is related to behavioral manifestations of cognitive fatigue (choice bias), it is expressed even when the behavioral performance is not clearly affected by fatigue (during cognitive work). Also, while the increase in choice bias and ERP saturated at the middle of the day (about 3-4 hours of work), the increase in SW density was prolonged until the end, following more faithfully the duration by difficulty interaction. A potential issue is yet that SW density is also affected by other factors, such as food intake and sleep pressure, which might question its specificity regarding cognitive fatigue. Future studies should improve our understanding of how these different factors concur to trigger brain slow waves and related behavioral changes.

Materials and Methods

The study was approved by the ethical committee ('Comité de Protection des Personnes', CPP no 113-15, ID RCB: 2015-A01445-44) of the Pitié-Salpêtrière Hospital and insured by Inserm ('Institut de la Santé et de la Recherche Médicale', protocol n°C15-59). A total of 40 participants were recruited from the Ile-de-France community via the RISC platform ('Relai d'Information sur les Sciences de la Cognition'), with n = 20 in the hard group (mean age 23.7±3.1 years, 10 women), n = 20 in the easy group (mean age 24.6±3.9 years, 10 women). For more information on participants and full details of EEG data recording and analysis, see SI Materials and Methods. All Matlab and

Python codes used to analyze behavioral and EEG data are publicly available at www.github.com/transpersonify/fatigue-eeg.

Behavioral protocol

Details of the behavioral protocol are provided in our previous paper (Wiehler et al., 2022). The 39 participants came to the lab three times within a single week, for training on cognitive control tasks on the first day, calibration of economic choices on the second day, and the actual experiment with both tasks and choices combined with EEG recording on the third day.

Training lasted about 3 hours, starting with the lowest difficulty level (1-back and 1-switch) and ending when accuracy reached a criterion of 90% correct in two consecutive blocks for all difficulty levels (up to 3-back and 12-switch). The two tasks were programmed using the Matlab Psychtoolbox (Kleiner et al., 2007). They presented a series of lower-case or upper-case letters, using green or red font. In the N-back task, participants indicated at every trial whether the letter on screen was the same as the letter presented in N trials before that. In the N-switch task, participants indicated whether the letter on screen was a vowel / consonant, or upper / lower case, depending on its color (red or green, counterbalanced over participants), which was switched N times per block.

Calibration of economic choices included familiarization with the different effort levels for cognitive and physical effort and one session of the choice task in which options were progressively updated toward indifference points, using a staircase procedure. Cost levels were 0 / 12.5 / 25 / 37.5 / 56.25 / 75% of the participant's maximum power level (determined beforehand) for physical effort (30-min session of pedaling on stationary bike), 0 / 2 / 4 / 6 / 9 / 12 switches within a 24-trial block for cognitive effort (30-min session of N-switch task), 0 / 3 / 7 / 30 / 90 / 365 days for delay (between the experiment and reward delivery), 0 / 18 / 54 / 90 / 126 / 162 minutes for wait (staying in an empty room, without personal belongings, before leaving the lab). All choices presented a variable small reward associated with one of the two lowest cost levels and a fixed big reward (50€) associated with one of the non-zero cost levels. The staircase procedure determined, for each possible pair of cost levels, the value of the small reward at which participants were indifferent between the two options (each being selected with a 50% rate).

On the experiment day, participants were randomly assigned to easy or hard groups, without their knowledge (so they ignored the existence of a different group performing tasks at a different difficulty level). The difficulty was 3-back and 12-switch for the hard group, 1-back and 1-switch for the easy group. All participants performed 5 sessions, with 10-min breaks after the second and fourth session, the first being the lunch break for which a sandwich was provided. Every session was divided into 65 blocks lasting 1 min each. One block presented 24 letters every 1.6s, to which

participants responded on a keyboard (by pressing the left or right arrow key, according to instructions of either the N-back or N-switch task). The two tasks were assigned to either the first or the second half of a session, in a counterbalanced order. The task to be performed was indicated on screen at the beginning of blocks. Each block ended with a series of 4 choices (one per cost type, in a random order), timed out at 3.25s after option onset, with a randomly jittered inter-trial interval of 1.25s (±0.33s). For each pair of cost levels, small rewards were systematically varied (across trials within a session) around pre-determined indifference points, such that in the absence of fatigue, choice rate would remain around 50%. Correct performance in cognitive control tasks was incentivized by instructing participants that each point above 80% correct would be paid 3€. Economic choices were also incentivized, by informing participants that at the end of the day, 2 choice trials would be randomly selected and that options selected in those trials would be implemented.

Before and after each session, participants rated their feelings by positioning a cursor on a visual analog scale between 0 and 100: fatigue (0 = top form / 100 = total exhaustion), stress (0 = perfectly relaxed / 100 = completely stressed), hunger (0: totally satiated / 100 = awfully starving) and motivation (0 = not at all motivated / 100 = fully motivated).

Dependent behavioral variables were subjective rating (z-scored at the participant level), performance in cognitive control tasks (correct response rate), choice (coded 1 when the low-cost option was selected, 0 otherwise) and choice response time (RT < 0.1s or > 3.25s were rejected). All variables were analyzed using mixed-effects linear models, within-participant factors (such as session) being estimated at the individual level and between-participant factors (such as task demand) at the group level.

Supplementary Methods

Computational Modeling

Choices were fitted using computational models that were previously validated (Heerema et al., 2023; Wiehler et al., 2022). We have replicated the Bayesian model comparison to check that the same models best explained the present dataset. These models included a same softmax choice function for all cost domains, which generated selection probability from the difference between subjective values of choice options:

$$Proba(choice = LC) = 1 / (1 + \exp(-(\beta.(Val_{LC} - Val_{HC}) + bias))) \quad (1)$$

with LC and HC designating low-cost and high-cost options, β a weight parameter on subjective values (also called inverse temperature) that adjusts for choice consistency and bias an intercept

parameter that captures the propensity to select low-cost options, irrespective of subjective values.

Subjective values were generated from objective attributes (rewards and costs) using discount functions that were multiplicative for delay (so the value remains positive, because a delayed reward is always better than nothing) and subtractive for true costs (so the value can be negative, because some rewards are not worth the effort or the wait in the lab):

$$Val = Rew \times \exp(-Kd.Delay) \quad (2)$$

$$Val = Rew - Kc.Cost^2 \quad (3)$$

with Kd and Kc designating discounting parameters that capture the weight of delay and other costs (different parameters being used for wait, physical effort and cognitive effort).

Computational models were fitted on each participant and session separately, using the Variational Bayes Analysis toolbox (VBA, https://mbb-team.github.io/VBA-toolbox), with priors informed by the choices made during the calibration session. Parameters were then regressed against a mixed model with a fitted power on session number to account for the concavity of time-on-task effects, as was done in a previous paper (Blain et al., 2016). Models were also fitted on all sessions together to obtain parameters used to generate choice probabilities and calculate choice residuals by comparison with observed choices.

Participants

All participants gave informed consent before participating in the study. The inclusion criteria for screening participants were: age between 18 and 30 years, no previous psychiatric or neurological condition, no psychotropic drug within the last 2 months, right handedness, no pregnancy, no glasses, no dreadlocks or braids. On the day of the EEG experiment, participants were asked to wash and dry their hair beforehand, and to avoid applying oil, gel or makeup. One participant in the easy group stopped the experiment after the first session and EEG data from 2 participants in the hard group and 3 participants in the easy could not be included, due to technical problems. In the end, 39 participants were included in the behavioral dataset and 34 participants in the EEG dataset.

On the experiment day, eating was restricted to one sandwich and one fruit taken during the first break. The only drink allowed (without restriction) was water. Participants received a fixed compensation of 70€ for their participation. In addition, they could win a 3€ bonus per point above 80% correct in the cognitive control task, and were offered 2 options randomly picked among those they selected in the choice task (for which they had to pay the associated cost in time or effort).

Event-Related Potentials

High-density scalp EEG signals were recorded using a BrainAmp system with 128 active electrodes brain Products GmbH). A ground electrode was placed at the nasion. Electrodes were referenced online to the fronto-central electrode (FCz). EEG activity was originally sampled at 500 Hz and stored in a BrainVision data format.

The EEG data time series were analyzed using the MNE-Python toolbox (Gramfort et al., 2013). The 5 sessions were analyzed separately for each of the 34 participants, resulting in 170 files spanning about 170 hours of EEG recording. The raw EEG signal was first high-pass filtered above 0.1 Hz and then resampled at 250 Hz. A notch filter was applied to remove line noise (at 50 Hz and harmonics). Time series were segmented into 4s long epochs around choice onset (from 1s before to 3s after option display. Bad channels identified as noisy throughout the recording were isolated and interpolated using auto-reject.

Ocular, muscle and motion artifacts were automatically detected and corrected via a homemade preprocessing pipeline that included the auto-reject (Jas et al., 2016), independent-component analysis (ICA) (Lee et al., 1999) and ICLabel (Pion-Tonachini et al., 2019) algorithms. After applying ICA on epochs of interest, the components labeled as 'Brain' by ICLabel were visually inspected based on their topography, time-series and spectral power before including them into the reconstructed EEG signal. A second pass of the auto-reject analysis was applied to the reconstructed signal to remove any epoch with remaining artifacts. Before statistical analysis, common average reference and non-causal 1-35 Hz band-pass filter were applied to each epoch of choice-related EEG activity and baseline activity (averaged over the 500 ms preceding option display) was subtracted. The scalp topographies were transformed using current source density (CSD) to achieve more accurate maps and to reduce the effect of volume conduction (Perrin et al., 1987).

To identify neural correlates of the fatigue-induced preference shift, EEG activity was regressed against (signed) choice residual, separately for each participant, channel and time point after option display. Regression coefficients were then taken to a second-level one-sample t-test, done separately for the easy and hard groups. Spatio-temporal clusters (i.e., channel by time windows) that survived significance threshold after permutation-based correction for multiple comparisons were identified separately for positive and negative correlation with choice residual. Permutations consisted in generating a null distribution of regression estimates by randomly shuffling labels, with 1024 iterations.

Background slow waves

To detect sleep-like SW, the same preprocessing pipeline was followed, with the exception that EEG time series were segmented per block and not per trial. Preserving the continuity of the EEG signal is important to detect background SW that are not necessarily time-locked to task events. Thus, we epoched the continuous data around each task and choice block, taking the mean block duration plus 1 s of padding before and after (40 s total for task epochs; 14 s for choice epochs) to avoid edge artifacts.

The SW detection algorithm was adapted from previous work on NREM sleep (Bernardi et al., 2015a; Riedner et al., 2007) and was modified to detect SW during wakefulness (Andrillon et al., 2021). SW were identified following a two-step preprocessing pipeline. First, EEG signals were down-sampled to 100 Hz and filtered using a zero-phase finite impulse response (FIR) band-pass filter (0.5–10 Hz) with automatically determined transition bandwidths, ensuring minimal edge artifacts while preserving waveform integrity. We then identified negative and positive zero-crossings in the filtered signal which were used to segment candidate SW. For each candidate wave, we computed the peak-to-peak (PTP) amplitude, that is the amplitude difference between the most positive and most negative peak between the start and end of the wave (consecutive zero-crossings). We then selected high-amplitude slow waves based on this PTP amplitude, which had to exceed a data-driven threshold, estimated for each channel and each participant in the first session (baseline). To compute this threshold, we fitted an ex-Gaussian distribution to the distribution of PTP amplitudes for each channel, session and participant (Virtanen et al., 2020). This ex-Gaussian fit provided 3 parameters: the mean (μ) and standard deviation (σ) of the Gaussian component and the Exponential tail (τ). To capture the tail of the Ex-Gaussian distribution, we defined the PTP threshold as twice the amplitude of the peak of the Ex-Gaussian. For each SW, we further extracted the following parameters: (1) Maximal negative slope (descending phase), representing the voltage decline (in μV/s) between the first negative zero-crossing and the negative peak crossing divided by the duration between the negative zero-crossing and the negative peak (in sec); and (2) Maximal positive slope (ascending phase), reflecting the voltage increase between the negative peak and the subsequent positive zero-crossing divided by the duration between the peak and the positive zero-crossing (in sec). Only waves with a descending and ascending slope between 0.25 and 2 μV/s were retained, ensuring the selection of physiologically meaningful SW. Finally, SW density was defined as the number of SW in each block (task or choice) divided by the duration of the corresponding block (40s or 14s respectively).

Slow-wave density was analyzed at each channel using a linear mixed-effects model (LME) to estimate the main effects of duration (session number) and difficulty (easy vs. hard group) and their interaction (session x group). We also added random intercepts for each subject. These LME were implemented in Python's statsmodels (Seabold and Perktold, 2010). For each channel, we

extracted the t-statistic for the session × difficulty interaction. To correct for multiple comparisons across channels, we performed a cluster-based permutation test: neighbors were defined by Delaunay triangulation of the 2D sensor coordinates from the MNE info structure. Candidate channels were those with uncorrected $p<.05$ and positive interaction t-values. Clusters of at least two adjacent channels were formed by iteratively merging neighboring candidates and the cluster statistic was defined as the sum of channel-wise t-values within each cluster. By randomly shuffling difficulty labels 1 000 times, we built null distributions of maximum cluster sums. Clusters from the original dataset were considered significant if their cluster-level p-value (Monte Carlo α) was $< .05$.

We tested the block wise relationship between SW density and choice residual. To remove common factors related to cognitive fatigue that could drive a correlation, we regressed out the effect of epoch (trial within block), session number, difficulty (group), and all their interactions on both SW density and choice residual, with a random intercept for each subject. Thus, both SW densities and choice residuals were placed in the null space of factors inducing cognitive fatigue. We finally tested the correlation between the two corrected measures (SW density and choice residual), to estimate their relationship independently from the effects of trial number, epoch, session, and difficulty. After this analysis we identified channels for which SW density was (1) impacted by cognitive fatigue (significant group-by-session interaction), (2) linked to choice residual after removing effects of cognitive fatigue. We also applied a cluster-permutation approach to this analysis, by shuffling the corrected measures of SW density (200 permutations). The definition and selection of significant clusters was identical to the permutation test analysis described above.

Acknowledgments

The research leading to these results has received funding from the national program “Investissements d’avenir” ANR-10- IAIHU-0006. We thank the staff of the Prisme facility (Paris Brain Institute), where the experiment took place. Shruti Naik was supported by a grant from the Agence Nationale de la recherche (‘X-fatigue’), Antonius Wiehler by a grant from the Paris Brain Institute (Big Brain Theory project ‘Biofatigue’), Fanny Lachat by an ERC Starting grant (‘Biomotiv’), and Arthur Le Coz by a grant from Ecole Doctorale Frontières de l’Innovations en Recherche et Education-Programme Bettencourt and the Fondation pour la Recherche Médicale (FDT202404018709).

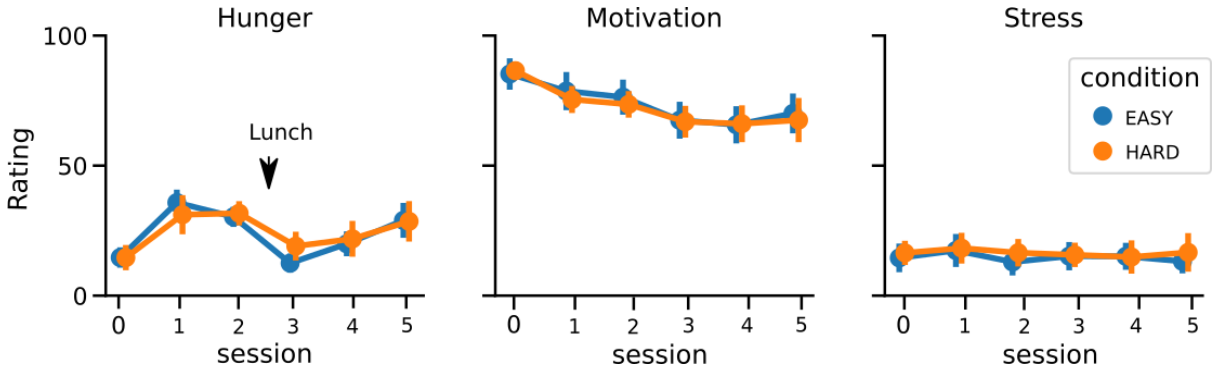

Figure S1.1: Self-reports of hunger, motivation and stress. All ratings were provided on a visual analog scale graded between 0 and 100. Data are averaged per group and session. Error bars show inter-participant Standard Error of the Mean (SEM).

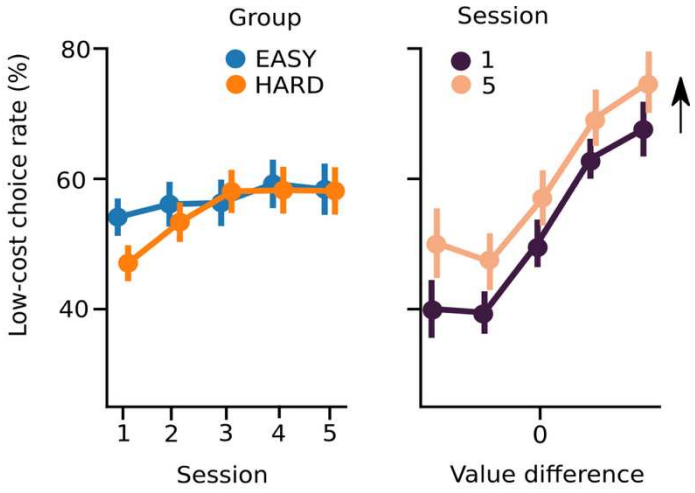

Figure S1.2: Choice rate. Choice rate is the percentage of trials in which the low-cost option was selected. It is plotted as a function of group and session (left graph) or binned decision value (right graph). Decision value is the difference between the two option values, estimated by a model initially fitted on all sessions together (i.e., without account for the fatigue effect on choices). The fatigue effect (i.e., the shift in the intercept of psychometric curves) was later captured by the choice bias parameter.

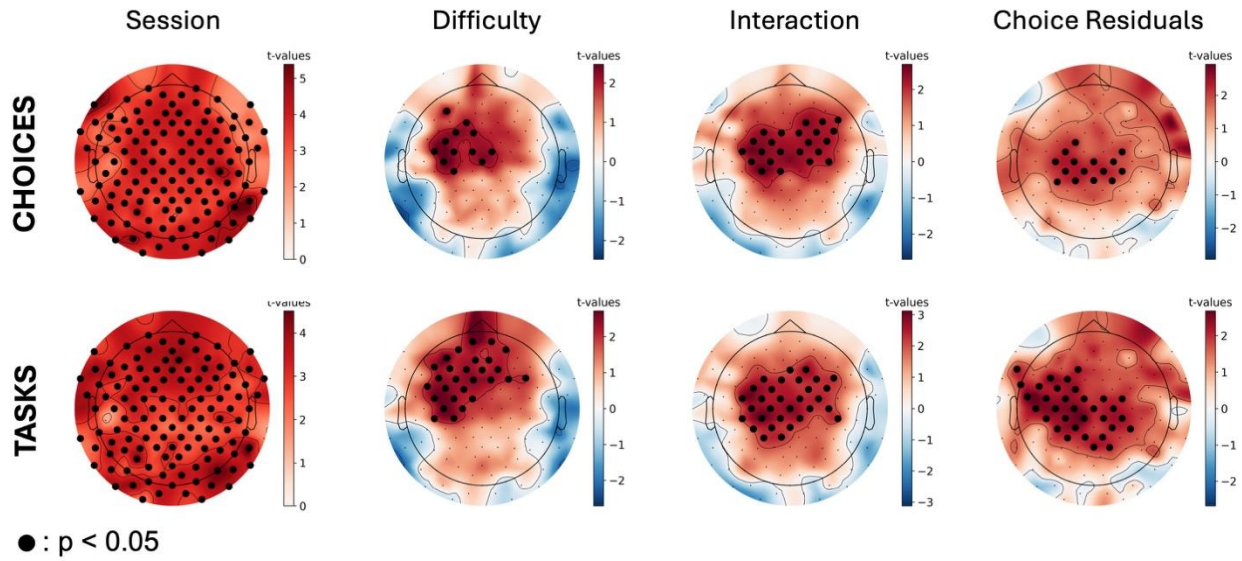

Figure S1.3. Scalp topographies of fatigue effects on slow wave density.

Scalp topographies show the distributions of color-coded t-values obtained for the following effects on slow wave density (from left to right): main effect of session (from 1 to 5), main effect of difficulty (easy vs. hard groups), group-by-session interaction and association with choice residuals (after removing the group-by-session interaction). Statistical tests were conducted separately for choice trials (top row) and task trials (bottom row). Significant channels are highlighted (big black dots).

Study 2
EEG Signature of Idiopathic Hypersomnia: Insights from Sleep Microarchitecture and Hypnodensity Metrics

In Review

Arthur Le Coz[1,2*#], Raphael Vollhardt[3,#], Pierre Champetier[1], Ruben Herzog[1], Smaranda Leu-Semenescu[3], Pauline Dodet[1,3], Valérie Attali[4,5], Ana Gales[3], Delphine Oudiette[1], Isabelle Arnulf[1,3,#], Thomas Andrillon[1,#*]

[1] Sorbonne Université, Institut du Cerveau - Paris Brain Institute - ICM, Inserm, CNRS, AP-HP, Hôpital de la Pitié Salpêtrière, Paris, France.

[2] Université Paris Cité, Paris, France.

[3] National Reference Center for Narcolepsies and Rare Hypersomnia, Sleep Clinic, DMU APPROCHES, Pitié-Salpêtrière Hospital, APHP- Sorbonne University, Paris, France

[4] AP-HP, Groupe Hospitalier Universitaire APHP-Sorbonne Université, Hôpital Pitié-Salpêtrière, Service des Pathologies du Sommeil (Département R3S), Paris, France

[5] Sorbonne Université, INSERM, UMRS1158 Neurophysiologie Respiratoire Expérimentale et Clinique, Paris, France

* Corresponding authors

# Equal contributions

2. 1. Digest

Idiopathic hypersomnia is characterized by excessive daytime sleepiness despite objectively sufficient or prolonged sleep. This paradox raises a central question for sleep research and fatigue science: how can extended, uninterrupted sleep fails to restore wakefulness? In this study, I explored whether neural alterations during sleep could account for the persistent daytime fatigue observed in IH. How does the macrostructure of sleep (hypnogram, hypnodensities) evolve in IH compared to controls? Are mesostructural features such as spectral power and infraslow dynamics altered? Does the microstructure of sleep (e.g., slow waves and spindles) show signs of abnormal homeostatic regulation or excessive stabilization? Finally, can a combination of these EEG markers support the identification of IH at the individual level? By addressing these questions in a large and homogeneous IH cohort, this study aims to clarify whether the roots of pathological fatigue in IH lie in subtle alterations of sleep dynamics or in impaired mechanisms of arousal.

2. 2. Study

Abstract

Background and Objectives: Patients with idiopathic hypersomnia with long sleep time (IH) report daytime hypersomnolence despite prolonged sleep time and normal sleep macrostructure. As they often have non-restorative sleep, we investigated whether the structure of their sleep is abnormal.

Methods: In polysomnography (PSG) recordings from 80 IH participants and 48 controls, we quantified hypnodensity metrics across the night (macro level), periodic and aperiodic spectral properties, infraslow fluctuations of sigma power within the night (meso level), slow waves, sleep spindles and their clustering (microstructure). Multivariate machine-learning models were used to classify IH vs. control sleep.

Results: Hypnodensity metrics were comparable between IH and controls, apart from more mixed wake/N1 sleep epochs in IH, and greater divergence between consecutive epochs of the same stage during NREM sleep in IH. Sigma power was increased in N2 sleep in IH and sleep spindles were more frequent and clustered. Slow wave density was also higher in IH. Higher average size of spindle cluster correlated with higher Epworth Sleepiness Scale scores. We leverage multivariate machine learning models to incorporate these features and achieved a balanced accuracy of 74% in distinguishing IH from controls.

Discussion: While spindles and slow waves are typically associated with good sleep quality, they are increased in IH patients. This could reflect higher need for sleep and increase the difficulty of awakening in IH, also marked by more mixed N1/waking stages.

Introduction

Idiopathic hypersomnia is a rare, chronic disorder of hypersomnolence, characterized by excessive daytime sleepiness despite normal or prolonged sleep duration. The disorder is often associated with i) a feeling of unrefreshing sleep, ii) marked difficulty in waking up – called sleep drunkenness or severe morning inertia – and iii) long unrefreshing naps (ICSD-3-TR, Sateia, 2014). The diagnostic framework requires demonstration of excessive daytime sleepiness in the absence of sleep debt or other explanatory conditions, as evidenced by a mean sleep latency test (MSLT) latency ≤8 minutes (and fewer than two sleep onsets in REM) and/or an excessive sleep need, as evidenced by a total sleep time greater than 11 hours/24 hours of PSG monitoring. Two forms of idiopathic hypersomnia have been described based on different symptoms, measures, and clustering analysis (Šonka et al., 2015). Idiopathic hypersomnia with long sleep time (IH) is considered as an independent, rare clinical entity and is closely associated with sleep time>11h on PSG. In contrast, idiopathic hypersomnia without long sleep time is evidenced exclusively with short MSLT latency, seems to closely resemble narcolepsy type 2, and is more frequent (1.5%) in epidemiologic studies (Billiard and Sonka, 2016; Fronczek et al., 2020; Gool et al., 2022; Plante et al., 2024). The cause of IH is unknown, but current hypotheses include a deficient arousal system (as in narcolepsy), a longer biological night (Lippert et al., 2014; Materna et al., 2018), the production of an endogenous hypnotic factor (Rye et al., 2012), or an abnormal sleep structure.

The diagnosis of IH requires that sleep duration is normal or prolonged and that sleep is not excessively fragmented. In a meta-analysis of 10 studies, participants with IH had increased total sleep time and REM sleep percentage, decreased sleep onset latency and N3 percentage, and similar sleep efficiency and REM sleep latency compared to controls (Plante et al., 2019). However, this meta-analysis mixed IH participants with and without long sleep time and included studies with low sample size. In another recent large study, longer sleep time, shorter sleep onset latency and higher percentage of REM sleep were confirmed in the IH group, while sleep efficiency was higher and N3 percentage was unchanged compared to controls (Evangelista et al., 2018). The arousal index was lower than in controls (Evangelista et al., 2018; Vernet and Arnulf, 2009). In conclusion, these studies suggest a longer and better consolidated sleep in IH, which contrasts with the complaint of excessive daytime sleepiness.

If the macrostructure of sleep is normal or even above normal, could an altered microstructure explain why sleep is not restorative in IH? Studies of microstructure in IH are scarce and yielded inconsistent results, potentially because they include heterogenous IH groups with small sample sizes and usually compare IH and narcolepsy type 1 rather than healthy sleepers. Quantitative EEG analyses led to mixed results, with slow wave activity either shown to be lower in IH (Pizza et al.,

2013; Sforza et al., 2000), or on the contrary higher with a faster dissipation during the night (Cairns and Bogan, 2019). Specifically, individuals with IH had a higher density of sleep spindles during N2 sleep than controls (Bové et al., 1994) and individuals with narcolepsy (Bové et al., 1994; Delrosso et al., 2014). The rate of cyclic alternating pattern (CAP, a marker of sleep instability) was lower in IH without long sleep time than in controls (Pizza et al., 2013). It is important to emphasize that these changes were typically subtle and tended toward better sleep in IH compared to narcolepsy type 1 and similar sleep microstructure between IH and controls.

Beyond the conventional sleep/wake classification and spectral EEG analysis, new fine-grained analyses of EEG signals have proven valuable in capturing subtle neural dynamics that better align with subjective assessments of sleep quality and quantity (Stephan and Siclari, 2023). First, hypnodensities constitute a probabilistic approach of sleep scoring, in contrast with the standard discrete sleep hypnograms. By computing the probability of the 5 different sleep stages (Wake, N1, N2, N3 and REM sleep) using an automatic sleep scoring algorithm (Herzog et al., 2025; Stephansen et al., 2018; Vallat and Walker, 2021), hypnodensities provide a good overview of hybrid sleep stages (i.e., epochs with a high probability of two or more sleep stages) and of the temporal variability of sleep stages (Herzog et al., 2025). Second, splitting the study of EEG dynamics between an aperiodic background activity and the (periodic) brain oscillations allows a more precise analysis of brain rhythms (Donoghue et al., 2020). Third, recent studies have stressed the importance of infraslow modulations of sleep dynamics, with a time period of approximately 50 seconds during stable NREM sleep (Osorio-Forero et al., 2025, 2021). These infraslow fluctuations structure the temporal organization of sleep hallmarks such as sleep spindles (Osorio-Forero et al., 2025), and reflect modulations of noradrenergic activity during NREM sleep. Examining infraslow oscillations or the temporal clustering of sleep spindles could offer a window onto the neuromodulation of sleep and the period favorable for stage transition and arousals (Foustoukos and Lüthi, 2025). These aspects might be very relevant for IH as patients experience enormous difficulty waking up from. Therefore, we aimed to determine whether these new approaches to PSG analyses could reveal differences in IH and provide a more comprehensive understanding of its pathophysiology in a large, homogeneous group of participants with IH and controls. Our methodology included analyses of the macrostructure (hypnogram and hypnodensities), the mesostructure (power spectral density, periodic analysis, infra-slow activity), and the microstructure of sleep (slow waves, sleep spindles and their clustering). Lastly, we combined all EEG features extracted to classify IH vs. control sleep recordings using automated machine learning algorithms.

Participants

Participants with Idiopathic Hypersomnia

This is a retrospective study of clinical and PSG data collected in the Pitié-Salpêtrière Sleep Clinic, -a National Reference Centre for Narcolepsies and Rare Hypersomnias-, between July 2015 and February 2023 as part of the clinical diagnostic of IH. Criteria of inclusion for IH patients comprised: age > 18 years old, and diagnosis of IH as defined by international criteria: Patient had to experience daily irresistible urges to sleep or daytime sleep episodes for at least three months, without any presence of cataplexy. Polysomnography and the MSLT should not support a diagnosis of narcolepsy type 1 or 2 (Sateia, 2014). At least one of the following conditions had to be met: the MSLT showed a mean sleep latency of less than or equal to 8 minutes, or the total sleep time over 24 hours was greater than or equal to 660 minutes, as measured by a 24-hour polysomnographic recording on night 2 and day 3. All patients had a standardized 48-hour sleep recording protocol, which included a first night of sleep with a 8-hour sleep opportunity window (night 1), followed by a MSLT with 5 nap opportunities (day 2), a second night and day of unrestricted sleep (*ad libitum*, night 2 and day 3 with two unlimited naps, stopped at 4 pm), which allowed measurement of unrestricted sleep time over a period of 18 hours (Arnulf et al., 2022; Vernet and Arnulf, 2009). Only the first night of sleep was analyzed in the present study. The diagnosis of IH was excluded if hypersomnolence or MSLT results were better explained by other sleep disorders, medical or psychiatric conditions, or the use of drugs or medications. Individuals were tested without sleep restriction to exclude a prolonged sleep duration due to chronic sleep deprivation, as confirmed by their sleep diary. Following international recommendations for MSLT, psychotropic medications, if present, were withdrawn for at least five half-lives for wake-enhancing drugs and stimulants, and at least three months for benzodiazepines, neuroleptics, antiepileptics, or antidepressants. This allowed to eliminate the effects of metabolites with long half-life (especially antidepressants) and potential rebound phenomena. For this study, only patients with IH with long sleep time (total sleep time >660 min/18h) were analyzed (N = 80).

Control Group

We retrospectively analyzed polysomnographic data of the control group from two datasets. The first dataset consisted of healthy individuals who participated in a study of the effects of verbal violence on sleep (ethics committee-approved study, clinicaltrial.gov reference: NCT03074578). These controls spent two nights in the sleep clinic, but we analyzed only the first (baseline) night, which was obtained under the same conditions as night 1 of the 48-hour protocol of the IH patients.

The second data set consisted of young adults who were referred to the sleep clinic for a systematic screening for sleep apnea syndrome during the preoperative evaluation of facial dysmorphia. As part of their evaluation, they underwent one night of PSG under the same conditions as night 1 of the 48-hour protocol. Participants with a sleep time lower than 360 min, a sleep efficiency lower than 75%, a periodic leg movement index greater than 15 and an apnea-hypopnea index greater than 10 were excluded. All participants underwent a medical interview with a sleep specialist to determine the absence of any medical, sleep, or psychological complaints. Only individuals not taking any psychotropic medications or drugs were selected. Other exclusion criteria included the presence of another sleep disorder (e.g., parasomnias, all polysomnograms include a video-audio recording that is analyzed by the physician, or restless legs syndrome), comorbid neurological or psychiatric disorders, moderate to severe depressive symptoms, sleep debt prior to sleep testing as assessed by sleep diary, interview, or current or past night or shift work. For this study, n = 48 controls were analyzed.

Ethics

Patients and preoperative control participants did not object to the anonymous reuse of their clinical and polysomnographic data for future research, as documented in their medical records, collected as part of their routine care and stored in a database declared to the National Commission for Data Protection and Liberties, in accordance with French law. Healthy controls were recruited from individuals who attended the sleep clinic as part of an ethics committee-approved research protocol and provided written informed consent, including permission for the anonymized reuse of their data.

Clinical measures

An experienced neurologist collected detailed information from the medical records of both patients and controls. These records included data obtained during a face-to-face interview with a sleep specialist, results from clinical scales, and a systematic self-report questionnaire completed upon entry to the sleep laboratory. The collected information covered: age, sex, body mass index, usual sleep and wake times during weekdays and weekends, presence of daily naps, occurrences of sleep drunkenness, sleep attacks, hypnagogic hallucinations, and sleep paralysis. Additionally, data on Epworth Sleepiness Scale scores at the time of the PSG, ongoing treatments, recreational drug use, depressive symptoms, and comorbid sleep, medical, neurological, and mental disorders were recorded.

Polysomnography

The PSG was conducted following the American Academy of Sleep Medicine (AASM) guidelines (Troester et al., 2023). The EEG montage included three electrodes at frontal (F3), central (C3), and occipital (O1) sites, contralateral mastoid (A2), and a ground channel on the forehead. Additional channels included left and right electrooculography and surface electromyography from the chin muscle and left and right tibialis anterior muscles. These channels were recorded at a minimum sampling frequency of 256Hz using a Grael amplifier (Compumedics Ltd, Australia). Cardiorespiratory measures included nasal pressure, nasal-oral thermistor airflow, tracheal sound sensor, thoracic and abdominal respiratory inductance plethysmography, position sensor, pulse oximetry, and electrocardiographic DII derivation. All recordings featured infrared video monitoring and ambient room sound recording. Sleep stages, micro-arousals, respiratory and motor events were scored on 30s epochs by certified sleep specialists according to the AASM manual version 2.4 (Berry et al., 2017), using Profusion Sleep 4 software (*Compumedics Ltd, Australia*).

Data Analysis

Preprocessing

We analyzed the EEG (F3, C3, and O1), electromyography (EMG, chin derivation), and electro-oculography (EOG) channels. All channels were resampled to a common sampling rate of 256 Hz. To minimize the impact of electrical noise, data were notch-filtered at 50 Hz and 100 Hz using a zero-phase notch filter. A zero-phase finite impulse response (FIR) band-pass filter was then applied to retain frequencies between 0.5 and 40 Hz. The EEG signals were re-referenced to the opposite mastoid (A2) electrode, providing a common reference point across recordings.

Automated Sleep Staging Algorithm and Extraction of Hypnodensity

Traditional sleep scoring by human experts is the gold-standard method for the identification of the different sleep stages. However, scoring is discrete and can vary between individual scorers (Nikkonen et al., 2024; Norman et al., 2000). The YASA package (Vallat and Walker, 2021) was used here for the automated sleep staging but other existing algorithms could be used (see(Hanif et al., n.d.) for a benchmark). For each 30s-epoch, the YASA algorithm computes a probability of each stage (wake, N1, N2, N3 and REM sleep), providing both hypnodensities (graded evaluation of sleep stages, Stephansen et al., 2018; Vallat and Walker, 2021) and a standard hypnogram (by selecting the stage with the highest probability for each epoch). To evaluate the agreement between expert sleep scoring and YASA's automated scoring, we computed Cohen's kappa using the scikit-learn package (Pedregosa et al., 2011). We also computed confusion matrices to compare the expert and automated sleep scoring.

Intrusions and Variability

To characterize sleep dynamics, we employed two information theory measures: entropy (H) and Kullback-Leibler divergence (D_{KL}) (Cover and Thomas, 2005). These metrics were computed at the epoch level based on the distribution of hypnodensities (probability of Wake, N1, N2, N3 and REM) to quantify the scoring ambiguity (which can be due to stage mixing , Huijben et al., 2023) and epoch-to-epoch variability, respectively. To maximize the interpretability of hypnodensities, and the derived metrics, we analyzed in conjonction with human expert scoring.

Entropy (H) measures the uncertainty associated with a probability distribution:

$$H(x) = -\sum_{i \in \Omega} p_i \log_2(p_i)$$

Where x represents a given epoch, Ω represents the five possible stages (wake, N1, N2, N3, REM sleep), and p_i is the probability of each stage. Higher entropy indicates greater stage ambiguity, potentially reflecting intrusions from other stages.

To measure variability between consecutive epochs, we used D_{KL}. For two probability distributions P(x) and Q(x) (i.e., the hypnodensity of two consecutive epochs) the D_{KL} follows:

$$D_{KL}(P \parallel Q) = \sum_{i \in \Omega} p_i \log_2\left(\frac{p_i}{q_i}\right)$$

Where p_i and q_i is the probability of the stage i for the P and Q hypnodensity, respectively

A D_{KL} of zero indicates minimal variability (identical distributions), while higher values suggest greater differences between epochs in the distribution of hypnodensities. To examine the epoch-to-epoch variability of sleep stages above and beyond stage transitions, D_{KL} was computed only on consecutive epochs of the same sleep stage according to the automated sleep scoring.

Spectral Analysis

Spectral analyses were performed on raw EEG data using the MNE-Python library (Gramfort et al., 2013). We excluded wake periods before and after the night sleep ("lights out" period), as well as epochs containing micro-arousals. Power Spectral Density (PSD) was computed for channels F3, C3, and O1 on each epoch using the Welch method with a Hamming window (0.5-40 Hz frequency range, 1024-point Fast Fourier Transform (FFT) with 50% overlap). The PSD of the EEG signal can be decomposed into its periodic and aperiodic components (Donoghue et al., 2020). The periodic component is thought to reflect brain oscillations (e.g., alpha oscillations, sleep spindles), and the aperiodic component the non-oscillatory background activity. We used the FOOOF package (Donoghue et al., 2020) to model these periodic and aperiodic components with fixed aperiodic

mode and peak width limits set to (0.5, 4) Hz. Before fitting FOOOF, we applied locally weighted scatterplot smoothing (LOWESS, span=0.075) to the PSD of each epoch to improve the robustness of the fit.

The aperiodic component follows a power law:

$$P_{aperiodic}(f) = \beta \cdot f^{-\alpha}$$

Where $P_{aperiodic}(f)$ is the aperiodic power for a given frequency f, α is the exponent of the power law, and β the offset. Subtracting the fitted aperiodic activity to the original PSD allowed to estimate the periodic power:

$$P_{periodic}(f) = \mathrm{PSD}(f) - \beta \cdot f^{-\alpha}$$

Absolute and relative periodic band power were computed for five frequency bands: delta (1–4 Hz), theta (4–8 Hz), alpha (8–12 Hz), sigma (12–16 Hz), and beta (16–30 Hz). For each 30s epoch, absolute band power was estimated by integrating the power spectral density within each frequency range in the periodic power spectrum. Relative band power was then computed by normalizing each band's absolute power by the total power across all bands. All band power values were log-transformed to approximate a normal distribution.

Sleep Spindle and Slow Wave Automatic Detection

Sleep spindles and slow waves were automatically detected using custom Python scripts incorporating the MNE (Gramfort et al., 2013) and YASA (Vallat and Walker, 2021) packages. For both spindles and slow waves, event density was calculated as the number of detected events within each sleep stage, divided by the total duration of that stage. To exclude wake periods unrepresentative of resting states, the analysis excluded wake epochs before and after sleep (lights-out and final awakening).

Slow waves were identified in all sleep stages, following a two-step preprocessing pipeline. First, EEG signals were down-sampled to 100 Hz and filtered using a zero-phase finite impulse response (FIR) band-pass filter (0.5–8 Hz) with automatically determined transition bandwidths, ensuring minimal edge artifacts while preserving waveform integrity. The filtered signal was then analyzed to identify negative and positive zero-crossings, which were used to segment potential slow waves. For each candidate wave, we computed the peak-to-peak (PTP) amplitude, that is the amplitude difference between the most positive and most negative peak between the start and end of the wave (consecutive zero-crossings). We then selected high-amplitude slow waves based on this PTP amplitude, which had to exceed a data-driven threshold, estimated for each channel and each participant. To compute this threshold, we fitted an exponentially modified Gaussian distribution (Ex-Gaussian) distribution to the distribution of PTP amplitudes for this channel, session and

participant (scipy.stats, Virtanen et al., 2020). This Ex-Gaussian fit provided 3 parameters: the mean (μ) and standard deviation (σ) of the Gaussian component and the Exponential tail (τ). To capture the tail of the Ex-Gaussian distribution, we defined the PTP threshold as twice the amplitude of the peak of the Ex-Gaussian. In N2 sleep and REM sleep, waves with PTP < 150μV were retained, while in N3 sleep, a higher threshold of 250μV was used to accommodate the larger amplitude of slow waves in N3 sleep. For each slow wave, we further extracted the following parameters: (1) Maximal negative slope (descending phase), representing the voltage decline (in μV/s) between the first negative zero-crossing and the negative peak crossing divided by the duration between the negative zero-crossing and the negative peak (in seconds); and (2) Maximal positive slope (ascending phase), reflecting the voltage increase between the negative peak and the subsequent positive zero-crossing divided by the duration between the peak and the positive zero-crossing (in seconds). Only waves with a descending and ascending slope between 0.25 and 2 μV/s were retained, ensuring the selection of physiologically meaningful slow waves. Slow waves were detected in each 30s epoch for EEG channels F3, C3, and O1, and stored for further analysis. Finally, slow wave density was defined as the number of slow waves per epoch of a given sleep stage.

Sleep spindles were identified in N2 sleep and N3 sleep using the YASA spindle detection algorithm (Vallat and Walker, 2021), which applies both time-domain and frequency-domain criteria. EEG signals were first filtered between 12 and 15 Hz using a zero-phase FIR band-pass filter with a 1.5 Hz transition bandwidth on each side, ensuring that the -6 dB cutoff points were at 11.25 Hz and 15.75 Hz. To enhance specificity, spindles were detected within a broadband range of 1–30 Hz, which allowed for the computation of relative spectral power. Detected spindles were required to meet the three following morphological and spectral thresholds. First, duration constraint: events had to last between 0.5 and 2.5 seconds. Second, minimum inter-spindle interval: spindles occurring less than 500ms apart were merged into a single event. Third, two signal-based thresholds: (i) Root Mean Square (RMS) threshold, where spindles had to exceed 1.5 standard deviations above the mean RMS of the 12–15 Hz filtered signal; (ii) Moving correlation threshold, requiring a correlation of ≥ 0.65 between the broadband and spindle-band filtered signals. Spindles were further characterized based on their PTP amplitude (μV), RMS power (μV), absolute power (log-transformed μV^2), relative power (proportion of power in the spindle band relative to broadband), frequency (Hz), number of oscillations (count of positive peaks per event), and symmetry (location of the most prominent peak within the spindle, normalized between 0 = start and 1 = end).

Additionally, spindle clusters were analyzed using custom Python scripts. Clusters were defined as contiguous spindles separated by ≤6 s. Cluster size was defined as the number of spindles in

each bout. Inter-cluster interval was computed as the time difference between the last spindle of a cluster and the first spindle of the subsequent bout, with temporal distances ≥300 s discarded. For each subject and channel, total spindle counts and the percentage of clusters for sizes 1–5 (with clusters ≥5 aggregated as "5") were calculated.

Infraslow Rhythms

We adapted our analysis of fast spindle band power fluctuations from the literature (Champetier et al., 2023; Lecci et al., 2017). Briefly, for each participant, we selected consecutive 120-s periods of artifact-free N2 and N3 sleep. Time–frequency power was computed in 100-ms bins with 0.2 Hz steps using a continuous wavelet transform with Morlet wavelets (four-cycle length). The resulting power time courses were smoothed with a symmetric 4-s moving average and normalized to the average absolute power in the sigma band (12 to 16 Hz) across all NREM sleep epochs. For each bout, power spectra in the 0.5–24 Hz range were computed every 0.1 s in steps of 0.2 Hz using a four-cycle Morlet wavelet transform, and the average power in conventional frequency bands (including the sigma band, 11–16 Hz) was determined. These power time courses were then smoothed using a 4-s symmetric moving average to highlight infraslow periodicities and normalized using the average absolute power computed over all N2 and N3 sleep epochs during the night. Finally, the spectral profiles of these power time courses were obtained via a continuous wavelet analysis in the 0.001–0.12 Hz range (with 0.001 Hz resolution) and averaged across bouts weighted by their duration.

Machine Learning Algorithm

We used machine learning models both for classifying the PSG of IH participants vs controls, and to regress sleep parameters based on EEG-derived features. To enhance interpretability and reduce noise in our high-dimensional EEG dataset, we applied a feature selection procedure based on the Minimum Redundancy Maximum Relevance (MRMR) algorithm (Ding and Peng, 2003). For both classification and regression tasks, MRMR ranked the 26 EEG features by evaluating their relevance—using a random forest performance metric—and penalizing redundancy, which was quantified as the mean correlation with all other features (see Supplemental Table 1 for the list of features used). Features were then progressively incorporated into the prediction models according to their MRMR ranking. For each subset, cross-validated (5-fold validation scheme) performance was computed (balanced accuracy and confusion matrices for classification and root-mean-square error (RMSE) for regression). The optimal feature subset was determined as the smallest set beyond which additional features did not yield statistically significant performance improvements (assessed via a Wilcoxon rank-sum test). For classification, MRMR followed by repeated cross-validated modelling on both the full sample (n=128; 48 CT, 80 IH) and

a balanced subsample obtained by bootstrapping the IH group 30 times. All classification and regression analyses were conducted using the XGBoost algorithm (Chen and Guestrin, 2016), which builds a series of decision trees in a boosting framework, offering strong performance and robustness in high-dimensional datasets. For diagnostic group classification, we employed a softprob objective function with logloss as the evaluation metric, a learning rate of 0.1, a maximum tree depth of 3, 80% subsampling for both subjects and features, and a gamma regularization parameter of 0.1. In regression tasks aimed at predicting continuous sleep quality metrics (e.g., sleep efficiency, total sleep time, wake after sleep onset), the objective function was set to minimize RMSE while retaining the same parameter settings. Model performance was rigorously evaluated using a repeated 5-fold cross-validation procedure (typically 60 training-testing iterations). In each iteration, data were partitioned into five balanced and stratified folds, with the model trained on four folds and validated on the remaining fold. This systematic procedure ensured that performance metrics—including balanced accuracy for classification and RMSE for regression—were robust and generalizable across the dataset.

Statistics

We employed linear mixed-effects models to analyze sleep-related metrics, using the *statistical models* package in Python (Seabold and Perktold, 2010). These models were designed to account for individual variability by including random effects based on subject identifiers. The linear mixed effects statistics were used on several EEG features including slow waves density, sleep spindle density, hypnodensities features (entropy, D_{KL}, distribution), and scoring confusion matrices. These features were computed at the level of each epoch and averaged across epochs of a given sleep stage or directly computed for a given sleep stage. For each metric, the models included fixed effects for age and gender and interactions between sleep stage, group, and channel, where applicable. To ensure the robustness of our findings, we applied the false discovery rate (FDR) method to correct for multiple comparisons(Benjamini and Hochberg, 1995). However, for the power analysis, where p-values were computed for each frequency bin (0.25 Hz bin), we employed a cluster-based multiple comparison correction, which better accounts for the inherent spectral structure by identifying significant clusters of adjacent frequencies (Maris and Oostenveld, 2007). Additionally, demographic characteristics were analyzed using non-parametric tests, including the Mann-Whitney U test and Chi-squared test, to compare groups on variables such as age, body mass index, and scores at the Epworth sleepiness scale.

Data Availability

The anonymized data of this study are available from the corresponding author on reasonable request.

Clinical and Sleep Characteristics of the Groups

Of the 384 patients diagnosed with idiopathic hypersomnia during the study period, 289 were excluded because they had an idiopathic hypersomnia without long sleep time, were taking a psychotropic treatment (N = 123) or an illicit substance (N = 4), had moderate to severe depressive symptoms (N = 95), had a comorbid sleep, neurological, medical or psychiatric disorder (N = 141), slept less than 360 minutes on night 1 and/or had a sleep efficiency of less than 75% (N = 38), and/or their PSG was not accessible (N = 1). Thus, 80 participants with IH (with long sleep time) and 48 control participants were included in the analysis (Table 1). The total sleep time was longer than 11h/18h of recording in all 80 patients with IH including a total sleep time of 626.4 ± 102.9 min during night 2 and 715.5 ± 78.5 min during 18h recording. The mean MSLT latency was 11 ± 4.5 min in the IH group, and 21/80 (26.3%) participants had an MSLT latency ≤ 8 min. The prevalence of females was higher in the IH group than in the control group, but age and body mass index did not differ between groups. As expected from the characteristics of IH, usual weekday and weekend sleep times were longer in the IH than in the control group, and IH participants were more likely than controls to report sleep drunkenness, sleep attacks, daily naps, hypnagogic hallucinations and sleep paralysis. The Epworth sleepiness scale score was higher in the IH group than in the control group. During the first night of PSG (which was stopped at 6:30 AM in all groups), IH had higher sleep efficiency and N3 percentage, but lower wake after sleep onset and REM percentage compared to controls. The other measures, including sleep latencies, total sleep time, N1 and N2 percentage, as well as arousal index, periodic leg movement index and apnea-hypopnea index did not differ between groups.

Automated Sleep Staging and Hypnodensities

The hypnogram was computed with the YASA algorithm and compared to the expert scoring. There was a good overall agreement (**κ** = 0.693 ± 0.009 – **Supplemental Figure 2.1**) even if the YASA algorithm had not been trained on IH data (Vallat and Walker, 2021). The agreement between expert and YASA scoring for REM sleep was higher in the IH group than in the control group (**Figure 2.1b**, ß = 0.054, p = 0.006), indicating more accurate automated detection of REM in IH patients. The entropy values of hypnodensities did not differ between groups. The epoch-to-epoch variability in these distributions, assessed by D_{KL} showed a higher variability in the IH group (larger D_{KL}) than in control group during N1 sleep (β = 0.041, p = 0.043), N2 sleep (β = 0.043, p = 0.042), and N3 sleep (β = 0.046, p = 0.042) epochs (**Figure 2.1d**). The hypnodensity-derived probability distributions of automated vs. traditional expert sleep scoring had similar profiles in

IH and control groups (**Supplemental Figure 2.1b**). This suggests that hybrid sleep states—where features of multiple sleep stages overlap—were as prevalent in participants with IH as in controls.

Table 1: Demographic, clinical and sleep measures in participants with idiopathic hypersomnia with long sleep time and controls.

Participants	Idiopathic hypersomnia	Controls	Effect size	p
Demographic and clinical information				
Number of women/men (%)	64 /80 (80)	23/48 (48)	12.75	< 0.001
Age, years	26.5 ± 7.1	29.8 ± 9.7	1617.5	0.14
Body mass index, kg/m^2	23.9 ± 5.3	21.9 ± 3.0	2137.5	0.09
Epworth sleepiness score, 0-24	15.7 ± 3.9	5.9 ± 3.0	3015.0	< 0.001
Usual sleep time during weekdays, min	570.1 ± 112.3 (N=77)	453.4 ± 10.0 (N=44)	2857.0	< 0.001
Usual sleep time during weekend, min	731.4 ± 122.4 (N=77)	501.1 ± 12.0 (N=44)	3244.0	< 0.001
Sleep drunkenness, N (%)	58/76 (76.3)	1/36 (2.8)	50.1	< 0.001
Regular daily naps, N (%)	49/78 (62.8)	6/32 (18.8)	15.9	< 0.001
Sleep attacks, N (%)	40/65 (62)	0/25 (0)	25.26	< 0.001
Hypnagogic hallucinations, N (%)	16/70 (23)	1/11 (9)	0.41	0.52
Sleep paralysis, N (%)	11/69 (17)	2/11 (18)	0	1.00
Sleep measures during night 1				
Sleep onset latency, min	18.1 ± 19.2	27.3 ± 36.2	1626.5	0.15
REM sleep latency, min	110.6 ± 62.6	94.5 ± 48.4	2286.0	0.07
Sleep efficiency, %	93.0 ± 4.9	90.9 ± 5.7	2347.5	0.04
Wake after sleep onset, min	32.1 ± 37.6	55.4 ± 35.3	1090.5	< 0.001
Total sleep time, min	456.1 ± 23.3	459.0 ± 54.2	1876.5	0.83
Sleep stages (% of total sleep time)				
N1	2.8 ± 2.5	2.3 ± 2.0	2134.5	0.29
N2	50.3 ± 9.3	53.3 ± 6.3	1582.0	0.10
N3	26.3 ± 9.0	21.5 ± 6.5	2515.0	0.003
REM	20.7 ± 4.9	22.4 ± 5.3	1506.0	0.042
Events/ h of sleep (index)				
Arousals	7.2 ± 4.7	8.2 ± 4.7	1645.5	0.18
Periodic leg movements	1.6 ± 2.8	1.2 ± 3.2	2305.0	0.02
Apnea-hypopnea	1.0 ± 1.4	1.5 ± 1.9	1706.5	0.29

Measures are mean ± standard deviation or N (%)

However, using the YASA scoring as a reference (**Supplemental Figure 2.1a**), the participants with IH have a lower probability of scoring wake during wake (0.78 < 0.82, ß = -0.0375, p = 0.0004) and a higher probability to score N1 sleep during wake (0.15 > 0.12, ß = 0.026, p = 0.00995) than controls. During N3 sleep, there was a higher probability for YASA to score N3 in participants with IH than in controls (0.85 > 0.84, ß = 0.016, p = 0.037).

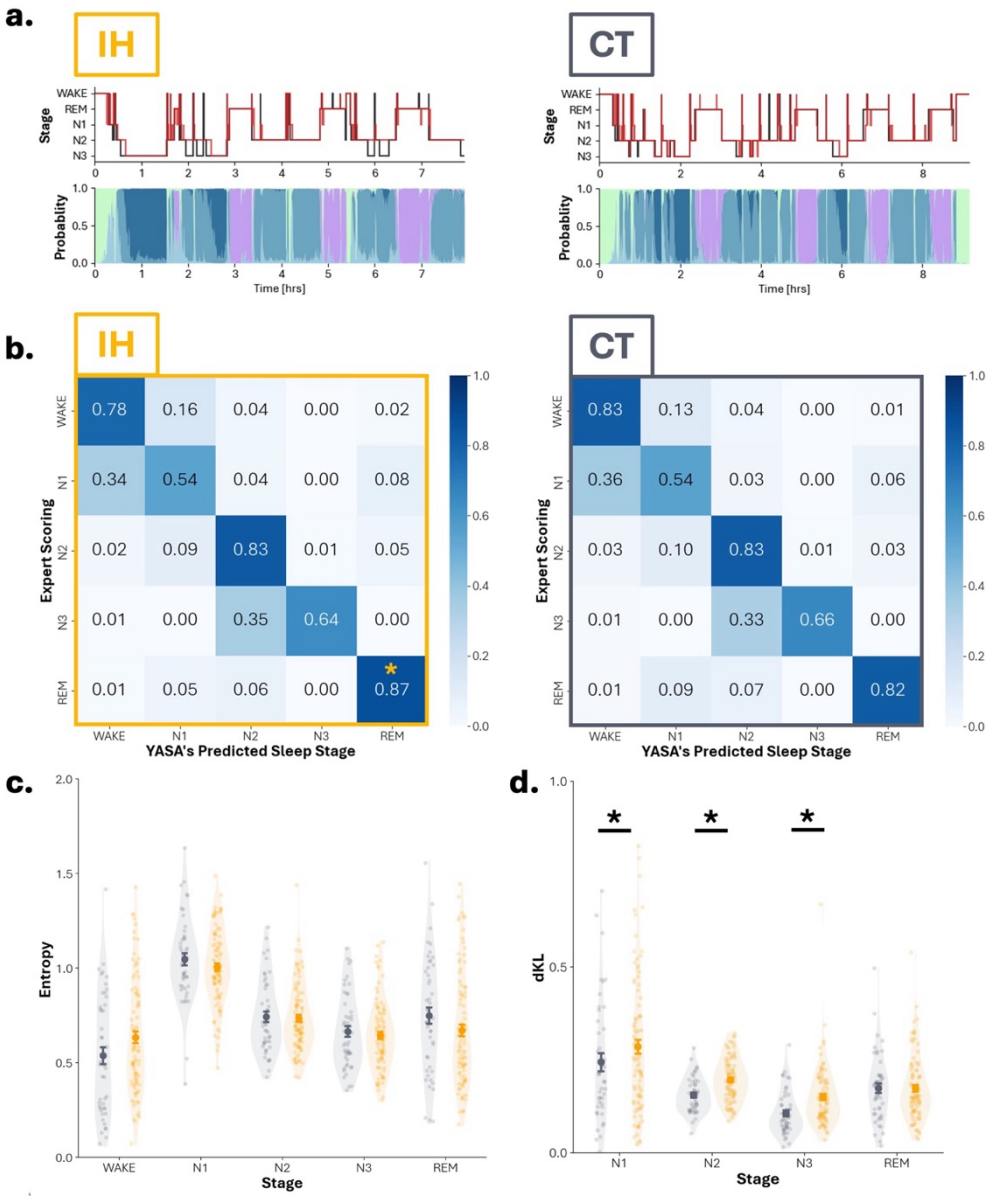

Figure 2.1: Participants with idiopathic hypersomnia do not have hybrid sleep states. a On the top row, hypnogram from experts scoring (black), and YASA scoring (red). On the bottom row, hypnodensities obtained with YASA in participants with IH (left panel) and controls (right panel). **b** Confusion matrices (experts vs YASA scoring). **c** Entropy (H) and epoch-to-epoch variability (DKL) extracted on YASA's hypnodensity in the different sleep stages, participants with IH (yellow) and controls (grey). Statistics: linear mixed models with age and gender as covariate, correction for multiple comparisons (false discovery rate), p < 0.05: *, p < 0.01: **, p < 0.001: ***.

Periodic Sigma Power

When comparing the EEG dynamics between groups, including the periodic and aperiodic power across sleep stages, there was an increase in the periodic power within the sigma band over the occipital (cluster: [12.5-17]Hz, $p_{CLUSTER}<0.001$) and central electrode (cluster: [12.5-15.75]Hz, $p_{CLUSTER}<0.001$) in N2 sleep in the IH group compared to the control group (**Figure 2.2b**). A similar increase of the frequency comprised between 12 and 18 Hz (which include the sigma band) was found in N1 sleep in all electrodes in the IH group compared to the control group (supplementary, **Figure 2.3b** $p < 0.001$). Other metrics of the periodic and aperiodic PSD did not differ between groups.

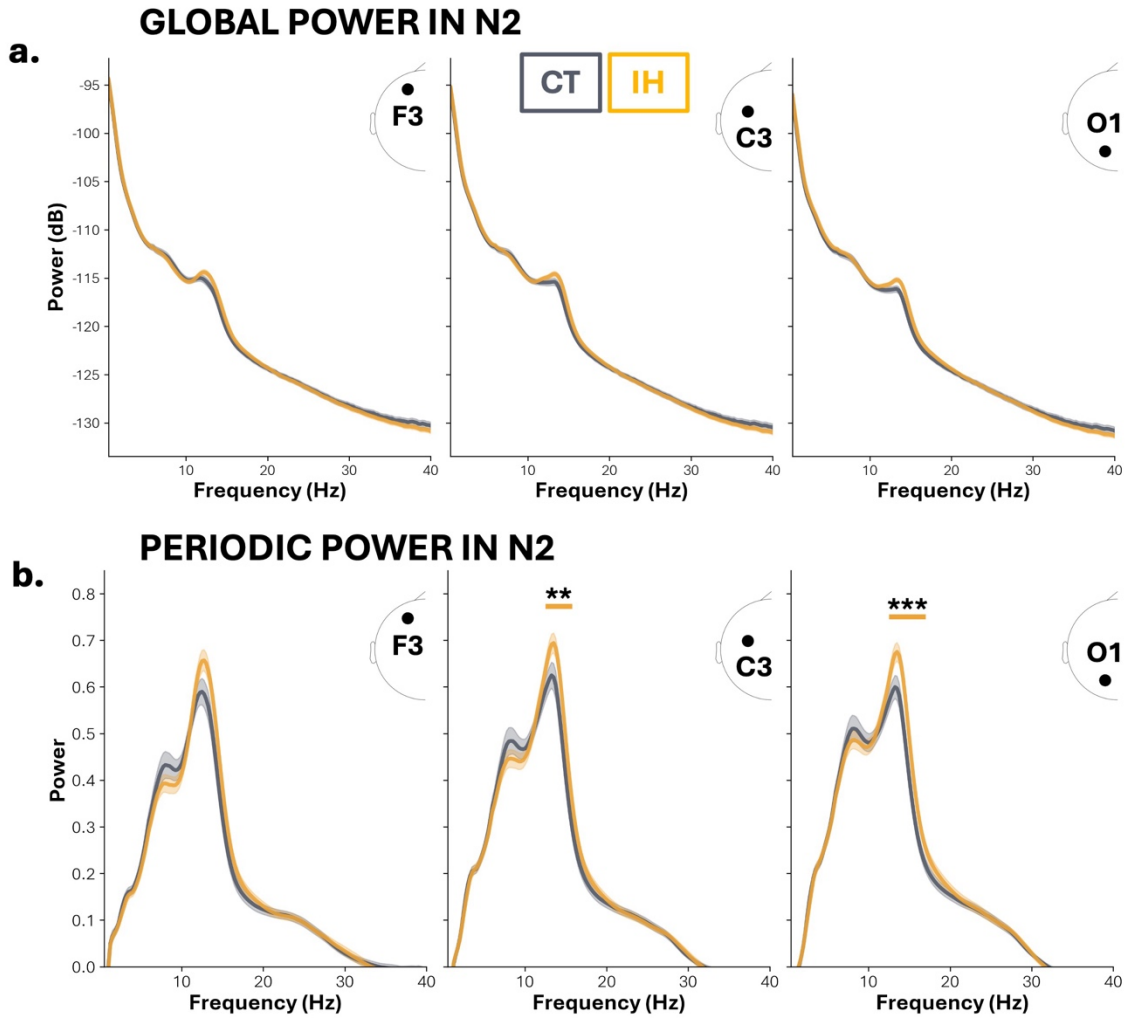

Figure 2.2: Participants with idiopathic hypersomnia have a higher power in the sigma band than controls. a Global, and **b** periodic power during N2 sleep, at channel F3, C3, and O1 (left, middle, and right respectively) in participants with idiopathic hypersomnia (yellow) compared to controls (grey). The yellow bar above the PSD in b at C3 and O1 indicates statistical differences. Statistics: linear mixed models with age and gender as covariate corrected with cluster-based multiple comparisons, $p_{CLUSTER} < 0.05$: *, $p_{CLUSTER} < 0.01$: **, $p_{CLUSTER} < 0.001$: ***. Shadings show the standard-error-of-the-mean (SEM) across participants.

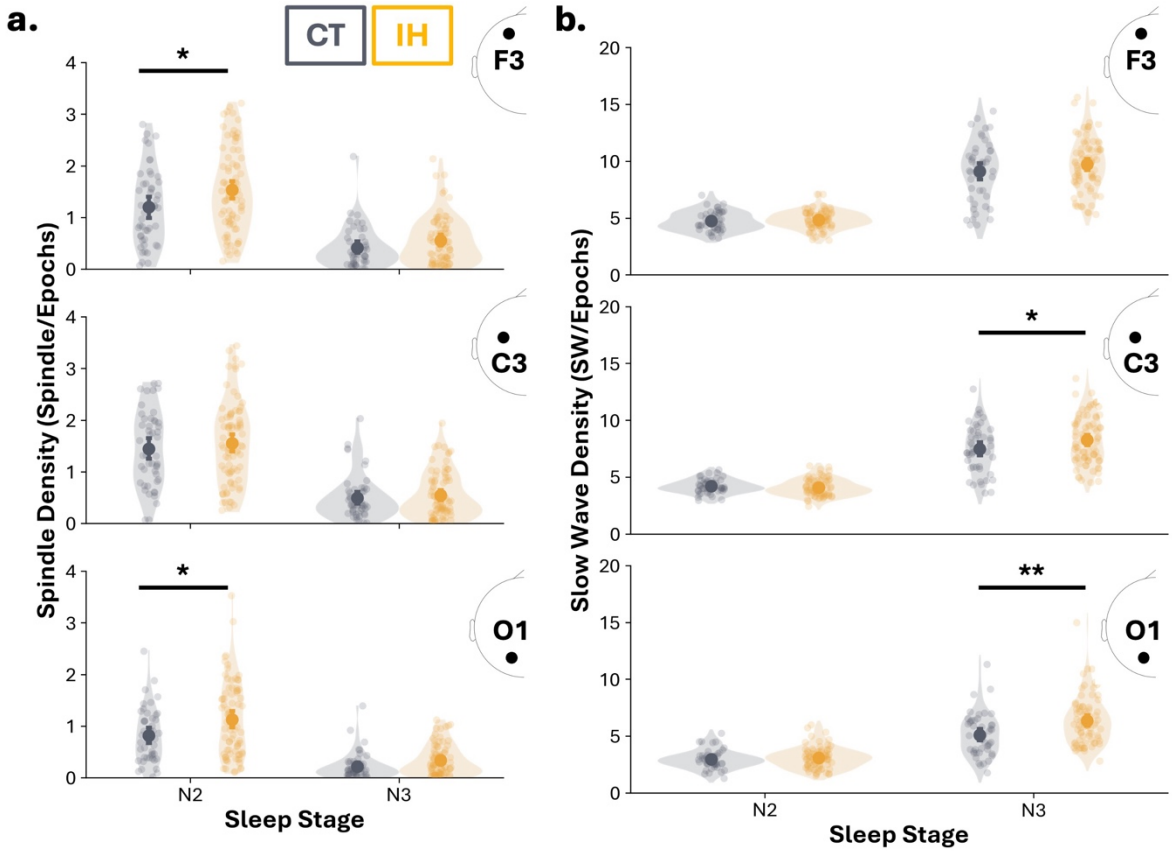

Figure 2.3: Sleep spindle and slow wave density were higher in IH in N2 and N3. a Sleep spindles density (number of sleep spindles divided by the number of epochs in a given sleep stage) in N2 and N3 for the IH (yellow) and control (grey) group. Small dots show individual data and large dots the population average. Error bars denote the standard error of the mean (SEM). **b** Slow wave density (number of slow waves divided by the number of epochs in a given sleep stage) in N2 and N3. F3 electrode on the top row, C3 in the middle, and O1 at the bottom. Statistics: linear mixed models with age and gender as covariate, with correction for multiple comparisons (false discovery rate), $p < 0.05$: *, $p < 0.01$: **, $p < 0.001$: ***.

Spindle and Slow Wave Density

The increase in power in the sigma band was also reflected in the detection of sleep spindles: there was an increase in sleep spindle density in N2 sleep at the frontal (ß = 0.342, p = 0.008) and occipital electrodes (ß = 0.321, p = 0.008) in the IH group compared to control group (**Figure 2.3a**). There was an increase in slow waves in N3 sleep in the central (ß = 0.713, p = 0.047), and occipital electrode (ß = 1.165, p < 0.001) in the IH group compared to the control group (**Figure 2.3b**). The analysis of spindle clustering indicated that at F3 and O1, isolated spindles (cluster size = 1) were less frequent in the IH group than in the control group (**Figure 2.4a**, ß = -0.045, p < 0.001, and **Supplemental Figure 2.4a**, ß = -0.040, p < 0.001). At F3, pairs of spindles were more frequent in the IH group than in the control group (**Figure 2.4a**, ß = 0.026, p = 0.039). There was no group difference for clusters of sizes three, four, and above five spindles.

The results showed a non-significant higher average cluster size in IH group than in control group at F3 and O1 (**Figure 2.4b**, ß = 0.084, p = 0.55; ß = 0.071; p = 0.069 respectively). A linear regression

analysis was conducted to examine the association between average spindle cluster size and Epworth sleepiness scale scores, controlling for age and gender. Higher average cluster sizes were associated with higher sleepiness scores at F3 and O1 (**Figure 2.4c**, ß = 6.88, SE = 2.84, t = 2.42, p = 0.011; ß = 8.13, SE = 3.48, t = 2.34, p = 0.011 respectively), with the model accounting for 12.5%, and 15% of the variance in sleepiness scores. The spindle cluster size in the IH participants with and without sleep drunkenness was similar (**Supplemental Figure 2.4a**, ß = 0.017, p = 0.720). We replicated previous findings showing an infraslow modulation (0.018 Hz) of the sigma power for F3, C3, and O1 electrodes (**Figure 2.5**). However, there was no differences between the IH group and the control group in any electrode (all $p_{CLUSTER} > 0.05$).

Prediction of Idiopathic Hypersomnia Diagnosis via Sleep Metrics

Multivariate EEG -based models were developed to classify groups and predict a range of sleep quality metrics. As shown in **Figure 2.6a** (left panel), the area under the curve increased with the number of features, reaching a peak of approximately 0.81 for 11 features for the full sample and 0.74 for the balanced sample with 13 features (**Supplementary Table 2**). The red marker in **Figure 2.6a** indicates the optimal feature set (feature names in supplementary Table 2), while the accompanying confusion matrices (**Figure 2.6a**, middle and right panels) revealed that correct classification rates in the balanced dataset were significantly above chance-level (50%) but remained modest— 69% for the control group and 64% for the IH group (**Figure 2.6a**, left panel). For the regression analyses, separate models were constructed to predict objective sleep measures (wake time after sleep onset and sleep efficiency), subjective sleep metrics (sleep duration during the weekend and score at the Epworth sleepiness scale), as well as total sleep time measured on night 2 and over 18 hours. In each case, features were sequentially added (up to 50 features), and model performance was evaluated using repeated 5-fold cross-validation (20 iterations). The optimal number of features was chosen based on the minimum RMSE, with error bars representing ± 1 standard deviation (**Figure 2.6b–6d**, left panels). Scatter plots comparing predicted versus true values (**Figure 2.6b–6d**, right panels) show a broad dispersion around the identity line, and the squared Spearman correlation coefficients (used as a proxy for R^2) ranged from approximately 0.10 to 0.30 across the different metrics. These findings indicate that while the EEG-derived features are moderately associated with both objective and subjective sleep parameters, their overall predictive power remains limited. Collectively, these results demonstrate that the EEG-based modelling approach can capture some variability in sleep quality and subtype discrimination—yielding a good peak area under the curve (≈ 0.81; **Figure 2.6a**) and regression R^2 values between 0.10 and 0.30 (**Figure 2.6b–6d**)—but underscore the need for further model refinement and the incorporation of additional predictors to achieve clinically robust performance.

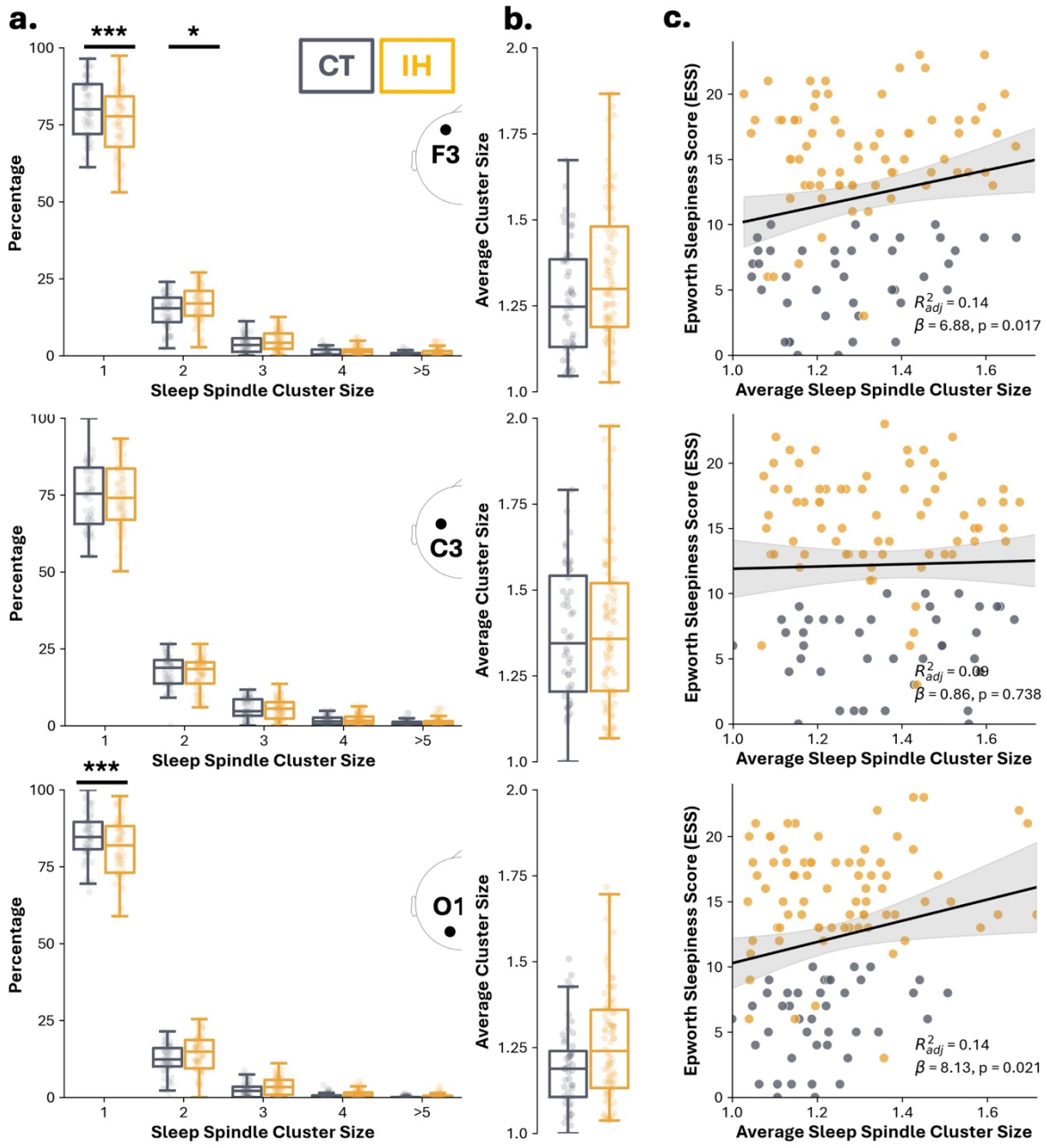

Figure 2.4: Sleep spindles were more clustered in the IH and predict the level of subjective sleepiness. **a** Percentage of sleep spindle clusters across size for the IH (yellow) and control (grey) groups. **b** Average sleep spindle cluster size per group. **c** Linear regression between average sleep spindle cluster size and Epworth sleepiness scale scores is represented by the solid black regression line (shading depicts the 95% CI). F3 electrode on the top row, C3 in the middle, and O1 at the bottom. Statistics for **a** and **b**: linear mixed models with age and gender as covariate with correction for multiple comparisons (false discovery rate), $p_{CORRECTED}$ <. 0.05: *, $p_{CORRECTED}$ < 0.01: **, $p_{CORRECTED}$ < 0.001: ***. In **a** and **b**, box plots show the median (middle line), 1st (bottom) and 3rd (top) quartiles. Whiskers extends to the most extreme non-outlier values (within 1.5×IQR). In all plots, dots show individual data points.

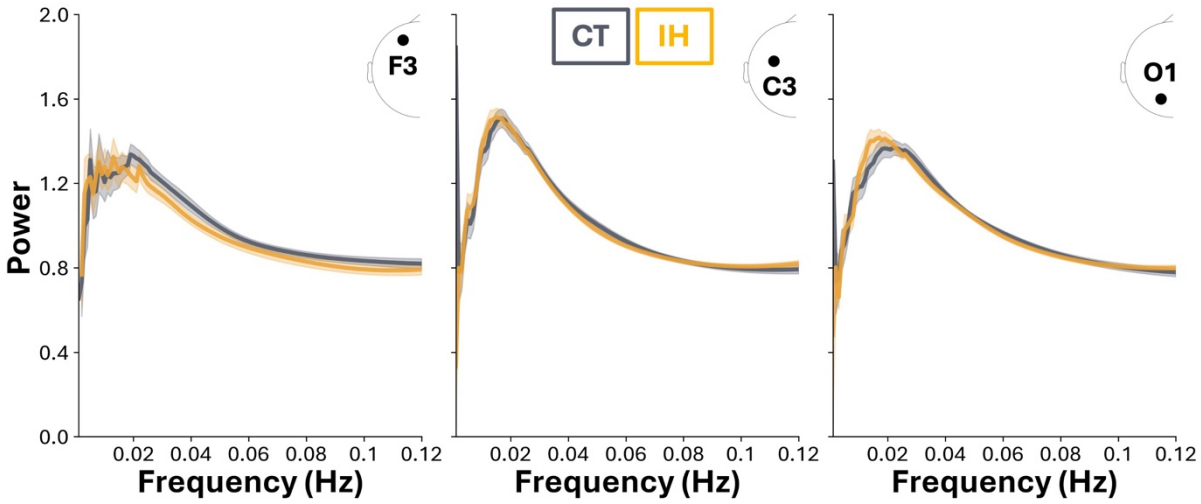

Figure 2.5: Infraslow sigma oscillations did not differ between groups. Normalized spectrum of 0.02 Hz oscillations in stable NREM sleep at F3 (left), C3 (center), and O1 (right) for the IH (yellow) and control (grey) groups. Shading area represents the standard error of the mean of the population per frequency bin. Statistics: linear mixed models with with age and gender as covariate cluster correction for multiple comparison, $p_{CLUSTER} < 0.05$: *, $p_{CLUSTER} < 0.01$: **, $p_{CLUSTER} < 0.001$: ***.

Discussion

In this controlled study of sleep EEG in 80 participants with IH with long sleep time, the proportion of N3 and sleep efficiency were increased, while the proportion of REM sleep and wake after sleep onset were reduced in the IH group compared to the control group. Such an increase in the percentage of N3 sleep was also found in a previous study of 35 patients with IH (Evangelista et al., 2018), although a meta-analysis of 10 previous studies (mixing IH participants with and without long sleep duration) did not replicate this finding (Plante et al., 2019). The restriction of our sample to IH with long sleep time, where well-consolidated sleep is expected (whereas sleep in IH with normal sleep time may be disrupted, as in narcolepsy type 2), may explain this slight discrepancy. However, the high percentage of N3 compared to the low percentage of REM sleep in our IH group may also reflect the way the sleep test was performed in our sleep clinic. Participants were awoken at 6:30 am before the first MSLT. This procedure could have shortened the total sleep time in IH (normalizing its duration compared to controls) and reduced the amount of REM sleep (which increases at the end of the night) in favor of N3 sleep.

Beyond the absolute or relative quantity of sleep stages, we examined qualitative differences across groups by extracting and analyzing hypnodensities. Group-level hypnodensity profiles were broadly comparable between IH and control groups, except for more mixed wake/N1 sleep epochs in IH. This finding contrasts with similar analyses in narcolepsy type 1, where dominant probabilities were more mixed with other sleep stages, suggesting more hybrid stages (Stephansen et al., 2018). Still, we found that wakefulness after sleep onset (intra-sleep wakefulness) had a

higher probability of N1 in IH individuals. These intrusions of sleep into wakefulness may be a marker of the difficulty of awakening from sleep in IH individuals.

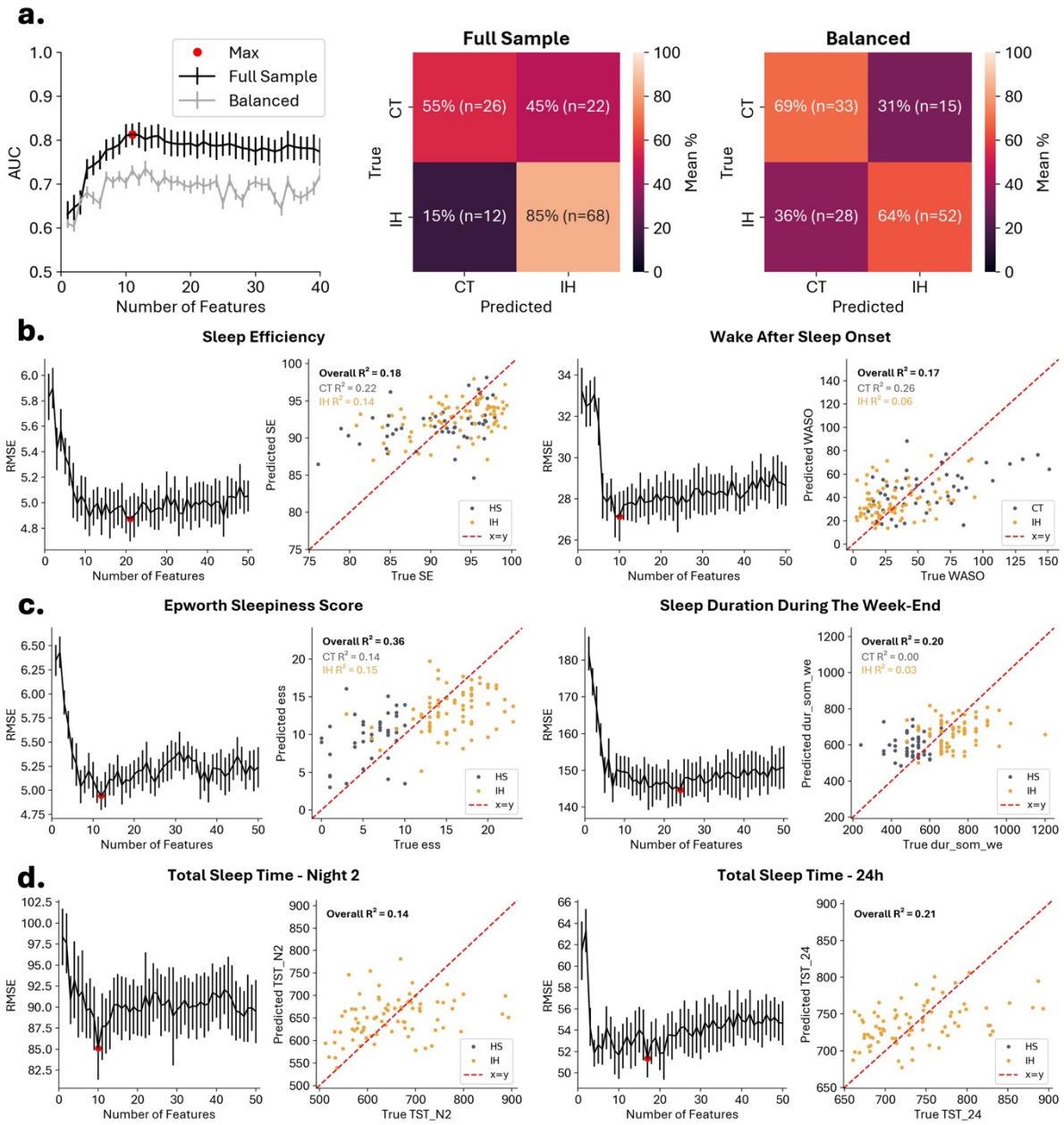

Figure 2.6: EEG-based features multivariate analyses predict group identify and sleep metrics. A Classifier results showing area under the curves and confusion matrices for both full (black) and balanced (dark grey) samples. The red marker highlights the optimal feature set, and confusion matrices display the percentage and count of correct classifications for control (grey) and idiopathic hypersomnia (yellow) groups. **b** Objective sleep measures (wake after sleep onset time and sleep efficiency) are evaluated via RMSE curves (left panels) and scatter plots (right panels) comparing predicted vs. true values. Data points are color-coded by group (control in grey, hypersomnia in yellow) with the red dashed line indicating the x=y identity line. **c** Subjective sleep metrics (sleep duration during the week and score at the Epworth sleepiness scale) are presented in the same format as (B). **d** Total sleep time predictions are shown for night 2 and the 24 hours (the latter for idiopathic hypersomnia only), again with RMSE curves and scatter plots. Error bars denote ±1 standard deviation across repeated cross-validation iterations.

Analysis of epoch-to-epoch dynamics showed that consecutive NREM sleep epochs were less similar in the IH than in control recordings, suggesting greater moment-to-moment variability. Since there was no increase in hybrid sleep stages and since hypnograms did not reveal more awakenings in IH, this variability does not seem to result from a greater instability as recently shown in insomnia(Herzog et al., 2025). To further explore the dynamics of sleep in IH, it would be interesting to consider other markers of sleep (in)stablitity such as Cyclic Alternating Patterns (CAP) and compare the rate of CAP between IH and controls (Pizza et al., 2013).

In terms of microstructural analysis, increased sleep spindles and slow wave densities in IH were two notable findings. Here, IH participants had increased sigma power and a higher density of sleep spindles. Sleep spindles were also more clustered in IH compared to controls. These results confirm and extend the previous findings of two research groups, who found a higher density of sleep spindles during N2 sleep in IH than in controls and narcolepsy(Bové et al., 1994; Delrosso et al., 2014). This increased activity and clustering of spindle, may reflect an over-stabilization of thalamocortical networks, which may underlie the pathophysiology of IH. As previously suggested, this mechanism may contribute to severe sleep inertia(Bové et al., 1994; Delrosso et al., 2014). Moreover, given that periods with a higher density of sleep spindles have been associated with reduced sensitivity to external noise during sleep(Dang-Vu et al., 2010), an excess or abnormal clustering of spindles in IH might further diminish cortical responsiveness and impair efficient arousal mechanisms, potentially explaining sleep drunkenness. Importantly, these changes in spindle activity were not reflected in the infraslow rhythmic modulation of sigma power, suggesting that long-timescale regulatory mechanisms of sleep under the influence of noradrenergic activity could be similar in IH and controls (Osorio-Forero et al., 2025).

Regarding delta power in IH, previous studies have yielded inconsistent results, with an increase over night in some studies (including participants with IH and some psychiatric disorders) on one hand (Plante et al., 2019; Walacik-Ufnal et al., 2017), and a decrease in a study of 10 patients with IH without long sleep time on the other hand (Sforza et al., 2000). In our IH series, while a global spectral analysis did not reveal differences in overall delta power compared to controls, a targeted analysis of slow waves patterns during N3 sleep revealed higher slow waves density than in the control group. This finding suggests that global delta power measures may obscure specific microarchitectural changes in slow wave activity. The fact that delta power does not just reflect the number but also amplitude of slow waves could explain differences between SW density and delta power. Importantly, an increase in slow wave density in IH patients could promote sleep drunkenness in these patients, as the prevalence of slow waves is associated with sleep inertia (Trotti, 2017). One potential mechanism underlying this increase could be an enhanced homeostatic sleep regulation (Tononi and Cirelli, 2006). An elevated sleep drive may stem from a

greater restorative need, manifesting as an increased slow wave activity. Indeed, the synaptic homeostasis hypothesis proposes that slow waves activity plays a crucial role in downscaling synaptic strength accumulated during wakefulness, with higher slow waves density reflecting an amplified need for synaptic renormalization (Tononi and Cirelli, 2014). It is possible that individuals with IH tend to create and strengthen synaptic contact at a higher rate during wakefulness, which would lead to an increase in slow waves during sleep as proposed for other sleep disorders (Avvenuti and Bernardi, 2022). Alternatively, changes in brain metabolism have also been associated with an increase in slow waves and could represent the cause or source of the enhanced slow wave activity observed here during sleep (Krueger et al., 2019). Both hypotheses suggest that the ultimate cause of IH symptoms could be found during wakefulness rather than sleep, in line with our findings showing a mostly preserved sleep in IH.

The classification of IH is based on the exclusion of other hypersomnolence disorders, such as narcolepsy type 1, insufficient sleep syndrome, or other sleep disorders. Accordingly, the clinical categorization of IH based on conventional sleep measures remains inconsistent when compared to normal sleepers, with significant variability between studies (Evangelista et al., 2018; Maski et al., 2021; Plante, 2018; Sforza et al., 2016, 2000, 2000; Vanková et al., 2001; Vgontzas et al., 2000). This may be because IH is characterized by many small differences that are difficult to detect in isolation and in small samples. In this context, our findings show that, when integrating many indexes derived from the first night PSG recordings (but not MSLT latency or total sleep time during 24h recordings), our EEG-based model achieved a good balanced classification performance with an AUC of 0.74 and a correct classification rate around 65%. Our approach could therefore represent an interesting aid for the diagnosis of IH, based on a single night of PSG recordings. Yet, the predictive power of our models for objective sleep measures remained low, suggesting that a significant proportion of the inter-individual variability remains unaccounted for. Our results thus support the notion that leveraging a combination of EEG features rather than relying on conventional sleep staging or a small set of macrostructural sleep parameters may be key to refining our understanding of sleep disorders (Andrillon et al., 2020; Herzog et al., 2024; Stephan and Siclari, 2023).

Our study has several limitations, including EEG recordings limited to 3 channels (which limits the spatial analysis of EEG), and a control group smaller than the IH group. On the other hand, the IH group analyzed here was large (although IH is a rare disorder), well-characterized (using not only MLST but also long-term bed rest recordings), untreated, without any individuals with possible psychiatric hypersomnia, resulting in homogeneity and robustness in the results. In addition, measurements were adjusted for sex and age.

In conclusion, our findings show that IH with long sleep time is characterized by distinct but subtle EEG signatures that paradoxically suggest a seemingly 'better-than-normal' sleep structure. This dissociation between normal nocturnal sleep microarchitecture and daytime hypersomnolence underscores the need to further explore daytime neural mechanisms and suggests a potentially deficient arousal system in IH. Ultimately, these findings may lead to a refinement of the diagnostic criteria for IH.

Acknowledgements

We thank the medical and para-medical staff for their never-stopping care for the patients, their scrutinous work for the acquisition and scoring of sleep recordings, and the sharing of their clinical expertise. ALC was supported by a grant from Ecole Doctorale Frontières de l'Innovation en Recherche et Education–Programme Bettencourt and the Fondation pour la Recherche Médicale (FDT202404018709). TA was supported by a grant from the Agence Nationale pour la Recherche (ANR-22-CE37–0006-01) and from the European Research Council (ERC-StG SleepingAwake 101116748). DO was supported by a grant from the European Research Council (ERC-Cog Creadoze 101087031).

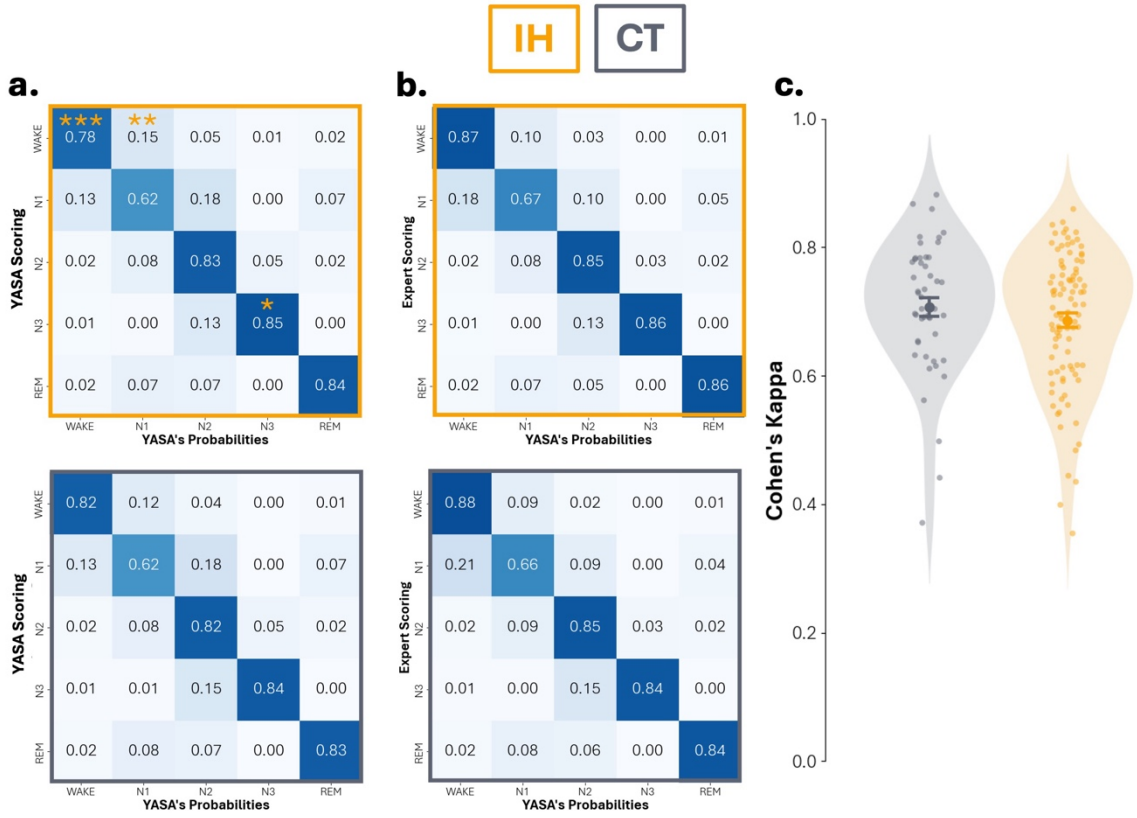

Supplemental Figure 2.1: Hypnodensity matrices for the automated and human scoring. Hypnodensities according to the sleep stage scored by **a** YASA, and **b** experts of participants with IH on the upper part (yellow squares) and controls on the lower part (grey squares). **c** Cohen's Kappa of YASA automatic sleep staging against expert scorers. Participants with IH in yellow compared to controls in grey. Statistics: Linear Mixed Models with age and gender as covariate correction for multiple comparison (false discovery rate), $p < 0.05$: *, $p < 0.01$: **, $p < 0.001$: ***.

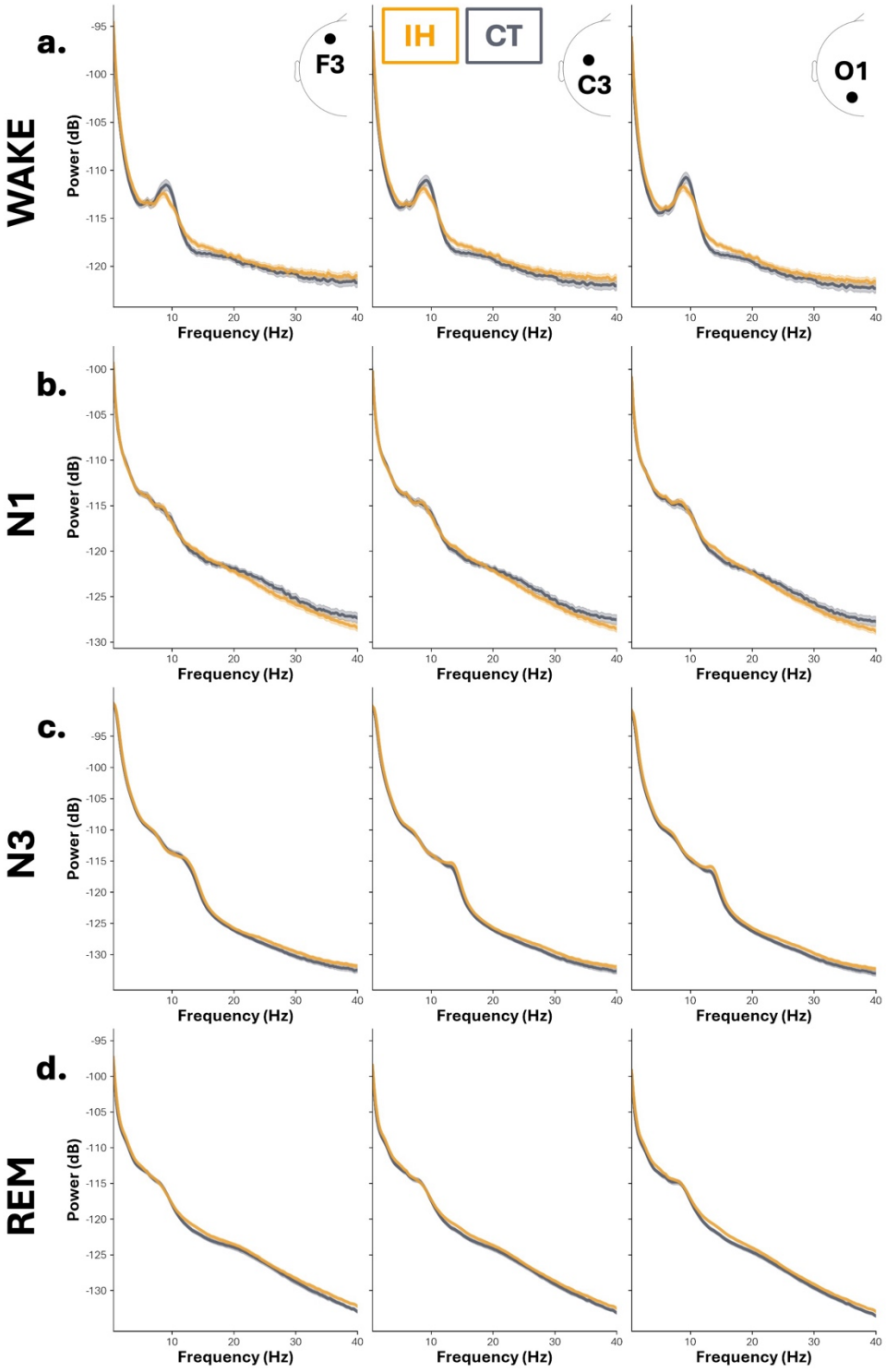

Supplemental Figure 2.2: Global power in wake during the night, N1, N3 and REM sleep. Global power in **a** wake during the night, **b** N1, **c** N3, and **d** REM sleep at channel F3, C3, and O1 (left, middle, and right, respectively) in participants with IH (yellow) compared to controls (grey). Shading area represents the standard error of the mean of the population per frequency bin.

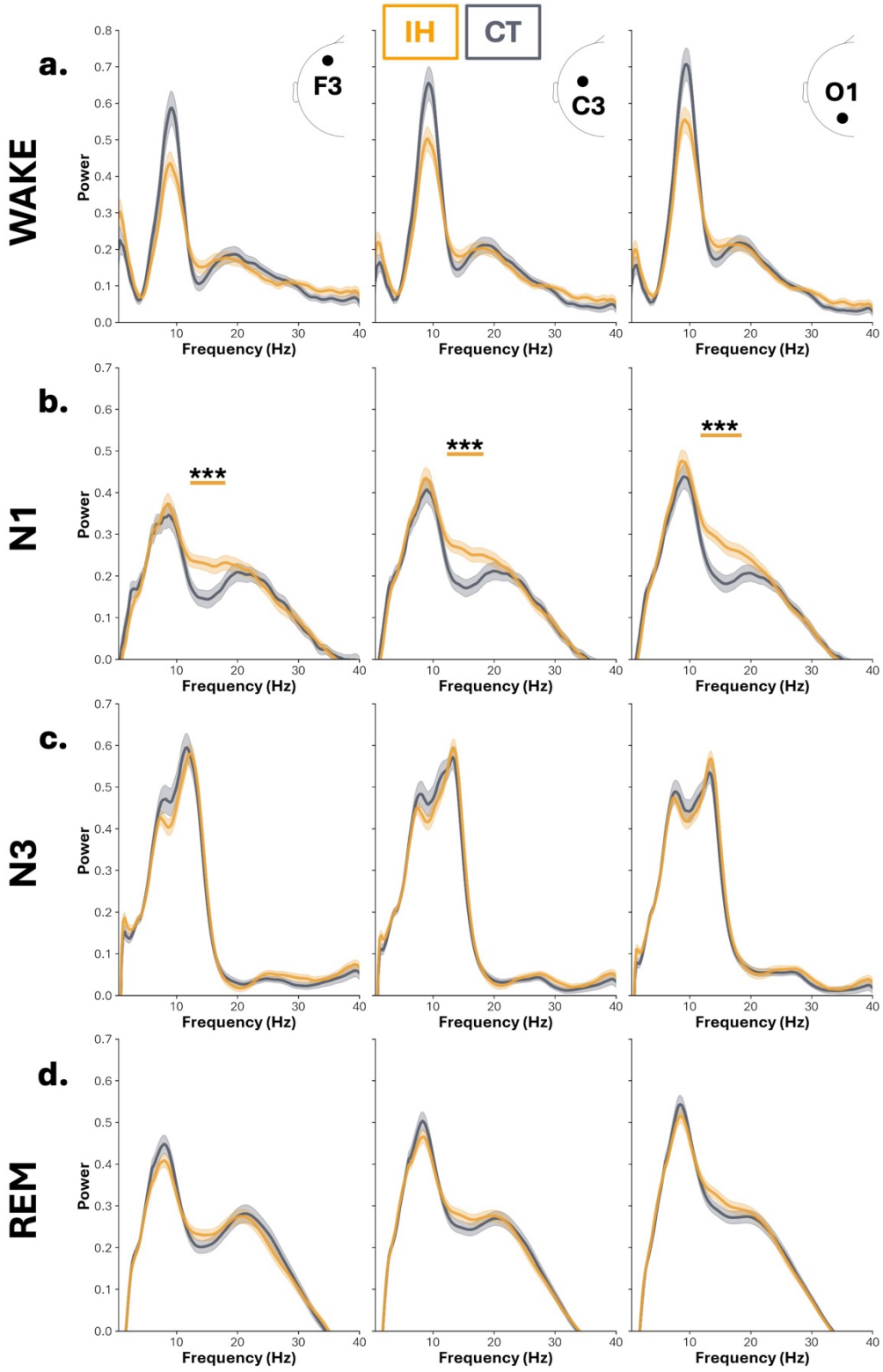

Supplemental Figure 2.3: Periodic power in wake during the night, N1, N3 and REM sleep. Periodic power in **a** wake during the night, **b** N1, **c** N3, and **d** REM sleep at channel F3, C3, and O1 (left, middle, and right, respectively) in participants with IH (yellow) compared to controls (grey). The yellow bar above the PSD in **b** indicates statistical differences. Shading area represents the standard error of the mean of the population per frequency bin. Statistics: linear mixed models with age and gender as covariate corrected with cluster correction for multiple comparisons, $p_{CLUSTER} < 0.05$: *, $p_{CLUSTER} < 0.01$: **, $p_{CLUSTER} < 0.001$: ***.

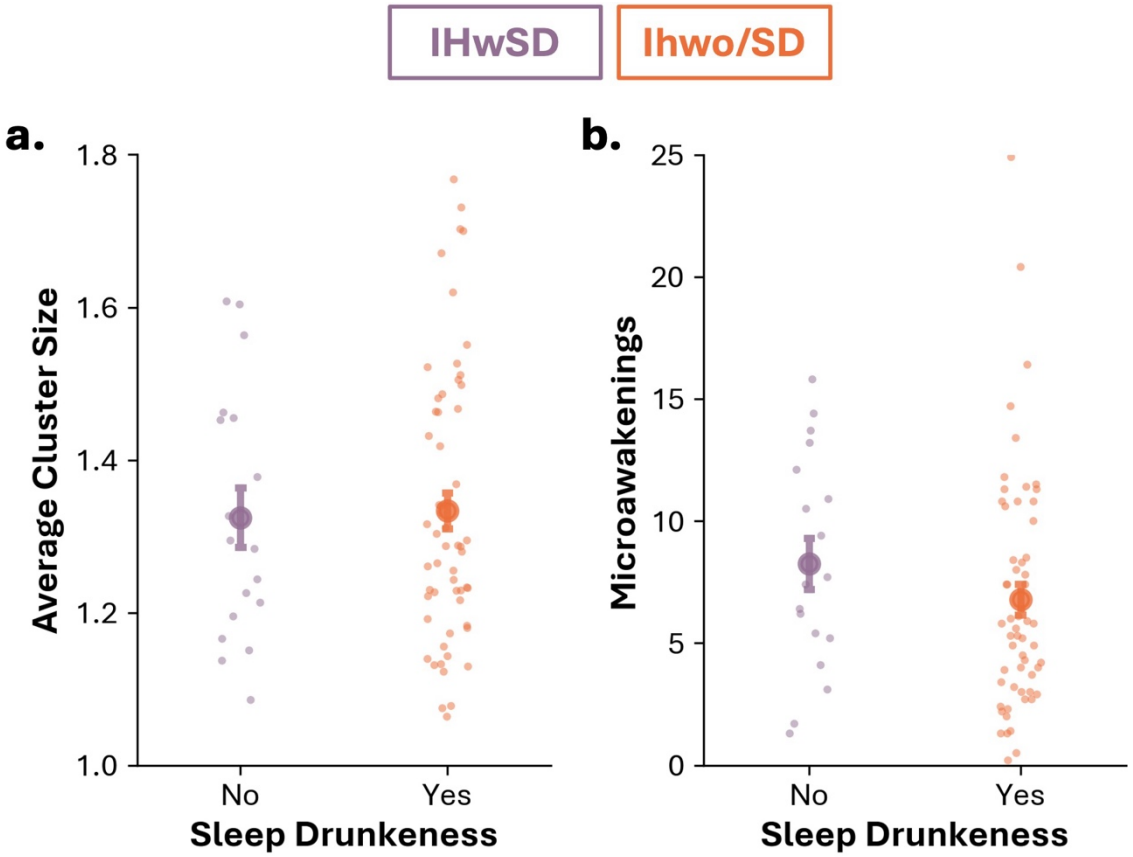

Supplemental Figure 2.4: Spindle cluster size and microawakenings for IH with (IHwSD) and without sleep drunkenness (IHwo/SD). a Average cluster size and **b** microawakening index in IH with (purple) and without (orange) sleep drunkenness. Statistics: linear mixed models with age and gender as covariate, corrected for multiple comparisons (false rate discovery), $p < 0.05$: *, $p < 0.01$: **, $p < 0.001$: ***.

Supplemental Table 2.1: Demographic, clinical and sleep measures in participants with idiopathic hypersomnia with long sleep time and controls.

Category	Feature	Definition / Unit	Channels	Sleep stage(s)
Event counts	Slow wave count	Number of events detected	F3, C3, O1	All (Wake, N1, N2, N3, REM)
	Sleep spindle count			N2 and N3
Event density	Slow wave density	Events per 30-s epochs	F3, C3, O1	All
	Sleep spindle density			N2 and N3
Amplitude / morphology	Slow wave and sleep spindle amplitude	Peak-to-peak (µV)	F3, C3, O1	All
	Slow wave downward and upward slope	µV·s-1		All
	Sleep spindle duration	duration (s)		N2 and N3
	Sleep spindle frequency	Median instantaneous frequency of spindle (in Hz)		N2 and N3
	Slow wave frequency	Hz		All
Spectral Absolute power	Absolute power in the delta, theta, alpha, sigma and beta frequency ranges	$\mu V^2/Hz$	F3, C3, O1	All
	Sleep spindle absolute power	Median absolute power (in log10 μV^2)		
Spectral Relative Power	Relative power in the delta, theta, alpha, sigma and beta frequency ranges	% of total power 0.5 to 40Hz	F3, C3, O1	All
	Sleep Spindle Relative Power	Median % [11.25; 15.75Hz] of total power 1 to 30		N2 and N3
Aperiodic Fit	Exponent, Offset	1/F Slope and intercept	F3, C3, O1	All
Hypnodensity-derived features	dKL, Entropy		C3, Chin EMG, Left EOG	All

Supplemental Table 2.2: Top 13 mRMR-Ranked EEG Features for Classifying IH and HS subjects.

Rank	EEG Feature name	Stage	Electrode
1	dKL	N3	
2	Sleep Spindle Count	N3	O1
3	Slow Wave Count	REM	C3
4	Slow Wave Density	N3	O1
5	Absolute Beta Power	N3	O1
6	Hypnodensities	N1	
7	S̄leep Spindle	N2	F3
8	d̄KL	N2	
9	Sleep Spindle	N3	F3
10	S̄low Wave Count	N3	O1
11	Slow Wave Frequency	N1	O1
12	Absolute Sigma Power	REM	C3
13	Sleep Spindle Count	N2	O1

Study 3
Neither Here nor There: Capturing Hallucinatory States in Narcolepsy Type 1

In Preparation

Arthur Le Coz[1,2*], Raphael Vollhardt[3], Sophia Snipes[1], Cécile Londner[4], Smaranda Leu-Semenescu[3], Pauline Dodet[1,3], Delphine Oudiette[1], Isabelle Arnulf[1,3], Thomas Andrillon[1*]

[1] Sorbonne Université, Institut du Cerveau - Paris Brain Institute - ICM, Inserm, CNRS, AP-HP, Hôpital de la Pitié Salpêtrière, Paris, France.

[2] Université Paris Cité, Paris, France.

[3] National Reference Center for Narcolepsies and Rare Hypersomnia, Sleep Clinic, DMU APPROCHES, Pitié-Salpêtrière Hospital, APHP- Sorbonne University, Paris, France

[4] AP-HP, Groupe Hospitalier Universitaire APHP-Sorbonne Université, Hôpital Pitié-Salpêtrière, Service des Pathologies du Sommeil (Département R3S), Paris, France

* Corresponding authors

3. 1. Digest

Participants with NT1 are characterized by fragmented boundaries between sleep and wakefulness, leading to excessive daytime sleepiness, cataplexy, and vivid hallucinations around sleep onset and awakening. These hallucinations are not mere reporting errors but reflect genuine alterations in conscious experience, often blurring the distinction between perception and dreaming. In this study, during a long SART, we combined EEG analyses, and experience sampling to investigate their neural underpinnings. The results suggest that these hallucinatory episodes, along with their behavioral and electrophysiological signatures, expand the concept of local sleep intrusions. Beyond NREM slow waves, fragments of REM physiology may transiently intrude into wakefulness, offering new insight into chronic fatigue and altered experiences in NT1.

3. 2. Study

Abstract

Hallucinations and illusions are vivid spontaneous mental experiences in which people perceive things that are not there or misperceive what is present in the environment. Hallucinations are normally absent in healthy individuals but frequent in psychiatric or neurological disorders. Yet, even in these populations, hallucinations and illusions remain rare and unpredictable events, limiting their empirical study. Here, we captured spontaneous reports of hallucinations and illusions from wakeful participants with Narcolepsy Type 1 (NT1), without any form of induction. Participants with NT1 and matched controls performed a sustained attention task interspersed with experience-sampling probes allowing for the report of various mental states including hallucinations and illusions. Compared to other spontaneous states, hallucinations or illusions in NT1 were associated with higher subjective sleepiness, reduced intentionality, and increased behavioral errors. When examining high-density EEG data, we found that hallucinations were associated with a distinct increase in occipital theta power and a decrease in posterior beta activity. Regardless of the occurrence of hallucinations and illusions, NT1 participants exhibited a parieto-occipital increase in the occurrence of theta bursts, which are usually observed in NREM Stage 1 and REM sleep and were absent in wakeful controls. Besides, these bouts of theta activity were associated with the presence of hallucinatory and illusory reports. Altogether, this pattern of results is consistent with an association between hallucinatory and illusory experiences in NT1 and the intrusion of sleep-like activity in wakefulness. These findings reveal that hallucinations and illusions can be reliably captured with standard sustained-attention tasks in individuals with NT1. While mind-wandering, that is stimulus-independent and task-unrelated experiences, has been linked to NREM-like slow wave intrusions, we identified a potential new type of sleep intrusion in NT1 individuals, possibly involving REM-like dynamics and associated with dream-like experiences. Hallucinations and illusions may reflect a hybrid brain state at the boundary between wakefulness and dreaming.

Introduction

Reverie ˈrɛv(ə)ri

Noun – A state of being pleasantly lost in one's thoughts; a daydream.

This word originates from old French, using the root of the word *rêve* (dream) captures the essence of spontaneous mental life. When our attention drifts from the task at hand, it gives rise to a wide spectrum of inner experiences. The term mind wandering has been recently proposed to describe the wide range of task-unrelated, stimulus-independent experiences that constitute the stream of consciousness (Smallwood and Schooler, 2015). Sometimes, the mind goes nowhere, leading to brief moments of mind-blanking (Andrillon et al., 2021; Mortaheb et al., 2021; Munoz-Musat et al., 2025; A. Ward and Wegner, 2013). During sleep, spontaneous mental content can emerge that is usually unrelated to the external environment: these are dreams. While mind-wandering may share some features and underlying mechanisms with dreaming (Fox et al., 2013), it has been suggested that task-focused thought, mind-wandering, and dreaming lie on a continuum of conscious states shaped by the level of cognitive control (Christoff et al., 2016). Still, despite this proposed continuum, mind-wandering and dreaming are thought to occur in distinct physiological states: wakefulness and sleep, respectively.

Within this "dynamic framework" for spontaneous experiences, hallucinations hold a special place. In the literature, a distinction is made between illusions which are defined as perception of real objects or persons in a distorted manner and hallucinations which are defined as perceptions without any real objects to be perceived (Leu-Semenescu et al., 2011). Here, we will examine both hallucinations and illusions conjointly. Vivid, involuntary, and often immersive, hallucinations and illusions break into the stream of consciousness with content that adds to or transforms external reality. While often associated with psychiatric (Goodwin and Rosenthal, 1971) or pharmacological states (Rolland et al., 2014), hallucinations in particular can also emerge in healthy individuals when the brain and body are pushed to their limits (Huang et al., 2021; Hurdiel et al., 2015; Pallesen et al., 2018; Waters et al., 2018). For example, during periods of extreme sleep deprivation such as those experienced by ultramarathon runners, hallucinatory visual percepts are often reported (Huang et al., 2021; Hurdiel et al., 2015). Yet, despite their relevance to the architecture of conscious experience, their rarity has made hallucinations poorly integrated into the study of spontaneous thoughts.

One major challenge is that hallucinations and illusions are rare, unpredictable, and difficult to induce under controlled conditions. This contrasts with the ubiquity of mind wandering during wakefulness and dreaming during sleep. This rarity makes hallucinations and illusions a robust clinical marker but severely limits their empirical study compared to MW, MB, or even dreams,

which can be reliably captured in the lab (Andrillon et al., 2021; Siclari et al., 2017). Hence, a key question remains unanswered: what distinguishes hallucinations from other form of spontaneous experiences? Better understanding the mechanisms of hallucinations could help us understand why they tend to occur in specific clinical populations and not in normal individuals except in exceptional circumstances.

To address this, we leveraged a unique opportunity offered by a sleep disorder: NT1. Rather than focusing on the disorder itself, we leveraged the unique profile of NT1 as a window onto hallucinations, which can be observed in this population without the use of pharmacological agents (Leu-Semenescu et al., 2011). NT1 is indeed characterized by a dysregulation of the sleep-wake system, with frequent and abnormal transitions from wakefulness to REM sleep (SOREM, Sleep Onset Rapid Eye Movement). One of the core subjective symptoms of NT1 is the presence of hallucinations or illusions. Hallucinatory experiences are reported by 59% of participants with NT1, including 13% who described perceptual illusions (Leu-Semenescu et al., 2011). In participants with NT1 these experiences often combined at least two sensory modalities, most commonly visual, auditory, kinesthetic, or tactile (Leu-Semenescu et al., 2011). Notably, about one-third of those reporting hallucinations experienced them while being fully awake, outside of sleep transitions (Leu-Semenescu et al., 2011).

These hallucinations often entail vivid dream-like imagery and increase at sleep onset (hypnagogic) or offset (hypnopompic), illustrating their association with the abnormal regulation of sleep and wakefulness in these patients. However, not all hallucinations occur during sleep. It has been proposed that the powerful sleep drive experienced by NT1 individuals could manifest as intrusions of sleep-like phenomena into wakefulness. According to this hypothesis, vivid hallucinations observed in wakeful NT1 patients would be associated with a covert or incomplete hypnagogic process (Leu-Semenescu et al., 2011), reflecting sleep-related mechanisms, particularly involving REM sleep (Leu-Semenescu et al., 2011).

To investigate hallucinatory experiences during wakefulness, we adapted a well-established sustained attention to response task (SART, Robertson et al. 1997). We used an experience sampling approach to collect subjective reports of participants undergoing the SART and specifically allowed participants to report hallucinations or illusions along episodes of mind wandering or mind blanking (Andrillon et al., 2021). This allowed us to capture hallucinatory episodes, particularly in participants with NT1. We then compared the behavioral and electrophysiological signature of these reports in contrast with mind-wandering or mind-blanking. Finally, we explored markers of sleep intrusions with sleep-like slow waves and theta bursts, typically observed in NREM2/NREM3 and NREM1/REM sleep respectively (Santamaria and Chiappa, 1987). Individuals with NT1 exhibited both more slow waves and theta bursts but only

theta bursts allowed us to dissociate hallucinations and illusions from other mind states. Theta bursts could thus reflect local, transient signatures of REM-like activity during wakefulness.

Methods

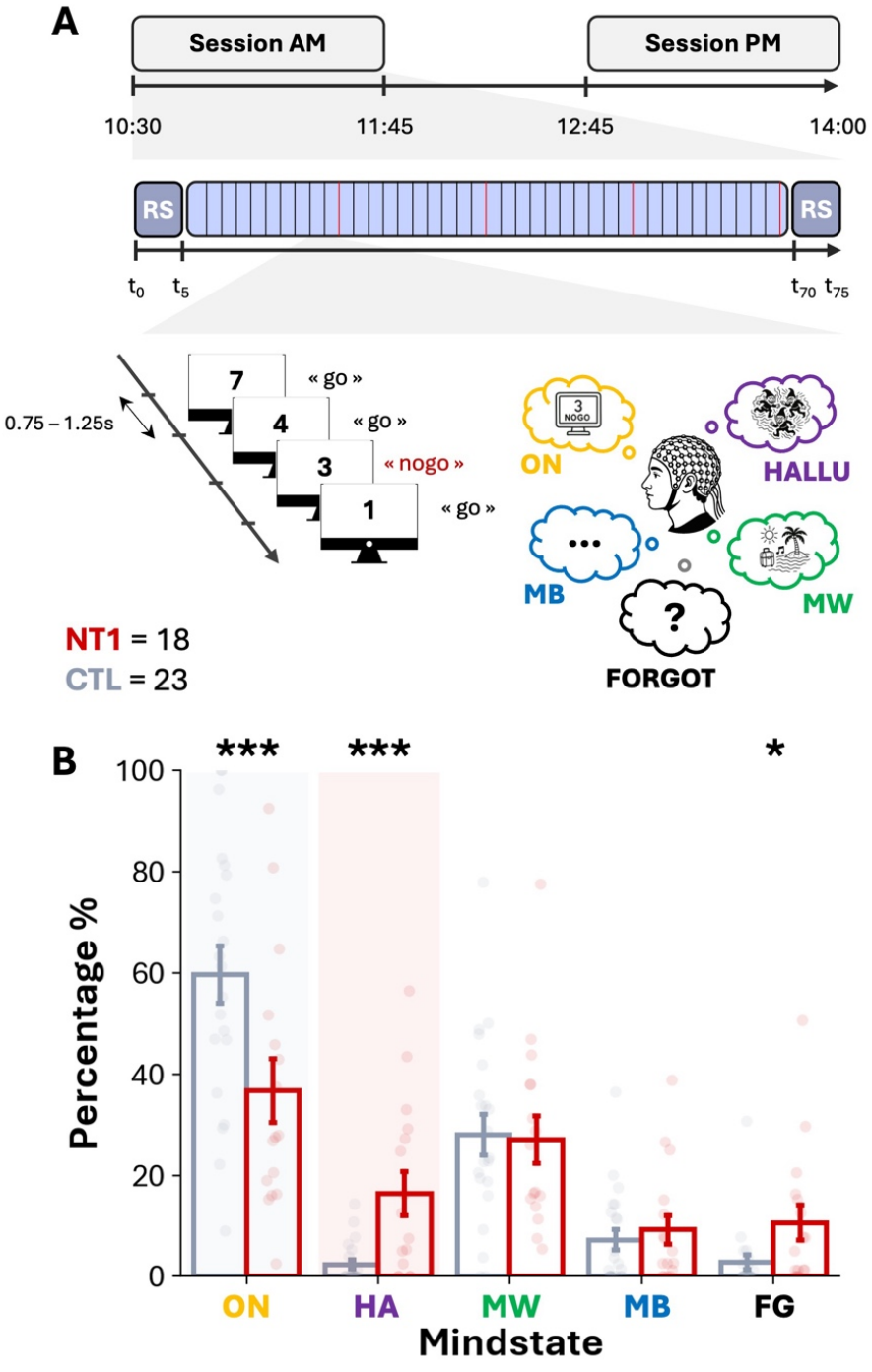

Figure 3.1. Experimental design and behavioral signature of mind states. A Experiment design with a morning (AM) and an afternoon (PM) session. During each session, participants did a SART with 40 probes indicated with vertical lines. Before and after the SART, participant did a closed eyes resting state of 5 minutes. **B** Percentage of each mind state according to the group. Statistics are linear mixed models corrected for multiple comparison with FDR. $p < 0.05$: *, $p < 0.01$: **, $p < 0.001$: ***

Participants

Participants with NT1 were recruited (n = 18, age = 27.9 ± 1.7, n = 7 women) through the sleep disorders unit at Pitié-Salpêtrière Hospital in Paris. All were adults (>18 years of age), fluent in written and spoken French, affiliated with the national health insurance system, and had provided informed consent prior to participation. The diagnosis of NT1 was established in accordance with ICSD-3 criteria, based on a standardized 48-hour clinical assessment including one night of polysomnography, a multiple sleep latency test (MSLT), and a second night of sleep recording (Sateia, 2014). Diagnosis was confirmed by either cerebrospinal fluid hypocretin-1 levels below 110 pg/mL or the presence of clear cataplexy symptoms in combination with a sleep latency below 8 minutes and at least two sleep-onset REM periods (SOREMPs). Participants followed regular sleep-wake schedules and were not under legal protection. They were either drug-free or had discontinued psychotropic medication for a period corresponding to five elimination half-lives. The diagnosis of NT1 was established in accordance with ICSD-3 criteria, based on a standardized 48-hour clinical assessment including one night of polysomnography, a MSLT, and a second night of sleep recording (Berry et al., 2017). Diagnosis was confirmed by either cerebrospinal fluid hypocretin-1 levels below 110 pg/mL or the presence of clear cataplexy symptoms in combination with a sleep latency below 8 minutes and at least two sleep-onset REM periods (SOREMPs). Pregnant participants were not excluded.

Healthy control participants were recruited (n = 23, age = 28.4 ± 1.4, n = 12 women), they were also adults fluent in French, insured under the national health system, and provided informed consent. They had no history of neurological or sleep disorders, followed regular sleep-wake rhythms, and were not taking psychotropic medication. They were screened for daytime sleepiness using the Epworth Sleepiness Scale, and only those with a score below 11 were included. Participants with irregular work schedules, insufficient sleep during the days preceding the experiment, or any other medical or psychiatric conditions known to affect sleep or vigilance were excluded.

SART

Participants completed a SART (Robertson et al., 1997) which designed was adapted from (Andrillon et al., 2021) using Psychtoolbox extension for Matlab (*Mathworks*, *Natick*, MA, USA). Participants were sitting in a Faraday Cages with dimmed light, chin rested. Single digit (from 1 to 9) was presented in random order at the center of the screen. Each digit appeared for a duration of 750 to 1250ms (random uniform jitter). Participants were instructed to press a key in response to every digit except the digit "3," which served as the no-go stimulus. Participants performed the SART for 4 blocks of between 12 to 15 minutes totaling around an hour of SART. They did a session in the

morning (10.30am) and another in the early afternoon (12.45pm). Each SART was surrounded by two eyes closed resting states session of 5 minutes (**Figure 3.1A**).

At pseudo-random intervals, the task was interrupted by experience-sampling probes assessing participants' current mental state. The inter-probe interval was between 40 and 70 seconds (random uniform jitter). Each probe asked participants to categorize their mental state using one of six options:

1. I was focused on the task (ON-task: ON)
2. I was distracted by something internal (thought, image, etc.; mind-wandering: MW)
3. I was distracted by something external (environment) (task interferences)
4. I was distracted by something imaginary (illusion, hallucination: HA)
5. I wasn't thinking about anything (mind-blanking: MB)
6. I don't remember (forgot: FG)

Following this first question, participants responded to two additional items: (1) whether the reported mental state occurred voluntarily or involuntarily, and (2) report their subjective feeling of sleepiness on the Karolinska sleepiness scale (See **Table 3.1** below for detail, KSS, Shahid et al. 2012).

Table 1. Karolinska Sleepiness Scale

Sleepiness level	KSS description
1	Extremely alert
2	Very alert
3	Alert
4	Rather alert
5	Neither alert nor sleep
6	Some signs of sleepiness
7	Sleepy, but no effort to keep awake
8	Sleepy, but some effort to keep awake
9	Very sleepy, great effort to keep awake, fighting sleep

EEG Recordings

High-density scalp EEG was recorded using an actiCap Snap system with 64 active electrodes connected to a BrainAmp amplifier (Brain Products GmbH). The ground electrode was placed at Fpz, and signals were referenced online to AFz. To monitor eye movements, electrooculogram (EOG) was recorded via electrodes placed above and below the left and right canthi. Electrocardiogram (ECG) was recorded using two additional electrodes, one positioned below the right deltoid and the other above the left hip. EEG, EOG, and ECG signals were sampled at 500 Hz. Eye movements and pupil diameter were also tracked from one eye using an EyeLink 1000 system (SR Research), although these data were not analyzed in the present study. A respiratory belt was used to monitor thoracic breathing.

Data Analysis

Preprocessing

EEG preprocessing was performed using MNE-Python (Gramfort et al., 2013). Raw high-density EEG were resampled at 256 Hz and epoched around two types of events: (i) Go and NoGo trials (–200 ms to +1200 ms), and (ii) thought probes (–10 to 0 s before the probe onset). Trials epochs were excluded if an electrode exhibited flat signals (max absolute amplitude <1 μV). For artifact correction, we applied Independent Component Analysis (ICA, Lee et al. 1999) on the trial epochs after a 1 Hz zero-phase high-pass filter. Components reflecting ocular, cardiac, or muscle artifacts were removed automatically based on their time courses and topographies. The components marked as artefacts were then removed by applying ICA weights to both trial and probe data subject by subject. Trial epochs were further denoised using the AutoReject algorithm (Jas et al., 2016) with Bayesian threshold optimization, calibrated on the first 20% of epochs. All trial and probe epochs were then re-referenced to TP9 and TP10 and baseline-corrected (–200 ms to 0 ms for trial epochs). Cleaned epochs were saved for subsequent analyses.

Spectral Analysis

Spectral analyses were conducted on probe-locked EEG epochs using the MNE-Python (Gramfort et al., 2013) and SpecParam libraries (previously FOOOF, Donoghue et al. 2020). Power spectral density (PSD) was computed using the Welch method with a Hamming window (0.5–40 Hz), using 1024-point Fast Fourier Transforms (FFT), with a 50% overlap (e.g. 4s with 2s overlap). For each channel and epoch, the PSD was smoothed using locally weighted scatterplot smoothing (LOWESS, span=0.075) to improve fit robustness.

The PSD of each epoch was then decomposed into periodic and aperiodic components using the FOOOF algorithm (aperiodic mode: “fixed”; peak width limits: 0.5–6 Hz, Donoghue et al. 2020). Epochs with poor model fits ($R^2 < 0.95$ or error > 0.1) were excluded from further analysis. The aperiodic fit followed a power-law model of the form:

$$P_{aperiodic}(f) = \beta \cdot f^{-\alpha}$$

Where $P_{aperiodic}(f)$ is the aperiodic power for a given frequency f, α is the exponent of the power law, and β the offset. Subtracting the fitted aperiodic activity to the original PSD allowed to estimate the periodic power:

$$P_{periodic}(f) = \mathrm{PSD}(f) - \beta \cdot f^{-\alpha}$$

For each channel and epoch, absolute periodic power was computed by averaging periodic power within canonical frequency bands: delta (0.5–4 Hz), theta (4–8 Hz), alpha (8–12 Hz), beta (12–30 Hz),

and gamma (30–40 Hz). Relative power was computed by normalizing absolute power in each band by the total periodic power across all bands. Both absolute and relative power were extracted at the single-trial level and later log-transformed prior to statistical modeling.

Slow Wave Automatic Detection

Slow waves were automatically detected using custom Python scripts incorporating the MNE library (Gramfort et al., 2013). Slow waves were detected in each 10s epochs preceding probes for each EEG channel and stored for further analysis.

Slow waves were identified following a two-step preprocessing pipeline. First, EEG signals were down-sampled to 100 Hz and filtered using a zero-phase finite impulse response band-pass filter (0.5–8 Hz) with automatically determined transition bandwidths, ensuring minimal edge artifacts while preserving waveform integrity. The filtered signal was then analyzed to identify negative and positive zero-crossings, which were used to segment potential slow waves. For each candidate wave, we computed the peak-to-peak amplitude, that is the amplitude difference between the most positive and most negative peak between the start and end of the wave (consecutive zero-crossings). We then selected high-amplitude slow waves based on this peak-to-peak amplitude, which had to exceed a data-driven threshold, estimated for each channel and each participant. Based on the distribution of peak-to-peak amplitude, we computed this threshold as the top 10th. This value was computed for each subject for each electrode. Then, for group comparison we computed an average control threshold per channel that we applied to both groups.

Event density was calculated as the number of detected events within the window preceding the mental state report, divided by the total duration of the window (i.e. 10s). For each slow wave, we further extracted the following parameters: (1) Maximal negative slope (descending phase), representing the voltage decline (in μV/s) between the first negative zero-crossing and the negative peak crossing divided by the duration between the negative zero-crossing and the negative peak (in seconds); and (2) Maximal positive slope (ascending phase), reflecting the voltage increase between the negative peak and the subsequent positive zero-crossing divided by the duration between the peak and the positive zero-crossing (in seconds). Only waves with a descending and ascending slope between 0.25 and 2 μV/s were retained, ensuring the selection of physiologically meaningful slow waves (Riedner et al., 2007).

Theta bursts automatic detection

We used an automatic detection pipeline inspired by the method proposed by Snipes et al. (2022) to identify transient theta bursts in resting and task-related EEG data. EEG recordings were first filtered between 1 and 40 Hz (zero-phase FIR filtering) and restricted to the 64 scalp channels.

Data were then filtered into several overlapping narrow bands, including a canonical theta band (4–8 Hz), using custom bandpass filters.

Burst detection was applied independently to each channel using a modified cycle-by-cycle analysis. A burst was defined as a sequence of oscillatory cycles meeting multiple criteria. First the cycle count needed to reach a minimum amount (at least 3 or 4 cycles, depending on the criteria set). Second, the period needed to be locally regular (period consistency ≥ 0.5–0.7). Third, amplitude and flanks needed to be consistent (≥ 0.4–0.6). Last, amplitude trend needed to be monotonic across cycles (≥ 0.4–0.9). These criteria correspond to a set of detection templates, ranging from strict to more inclusive profiles, consistent with previously published classification schemes (Snipes et al., 2022).

Detected bursts were aggregated across channels based on temporal overlap and frequency similarity (minimum clustering range = 1 Hz), and bursts not assigned to a cluster (i.e., detected on a single channel only) were excluded. For each burst, we extracted onset and offset, duration, central frequency, and average amplitude. Bursts within the theta range (4–8 Hz) were used for subsequent analyses, with exploratory comparisons also including adjacent bands (e.g., 2–6 Hz or 6–10 Hz).

Event density was calculated as the number of detected events within the window preceding the mental state report, divided by the total duration of the window (i.e. 10s).

Statistical Analysis

Behavioral data were analyzed using linear mixed-effects models implemented in RStudio with the lme4 (Bates et al., 2015), lmerTest (Kuznetsova et al., 2017), and emmeans package (Lenth et al., 2025). Fixed effects included mental state and group (NT1 vs. controls), and random intercepts were included for each participant. P-values for fixed effects were obtained using the lmerTest package, and post-hoc pairwise comparisons were corrected for multiple comparisons using the false discovery rate (FDR) method.

EEG data were analyzed in Python using the statsmodels package and custom scripts (Seabold and Perktold, 2010). Statistical comparisons across electrodes were conducted using cluster-based permutation tests to control for multiple comparisons (200 permutations), focusing on spatiotemporal clusters of significance rather than isolated electrodes.

Ethics

The study received approval from the Comité de Protection des Personnes (CPP Île-de-France VI, ID RCB: 2022-A01636-37) and was sponsored by the Assistance Publique – Hôpitaux de Paris (AP-HP). All participants provided written informed consent prior to inclusion.

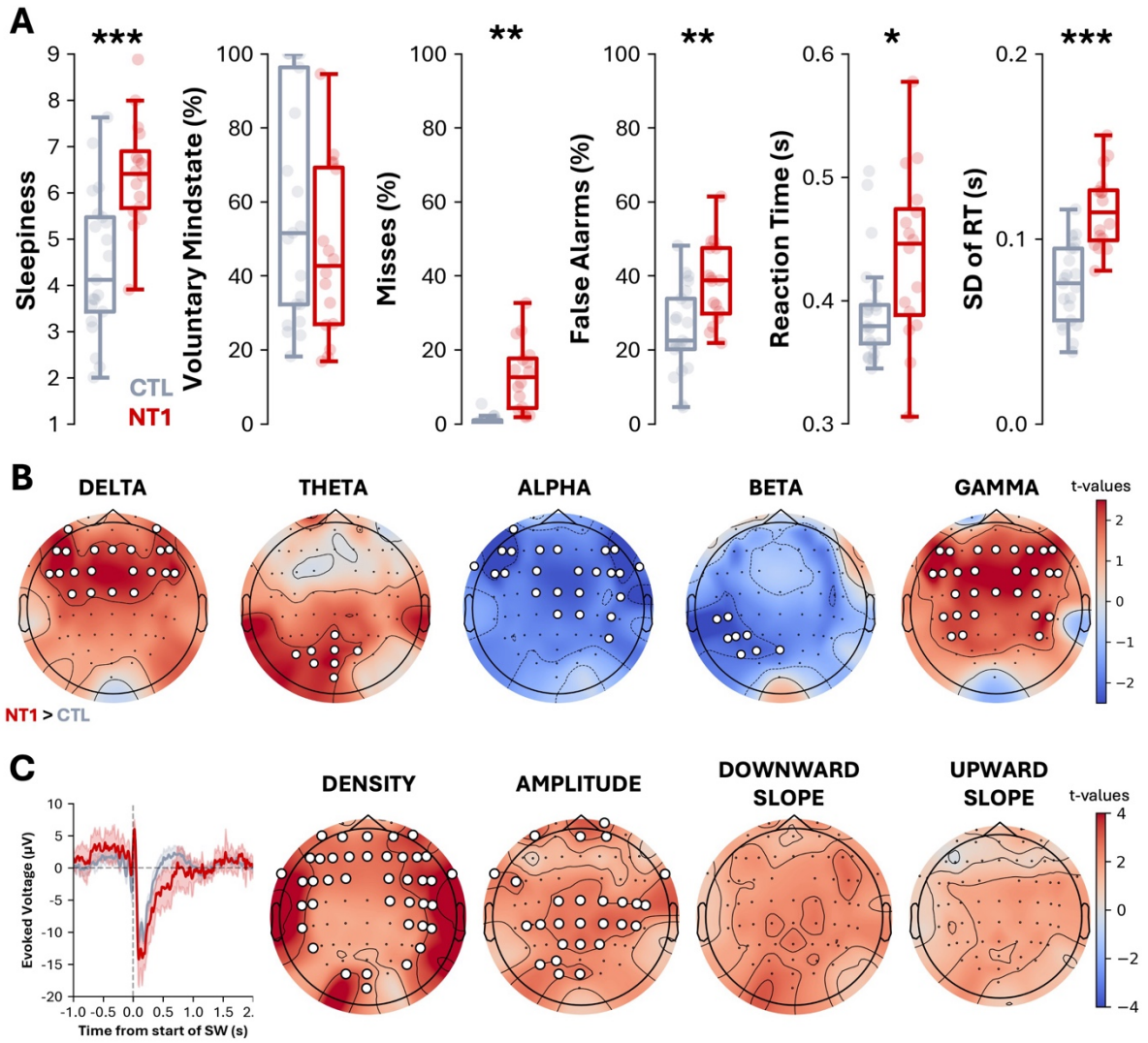

Figure 3.2. Group differences between NT1 and CTL. A By group from left to right, subjective sleepiness ratings on the Karolinska Sleepiness Scale (KSS), voluntary mind state percentage, miss rate, false-alarm rate, correct reaction time on Go trials, and its standard deviation. Boxplots show median, 25th–75th percentiles (IQR), whiskers to ±1.5×IQR, with subjects as individual points. Each subject is represented as transparent dot behind the boxplots. **B** NT1 vs CTL statistical maps of periodic band power within the different frequency bands (from left to right, delta, theta, alpha, beta, and gamma). **C** On the left, slow waves waveform per groups, shading represent the standard error of the mean per participants, then topographical maps of slow waves features are shown (from left to right, density, amplitude, downward, and upward slope). Statistics: linear mixed models with cluster correction for multiple comparison. $p < 0.05$: *, $p < 0.01$: **, $p < 0.001$: ***.

Results

Subjective and behavioral differences between NT1 and controls.

First, we compared subjective reports of participants with NT1 compared to controls. When comparing the percentage of mind-state report between CTL and NT1, we observed a decrease in ON report in NT1 (37.8 ± 4.7 vs. 60.3 ± 4.1; ß = -0.23, $p < 0.001$), and an increase in report of

hallucinations (16.7 ± 3.4 vs. 2.4 ± 0.8; ß = 0.14, p < 0.001). We observed an increase in forgot report in NT1 (10.8 ± 3.0 vs. 2.9 ± 1.3; ß = 0.08, p = 0.038, **Figure 3.1B**). We did not observe differences of percentage of MW nor MB. In terms of differences in subjective sleepiness, participants with NT1 reported higher level of subjective sleepiness on the KSS compared to CTL (6.3 ± 0.1 vs. 4.4 ± 0.1; ß = 1.96, p < 0.001; **Figure 3.2A**). In line with our hypothesis, hallucinations/illusions reports were commonly reported during wakefulness by participants with NT1, while controls almost never selected this option.

Beyond subjective experience, we examined objective behavioral performances during the SART. Compared to CTL participants with NT1 had higher rates of misses (12.8 ± 0.7 vs. 0.75 ± 0.1%; ß = 12.1, p < 0.001), false alarms (38.2 ± 1.1 vs. 25.8 ± 0.8%; ß = 12.5, p = 0.0019), slower response times (432.7 ± 3.3 vs. 392.7 ± 1.9ms; ß = 0.043, p = 0.025), and higher variability of response times (114.3 ± 1.9 vs. 75.6 ± 1.1ms; ß = 0.04, p < 0.001; **Figure 3.2A**). Altogether, these behavioral impairments reflect a state of hypovigilance in NT1, in line with the disorder's clinical profile and supporting the task's sensitivity to reveal modulations of attentional lapses in clinical groups.

EEG differences between NT1 and controls

Building on this behavioral profile of reduced vigilance in NT1, we next examined whether these differences were mirrored in the electrophysiological signal. Thus, to clarify the differences between the two groups we computed the relative power spectrum between group across the different frequency bands (see **Methods**). We observed clear differences in all bands (**Figure 3.2B**). Compared to CTL, participants with NT1 had higher frontal relative delta ($t_{CLUSTER}$ = 48.1, $p_{CLUSTER}$ ≤ 0.01), higher occipital relative theta ($t_{CLUSTER}$ = 17.6, $p_{CLUSTER}$ ≤ 0.01), and higher fronto-central relative gamma ($t_{CLUSTER}$ = 66.4, $p_{CLUSTER}$ ≤ 0.01). Yet, participants with NT1 had lower frontal relative alpha ($t_{CLUSTER}$ = -14.8, $p_{CLUSTER}$ ≤ 0.01) and left parieto-occipital relative beta (tcluster = -18.3, $p_{CLUSTER}$ ≤ 0.01).

Beyond spectral power differences, we investigated whether slow waves were more prevalent in NT1. These SW intrusions during wakefulness are typically associated with lapses of vigilance and increase with time spent awake (Andrillon et al., 2021). To this end, we automatically detected slow waves in the EEG signal preceding probe reports and compared their density and amplitude between groups (see **Methods** for details). Compared to CTL, NT1 had higher density of SW over fronto-temporal regions ($t_{CLUSTER}$ = 122.1, $p_{CLUSTER}$ ≤ 0.01) and occipital regions ($t_{CLUSTER}$ = 8.2, $p_{CLUSTER}$ ≤ 0.01). Participants with NT1 had higher SW amplitude than CTL across centro-posterior regions ($t_{CLUSTER}$ = 92.7, $p_{CLUSTER}$ ≤ 0.01) and frontal region ($t_{CLUSTER}$ = 13.1, $p_{CLUSTER}$ ≤ 0.01).

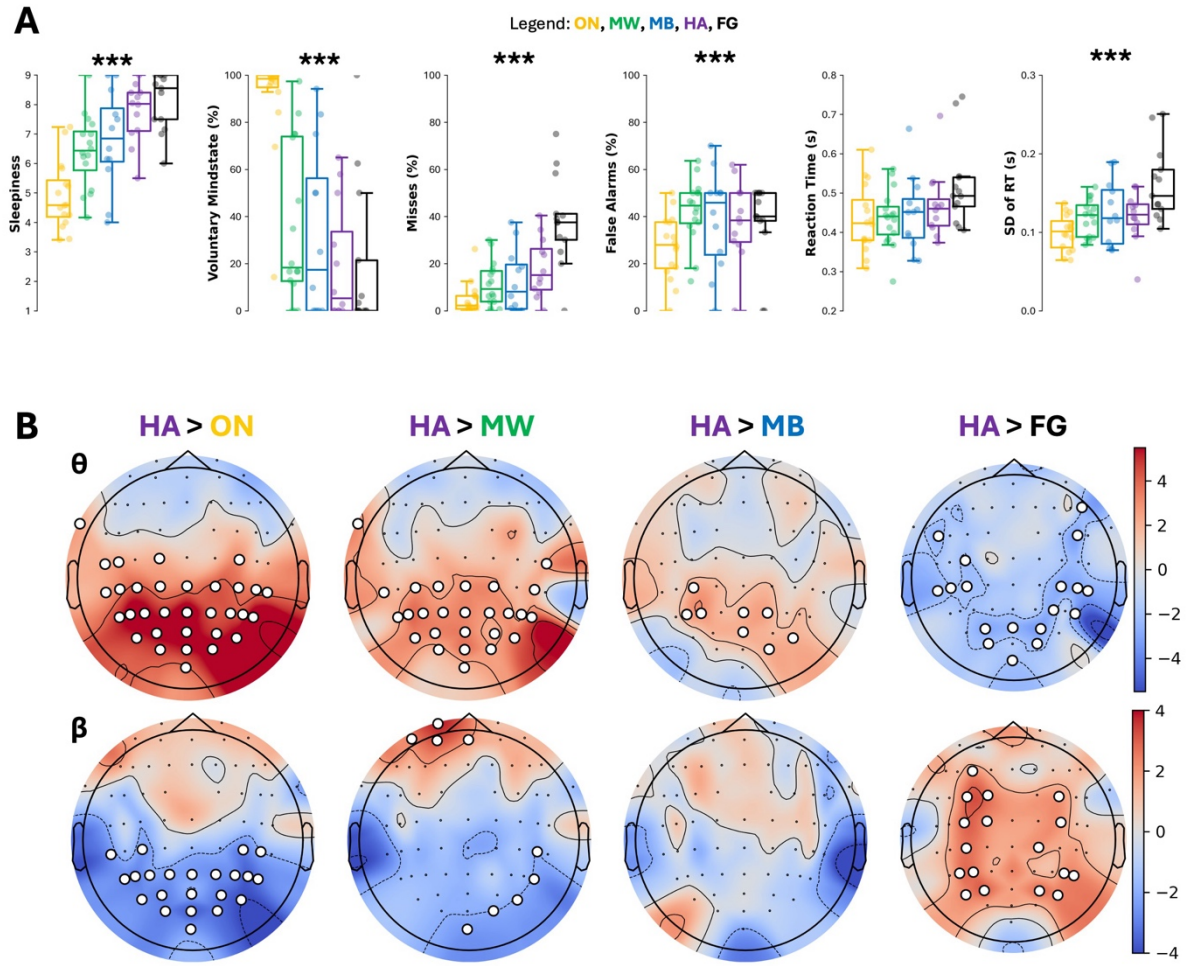

Figure 3.3. Hallucinations behavioral and electrophysiological signature. A By mind state within NT1 from left to right, subjective sleepiness ratings on the Karolinska Sleepiness Scale (KSS), voluntary mind state percentage, miss rate, false-alarm rate, correct reaction time on Go trials, and its standard deviation. Boxplots show median, 25th–75th percentiles (IQR), whiskers to ±1.5×IQR, with subjects as individual points. Each subject is represented as transparent dot behind the boxplots. Each subject is represented as transparent dot behind the boxplots. **B** Statistical maps of comparison between mind state within NT1. Relative periodic theta on the top row, relative periodic beta on the bottom row. From left to right, HA compared to ON, MW, MB, and FG. Statistics: linear mixed models with FDR correction for multiple comparison for the behavioral features, only main effect are showed here (see Results for post-hoc tests): $p < 0.05$: *, $p < 0.01$: **, $p < 0.001$: ***. linear mixed models with cluster correction for multiple comparison for the EEG features, white dot means $p < 0.05$.

In addition to SW which provide a marker of local NREM sleep intrusions, we investigated transient theta bursts. Theta bursts may capture different aspects of sleep-wake instability and possibly reflect early features of REM-like dynamics during wakefulness. We detected theta bursts and computed the density of these events preceding mind-states reports. Interestingly, participants with NT1 had a peak of density over parieto-occipital regions that the CTL group did not show (**Figure 3.4A**). When doing group comparisons, we did observe an increase in theta bursts density over parieto-occipital in participants with NT1 compared to CTL ($t_{CLUSTER} = 13.4$, $p_{CLUSTER} \leq 0.01$). Then we observed how theta bursts correlate with behavior in the two groups (**Figure 3.4B**).

In CTL, when frontal and parietal theta bursts density decreases, the rate of false alarms increases ($t_{CLUSTER}$ = -22.3, $p_{CLUSTER} \leq 0.01$, and $t_{CLUSTER}$ = -13.2, $p_{CLUSTER} \leq 0.01$ respectively). In both groups, when theta bursts density increases, the rate of misses increases (CTL: $t_{CLUSTER}$ = 14.9, $p_{CLUSTER} \leq 0.01$, NT1: $t_{CLUSTER}$ = 28.7, $p_{CLUSTER} \leq 0.01$).

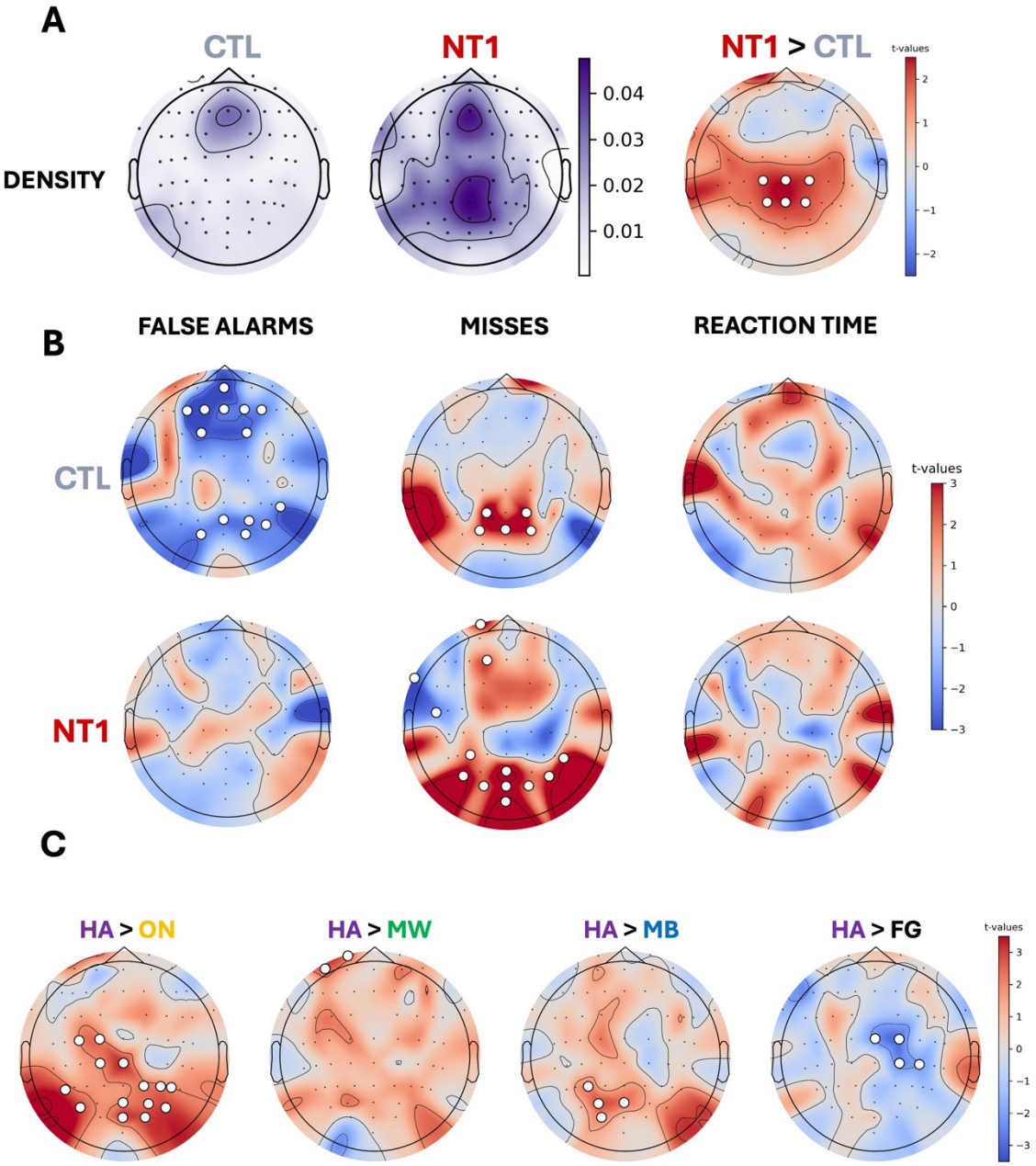

Figure 3.4. Hallucinations behavioral and electrophysiological signatures. A Topographies of theta burst densities according to the group, group comparison on the right. **B** Main effect of theta bursts density on behavioral metrics, from left to right: false alarms, misses, reaction time. **C** Statistical comparison between mind states within NT1 with HA, from left to right: HA compared to ON, MW, MB, and FG. Statistics: linear mixed models with cluster correction for multiple comparison for the EEG features, white dot means $p < 0.05$.

Hallucinations are not errors of report, and have clear behavioral and EEG signatures

We now turned to examining the behavioral and electrophysiological signature of hallucinations. To do so, we restricted our analysis to the NT1 group as they reliably reported hallucinations during the SART. Within NT1, HA reports were behaviorally different compared to the other mind states (**Figure 3.3A**). HA reports were associated with higher sleepiness compared to ON (ß = 2.825, $p < 0.001$), MW (ß = 1.306, $p < 0.001$), and MB (ß = 1.457, $p < 0.001$). HA reports were associated with higher rate of misses compared to ON (ß = 15.10, $p < 0.001$), MW (ß = 8.11, $p < 0.001$), and MB (ß = 9.26, $p < 0.001$) but lower rate of misses compared to FG (ß = 11.88, $p < 0.001$). HA reports compared to ON were associated with higher rate of false alarms (ß = 14.627, $p < 0.001$) and variability of reaction time (ß = 0.02837, $p < 0.001$). HA reports were associated with less intentionality compared to ON (HA: ß = -0.67, $p < 0.001$).

Within NT1, HA reports are associated with different electrophysiological signatures than the other mind states report (**Figure 3.3B**). HA reports are associated with increased relative occipital theta compared to ON ($t_{CLUSTER} = 139.8$, $p_{CLUSTER} \leq 0.01$), MW ($t_{CLUSTER} = 73.4$, $p_{CLUSTER} \leq 0.01$), and MB ($t_{CLUSTER} = 7.5$, pcluster = 0.01). Yet, HA reports are associated with lower temporo-occipital theta compared to FG ($t_{CLUSTER} = -11.5$, $p_{CLUSTER} \leq 0.01$). HA reports are associated with lower occipital beta compared to ON ($t_{CLUSTER} = -62.7$, $p_{CLUSTER} \leq 0.01$), MW ($t_{CLUSTER} = -10.6$, $p_{CLUSTER} \leq 0.01$). Yet HA reports are associated with increase left frontal beta compared to MW ($t_{CLUSTER} = 11.4$, $p_{CLUSTER} \leq 0.01$), and increased central beta compared to FG ($t_{CLUSTER} = 26.3$, $p_{CLUSTER} \leq 0.01$).

Lastly, we observed within NT1, how the theta bursts density would change in all mind states compared to HA. HA reports were associated with increased theta bursts density around occipital regions compared to ON ($t_{CLUSTER} = 29.5$, $p_{CLUSTER} \leq 0.01$), and MB ($t_{CLUSTER} = 9.3$, $p_{CLUSTER} \leq 0.01$). HA reports were associated with increased in theta bursts over left frontal regions compared to MW ($t_{CLUSTER} = 5.1$, $p_{CLUSTER} \leq 0.05$). HA reports were associated with decreased density in theta bursts around right central area compared to FG ($t_{CLUSTER} = -9.3$, $p_{CLUSTER} \leq 0.01$).

Distinct subjective and behavioral profiles of non-hallucinatory mind-states in NT1

To further explore the diversity of subjective states experienced by participants with NT1, we compared all reported mind states in terms of subjective experience and objective performance.

FG reports were associated with higher sleepiness compared to ON (ß = 3.146, $p < 0.001$), MW (ß = 1.626, $p < 0.001$), and MB (ß = 1.778, $p < 0.001$). FG reports were associated with higher rate of misses compared to ON (ß = 26.98, $p < 0.001$), MW (ß = 19.99, $p < 0.001$), MB (ß = 21.14, $p < 0.001$). FG reports were associated with higher rate of false alarms compared to ON (ß = 16.762, $p < 0.001$). FG reports were associated with higher variability of reaction time compared to ON (ß = 0.04346,

p < 0.001), MW (ß = 0.023, p = 0.003), and MB (ß = 0.02710, p = 0.003). FG reports were less intentional than ON (ß = -0.72, p < 0.001), MW (ß = -0.19, p = 0.032), and MB reports (ß = -0.20, p = 0.036).

MW and MB reports were associated with increased sleepiness and degraded performance compared to ON. Participants reporting MW or MB exhibited higher subjective sleepiness than ON (MW: ß = 1.519, p < 0.001; MB: ß = 1.368, p < 0.001). These off-task states were also linked to more frequent misses (MW: ß = 6.99, p < 0.001; MB: ß = 5.83, p = 0.011), more false alarms (MW: ß = 13.135, p < 0.001; MB: ß = 14.359, p < 0.001), and greater variability in reaction times (MW: ß = 0.02, p < 0.001; MB: ß = 0.016, p = 0.035) relative to ON reports. MW and MB reports were less intentional than ON (MW: ß = -0.53, p < 0.001; MB: ß = -0.52, p < 0.001).

Discussion

Individuals diagnosed with NT1 share very specific sleep and wakefulness disruptions such as excessive daytime sleepiness and sleep attacks, sudden episodes of cataplexy, fragmented nighttime sleep, and abnormal transitions between sleep stages, particularly from wakefulness into REM sleep. These symptoms reflect the loss of hypocretin-producing neurons in the hypothalamus, which disrupts the regulation of arousal and REM sleep. NT1 also impacts the subjective experience with an increase in dreaming and lucid dreaming overnight (Dodet et al., 2015), a struggle to sustain attention for long periods of time during the day and may also experience increased creative thinking (Lacaux et al., 2019). Relatedly, individuals with NT1 also experience hallucinations or illusions characterized by vivid imagery that occurs at the boundary between wakefulness and sleep. It has been hypothesized that these experiences result from the intrusion of sleep features, especially REM sleep, into wakefulness, yet testing this hypothesis has proven challenging given the elusiveness of hallucinations.

Here, we compared two groups of individuals: one group diagnosed with NT1, and one group composed of controls matched for age and gender. Every participant performed a long sustained-attention task, which is known to elicit many attentional lapses. The controls showed a typical pattern of responses with only 60% of task-focused responses, the remaining 40% being mostly split between MW, MB and not remembering. Unsurprisingly, control participants only rarely selected the hallucination/illusion option. In contrast, the individuals within the NT1 group showed a subjective and behavioral profile in line with the standard clinical characterization of NT1. NT1 patients made both more false alarms and more misses, illustrating an increase in behavioral variability through a mixture of impulsivity (false alarms) and sluggishness (misses, slow response times). This volatile behavior is reflected in the increase in response time variability at the behavioral level. At the subjective level, NT1 patients reported the same amount of MW, MB

and not remembering but also reported a large amount of hallucinations/illusions at the expense of task-focused states. Participants with NT1 also declared being sleepier and engaging in task-related or unrelated thoughts less intentionally. Overall, these results suggest that NT1 patients experience more frequent lapses of attention compared to controls and that part of these lapses underlie a very specific kind of experiences: hallucinations and illusions.

Our study demonstrates that hallucinatory episodes can be reliably captured and studied in controlled cognitive settings, alongside other forms of spontaneous mental states. Compared to on-task reports, hallucinations were associated with higher subjective sleepiness, reduced voluntary control, and impaired behavioral performance. Compared to MW and MB, HA reports were associated with increased subjective sleepiness and misses. Based on these results, it is unlikely that participants picked the hallucination/illusions options at random. Rather, hallucinations/illusions could form a category of conscious experience distinct of other classical forms of attentional lapses such as MW and MB. When considering sleepiness, intentionality, or performance, hallucinations/illusions were closest to "not remembering". In particular, both mind states had very high sleepiness rating which could suggest that they both represent states of low arousal and the transition toward sleep.

More generally, much like psychedelic states or dreaming, hallucinations reported by participants with NT1 can be situated on the conceptual landscape of the dynamical framework of thoughts (Girn et al., 2020). Indeed, participants reported very low levels deliberate constraints when experiencing hallucinations. Moreover, the increase in sleepiness and behavioral lapses suggests a loosening of automatic constraints as well. Hallucinations may represent the upper extreme of spontaneity during wakefulness, very close to dreaming.

From the electrophysiological perspective, our findings suggests that the brains of participants with NT1 can sometimes operate at the boundary between wakefulness and sleep. During hallucinatory reports, we observed a pronounced increase in occipital theta activity compared to ON, MW, and MB states. While theta activity has often been linked to cognitive control when expressed over frontal regions (Cavanagh and Frank, 2014; Snipes et al., 2022), its increase has been observed during NREM stage 1 (Santamaria and Chiappa, 1987) and following sleep deprivation (Snipes et al., 2022). This pattern may reflect a disengagement from sensory processing or an early signature of local sleep intrusion. In parallel, beta power decreased over posterior regions, consistent with reduced cortical activation and cognitive engagement (Lundqvist et al., 2024). We also observed an increase of beta power in frontal regions compared to MW, the origins of which remain unknown. Participants with NT1 compared to CTL had a higher SW density over frontal, temporal and occipital regions. SW amplitude was also higher over central and parietal regions in NT1 compared to CTL. Participants with NT1 also exhibited a distinctive

peak of theta burst density over parieto-occipital regions, a feature absent in controls. Their spatial topography in NT1 is reminiscent of theta oscillations at sleep onset (Santamaria and Chiappa, 1987) or REM sleep (Hutchison and Rathore, 2015), raising the possibility that they may constitute localized expressions of REM-like dynamics during wakefulness. Nonetheless, caution is needed in interpreting these results. Rather than conforming neatly to wake, NREM, or REM classifications, these oscillatory patterns might reflect a hybrid state, shaped by the unique instability of sleep-wake architecture in NT1.

The electrophysiological analyses revealed that hallucinations in NT1 were not only subjectively distinct but also associated with specific patterns of brain activity. These episodes were marked by increased theta power over occipital regions and decreased beta power in posterior areas. Both features typically observed during transitions toward sleep and early stages of NREM sleep. Intriguingly, hallucinations were also accompanied by an increase in theta bursts, particularly over parieto-occipital regions, which were largely absent in controls. While the functional role of these bursts remains debated, their topography and temporal dynamics resemble the early manifestations of REM sleep or REM-related oscillations such as sawtooth waves. Interestingly, in animal models, during REM sleep onset, ponto-geniculo-occipital (PGO) waves: phasic bursts originating in the pons and propagating to the occipital cortex have been associated with dreaming and appear during wakefulness under LSD (Brooks, 1975). In addition, a correlation between theta bursts pontine waves has been observed in rodents (Karashima et al., 2005). Although their human equivalent remains elusive, the spatial distribution and timing of the theta bursts observed here may echo such mechanisms. This raises the question of whether these parieto-occipital bursts could reflect a homologous process or represent the cortical echo of subcortical REM-related activity. Given that individuals with NT1 are prone to sleep-onset REM periods and that hallucinations often occur at sleep-wake boundaries, one possibility is that these episodes reflect brief, localized expressions of REM-like activity during wakefulness. However, this interpretation must be approached with caution. The observed electrophysiological patterns could reflect a hybrid state that combines elements of both wakefulness and different sleep stages. These results reaffirm a growing view in sleep research: that brain states may be better conceptualized on a continuum with overlapping dimensions rather than as strictly discrete stages (Andrillon and Oudiette, 2023).

While our investigation focused on NT1, the specific neural and behavioral signatures observed in hallucinatory episodes raise the question of whether similar mechanisms could be at play in other clinical populations. Hallucinations are also common in disorders such as Parkinson's disease, Lewy Body Dementia, Kleine-Levin Syndrome, or schizophrenia. Interestingly, these conditions are often marked by comorbid sleep disturbances, excessive daytime sleepiness, and altered REM

sleep dynamics. For instance, sleep-onset REM periods have been documented in Parkinson's disease (Bargiotas et al., 2019), and fragmented sleep is a hallmark of schizophrenia (Ferrarelli, 2021). Could hallucinations in these populations also reflect transient intrusions of sleep-like activity into wakefulness, as suggested here in NT1? Although these disorders differ in etiology and pathophysiology, they may share vulnerability to sleep-wake boundary instability. Investigating whether electrophysiological markers like those identified in NT1, such as theta bursts or hybrid spectral profiles in these populations, could provide new insights into the mechanisms underlying hallucinations across conditions.

Acknowledgements

ALC was supported by a grant from Ecole Doctorale Frontières de l'Innovation en Recherche et Education–Programme Bettencourt and the Fondation pour la Recherche Médicale (FDT202404018709). TA was supported by a grant from the Agence Nationale pour la Recherche (ANR-22-CE37–0006-01) and from the European Research Council (ERC-StG SleepingAwake 101116748). The data collection took part in the CENIR platform of the Paris Brain Institute. Sincere thank goes to Marie, Laurent, Amandine, and Berenice.

3. 3 Appendix

Note on the Appendix of Study 3:

For **Study 3**, I collected data from 23 healthy controls, 18 participants with NT1, and 7 participants with idiopathic hypersomnia with long sleep time (IH). The aim was to compare the impact of excessive daytime sleepiness on sustained attention in two clinical groups with different underlying neurological mechanisms. Recruiting participants with IH proved more difficult than recruiting those with NT1, as discontinuing treatment was too complicated for most of the individuals contacted. Data collection in the IH group is therefore still ongoing.

While the focus of this study is on hallucinations reported by NT1 participants, the supplementary appendix presents preliminary and uncorrected results comparing IH to controls. This appendix offers a complementary perspective on how hypersomnolence manifests across distinct neurological conditions. My goal is to publish the results obtained with IH individuals in a separate publication once data collection will be completed.

Appendix of Study 3

Idiopathic hypersomnia with long sleep time (IH) is a rare sleep disorder characterized by excessive daytime sleepiness despite normal or prolonged sleep duration (Sateia, 2014). This disorder is also associated with difficulties with awakening, despite normal or better than normal sleep architecture (See **Study 2**). While patients often report severe impairments in daytime vigilance and attention, the neural correlates of these symptoms remain poorly understood (Billiard and Sonka, 2022). In this appendix, I present preliminary comparisons between IH participants and healthy controls based on a sustained attention to response task (SART) and concurrent EEG recordings. These results aim to provide an initial electrophysiological characterization of attentional lapses in IH, complementing **Study 3**.

We first compared the subjective experience and behavioral performances of IH to controls. Participants with IH reported being less often ON (ß = -0.1, p = 0.003). This is due to a higher proportion of MW (ß = 0.12, p = 0.01) as the proportion of MB, HA and FG were similar across groups. Furthermore, participants with IH reported higher levels of subjective sleepiness than controls (ß = 2.3, p = 0.004). Participants with IH had worse performance than controls, with a higher proportion of missed responses (ß = 5.0, p = 0.049), longer reaction times (ß = 0.05, p = 0.02), and greater variability in reaction times (ß = 0.02, p = 0.01; **Figure SA 3.1**).

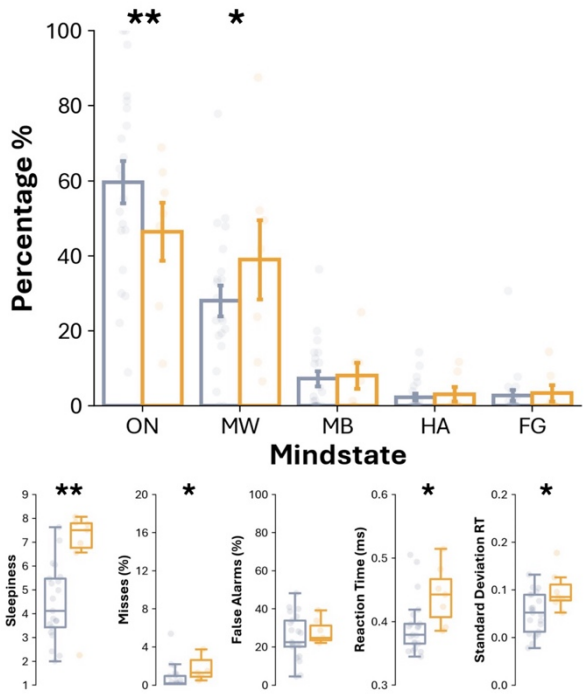

Appendix Figure 3.1: Subjective and behavioral differences between groups. Top row, percentage of each mind state according to the group. Bottom row, by group from left to right, subjective sleepiness ratings on the Karolinska Sleepiness Scale (KSS), miss rate, false-alarm rate, correct reaction time on Go trials, and its standard deviation. Boxplots show median, 25th–75th percentiles (IQR), whiskers to ±1.5×IQR, with subjects as individual points. Each subject is represented as transparent dot behind the boxplots. Statistics are linear mixed models, corrected for multiple comparison with FDR; p < 0.05 : *, p < 0.01 : **, p < 0.001 : ***.

To characterize the differences between the two groups in terms of brain activity, we compare the electrophysiological signature between groups. Despite behavioral and subjective differences, classical EEG markers including band power of the periodic activity and slow wave density did not significantly differ between IH and controls (**Figure Appendix 3.2**). However, IH participants exhibited a higher density of theta bursts. This increase in theta bursts

for IH patients had a different spatial distribution than the one observed in NT1 patients (**Figure 3.4A**). In IH, theta bursts seem more diffusely distributed across occipital areas, whereas in NT1 they were more focal and of greater density (**Figure Appendix 3.3**).

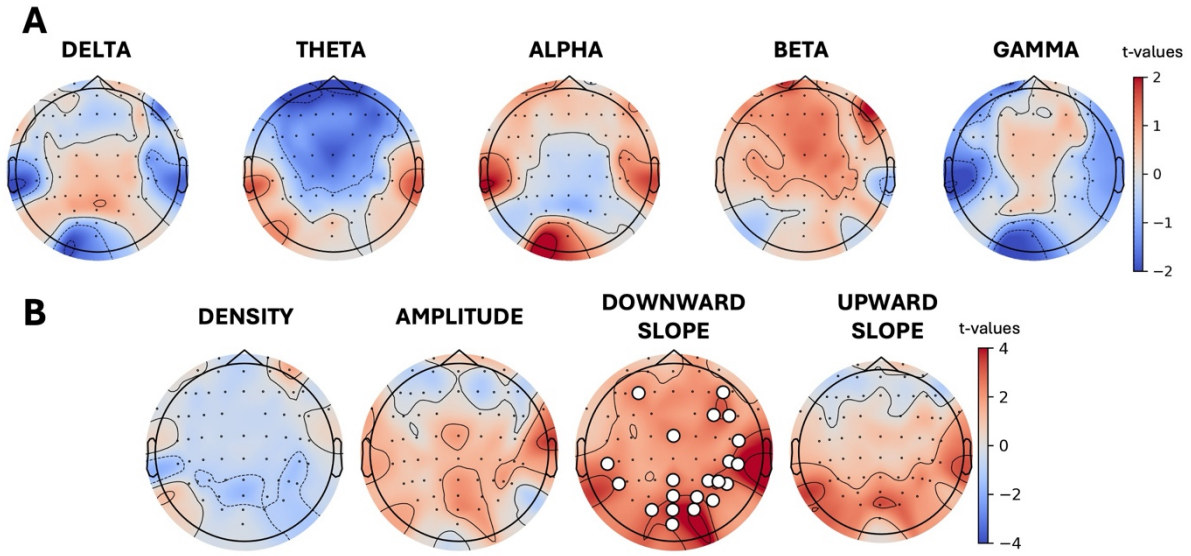

Appendix Figure 3.2: A IH vs CTL statistical maps of relative periodic band power within the different frequency bands (from left to right, delta, theta, alpha, beta, and gamma). B Topographical maps of slow waves features are shown (from left to right, density, amplitude, downward, and upward slope). Statistics: linear mixed models, white circle means $p < 0.05$.

In controls, higher theta burst density was associated with fewer false alarms. This relationship was not observed in IH participants (nor in NT1, **Figure 3.4B**). In contrast, higher theta burst density in IH was positively associated with increased misses, especially in occipital regions (**Figure Appendix 3.3**). Additionally, theta burst density in occipital electrodes correlated with longer reaction times in the IH group. This pattern was not observed in controls or NT1 (**Figure 3.4B**). It is important to note however the relative small size of the IH sample.

Comparing ON reports within IH revealed a consistent increase in occipital theta bursts density during HA, MB, and FG compared to ON. These three states shared a very close topographical pattern. A distinct centro-parietal increase in theta burst density was observed during MW compared to ON. While reports of HA and FG states were rare in this group, the preservation of these categories allows for consistency with the comparisons presented in **Study 3**.

In summary, preliminary findings indicate that individuals with IH exhibit distinct electrophysiological patterns characterized by increased theta burst density. Unlike NT1, where theta bursts were focal and parieto-occipital, theta bursts in IH seems to show a more diffuse occipital distribution and were not specifically linked to hallucinations. Instead, these theta bursts have a similar signature in all off-task mind states compared to on-task (**Figure Appendix 3.3**). These observations suggest that theta bursts represent a heterogeneous phenomenon, potentially

differentiating between REM-like intrusions associated with vivid experiences in NT1, and more diffuse, NREM-like arousal reductions linked to cognitive sluggishness in IH.

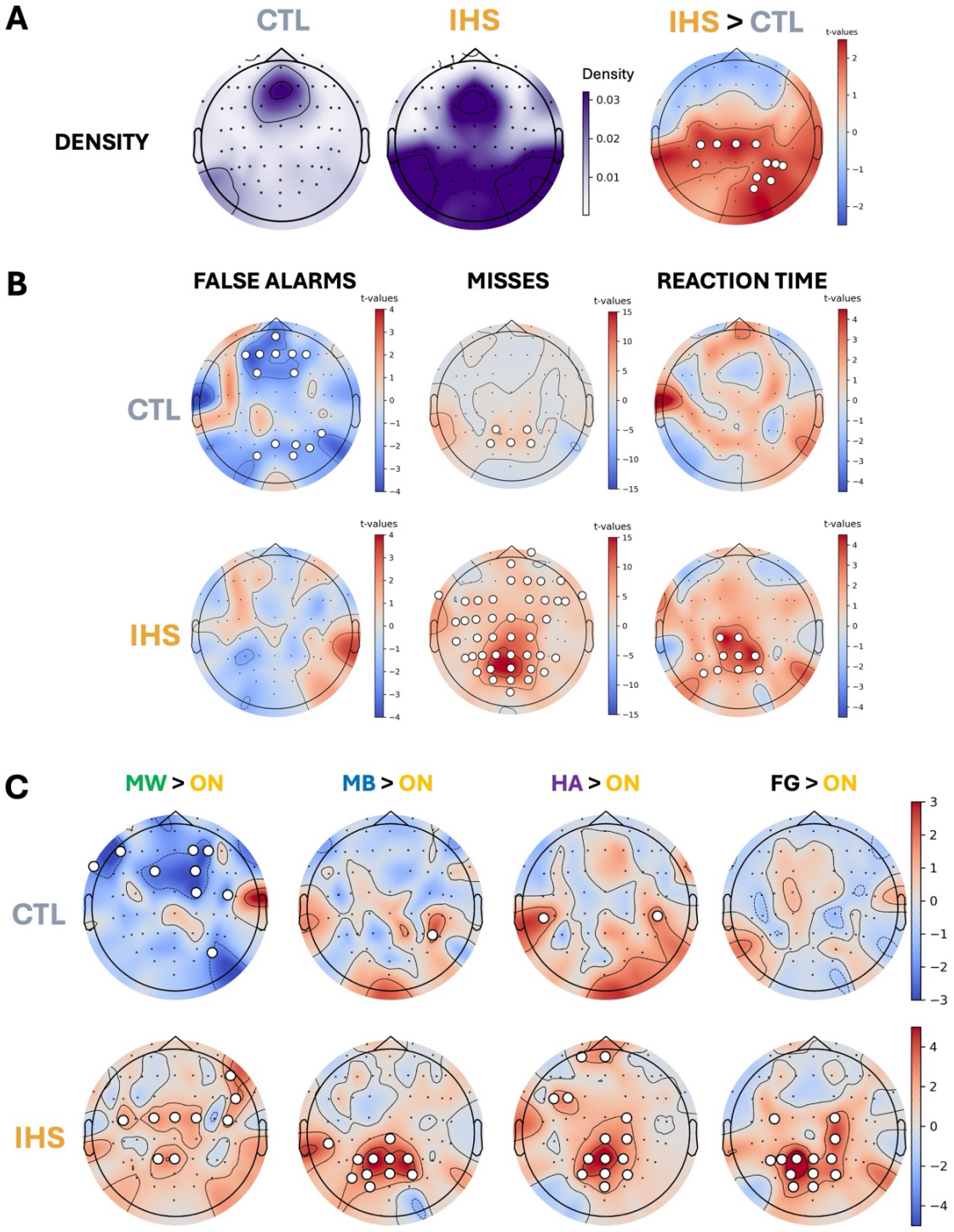

Supplemental Appendix Figure III. 3. Differences in theta burst density between groups and mind states. A Topographies of theta burst densities according to the group, group comparison on the right. **B** Main effect of theta bursts density on behavioral metrics, from left to right: false alarms, misses, reaction time. **C** Statistical comparison between mind states within CTL (top row), and IH (bottom row) with ON, from left to right: MW compared to ON, MB, HA, and FG. Statistics: uncorrected linear mixed, white dot means $p < 0.05$.

Study 4
Spontaneous Thoughts from Laboratory Settings to Real Life

In Preparation

Arthur Le Coz[1, 2*], Guillaume Oiry[1], Julissa De Los Santos[1],
Conor Shatto[3], Alfredo Spagna[3], Thomas Andrillon[1*]

[1] Sorbonne Université, Institut du Cerveau - Paris Brain Institute - ICM, Inserm, CNRS, AP-HP, Hôpital de la Pitié Salpêtrière, Paris, France.

[2] Université Paris Cité, Paris, France.

[3] Columbia University, Psychology Dept., NY, USA

* Corresponding Authors

4. 1. Digest

Mind wandering is often presented as a core aspect of human cognition. Accordingly, humans would spend a third of their life thinking about something else than the task at hand. Yet, research on mind wandering is often performed in the context of a lab or activities that are far from our everyday life (e.g., SART task). This particular setting enables researchers to control what participants are supposed to do and their environment. It also allows them to collect neuroimaging data to understand the brain mechanisms associated with mind wandering and the generation of spontaneous experiences. But are these methods, which I have extensively used in the previous Chapters, suited to explore how spontaneous experiences occurs throughout our life and impact cognition? In this Chapter, I sought to complement the traditional lab-centred investigation of mind wandering by devising a methodological approach allowing to catch mind wandering (and other types of spontaneous experiences) “in the wild”. The following chapter present a pilot study and a proof of concept to conduct experience sampling and EEG recordings in real-life situation. I am currently developing this approach toward translational applications with applications to start-up incubators and funding.

4. 2. Study

Abstract

Objectives: This study aimed to investigate spontaneous experiences (SE), their phenomenology, and their electrophysiological correlates in everyday life activities. Healthy participants were tested while working at their desk, or during meetings or lectures, which we compared to a standard controlled cognitive task commonly used in laboratory research (Sustained Attention to Response Task, SART). Our goal was here to test the impact of the task and context on the type and frequency of SE and their neural correlates.

Methods: We recruited 25 healthy adults (aged 18–37; 13 women). Brain activity was recorded using portable 8-channels EEG headsets. Each participant took part in one to three experimental conditions: (1) working on a computer (self-direct work), (2) an in-person lab meeting, (3) a classroom lecture and (4) a SART. During each session, participants were frequently probed to report: (1) their current mental state, (2) their confidence in the report, (3) whether the state was voluntary, and (4) their level of subjective sleepiness.

Results: Participants reported being more frequently focused when working on their own compared to during the meetings, lectures or SART. Task-unrelated thoughts (TUT) were most prevalent during the SART, followed by lectures, and were least frequent when participants were working on their own. Confidence in mental state reports was highest during self-direct work sessions, and lowest during the SART, with intermediate levels during meetings and lectures. Mental states were more often reported as voluntary during self-directed work sessions than during meetings or the SART, and more during meetings than during the SART. Subjective sleepiness followed a similar pattern: it was highest during the SART, followed by meetings, and lowest during self-directed work sessions. Spectral analyses are preliminary but revealed that theta power was higher during the SART compared to all other contexts, and higher during self-directed work compared to meetings and lectures. Delta power was elevated in classroom recordings relative to all other conditions.

Conclusion: Activities in which participants were allowed to work on their own were associated with fewer distractions, greater cognitive engagement, and more voluntary control over thought. The SART was characterized by a specific pattern of SE, which highlight the limitations of the classical approach of mind wandering research in generalizing to real-world settings. Our findings demonstrate that portable EEG can be used to detect classical neural markers of attention and mind wandering (e.g., spectral power) outside the lab. However, improving methods for cleaning

low-density EEG data collected in noisy real-life environments are needed to ensure sufficient signal quality for future applications.

Introduction

We spend up to half of our waking life thinking about something different than the task at hand (Kane et al., 2017). This phenomenon is often referred to as mind wandering (MW). MW has been linked to adaptive functions such as creativity (Baird et al., 2012) and future planning (Smallwood and Schooler, 2015), and detrimental outcomes such as reduced task performance (Andrillon et al., 2021) and may lead to increased risk of road accidents (He et al., 2011; Lemercier et al., 2014). More recently, another spontaneous mental state has gained attention: mind blanking (MB), during which individuals report an absence of mental content (Andrillon et al., 2025; A. Ward and Wegner, 2013). Yet, most research on MW and MB has been conducted in the laboratory, using experimental paradigms that are far from everyday life activities.

Mind wandering and MB are subjective, spontaneous, and private experiences. This makes them difficult to study systematically and objectively. Researchers have addressed this challenge by testing participants in controlled environments (e.g., the laboratory) and using simple and highly repetitive cognitive tasks such as the Sustained Attention to Response Task (SART, Robertson et al., 1997). This approach has several important pitfalls. A monotonous task like the SART can fail to motivate individuals to pay attention to it and may put them in a state of hypo-arousal, which could favor a certain type of spontaneous experiences. It is therefore no surprise that this approach has revealed a tight relationship between MW and MB and sleepiness, and its association with sleep-like activity in EEG recordings for example (Andrillon et al., 2021). Alternatively, mind wandering has been extensively studied in the context of reading or listening (Unsworth and McMillan, 2013; Varao-Sousa et al., 2018). These tasks have more ecological relevance compared to the requirements of working or studying, but participants are classically required to complete these tasks independently of their own goals, which could impact concentration and performance.

A large body of research has used the SART and other attentional tasks to investigate the neural underpinnings of MW. In terms of event-related potentials (ERPs), studies have shown that sensory-evoked components such as the P1, N1, and P3 are attenuated during MW, suggesting a functional decoupling from the external environment (Kam et al., 2022). This sensory decoupling could impair the optimal processing of sensory information and efficient completion of the task at hand. Spectral analyses have further shown that MW is often accompanied by increased low-frequency activity and decreased high-frequency activity (delta: 1-4Hz, theta: 4-8Hz vs beta: 16-30Hz respectively, Kam et al., 2022). Alpha activity (8-12Hz) has a complex relationship with MW because alpha oscillations are also affected by vigilance or the type of task at hand (e.g., visual or auditory task Bazanova and Vernon, 2014). Consequently, while some studies report increased

alpha power during MW (Bazanova and Vernon, 2014), others suggest more nuanced modulations depending on task demands and the nature of thoughts (Kam et al., 2022).

Beyond traditional EEG metrics, recent work has highlighted the association between MW and sleep-like slow waves (SW) during wakefulness. Detected during tasks like the SART, these transient local events in the EEG resemble the SW observed during NREM sleep (Andrillon et al., 2021). These SW appear to index fluctuations in arousal and sleepiness. In human and animal intracranial recordings, sleep-like SW have been associated with a reduction of neuronal firing rate (Sheybani et al., 2023; Vyazovskiy et al., 2011), which could result in behavioral errors (Vyazovskiy et al., 2011). In non-invasive recordings performed in humans, the spatial distribution of these SW appears to distinguish types of behavioral errors: SW over prefrontal electrodes is associated with impulsive responses such as faster responses and false alarms; whereas SW over posterior electrodes are linked to a form behavioral sluggishness, with slower response times and missed responses (Andrillon et al., 2021). These findings support the emerging paradigm of local sleep: the idea that certain cortical regions can briefly enter sleep-like states while the rest of the brain remains awake (Andrillon et al., 2019; Andrillon and Oudiette, 2024). Originally described in sleep-deprived animals (Vyazovskiy et al., 2011), local sleep can occur even in well-rested individuals and tends to increase with cognitive load and time-on-task (Bernardi et al., 2015b; Hung et al., 2013). Interestingly, the spatial distribution of these SW appears to differentiate mental states: larger SW over prefrontal electrodes is associated with MW whereas larger SW over posterior electrodes are linked to MB (Andrillon et al., 2021). These results suggest that spontaneous fluctuations of arousal could dynamically affect cortical activity with a slowing down associated with errors and lapses of attention.

However, most of these insights stem from highly controlled lab settings using a narrow range of cognitive tasks. Whether the same neural signature of MW and MB apply in real-life settings such as work, study, or commuting remains an open question. According to the contextual regulation hypothesis, the frequency and nature of SE are shaped by the cognitive demands of the environment (Andrews-Hanna et al., 2010; Smallwood and Schooler, 2015). Low-demand contexts promote task-unrelated thoughts (TUT) that may support creativity, while high-demand contexts suppress them due to their potential cost (Andrews-Hanna et al., 2010; Smallwood and Schooler, 2015). In addition, it is possible that lab settings and monotonous tasks could promote sleepiness, putting participants in a hypo-vigilant state that is not necessarily representative of their everyday life. This could be particularly relevant for certain populations, like individuals with ADHD or sleep disorders, who might struggle to stay focused on lab experiments (Pinggal et al., 2025; Van den Driessche et al., 2017).

In addition, MW is not a unitary phenomenon. Previous research has stressed the importance to distinguishing between mind wandering "with and without intention" since voluntary and involuntary MW differ in terms of phenomenology, cognitive consequences and electrophysiological correlates (Seli et al., 2016). Voluntary MW is often associated with increased alpha power (Martel et al., 2023) and short-term academic costs (Wammes et al., 2016). Whereas involuntary MW is linked to broader attentional failures and poorer long-term academic performances (Wammes et al., 2016). Moreover, participants are classically asked to report MW whenever they engage in stimulus-unrelated and task-unrelated thoughts. Yet, the divide between task-related and unrelated thoughts could be harder to grasp when participants engage in everyday life activity. Capturing this heterogeneity could prove essential for understanding how spontaneous cognition arises outside the lab.

Supporting this, experience sampling studies across extended periods have shown that predictors of MW identified in the lab, such as working memory capacity, fail to generalize to everyday life (Kane et al., 2017). Real-life contexts are marked by more fluctuating stress levels, which significantly modulate the frequency and nature of spontaneous thoughts (Linz et al., 2021). Distractions are more prevalent in real life compared to lab settings (Varao-Sousa et al., 2018). This suggests that MW and MB in real-life settings may be driven by different mechanisms, modulated by context, time of day, and cognitive demand.

In this study, we aim to bridge the gap between laboratory findings and real-life cognitive experience. Using experience sampling probes administered in diverse everyday contexts in the same individuals, we investigate how often people report task-related thoughts (TRT), TUT and MB. TRT refers to thoughts related to the ongoing task or activity. TUT captures thoughts unrelated to the current task, often spontaneous or internally driven. MB describes a state in which individuals report the absence of mental content. In addition, we explore how their brain activity fluctuates across both mental states and settings. This approach allows us to test whether the behavioral and neurophysiological markers identified in the lab hold in naturalistic environments.

Methods

Participants

Twenty-five healthy adult volunteers (aged 18 to 37; 13 women) were provided written informed consent prior to participation. Exclusion criteria included a diagnosis of attentional disorders, a history of neurological and/or psychiatric conditions, uncorrected hearing impairments, and physical characteristics that could interfere with EEG cap placement (e.g., bald scalp, braids,

dreadlocks). The study protocol was approved by the Sorbonne Ethics Committee (CER project ID: CER-2023-LE-COZ-EPICE).

Participants were recruited from the host laboratory and among students enrolled in cognitive science courses participating in the project (UEs from the Cogmaster, PSL-UPC-EHESS). Each participant took part in one to three of the four experimental contexts (SART, work, meeting, lecture), described in detail in **Table 1**. A total of 63 EEG recordings were collected. Twenty recordings were excluded from the analyses due to excessive artifacts. Additionally, five participants responded to in-task questionnaires without EEG recording within the class context.

Contexts

SART: Participants completed a standard sustained attention task (SART, Robertson et al., 1997), following the parameters described in (Andrillon et al., 2021). The SART was preceded and followed by 5-minute resting-state periods (RS1 and RS2, respectively), during which participants were instructed to remain awake with their eyes closed. EEG data were recorded throughout using a portable EEG headset. The task was implemented in PsychoPy (Peirce, 2007).

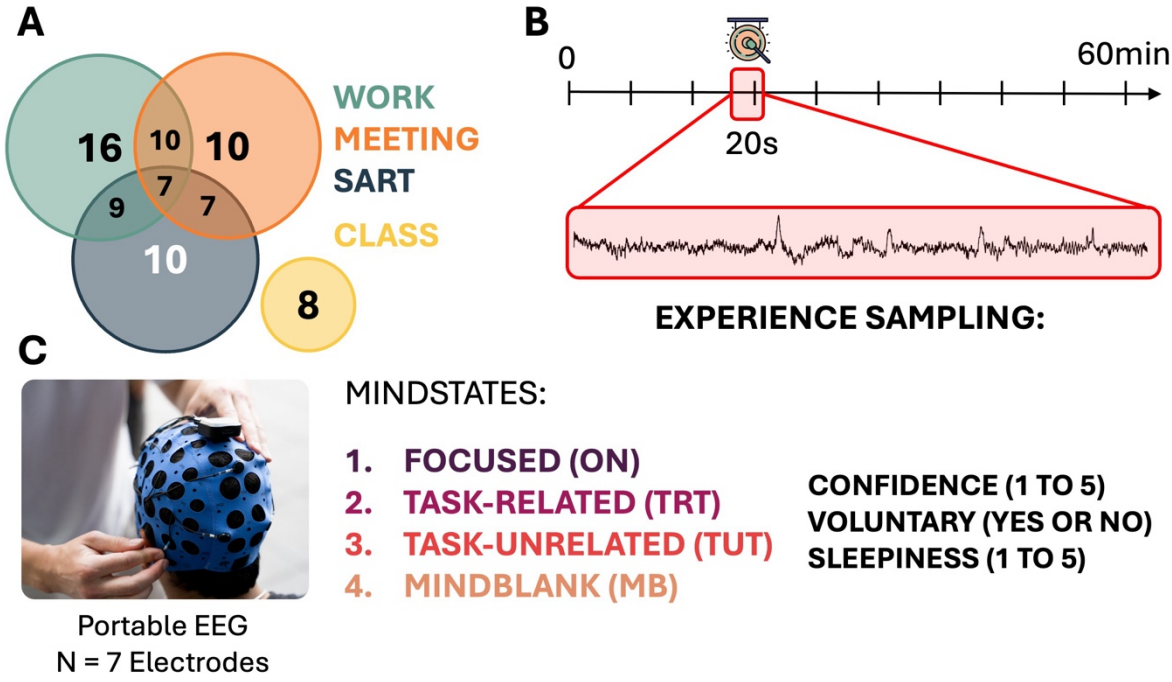

Figure 4.1: Experimental set up. A Amount of participant recruited, and which context they participated to. In green work, orange meeting, black SART, and yellow the class; total n = 25 participants. **B** Illustration of approximately 9 sound probe every 60 minutes of a given task. 20 seconds before each sound was analyzed and associated to the reported mindstate. **C** Picture of the portable EEG cap and amplifier used for the experiment. The participant could report being focused (ON), having task-related thoughts (TRT), task-unrelated thoughts (TUT), or mind blanking (MB). Then they reported how confident they were in this report on a scale of 1 to 5, if the mindstate was voluntary or not, and how sleepy they were on a scale of 1 to 5.

The SART is a Go/NoGo task where digits from 1 to 9 are presented in a pseudorandom order. Each digit was displayed for a duration randomly drawn from a uniform distribution ranging from 750 to 1250 ms. Participants were instructed to press the spacebar as quickly as possible whenever a digit appeared, except when the digit "3" was shown, in which case they had to withhold their response. Failure to press the spacebar for digits other than "3" was classified as a miss (omission error), while pressing the spacebar for the digit "3" was classified as a false alarm. Response time (time from digit onset to response) was also recorded. The task comprised four blocks with self-paced breaks between blocks, totalling approximately an hour of task time (excluding resting-state periods)

Table 2: Participants ID and the contexts they participated in. In the class context, some participants only answered to the thought sampling questionnaires noted "Q".

ID	WORK	MEETING	SART	CLASS	
129	✓	✓	✓		
175	✓	✓	✓		
525	✓	✓	✓		
527	✓	✓	✓		
255	✓	✓	✓		
910	✓	✓	✓		
495	✓	✓	✓		
738	✓	✓			
807	✓	✓			
524	✓	✓			
238	✓		✓		
331	✓		✓		
692	✓				
707	✓				
439	✓				
458	✓				
427			✓		
510				✓	
526				✓	
621				✓	
808				✓	
994				✓ + Q	
786				Q	
900				Q	
387				Q	
Totals:	16	10	10	5 + 4Q	**41 + 4Q**

Work: In this real-life context, participants—members of the research team—performed routine professional tasks (e.g., reading, writing, coding, data visualization or analysis, preparing presentations). As in the SART condition, the session was framed by two 5-minute resting-state periods (RS1 and RS2). EEG was continuously recorded using a portable EEG headset. Each session lasted approximately two hours.

Meeting: This condition took place in a real professional setting. Participants were recorded while attending a regular lab meeting that included a presentation (by someone not participating in the

EEG recording) followed by a group discussion. Participants wore a portable EEG headset for the duration of the meeting, which lasted approximately one hour.

Lecture: In this condition, participants attended a graduate-level lecture (Master 1, Research Master in Cognitive Science, ENS-EHESS-Université Paris Cité). Recordings were conducted with the agreement of the Cogmaster program administration, course coordinators, and lecturers. Due to the constraints of the setting, no resting-state periods were recorded. Some participants wore a portable EEG headset during the entire class. In order to estimate the influence of the EEG headset, we also asked other students attending the class to complete the self-report questionnaire (described later). Sessions lasted between 1.5 and 3 hours.

Thoughts Sampling

During all experimental contexts (excluding resting-state periods), participants were interrupted by auditory probes prompting them to report their mental state. In the meeting and lecture contexts, participants responded using paper questionnaires, while in the SART and work contexts, digital questionnaires were used. However, the same questions were provided to all participants. In the lecture, meeting, and work contexts, the number of mental probes per hour was set to nine. The inter-probes timings were computed following a Poisson's distribution ($\lambda = 9$).

In the SART task, the probe occurred every 30 to 70 seconds, based on a uniform random distribution. Each block included a fixed number of 15 probes.

At each probe, participants were asked to report their mental state immediately preceding the interruption. The probes were presented in English, as it was the shared language among all participants. They were asked to choose one of five attentional states:

(1) Focused on the task at hand (On Task, ON)
(2) Thinking about something related to the task (Task-Related Thought, TRT)
(3) Thinking about something unrelated to the task (Task-Unrelated Thought, TUT)
(4) Not thinking about anything (Mind Blanking, MB)
(5) Forgot (Forgotten, FG)

Participants also reported their confidence in their response on a scale from 1 ("Not at all confident") to 5 ("Extremely confident"), whether the mental state was intentional or not, and their level of sleepiness on a scale from 1 ("Very awake") to 5 ("About to fall asleep"). For paper questionnaires, they were also asked to note the time of the probe.

In total we collected 1,369 probes: 97 during meetings, 224 during lectures, 421 during work sessions, and 600 during SART.

EEG Recordings

We used portable EEG headsets (*Explore+* models) manufactured by *Mentalab*. These devices are equipped with nine dry electrodes positioned according to the international 10–20 system at the following locations: Fp1, Fp2, Fz, Cz, Pz, O1, O2, with M1 used as ground and M2 as the secondary reference. Data were recorded at a sampling rate of 250 Hz. These headsets have been validated and shown to provide reliable spectral analysis during resting-state recordings (Dirik et al., 2023).

Table 2: Quantity of epochs analyzed depending on the maximum amplitude threshold set per conditions (context or resting states), and per length of epochs (20 and 5 seconds).

Threshold	T20	T5	W20	W5	M20	M5	S20	S5	C20	C5	RS20	RS5
n	215	2772	40	1334	11	176	163	960	1	302	683	3298
%	21,8	70,4	34,0	50,0	11,8	98,7	24,4	97,8	0,8	62,4	71,9	86,8
ø	984	3936	338	1352	45	180	480	1920	121	484	936	3801

T: Totals (i.e. all context combined), W: Work, M: Meeting, C: Class, S: SART, RS: Resting State, 20: 20 seconds epochs, 5: 5 seconds epochs, ø: no threshold applied.

EEG Analyses

A subset of recordings (N = 20 out of 63) was excluded from analysis due to excessive artifacts. EEG preprocessing and analysis were conducted using the MNE-Python library (Gramfort et al., 2013).

Preprocessing

EEG channels were re-referenced to the average of the two mastoids (M1 and M2). The continuous signal was filtered using a zero-phase high-pass filter at 0.5 Hz, a low-pass filter at 40 Hz, and a notch filter at 50 Hz to remove electrical line noise. Bad channels were identified through visual inspection and excluded.

Data were first segmented into 20 second epochs preceding each probe onset. SW detection was performed on these 20 second segments. For more stringent artifact rejection in the spectral analysis, which is particularly sensitive to noise, these 20 second epochs were further divided into four non-overlapping 5 second segments prior to each probe. Only segments with a peak-to-peak

amplitude below 350 μV (threshold determined via visual inspection of segment-wise amplitude distributions) were retained for spectral analyses (see **Table 2** for quantities of epochs conserved per epochs length with this threshold). After rejection threshold, 21.8% of the 20s epochs and 70.4% of the 5s epochs were conserved and analyzed. Resting-state recordings were also segmented into 5 second epochs for spectral power analysis and 20 second epochs for SW detection, using the same amplitude threshold criteria. The same amplitude threshold were applied to the resting states recordings, 71.9 % of the 20s epochs and 86.8% of the 5s epochs were conserved and analyzed.

Spectral analysis

Power spectral density (PSD) was computed using Welch's method with Hamming windows, applied to 2 second epochs with 1 second overlap. PSDs were first averaged across segments for each probe, then across attentional states, sessions, and finally across subjects.

Spectral power was averaged within standard frequency bands: delta (1–4 Hz), theta (4–8 Hz), alpha (8–12 Hz), and beta (12–30 Hz). Both absolute power (mean power within each frequency band) and relative power (power in each band normalized by the sum of all bands) were computed.

Sleep-like slow waves

The SW detection was adapted from previous work on NREM sleep (Bernardi et al., 2015b; Riedner et al., 2007) and was modified to detect SW during wakefulness(Andrillon et al., 2021). SW were identified following a two-step preprocessing pipeline. First, EEG signals were down-sampled to 100 Hz and filtered using a zero-phase finite impulse response (FIR) band-pass filter (0.5–10 Hz) with automatically determined transition bandwidths, ensuring minimal edge artifacts while preserving waveform integrity. We then identified negative and positive zero-crossings in the filtered signal which were used to segment candidate SW. For each candidate wave, we computed the peak-to-peak (PTP) amplitude, that is the amplitude difference between the most positive and most negative peak between the start and end of the wave (consecutive zero-crossings). We then selected high-amplitude SW based on this PTP amplitude, which had to exceed a data-driven threshold, estimated for each channel and each participant in the first session (baseline). This threshold corresponded to the top 10th percentile on the distribution of PTP amplitude for each participant, electrode, within each condition (class, meeting, SART, work) and within resting-state recordings. For each SW, we further extracted the following parameters: (1) Maximal negative slope (descending phase), representing the voltage decline (in μV/s) between the first negative zero-crossing and the negative peak crossing divided by the duration between the negative zero-crossing and the negative peak (in sec); and (2) Maximal positive slope (ascending phase), reflecting the voltage increase between the negative peak and the subsequent positive zero-crossing divided

by the duration between the peak and the positive zero-crossing (in sec). Only waves with a descending and ascending slope between 0.25 and 2 μV/s were retained, ensuring the selection of physiologically meaningful SW. Finally, SW density was defined as the number of SW in each epoch before a thought probe divided by the duration of the epochs (20s). Event-related potentials (ERPs) time-locked to the onset of SW were computed using the filtered EEG signal (0.5–40 Hz).

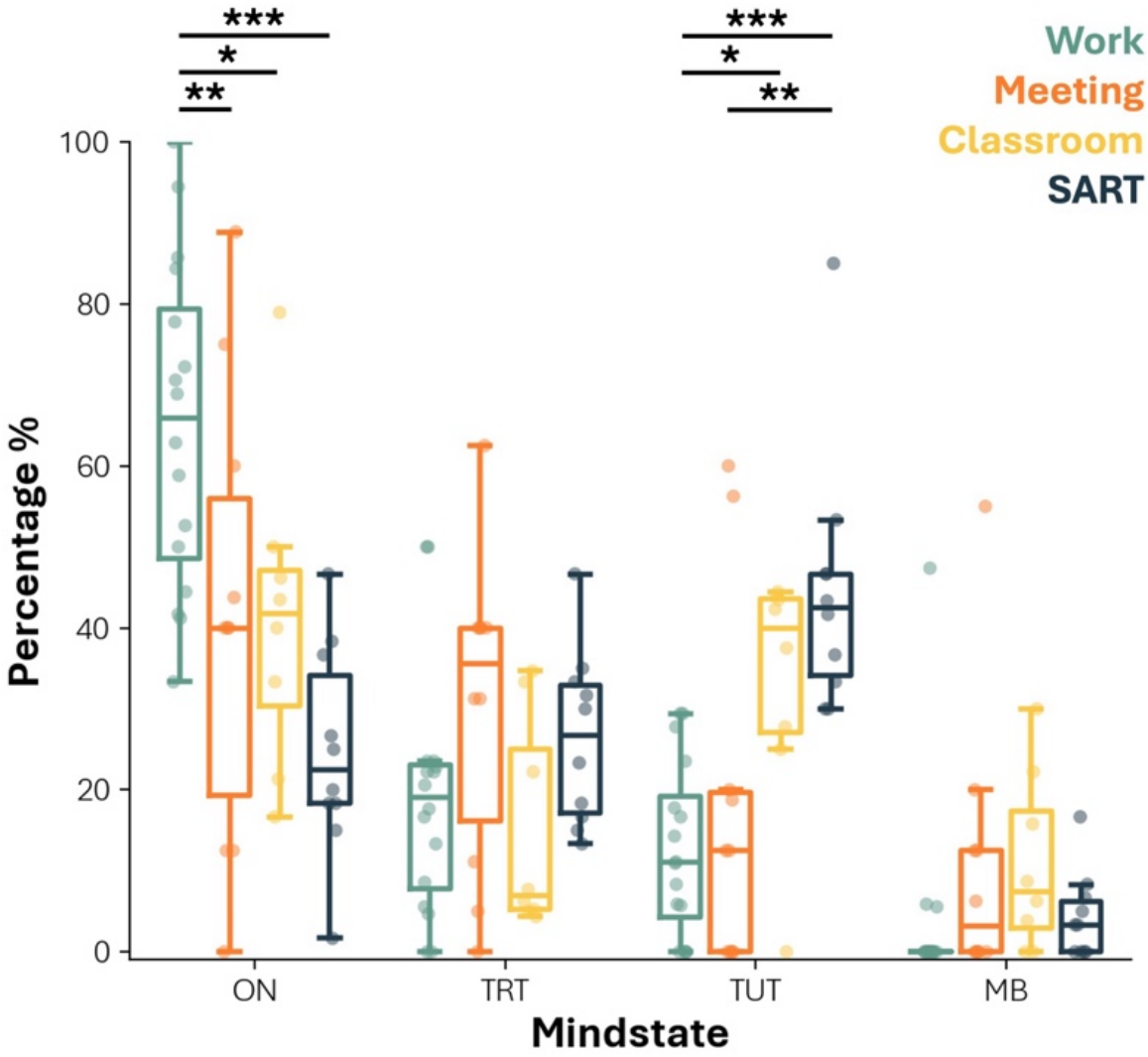

Figure 4.2: Distribution of mind-states (%) across contexts. Boxplots represent the percentage of time spent in each attentional state: ON (focused), TRT (task-related thoughts), TUT (task-unrelated thoughts), and MB (mind-blanking), across four contexts: Work, Meeting, Class, and SART. Each dot corresponds to a single participant. In each boxplot, the central line indicates the median, the box spans the interquartile range (IQR; 25th to 75th percentile), and the whiskers extend to the most extreme data points within 1.5 × IQR. Statistical analysis: Linear mixed-effects models with false discovery rate (FDR) correction for multiple comparisons. $p < 0.05$: *, $p < 0.01$: **, $p < 0.001$: ***.

Statistical analyses were conducted using the statsmodels library in Python (Seabold and Perktold, 2010), and lme4 (Bates et al., 2015), lmerTest (Kuznetsova et al., 2017), and emmeans package (Lenth et al., 2025) in R. To examine interactions between variables, we used linear mixed-effects models (LME), with participant ID included as a random effect. Experimental context and attentional state were included as fixed categorical factors, while confidence and sleepiness ratings were treated as continuous covariates. Multiple comparisons were corrected using the False Discovery Rate (FDR) procedure.

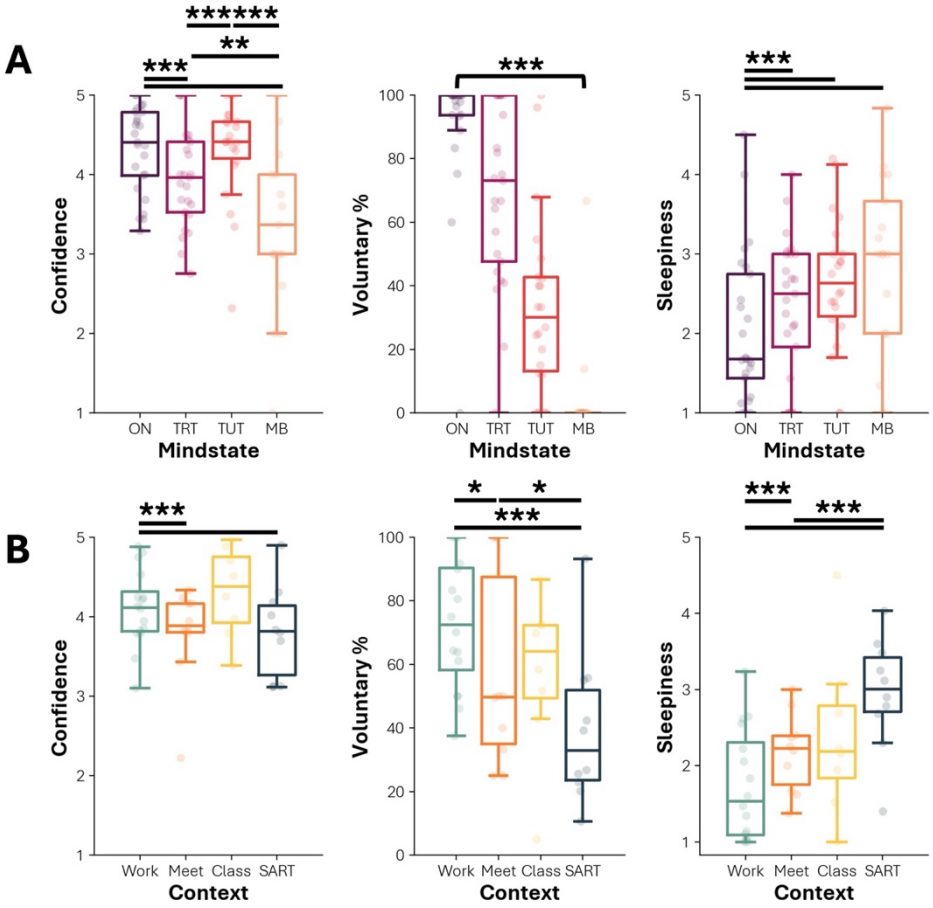

Figure 4.3: Vigilance, intentionality, and sleepiness ratings across mental states and task contexts. Confidence in the mind-state report, intentionality ratings (percentage), and sleepiness ratings according to **A** the reported mind-state: focused (ON), task-related thoughts (TRT), task-unrelated thoughts (TUT), and mind blanking (MB), and **B** the task context: Work, Meeting, Class, and SART. Boxplots display the distribution of ratings across conditions, with vigilance and sleepiness measured on a 1–5 scale and voluntariness as percentage. In each plot, boxplots show median, 25th–75th percentiles (IQR), whiskers to ±1.5×IQR, with subjects as individual points. Statistical analysis: Linear mixed-effects models were applied with subjects as random effects. Pairwise comparisons of estimated marginal means were conducted. Significance levels are indicated as follows: $p < 0.05$: *, $p < 0.01$: **, $p < 0.001$: ***.

Subjective reports

When comparing the distribution of mind-state reports across different contexts, we observe that mind-states are modulated according to the task at hand (**Figure 4.2**). Participants reported being on task more frequently when working (64.9 ± 5.0%, mean ±SEM) compared to during meetings (41.3 ± 8.9%, ß = 0.24, p = 0.007), in class (41.2 ± 6.8%, ß = 0.24, p = 0.01), and during SART tasks (24.7 ± 4.1%, ß = 0.40, p < 0.001). Conversely, participants reported more TUT during SART tasks (44.7 ± 5.1%) compared to working (12.6 ± 2.7%, ß = 0.32, p < 0.001) or during meetings (18.0 ± 7.1%, ß = 0.27, p = 0.006). Participants also showed a higher percentage of TUT during class (33.1 ± 5.4) than during work (12.6 ± 2.7%, ß = 0.21, p = 0.041).

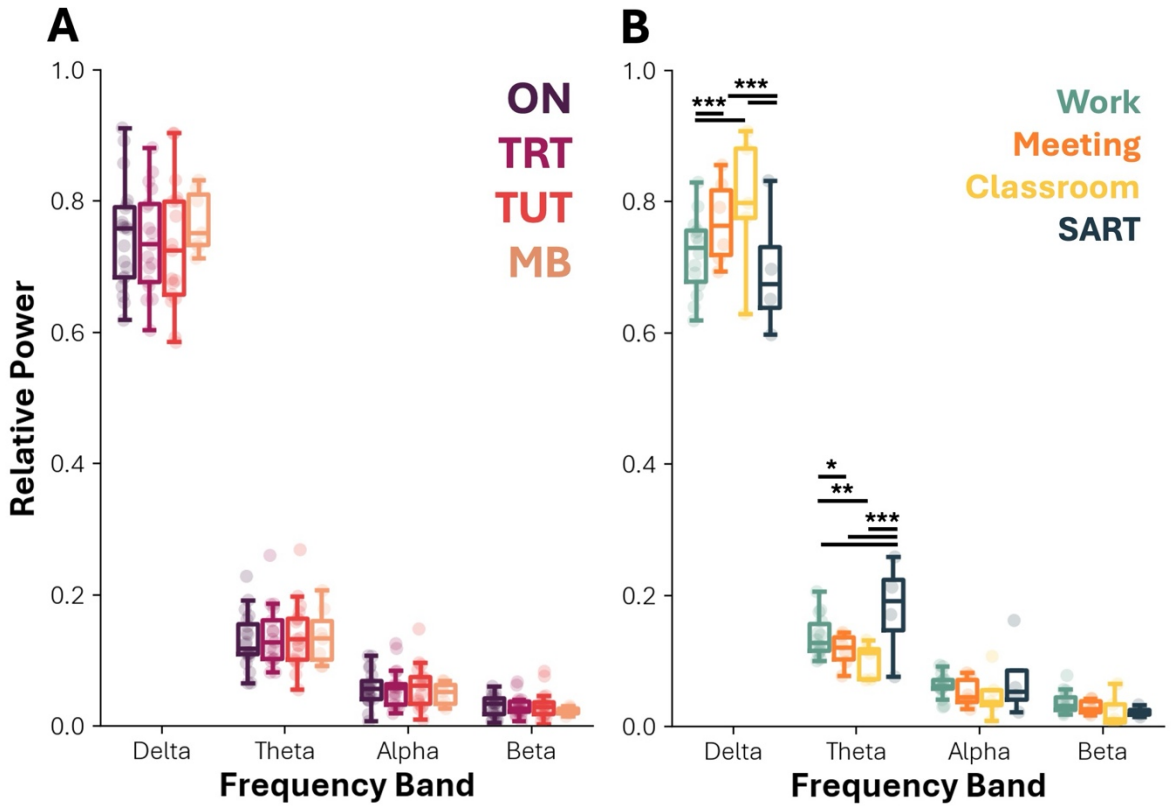

Figure 4.4: Relative band power across task contexts and mind-states. Relative band power **A** according to the mind-states, and **B** in the different task contexts (Work, Meeting, Class, and SART). In each plot, the horizontal line in the middle of the box represents the median value; boxplots show median, 25th–75th percentiles (IQR), whiskers to ±1.5×IQR, with subjects as individual points. Statistical analysis: Linear mixed-effects models were applied with subjects as random effects. Correction for multiple comparison with FDR. Significance levels are indicated as follows, p < 0.05 : *, p < 0.01 : **, p < 0.001 : ***.

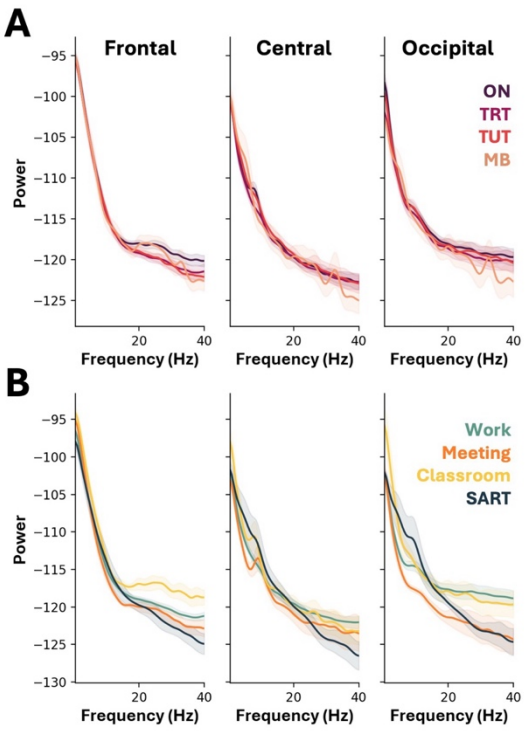

Figure 4.5: PSD according to the mind-state and tasks. Power spectral density according to **A** the different mind-states (ON, TRT, TUT, MB) and **B** the tasks (work, meeting, class, SART). Each column corresponds to a scalp localization (from left to right: frontal, central, occipital). Shaded areas represent the standard error of the mean across participants.

Participants were more confident when reporting being ON compared to TRT (ß = 0.34, $p < 0.001$) or MB (ß = 0.78, $p < 0.001$). They were also more confident when reporting TUT than TRT (ß = 0.34, $p < 0.001$) or MB (ß = 0.78, $p < 0.001$; **Figure 4.3A, left**). Finally, they were more confident when reporting TRT than MB (ß = 0.44, $p < 0.001$). ON reports led to the highest proportion of voluntary mind-states compared to TRT (ß = 0.29, $p < 0.001$) TUT (ß = 0.55, $p < 0.001$), or MB (ß = 0.81, $p < 0.001$). TRT reports led to higher proportion of voluntary mind-states compared to TUT (ß = 0.26, $p < 0.001$), or MB (ß = 0.52, $p < 0.001$).

Participants showed a higher percentage of voluntary mind-state reports when reporting TUT than MB (ß = 0.26, $p < 0.001$; **Figure 4.3A, middle**). Participants reported lower sleepiness when ON compared to TRT (ß = -0.29, $p < 0.001$), TUT (ß = -0.36, $p < 0.001$), or MB (ß = -0.42, $p < 0.001$; **Figure 4.3A, right**). Participants reported greater confidence in their mental state reports when working compared to during lab meetings (ß = 0.40, $p < 0.001$) or during SART tasks (ß = 0.33, $p < 0.001$; **Figure 4.3B, left**). Similarly, participants showed a higher percentage of voluntary mindstate reports during work compared to meetings (ß = 0.13, $p = 0.076$) or during SART tasks (ß = 0.29, $p < 0.001$). Participants also showed a higher percentage of voluntary mindstate reports during

meetings than during SART tasks (ß = 0.15, $p = 0.0078$; **Figure 4.3B, middle**). Participants reported lower sleepiness when working compared to during meetings (ß = -0.51, $p < 0.001$) or during SART tasks (ß = -0.89, $p < 0.001$). They also reported lower sleepiness during meetings compared to during SART tasks (ß = -0.38, $p < 0.001$; **Figure 4.3B, right**).

EEG Analysis

The resting states show typical power spectra with a 1/f relationship between power and frequency and a clear alpha peak maximal over the occipital channel, which stresses the quality of the recordings despite the use of a portable EEG system, equipped with dry electrodes and recording in a noisy environment. During the different tasks, the alpha peak is not visible, which

could be due to the fact that participants were engaged in a specific task. Similarly, we could detect sleep-like SW with a similar waveform as those recorded in the lab using state-of-the-art EEG systems. These SW show a larger amplitude for the frontal channel, which is in line with previous findings. Interestingly, these SW were smaller during the activity than in the resting state, possibly because participants were engaged in a specific task outside of resting state sessions. Overall, these first analyses show that our EEG recordings allow the recording of some of the most classical EEG markers of attention lapses (SW, alpha oscillations).

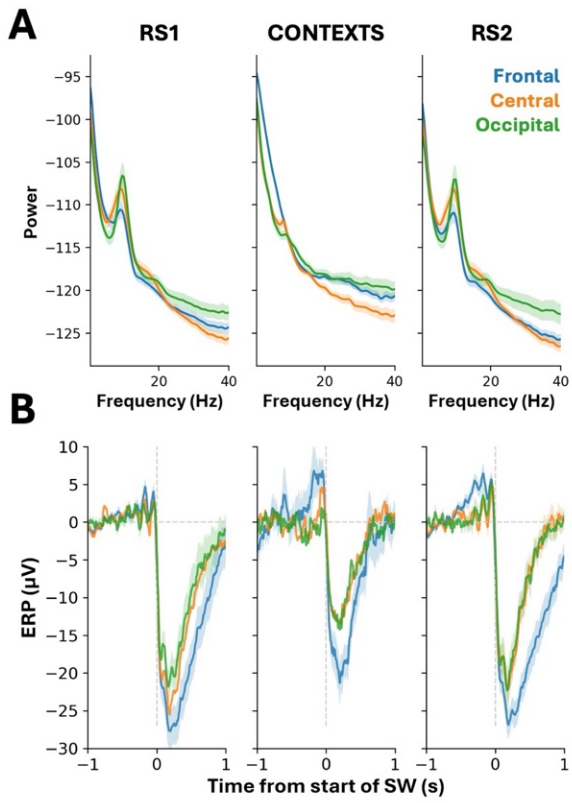

Figure 4.6: EEG activity in resting states and task-related contexts. A Power spectral density and **B** slow waves waveforms are shown according to the type of activity (resting states and averaged across contexts) and scalp localization (frontal: blue, central: orange, occipital: green). Shaded areas represent the standard error of the mean across participants.

When comparing now the different types of activity, we found that, in class, delta relative power was higher than in work (ß = 0.09, $p < 0.001$), meeting (ß = 0.02, $p < 0.001$), and SART (ß = 0.1, $p < 0.001$; **Figure 4.4B**). Theta power was higher in work than in meetings (ß = 0.03, $p = 0.04$), and class (ß = 0.04, $p = 0.008$). Theta power was higher in SART compared to work (ß = 0.05, $p = 0.005$), meetings (ß = 0.08, $p < 0.001$), and class (ß = 0.09, $p < 0.001$).

We did not observe differences in relative power according to the mind state (**Figure 4.4A**). We did not observe differences either in SW density (**Figure 4.7**).

Discussion

We show that the frequency and nature of mental states were strongly influenced by the context in which they occurred. Participants were more likely to report being focused when they were working on self-directed tasks, compared to when they were listening passively in a lecture or participating in the SART. In the same spirit, TUT were more frequent during the SART and passive lecture context, and least frequent during work. These findings align with the contextual regulation hypothesis which claims that the cognitive demands and motivational salience of the

task at hand regulate the occurrence of SE (Andrews-Hanna et al., 2010; Smallwood and Schooler, 2015).

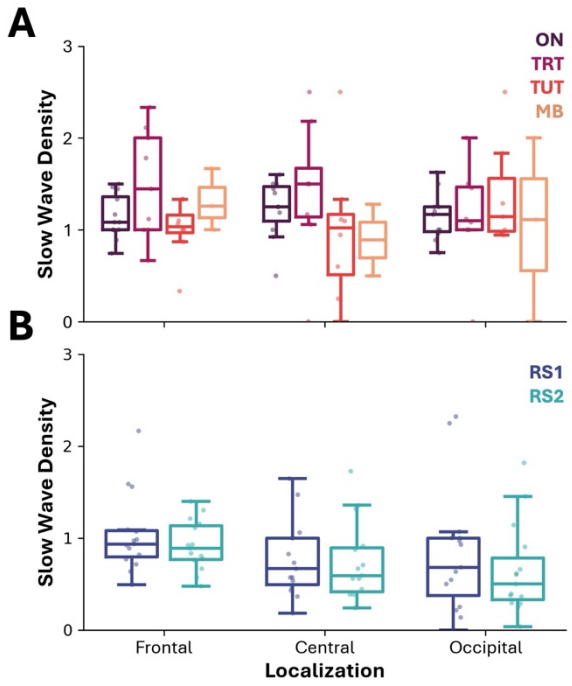

Figure 4.7: Slow wave density within contexts and resting states, according to the localization. Slow wave density according to the different electrode localization (from left to right: frontal, central, occipital), **A** within the different mind states, and **B** according to the resting state. In each plot, the horizontal line in the middle of the box represents the median value; boxplots show median, 25th–75th percentiles (IQR), whiskers to ±1.5×IQR, with subjects as individual points.

Passive contexts (e.g. lecture and meetings) were associated with greater subjective sleepiness and lower confidence in mental state reports. In addition, the proportion of involuntary mental states was higher. These results suggest that decreased engagement and increased fatigue in passive contexts may predispose individuals to attentional lapses. The low level of sleepiness suggests that participants working on self-directed tasks reported not only greater focus and voluntary control over their thoughts, but also higher confidence in their self-reports.

These observations reflect a continuum in the different balance between internal and external constraints, consistent with the Dynamic Framework of Thought (DFT) (Christoff et al., 2016). According to this framework, the stream of consciousness emerges from dynamic interactions between processes that generate variability (e.g. SE) and those that impose constraints. These constraints can be external, such as task demands or environmental structure. These constraints can also be internal, including cognitive goals and executive control. The relative balance between these opposing forces determines whether thoughts are more spontaneous and unconstrained, or more deliberate and task oriented.

Within this framework, passive contexts reduce the influence of external constraints, allowing variability-driven processes to dominate and increase the likelihood of spontaneous, often involuntary, thoughts such as MW and MB. In contrast, active engagement in self-directed tasks likely increases internal constraints through deliberate goal-setting and sustained attention, fostering more stable and intentional thought patterns.

Using portable EEG, we were able to replicate some previously reported spectral markers of fatigue and attentional disengagement in real-life settings. Relative theta power was higher in the

SART compared to the other contexts, echoing the increase in subjective sleepiness, which reminds of the signature of sleep onset (Santamaria and Chiappa, 1987). Interestingly, relative theta power was higher in work which could be linked with cognitive control rather than drowsiness (Cavanagh and Frank, 2014; Snipes et al., 2022) although we cannot rule out the possibility of artefacts driving this effect. We also observe an increase in delta power during meetings or lectures compared to work or the SART. This increase could be due to the specific context in which the brain activity was recorded more than an index of drowsiness since sleepiness ratings (**Figure 4.3B**) do not align with the modulation of delta (**Figure 4.4B**). During the SART and the work conditions, participants were installed in front of a computer and answered the thoughts probes digitally. Whereas in class and during meetings, people were less stable and answered on paper. This could lead to more low amplitude artifacts that would be reflected in the delta band.

Besides, we did not observe consistent modulation of spectral power between the reported mental states, in contrast to prior findings from lab-based studies (Compton et al., 2019; Kam et al., 2022; Munoz-Musat et al., 2025). This could be explained by a higher signal variability in real-life recordings or the overlapping of mental states in ecologically complex situations. It could simply be due to lack of statistical power due to the exclusion of 30% of the 5-second epochs. It also stresses the importance of assessing the robustness of state-specific spectral signature outside of laboratory-settings paradigms.

We successfully detected SW during wakefulness. The 21.8% of artifact-free data was not enough for further interpretation (**Table 2**, **Figure 4.7**). The waveform of the SW detected (see **Figure 4.5A**) is very similar to those we observe during sleep, and the one detected in laboratory settings (Andrillon et al., 2021) and they seem to share a similar distribution on the scalp with more and larger SW detected over frontal electrodes. The presence of SWs in real-life contexts represents a promising lead to test the local sleep hypothesis “in the wild”, but more refined detection pipelines, and higher spatial resolution may be required to link it with behavioral performances.

Several limitations should be acknowledged regarding these pilot data. The relatively small number of participants per context may limit statistical power and generalizability. Having recorded the same participant within different contexts counterbalance the small sample size (Banville et al., 2025) but this could not be done systematically. The use of dry-electrode portable EEG devices allowed to record brain activity in real-life settings but imposes trade-offs in terms of signal quality and spatial resolution. The differences in sampling methods across contexts (e.g., paper vs digital probes) may introduce uncontrolled variance. The class sample consisted of participants who did not overlap with other contexts, which may confound inter-context comparisons.

Importantly, while our findings demonstrate the feasibility of using portable EEG to investigate brain activity in real-life contexts, current methods for cleaning and preprocessing such data remain limited. As a result, we had to exclude a substantial portion of recordings to ensure signal quality (i.e. 78.2% of 20 seconds epochs, and 29.6% of the 5 seconds epochs) This constraint highlights the need for further methodological development to enhance data quality and artifact rejection for mobile EEG systems. Nevertheless, the prominent alpha peak during eyes-closed resting states closely resembles those observed in traditional laboratory recordings (**Figure 4.5**), supporting the validity of our setup. Some residual noise becomes more apparent when the data are subdivided by mind-state (**Figure 4.6A**) or by context (**Figure 4.6B**), which is likely due to reduced averaging and the inherent variability of mobile recordings. These limitations underscore the importance of collecting larger volumes of data per participant, including more frequent thought probes, to improve signal-to-noise ratio and allow for more granular analyses.

To conclude, despite these limitations, our pilot study demonstrates the feasibility and value of studying spontaneous mental states in real-life contexts using portable EEG. It opens the door to a richer understanding of SE as it unfolds outside the laboratory, constrained by both internal states and external demands.

General Discussion

I. Sleep-like slow waves, a unifying signature of fatigue

"All for One, and One for All"

Alexandre Dumas

Much like the motto of Dumas's musketeers, fatigue can take different forms—use dependent, time dependent, or chronic—yet they could all share a common physiological substrate: a shift of wakeful cortical dynamics toward sleep-like dynamics.

In **Study 1**, I investigated acute fatigue induced by the time spent awake (time-dependent) and by increased levels of cognitive effort (use-dependent). Cognitive effort was manipulated by varying task-difficulty between two groups of individuals (between-subject effect) (Blain et al., 2016; Pessiglione et al., 2025; Wiehler et al., 2022). These two groups engaged in the cognitive tasks for an entire day, allowing us to also capture time-dependent fatigue within subjects. Both "time" and "use" were associated with specific and, most importantly, overlapping, behavioral and electrophysiological signatures. Behaviorally, participants exhibited increased choice bias over time, as they favored low-effort, immediate rewards over more rewarding but also more demanding or delayed alternatives. This bias toward low-cost options was even more pronounced in the group assigned to the difficult task, revealing an influence of both time and use-dependent fatigue on choice impulsivity. Interestingly, subjective assessment of fatigue tracked time-dependent but not use-dependent effects. This pattern of results replicates here previous findings (Blain et al., 2016; Wiehler et al., 2022) and stresses the limitations of self-assessment of fatigue.

Electrophysiologically, SW density increased in both groups with session number (time-dependent effect), replicating previous findings on the homeostatic regulation of slow waves during wakefulness (Finelli et al., 2000). This time-dependent increase in SW density was even more pronounced for participants assigned to the most challenging version of the task (**Study 1**), revealing a use-dependent effect as well. Interestingly, the topographies of the time-dependent and use-dependent effects markedly differed (**Figure S1.3**). While the time-dependent effect (session) was visible in all electrodes uniformly, the use-dependent effect was only observed in central electrodes. Focusing on task-difficulty alone reveals a left frontal effect, which is reminiscent of the use-dependent hypo-activation observed in a previous fMRI study using the same protocol (Blain et al., 2016). Finally, we observed the SW effect throughout the different tasks, both in the cognitive task inducing fatigue and the choice task revealing it (**Figure 1.4C**).

From these results, we thus propose that the occurrence of sleep-like SW in wakefulness could reflect a general effect of fatigue as a "state", that is yet modulated locally by context-dependent processes. According to this model, the uniform increase in SW density over time would reflect a shift in cortical dynamics toward greater synchronization and sleep-like activity. This change in

cortical dynamics could be more expressed in certain networks under strain because of cognitive efforts, revealing more local use-dependent effect. These changes would be sustained in time, present in both the cognitive and choice tasks and not just confined to the moments in which participants are showing behavioral signs of fatigue (here, choice impulsivity). Yet, this pervasive and sustained change in background dynamics is still predictive of choice bias, above and beyond the effect of fatigue (mediation, **Figure S1.3**), which suggests that this shift toward sleep-like dynamics could have downstream effects on the decision-making processes.

What are the possible origins of these time and use-dependent effects on SW occurrence? Previous studies have suggested that, as time spent awake increases, so-called somnogenic molecules would accumulate and ensure the homeostatic regulation of sleep (Krueger et al., 2019). Various molecules have been proposed to fulfil this role such as adenosine, interleukins or tumor necrosis factor (Krueger et al., 2019). Interestingly, the cortical concentration of these molecules is use-dependent and has been linked to cognitive functions. In addition, these molecules were shown to have a direct effect on cortical dynamics and increase the likelihood to observe SW. Of particular interest here is the fact that the neurophysiological pathways involve glutamatergic receptors, bringing the gap between previous metabolic accounts of cognitive fatigue and slow waves. Accordingly, an increase in cognitive effort could lead to a local increase in somnogenic molecules via the accumulation of glutamate, triggering a shift toward sleep-like dynamics. These local effects could be coupled with global changes, occurring at the cortical or subcortical level. These changes may also be under neuromodulatory control. A strong noradrenaline drive is associated with optimal sensory processing, whereas reduced noradrenergic activity is typically linked to lapses of attention or sleep onset (Sara, 2009).

What could be the consequences of these SW increase? In sleep, slow waves are associated with a phenomenon of cortical bi-stability by which large assemblies of neurons will alternate between moments of synchronized activity (up-state or ON period) and silence (down-state or OFF period) (Vyazovskiy and Harris, 2013). This alternation has been shown to alter cognitive processing and could be responsible for the lack of responsiveness and consciousness associated with sleep (Andrillon and Kouider, 2020; Tononi and Massimini, 2008). Importantly, this relationship between slow waves and cortical bistability is not confined to sleep but has been observed in human intracranial recordings in the context of brain lesions (Massimini et al., 2024) but also in normal circuits (Sheybani et al., 2023). Brief interruptions of sustained cortical firing could thus mechanistically explain the occurrence of errors in the context of mental fatigue. The fact that these cortical silences could be local could also explain why fatigue results in a diverse range of behavioral outcomes, from sluggishness to impulsivity. Thus, a shift toward sleep-like dynamics could not only track the time and use-dependent accumulation of fatigue (marker) but also explain

the occurrence of behavioral lapses themselves (mechanism). Importantly here, this general shift being of cortical origin, it could reflect both global and local changes and constraints.

The regulation of sleep-like SW could reflect the same complex and multi-level regulation as sleep (Vyazovskiy and Andrillon, 2025). Namely, SW could increase as a function, as we mentioned above, of prolonged wakefulness and cognitive activity. Circadian factors could also come into play. The fact that the SW increase observed in **Study 1** was not monotonous could reflect such circadian modulation. This regulation could also affect cortical brain regions differently. Typically, previous studies showed a prevalence of the increase in SW over frontal electrodes (Andrillon et al., 2021; Bernardi et al., 2015a; Hung et al., 2013). This could be because of a regional vulnerability of frontal cortices that would be expressed through local SW. However, this could also be due to use-dependent processes. In fact, when dissociating both time and use-dependent effects, we observed a widespread time-dependent and a regional use-dependent processes. Targeting different neuronal circuits with use-dependent fatigue could help understand how fatigue is expressed in different brain regions. More research is needed to map out how these changes in cortical dynamics are driven predominantly by circadian factors, homeostatic sleep pressure, or their interaction. Addressing this question will require fitting the evolution of SW features to circadian and homeostatic models and track their influence on behavioral performances and subjective reports.

In addition to use and time-dependent cognitive fatigue, two forms of acute fatigue, in my thesis I also investigated chronic fatigue. To do so, I focused on two clinical populations, NT1 and IH, which are characterized by chronic fatigue and sleepiness. Studying these populations offers a way to investigate whether sleep-like slow waves occur more frequently during wakefulness in the context of long-term fatigue. In my thesis, I used a comparison paradigm to investigate SW expression in individuals with NT1 and IH (**Study 3**). These two populations are characterized by EDS, but distinct pathophysiological profiles (Sateia, 2014). In NT1, which involves well-documented dysregulation of sleep-wake mechanisms, I observed a clear increase in SW density during wakefulness compared to controls. This increase was associated to behavioral and subjective outcomes that can be associated with fatigue. For example, the behavioral profile of NT1 individuals combined both more sluggish responses and impulsive tendencies than controls, mirroring the mixed impairments observed under acute fatigue (Boksem et al., 2006, 2005; Faber et al., 2012; Lorist et al., 2000). These behavioral errors were correlated with sleep-like SW, as also shown previously within the healthy population (Andrillon et al., 2021; Pinggal et al., 2022). These results suggest that the chronic fatigue and sleepiness that represent a hallmark of NT1 as well as the associated behavioral profile could be explained by a chronic increase in sleep-like activity in the brain of these patients.

In contrast, individuals with IH are characterized by normal or even above-average sleep quality (Billiard and Sonka, 2022; Boulanger et al., 2024, **Study 2**). The IH group reported similar or even greater subjective sleepiness, but we did not observe a difference in SW density compared to controls (**Study 3, Supplemental Appendix Figure 3.2**). These results are still preliminary and could be explained by the limited sample size and statistical power of the current sample. However, if confirmed, these results suggest that subjective fatigue and objective electrophysiological markers can diverge in chronic conditions and that increases in sleep-like activity do not account, potentially, for all types of chronic fatigue as it raises the possibility that the mechanism underlying perceived sleepiness in IH may differ from those reflected by SW. Clinically, IH remains a puzzling condition that would require further investigation.

In summary, the different forms of fatigue converge toward a shared neurophysiological signature: sleep-like SW. Across experimental paradigms and clinical comparisons, SW reliably tracked fatigue-related changes even when subjective reports failed to do so. Behaviorally, fatigue was expressed as a combination of sluggishness (e.g., slower responses, increased omissions) and impulsivity (e.g., choice bias, false alarms), and the spatial distribution of SW helped predict the type of error observed. These findings position SW as a sensitive, task-relevant marker of fatigue across timescales and populations. Still, not all cognitive failures are preceded by SW, suggesting that they are part of a broader set of neurophysiological mechanisms contributing to cognitive decline under fatigue.

In addition to the question of SW as a marker or mechanism of fatigue, there is also the question of their potential function(s). As mentioned above, sustained cognitive effort leads to measurable physiological changes in the cortex. Spectroscopy and functional MRI studies have shown that intense or prolonged activation in regions such as the prefrontal cortex can result in local glucose depletion and the accumulation of metabolic waste and in particular glutamate (Blain et al., 2016; Wiehler et al., 2022). This metabolic strain is thought to reduce cortical excitability and may contribute to the emergence of SW during wakefulness (Krueger et al., 2019). In parallel, sustained cognitive activity could result in synaptic changes that can also promote the occurrence of local SW (Andrillon and Oudiette, 2023). This synaptic effect is not exclusive of the metabolic one, as the two processes are intimately related. Importantly, synaptic and metabolic homeostasis are among the proposed key restorative functions of sleep. In this view, SW may reflect a local protective mechanism, transiently silencing overused neural populations to maintain global function. Accordingly, SW could represent a protective feature rather than a failure, preventing potentially neurotoxic metabolite accumulation or harmful cortical dynamics such as epileptogenic activity. Indeed, extreme cases of sleep deprivation can induce epileptic activity (Malow, 2004), a fact known at least since the antiquity (Lloyd, 1983). Recent work has proposed

that wake SW could help regulate epileptic discharges (Sheybani et al., 2023). A related hypothesis, inspired by sleep research, links SW to glymphatic clearance. During NREM sleep, SW have been associated with increased cerebrospinal fluid flow and waste elimination through the glymphatic system (Fultz et al., 2019; Xie et al., 2013). While glymphatic activity is most prominent during sleep, recent work suggests it may also operate during quiet wakefulness (Yang et al., 2024). The possibility that SW might facilitate, or be triggered by, glymphatic-like activity during wakefulness remains speculative but intriguing.

Taken together, these hypotheses raise the possibility that local SW could serve a dual role: as markers of regional neural fatigue and as part of a homeostatic mechanism for restoring metabolic balance. Multimodal approaches combining EEG, spectroscopy, and structural imaging may offer a promising avenue to test these hypotheses in future studies.

II. Broadening the definition of local sleep

SW are arguably the main neurophysiological hallmark of sleep. They are used to identify and characterize sleep. They have been linked to sleep's core functions (memory consolidation, synaptic homeostasis, glymphatic regulation) and could explain both behavioral (unresponsiveness) and subjective (dreaming, dreamless sleep) changes associated with sleep. But sleep and SW can be dissociated. Some sleep stages are only weakly associated with SW, such as N1 or REM sleep. SWs are also observed in states different from sleep, in anesthesia (Chauvette et al., 2011), with the administration of certain psychedelics (Bréant et al., 2024) or following hyperventilation (Epstein et al., 1994). Likewise, there is more in sleep than just slow waves with sleep being also associated with thalamo-cortical oscillations (sleep spindles, De Gennaro and Ferrara, 2003; Fernandez and Lüthi, 2020) or volley of brainstem activation (PGO waves, Jouvet et al., 1959).

In this thesis, I focused mostly on SW. I documented the presence of SW across different populations and settings. In **Study 1**, SW density is an indicator of fatigue and choice bias. In **Study 3**, I observed increased SW in participants with NT1. This reflected the chronic expression of fatigue in a clinical condition characterized by sleep-wake instability (Sateia, 2014). In **Study 4**, I showed that SW can also be detected in naturalistic contexts using portable EEG in healthy individuals. I then confirm the ubiquity of SW and the feasibility for real-life observations. I showed that the occurrence of these SW can be associated with typical behavioral consequences of fatigue. They include a momentary decrease or slowing of responsiveness, leading to missed trials or delayed responses, or, conversely, an increase in impulsivity, reflected in fast reactions, choice impulsivity, or false alarms. I also showed that SW can account for changes in subjective experience associated with fatigue, namely an increase in subjective sleepiness, and in the likelihood to mind wander or to mind blank. Yet, even if these results offer a rich physiological, behavioral and phenomenological description of cognitive fatigue in the healthy populations, this portrait turned out not to be exhaustive,

Beyond consolidating the concept of local sleep, **Study 3** broadened the investigation of fatigue toward additional neurophysiological markers beyond SW, and toward cognitive consequences other than misses, false alarms, MW, and MB. I used experience sampling to probe the phenomenology of participants with NT1 during a sustained attention task. Individuals with NT1 frequently typically experience vivid hallucinations, often during sleep onset, as part of well-characterized disruptions of sleep-wake transitions (Leu-Semenescu et al., 2011). Up to a third of these hallucinatory episodes occur during wakefulness, outside of traditional sleep boundaries (Leu-Semenescu et al., 2011). To explore the neural origins of these atypical signs of fatigue, we

tested NT1 participants in a long SART. Participants were instructed to remain awake and perform the task to the best of their ability, although they made more errors than controls. However, during this SART, NT1 patients reported a high proportion of hallucinations and illusions (**Figure 3.1**). Furthermore, hallucinations and illusions were almost exclusively reported by participants with NT1, rarely by healthy controls or individuals with a different hypersomnolence disorder (IH, **Supplementary Appendix Figure 3.1**). Finally, hallucinations and illusions had a specific phenomenological profile and carried specific behavioral and electrophysiological features (**Figure 3.3**). They could thus represent a new, pathological form of sleep intrusions, different from the classical SW intrusions that I have focused on so far.

From a behavioral standpoint, hallucinations were associated with increased subjective sleepiness, lower intentionality, and more frequent misses, indicating a marked disengagement from the task (**Figure 3.3**). This dissociation from external goals, combined with low arousal, situates hallucinations near the extreme of spontaneous, involuntary mental states: closer to dreaming than to classic lapses such as mind-wandering or mind-blanking.

Electrophysiologically, hallucinations differed from on-task states by increased occipital theta power and decreased posterior beta power patterns typically observed during drowsiness and early NREM sleep (Santamaria and Chiappa, 1987). Importantly, hallucinations were also accompanied by short theta bursts over parieto-occipital regions, which were largely absent in controls (**Figure 3.4**). These bursts had a spatial and temporal profile reminiscent of REM-related oscillations, such as sawtooth waves and the theta activity observed at REM onset (Frauscher et al., 2020; Hutchison and Rathore, 2015; Jouvet et al., 1960). While their functional role remains debated, their topography echoes subcortical REM phenomena described in animals, such as PGO waves (Brooks, 1975; Karashima et al., 2005), which have been linked to visual dream content and shown to occur under hallucinogenic states (Brooks, 1975).

Interestingly, the occurrence of these theta bursts did not coincide with an increase in SW, which remained stable across hallucination and non-hallucination states. In fact, SW could distinguish hallucinations from fully alert states, but not from other disengaged mind states such as MW or MB. This suggests that while SW remain a hallmark of NREM-like local sleep, hallucinations may reflect a different mode of local intrusion, more consistent with REM physiology. This interpretation aligns with the known pathophysiology of NT1, where REM sleep mechanisms are dysregulated and prone to intrude into wakefulness (Leu-Semenescu et al., 2011).

Taken together, these findings support an extension of the local sleep framework: beyond NREM-like slow waves, REM-like dynamics may also manifest transiently and locally during wakefulness. This “REM-like local sleep” could represent a distinct path through which the brain disengages from the environment, with unique phenomenological and neurophysiological consequences.

Rather than a unitary phenomenon, local sleep may therefore encompass a broader taxonomy of microstates, shaped by the underlying architecture of NREM or REM sleep regulation.

Several neurological and psychiatric disorders are associated with spontaneous hallucinations and REM dysregulation. Parkinson's disease and dementia with Lewy bodies, for example, frequently involve visual hallucinations that precede cognitive decline and are often comorbid with REM sleep behavior disorder, suggesting early alterations in REM circuitry (Arnulf et al., 2000). In schizophrenia, hallucinations are typically auditory but have also been linked to fragmented sleep and abnormalities in REM sleep architecture (Ferrarelli, 2021). The presence of sleep-onset REM periods in some of these conditions further supports the idea that boundary instability could underlie hallucinatory episodes.

These observations raise the possibility that REM-like intrusions into wakefulness may not be unique to NT1, but rather a general mechanism emerging when REM-regulatory systems are destabilized. Testing this hypothesis will require investigation of hallucinatory states across conditions, allowing to identify potential shared neural signatures. The theta bursts identified in NT1, particularly over parieto-occipital regions, could serve as candidate biomarkers for such investigations. Whether these oscillatory events represent a shared mechanism or a syndrome-specific expression remains an open question.

Interestingly, a distinct pattern of theta bursts was also observed in participants with IH, although with different functional and topographical characteristics (**Appendix Study 3**). Compared to controls, individuals with IH exhibited increased theta burst density, particularly over occipital regions. However, unlike the parieto-occipital theta bursts observed in NT1, bursts in IH were more diffusely distributed and not specifically associated with hallucinatory episodes. Instead, they were linked to more general markers of disengagement and behavioral slowing, including increased reaction times, greater variability, and a higher proportion of missed responses.

Taken together, these findings point to a potential functional taxonomy of transient theta bursts. In NT1, theta bursts may reflect REM-like local intrusions associated with vivid, immersive experiences. In contrast, the more diffuse theta bursts seen in IH may correspond to low-arousal, NREM-like disengagement, contributing to sluggishness and impaired responsiveness. This distinction suggests that theta bursts are not a unitary phenomenon. Theta bursts could have subtypes with distinct roles in modulating behavior and arousal (Snipes et al., 2022).

Despite these results, caution is warranted. There are some conceptual limitations that will need to be addressed before this framework can be generalized.

First, while the observed theta bursts in NT1 exhibit spatial and temporal characteristics reminiscent of REM-related phenomena (e.g., sawtooth waves or PGO-like activity), the absence

of direct markers of REM physiology during wakefulness limits interpretability. In humans, PGO waves remain difficult to isolate non-invasively, and the classification of bursts as "REM-like" currently relies on indirect comparisons. Comparing the theta bursts detected in the different sleep stages within the same participants would be required to establish a more robust link.

Second, the functional role of these theta bursts remains uncertain. In NT1, they are associated with hallucinations and parieto-occipital topographies, whereas in IH, theta bursts are more diffusely distributed, associated with disengaged mind states (e.g., MW, MB, HA, FG), and correlate with slower responses and increased misses. This raises the possibility that distinct types of theta bursts may reflect qualitatively different neural mechanisms. However, this taxonomy remains preliminary and requires further investigation. Invasive recordings in epileptic patients could help better understand the underlying mechanisms and establish a taxonomy of theta bursts, following the example of approaches used to distinguish different types of slow waves (El-Kanbi et al., 2022).

Third, a broader conceptual challenge concerns the integration of these findings into the theoretical framework of local sleep. While NREM-like SW are now well established as local markers of cortical fatigue and attentional lapses (Andrillon et al., 2021; Bernardi et al., 2015a; Hung et al., 2013; Sheybani et al., 2023), the nature of transient REM-like events during wake could be debated. Importantly, differences in the regulation of NREM and REM sleep may shed light on the origin of these phenomena. A thorough comparison of homeostatic and circadian influence on NREM and REM regulation could help shed light on these distinct types of sleep intrusions.

Together, these findings support a broader conceptualization of local sleep. Local sleep could be expressed by both NREM-like and REM-like patterns. These patterns could emerge under physiological or pathological contexts. Understanding this spectrum will require integrative approaches combining subjective experience, behavioral dynamics, and multi-scale neurophysiological data across both healthy and clinical populations.

III. How to apply these findings to real life?

Fatigue is a major contributor to accidents and errors across high-stakes domains. In Europe, up to one in five road accidents is attributed to driver fatigue (Horne and Reyner, 1995). In aviation, fatigue has been implicated in approximately 20% of aviation accidents between 2001 and 2012 (Marcus and Rosekind, 2017). Even though safety protocols and automation aim to minimize human errors in aviation, decades of research on fatigue have shown that its physiological and cognitive signatures remain difficult to monitor and prevent in real life. In this thesis, I investigated the neurophysiological correlates of fatigue across three complementary axes. First, through a fundamental study examining task-induced fatigue (**Study 1**). Second, through clinical studies, characterizing electrophysiological markers of pathological sleepiness in hypersomnolence disorders (**Study 2 and 3**). Third, through an exploration in real-life settings, using portable EEG and thought sampling in naturalistic environments (**Study 4**). I aim to bridge experimental findings with ecologically valid observations.

The exploration of spontaneous experience as I did in **Study 3** relies on a constrained and often monotonous laboratory task. In **Study 4**, I extended the investigation of SE to everyday contexts. In this study, we sought to bring our research out in the real world by adapting our methodology to real-life situations rather than trying to translate these activities into well-controlled paradigms. This is particularly the case for the SART, introduced in 1996 by Robertson and colleagues precisely to provide a way to explore the "action slips common in the everyday lives of normal people" (Robertson et al., 1997). The SART allows researchers to quantify impairments in subjective attention that go beyond self-assessments and, when paired with neuroimaging, offers a window onto the underlying neurophysiological mechanisms. However, its simplicity and monotony make it difficult to extrapolate laboratory results to real-life settings, and there is only a weak relationship between SART performance and everyday-life reports of cognitive failure (Smilek et al., 2010). Another limitation of the SART is the constant interruption through the presentation of new visual stimuli every second and the associated request for simple and discrete responses (button presses). This is very different from more continuous activities such as listening to a lecture or driving. This approach could alter not only the frequency but also phenomenological properties of MW.

To examine whether the results obtained in the standard lab-based approach could be generalized, we implemented a pilot study to investigate fatigue in the real world. We ported the experience sampling technique and neurophysiological recordings to professional and academic activities such as attending a meeting or lecture, working on a computer, etc. For neurophysiological recordings, we used portable EEG systems allowing the recording of brain

activity *in situ*. This was for me the opportunity to develop new skills and work closely with start-ups developing these products (e.g., Mentalab).

In practice, we observed a modulation of the proportion of reported mind states by the context in which we did the recordings (**Figure 4.2**). Participants were more on-task during autonomous work sessions (65%) than while attending a professional meeting (41%), or a class (41%). The smallest proportion of on-task reports were recorded for the SART (25%). Conversely, TUT reports were highest during the SART (45%) but also frequent during classes (33%) and meetings (18%). These findings highlight the influence of cognitive and environmental demands on internal states. In addition, participants reported greater confidence in their mind-states report, lower sleepiness, and higher intentionality of their mind-sates during work sessions compared to the SART. This influence of context is in line with other findings, for example showing that fluctuating stress levels in real life modulate both the frequency and nature of SE (Linz et al., 2021). Distractions are also more present in real life context, suggesting a greater role of exogenous factor in shaping SE (Varao-Sousa et al., 2018). When participants were working in **Study 4**, they decided the task they had to complete. We propose that volition and goal-related tasks also act as exogenous factors shaping SE in real life.

Real life does not always mean ordinary, quite the contrary. In sports, some individuals can explore states of the mind and body that would be impossible and/or unethical to reproduce in the laboratory. Yet, these extreme cases can provide unique insights on the human mind and the functioning of the brain. For example, hallucinatory phenomena are not exclusive to clinical conditions. They can also arise in non-pathological contexts, marked by extreme fatigue (Huang et al., 2021; Hurdiel et al., 2015; Pallesen et al., 2018; Waters et al., 2018). For example, solo sailing can result in severely restricted and fragmented sleep and hallucinations are commonly reported (Hurdiel et al., 2012). Visual hallucinations are also reported during long running races (ultra-trail) (Huang et al., 2021), again in close association with sleep deprivation. These examples are fascinating as they offer an opportunity to bridge the gap between mental and physical fatigue. These extreme cases challenge the classical separation between the “normal” and “pathological” (Canguilhem, 2013), and instead suggest a continuum between normal spontaneous experiences (e.g., MW, MB) and those observed in clinical populations (e.g., hallucinations).

Accordingly, in **Study 3**, I demonstrated that participants with NT1 frequently reported hallucinatory or illusory experiences, particularly under conditions of reduced alertness and constraints. These hallucinations happen in the daily life of NT1 (Leu-Semenescu et al., 2011). Until now, it hasn’t been captured in laboratory settings. Monitoring participants with NT1 spontaneous experience at home could allow to better understand the phenomenology of these hallucinations.

Altogether, these findings highlight the importance of a dialogue between the study of internal states in controlled environment and ecologically valid settings. True, the complexity and variability of real-life dynamics pose significant challenges. A first challenge emerged when designing the paradigm. Which categories of thoughts are more present in real-life compared to laboratory settings? Based on prior literature, we selected the categories that seemed to best capture the spectrum of SE (Van den Driessche et al., 2025). Another question then arose: how frequently should participants be interrupted? Too short an interval between probes risks disrupting participants excessively. However, as revealed by the limited signal-to-noise ratio in portable EEG, obtaining a large number of mental state reports is essential to generate robust insights on the underlying physiological signatures. This leads to another point: experience sampling is a powerful tool, but it also introduces new methodological challenges. Experience sampling is instrumental in characterizing subjective states but remains interruptive by nature. In some cases, the probe may interfere with the ongoing process, especially for fleeting SE such as mind-blanking or hallucinations. It could be interesting to leverage recent development in signal processing and machine learning to detect the fluctuations in attention without interrupting participants, as I have contributed to in a recent study currently under review (Munoz-Musat et al., 2025).

Another key parameter of the experience sampling technique is the phenomenological space that is being explored, that is the propositions participants can choose from. As shown in **Study 3**, simply adding hallucinations/illusion as available options enabled us to capture such reports in surprising proportions even in a population of NT1 patients known to experience hallucinations. It is unlikely that these hallucination/illusion reports could be all explained by a response bias as these reports were associated with a distinct behavioral and physiological signatures. To a certain extent, a similar finding was obtained with MB. Until recently, MW research focused heavily on a binary approach by asking participants to indicate whether they were on or off task. Subsequent studies demonstrated the importance of considering subtypes of mind wandering, with a focus on dimensions of awareness, temporality, intentionality, etc. Yet, in 2013, Ward and Wegner showed that individuals can sometimes "blank", being neither on task nor mind wandering, but having simply no conscious content to report when probed (A. Ward and Wegner, 2013). Again, offering the MB option in experience sampling probes reveal a specific phenomenological state (Andrillon et al., 2025), distinct from both ON and MW states. This complexification of the phenomenological landscape goes further. In some studies, instances of "mind blanking" (no content to report) can be mixed with "forgetting" (content forgotten) (Andrillon et al., 2021; Fell, 2022; Munoz-Musat et al., 2025; Van den Driessche et al., 2017). In **Study 3**, we show this grouping might be approximative in some contents. Indeed, we observe clear differences between forgetting reports and other mind state reports (**Figure 3.3**). Forget reports are associated with a higher degree of sleepiness,

reduced volition, and poorer behavioral performance than MB. This difference could be driven by NT1 patients, who may drift into sleep and forget their prior thoughts once they reach a certain level of disconnection from the environment. It could be phenomenologically different from controls. As NT1 patients can hallucinate at sleep onset and during wakefulness (Leu-Semenescu et al., 2011), the forget states could be a mix between sleep onset without mental imagery, and brief loss of meta-awareness during wakefulness. The scientific investigation of subjective experience (SE) is thus at a crossroads, facing the challenge of striking an optimal balance between overly simplistic and excessively complex descriptions of SE. In this thesis, I have largely adopted the recently proposed 5-state Classification of Mental States (CoMS-5T, Van den Driessche et al., 2025) as a guiding framework.

Thus, like any tool used by researchers, experience sampling has its limitations, yet it was essential for collecting the data necessary to validate behavioral and physiological biomarkers. However, now we know better the behavioral and physiological signatures of these mind states, we can perhaps move toward a more continuous and less intrusive monitoring of internal states, enabling real-time assessments without relying on self-report. Behavioral signals provide the simplest and most accessible way to monitor internal states. Typing speed and keystroke variability can reflect changes in fatigue over time (Acien et al., 2022; Bastian and Sackur, 2013; Jong et al., 2018). Voice rhythm and tone can also be used to detect fatigue (Thoret et al., 2024). These signals can be collected continuously without requiring complex hardware. Cardiac and respiratory markers offer a second layer of information. Devices such as smartwatches now provide reliable estimates of heart rate variability and breathing rhythm, two proxies of autonomic regulation (Hoilett et al., 2018; Trimpop et al., 2017). In the context of fatigue, both increased variability and strong cardiovascular responses have been observed, reflecting divergent strategies of disengagement or compensatory effort (Wright et al., 2008; Zhao et al., 2012). These physiological signals are sensitive to fatigue but also to contextual factors such as stress or motivation (Herd, 1991), which must be accounted for when interpreting them. Pupillometry offers a third avenue for tracking internal states (van der Wel and van Steenbergen, 2018; Wiehler et al., 2022). Pupil diameter varies with arousal and effort and has been shown to dilate with fatigue (van der Wel and van Steenbergen, 2018), especially during fatigued economic decision (Wiehler et al., 2022). Eye-tracking systems are increasingly available in mobile formats and can be used to track blink rate, saccade dynamics, and gaze dispersion, already studied in attention and fatigue research (Pupil Labs, Berlin, Germany). Finally, EEG can give us precise information about fatigue and/or spontaneous experience with markers such as SW or theta bursts (Andrillon et al., 2021; Snipes et al., 2022, **Study 3**). In **Study 4**, we recorded SWs in everyday contexts using a portable, dry-electrode EEG system, replicating waveform characteristics previously reported in laboratory studies. These

results confirm the feasibility of using EEG to track fluctuations in vigilance and internal states outside the lab.

These associations of physiological and behavioral metrics can be used to passively monitor fatigue and attention. The available signals may vary depending on the context. Each can still provide useful information about internal states. Given the large variability in baseline physiology and fatigue responses, models should be personalized (Dongen et al., 2004; Zanoli et al., 2023). They should also integrate contextual factors such as task type, time of day, or prior sleep. This approach would allow continuous monitoring. It could help detect early signs of fatigue or attentional lapses such as MW, MB, or hallucinations.

In central hypersomnias (NT1, IH), these tools could be used and compared to discussed diagnostic strategies such as MSLT and maintenance wakefulness test (MWT). The MSLT measures the time an individual take to fall asleep 5 times during the day (Berry et al., 2017). The MWT is used to test the efficacy of a treatment and see if an individual can stay awake for 40 minutes (Berry et al., 2017). At home EEG coupled to actimetry could allow to monitor the time patients take to fall asleep and when during the day. Clinicians could also compare the sleep onset time without and with treatment. Coupled with objective sleepiness detected with voice recordings, clinicians could have an overview of the ability of a patient with hypersomnia to drive and work without and with treatment. In turn, we could explore a new dimension of research on arousal and fatigue with longitudinal recordings. This could be helpful in pathologies where fatigue is reported as one of the most disabling aspect of the condition (e.g., multiple sclerosis, Parkinson disease, major depressive disorder, Braley and Chervin, 2010; Friedman et al., 2007; Kluger et al., 2016; Nierenberg et al., 1999).

In the general population, this passive monitoring and prevention could prove useful. We have poor meta-awareness of our own fatigue level (Jones et al., 2006; Wiehler et al., 2022). We also usually realize too late that our mind drifted away. In truck driver or pilots, this tool could also help decrease the, still high, amount of fatigue related accidents (Garbarino et al., 2001).

Of course, this kind of passive monitoring and prevention comes with clear ethical considerations. The goal is not surveillance, but self-access. Enabling individuals to better understand their own physiology, and act upon it. Strict ethical frameworks should define the contexts and purposes of use: scientific, medical, or therapeutic. Transparency, informed consent, and interpretability of the biomarkers must be central. Objective indicators are not direct windows into consciousness, they are probabilistic inferences.

The core contribution of this thesis is not only to document internal cognitive states and their neural correlates, but also to provide a framework for translating these findings into ecologically valid, ethically responsible applications.

Fatigue, spontaneous thought, and hallucination-like phenomena are not confined to labs or clinical settings: they are embedded in real life experience. Understanding their neurophysiological substrates opens the door to real-time, personalized cognitive monitoring, with potential benefits in health, performance, and well-being.

Concluding Remarks

It has been quite a journey. Through this thesis, I explored fatigue, regardless of its origin (e.g., use-dependent, time-dependent, or chronic). I demonstrated that these different origins of fatigue share a common physiological substrate characterized by a shift in cortical dynamics towards sleep-like slow waves. These slow waves emerge as a sensitive and relevant marker of fatigue, capturing fluctuations in cortical states even when subjective self-reports fail to do so. Their spatial distribution predicts the type of behavioral errors, linking local cortical dynamics to cognitive lapses in real time. The precise molecular and synaptic processes governing the progressive destabilization of wakefulness remain to be uncovered. Likewise, the contribution of circadian and homeostatic processes to the emergence of slow waves needs further investigation. Beyond their role as a marker, could these slow waves regulate abnormal neuronal discharges? Facilitate metabolic clearance?

With this work, I strengthened the role of slow waves as a marker of fatigue. The accumulation of slow waves with fatigue mediates the low-cost decisions one may take. These slow waves allow us to differentiate healthy controls from populations of patients with chronic fatigue. Importantly, they can also be detected in real-life settings.

Beyond slow waves, the search for other forms of local sleep began before my PhD. Serendipitously capturing hallucinations report in NT1 opened the way for a broader definition of local sleep, encompassing microstates beyond NREM-like activity, with REM-like dynamics that may manifest through theta bursts in pathological conditions. A deeper investigation of these events, both in humans and with invasive recordings, could establish a more comprehensive taxonomy of local sleep intrusions.

Finally, this thesis points to crucial translational perspectives. The development of unobtrusive, multimodal tools for real-life monitoring of fatigue can improve safety, productivity, and clinical care. Personalized models, grounded in objective markers of physiological dynamics, have the potential to overcome the limitations of self-report measures and enable early, adaptive interventions. Ethical considerations will be essential in the deployment of such tools.

Taken together, this thesis provides a conceptual and methodological foundation to study fatigue as a neurophysiological process of local sleep intrusions. It opens avenues for mechanistic, ecological, and clinical research in the years to come.

To anyone who has read my thesis up to this point, I sincerely thank you for your time, interest, and patience. I hope my work has added meaningful pieces to the broader puzzle of understanding fatigue, a phenomenon that emerges at the intersection of two multifaceted states: sleep and wakefulness.

References

Acien, A., Morales, A., Vera-Rodriguez, R., Fierrez, J., Mondesire-Crump, I., Arroyo-Gallego, T., 2022. Detection of Mental Fatigue in the General Population: Feasibility Study of Keystroke Dynamics as a Real-world Biomarker. JMIR Biomedical Engineering 7, e41003. https://doi.org/10.2196/41003

Ackerman, P.L., 2011. Cognitive fatigue: Multidisciplinary perspectives on current research and future applications, Cognitive fatigue: Multidisciplinary perspectives on current research and future applications. American Psychological Association, Washington, DC, US. https://doi.org/10.1037/12343-000

Anderson, C., Horne, J.A., 2006. Sleepiness enhances distraction during a monotonous task. Sleep 29, 573–576. https://doi.org/10.1093/sleep/29.4.573

Andrews-Hanna, J.R., Reidler, J.S., Huang, C., Buckner, R.L., 2010. Evidence for the Default Network's Role in Spontaneous Cognition. Journal of Neurophysiology 104, 322–335. https://doi.org/10.1152/jn.00830.2009

Andrillon, T., Burns, A., MacKay, T., Windt, J., Tsuchiya, N., 2021. Predicting lapses of attention with sleep-like slow waves. https://doi.org/10.1101/2020.06.23.166991

Andrillon, T., Kouider, S., 2020. The vigilant sleeper: neural mechanisms of sensory (de)coupling during sleep. Current Opinion in Physiology, Physiology of sleep 15, 47–59. https://doi.org/10.1016/j.cophys.2019.12.002

Andrillon, T., Lutz, A., Windt, J., Demertzi, A., 2025. Where is my mind? A neurocognitive investigation of mind blanking. Trends in Cognitive Sciences 29, 600–613. https://doi.org/10.1016/j.tics.2025.02.002

Andrillon, T., Nir, Y., Cirelli, C., Tononi, G., Fried, I., 2015. Single-neuron activity and eye movements during human REM sleep and awake vision. Nat Commun 6, 7884. https://doi.org/10.1038/ncomms8884

Andrillon, T., Oudiette, D., 2024. Global and local sleep, in: Advances in the Psychobiology of Sleep and Circadian Rhythms. Routledge, New York, NY, US, pp. 1–16. https://doi.org/10.4324/9781003296966

Andrillon, T., Oudiette, D., 2023. What is sleep exactly? Global and local modulations of sleep oscillations all around the clock. Neurosci Biobehav Rev 155, 105465. https://doi.org/10.1016/j.neubiorev.2023.105465

Andrillon, T., Solelhac, G., Bouchequet, P., Romano, F., Le Brun, M.-P., Brigham, M., Chennaoui, M., Léger, D., 2020. Revisiting the value of polysomnographic data in insomnia: more than meets the eye. Sleep Med 66, 184–200. https://doi.org/10.1016/j.sleep.2019.12.002

Andrillon, T., Windt, J., Silk, T., Drummond, S.P.A., Bellgrove, M.A., Tsuchiya, N., 2019. Does the Mind Wander When the Brain Takes a Break? Local Sleep in Wakefulness, Attentional Lapses and Mind-Wandering. Front. Neurosci. 13. https://doi.org/10.3389/fnins.2019.00949

Arnau, S., Brümmer, T., Liegel, N., Wascher, E., 2021. Inverse effects of time-on-task in task-related and task-unrelated theta activity. Psychophysiology 58, e13805. https://doi.org/10.1111/psyp.13805

Arnau, S., Löffler, C., Rummel, J., Hagemann, D., Wascher, E., Schubert, A.-L., 2020. Inter-trial alpha power indicates mind wandering. Psychophysiology 57, e13581. https://doi.org/10.1111/psyp.13581

Arnulf, I., Bonnet, A.-M., Damier, P., Bejjani, B.-P., Seilhean, D., Derenne, J.-P., Agid, Y., 2000. Hallucinations, REM sleep, and Parkinson's disease. Neurology 55, 281–288. https://doi.org/10.1212/WNL.55.2.281

Arnulf, I., Leu-Semenescu, S., Dodet, P., 2022. Precision Medicine for Idiopathic Hypersomnia. Sleep Med Clin 17, 379–398. https://doi.org/10.1016/j.jsmc.2022.06.016

Asplund, C.L., Chee, M.W.L., 2013. Time-on-task and sleep deprivation effects are evidenced in overlapping brain areas. NeuroImage 82, 326–335. https://doi.org/10.1016/j.neuroimage.2013.05.119

Avvenuti, G., Bernardi, G., 2022. Chapter 3 - Local sleep: A new concept in brain plasticity, in: Quartarone, A., Ghilardi, M.F., Boller, F. (Eds.), Handbook of Clinical Neurology, Neuroplasticity. Elsevier, pp. 35–52. https://doi.org/10.1016/B978-0-12-819410-2.00003-5

Baiardi, S., Mondini, S., 2020. Inside the clinical evaluation of sleepiness: subjective and objective tools. Sleep Breath 24, 369–377. https://doi.org/10.1007/s11325-019-01866-8

Baird, B., Smallwood, J., Mrazek, M.D., Kam, J.W.Y., Franklin, M.S., Schooler, J.W., 2012. Inspired by Distraction: Mind Wandering Facilitates Creative Incubation. Psychol Sci 23, 1117–1122. https://doi.org/10.1177/0956797612446024

Balkin, T.J., Riedy, S.M., Rabat, A., Friedl, K.E., 2023. Toward a More Precise Definition of fatigue, in: The Handbook of Fatigue Management in Transportation. CRC Press.

Banville, H., Benchetrit, Y., d'Ascoli, S., Rapin, J., King, J.-R., 2025. Scaling laws for decoding images from brain activity. https://doi.org/10.48550/arXiv.2501.15322

Bargiotas, P., Lachenmayer, M.L., Schreier, D.R., Mathis, J., Bassetti, C.L., 2019. Sleepiness and sleepiness perception in patients with Parkinson's disease: a clinical and electrophysiological study. Sleep 42, zsz004. https://doi.org/10.1093/sleep/zsz004

Bastian, M., Sackur, J., 2013. Mind wandering at the fingertips: automatic parsing of subjective states based on response time variability. Front. Psychol. 4. https://doi.org/10.3389/fpsyg.2013.00573

Bates, D., Mächler, M., Bolker, B., Walker, S., 2015. Fitting Linear Mixed-Effects Models Using lme4. Journal of Statistical Software 67, 1–48. https://doi.org/10.18637/jss.v067.i01

Bazanova, O.M., Vernon, D., 2014. Interpreting EEG alpha activity. Neurosci Biobehav Rev 44, 94–110. https://doi.org/10.1016/j.neubiorev.2013.05.007

Benjamini, Y., Hochberg, Y., 1995. Controlling the False Discovery Rate: A Practical and Powerful Approach to Multiple Testing. Journal of the Royal Statistical Society: Series B (Methodological) 57, 289–300. https://doi.org/10.1111/j.2517-6161.1995.tb02031.x

Bernardi, G., Siclari, F., Yu, X., Zennig, C., Bellesi, M., Ricciardi, E., Cirelli, C., Ghilardi, M.F., Pietrini, P., Tononi, G., 2015a. Neural and Behavioral Correlates of Extended Training during Sleep Deprivation in Humans: Evidence for Local, Task-Specific Effects. J. Neurosci. 35, 4487–4500. https://doi.org/10.1523/JNEUROSCI.4567-14.2015

Bernardi, G., Siclari, F., Yu, X., Zennig, C., Bellesi, M., Ricciardi, E., Cirelli, C., Ghilardi, M.F., Pietrini, P., Tononi, G., 2015b. Neural and behavioral correlates of extended training during sleep deprivation in humans: evidence for local, task-specific effects. J Neurosci 35, 4487–4500. https://doi.org/10.1523/JNEUROSCI.4567-14.2015

Berry, R.B., Brooks, R., Gamaldo, C., Harding, S.M., Lloyd, R.M., Quan, S.F., Troester, M.T., Vaughn, B.V., 2017. AASM Scoring Manual Updates for 2017 (Version 2.4). Journal of Clinical Sleep Medicine 13, 665–666. https://doi.org/10.5664/jcsm.6576

Billiard, M., Sonka, K., 2022. Idiopathic Hypersomnia: Historical Account, Critical Review of Current Tests and Criteria, Diagnostic Evaluation in the Absence of Biological Markers and Robust Electrophysiological Diagnostic Criteria. Nat Sci Sleep 14, 311–322. https://doi.org/10.2147/NSS.S266090

Billiard, M., Sonka, K., 2016. Idiopathic hypersomnia. Sleep Medicine Reviews 29, 23–33. https://doi.org/10.1016/j.smrv.2015.08.007

Blain, B., Hollard, G., Pessiglione, M., 2016. Neural mechanisms underlying the impact of daylong cognitive work on economic decisions. Proceedings of the National Academy of Sciences 113, 6967–6972. https://doi.org/10.1073/pnas.1520527113

Blain, B., Schmit, C., Aubry, A., Hausswirth, C., Le Meur, Y., Pessiglione, M., 2019. Neuro-computational Impact of Physical Training Overload on Economic Decision-Making. Curr Biol 29, 3289-3297.e4. https://doi.org/10.1016/j.cub.2019.08.054

Boksem, M.A.S., Meijman, T.F., Lorist, M.M., 2006. Mental fatigue, motivation and action monitoring. Biol Psychol 72, 123–132. https://doi.org/10.1016/j.biopsycho.2005.08.007

Boksem, M.A.S., Meijman, T.F., Lorist, M.M., 2005. Effects of mental fatigue on attention: an ERP study. Brain Res Cogn Brain Res 25, 107–116. https://doi.org/10.1016/j.cogbrainres.2005.04.011

Boksem, M.A.S., Tops, M., 2008. Mental fatigue: costs and benefits. Brain Res Rev 59, 125–139. https://doi.org/10.1016/j.brainresrev.2008.07.001

Borbély, A.A., Achermann, P., 1992. Concepts and models of sleep regulation: an overview. J Sleep Res 1, 63–79. https://doi.org/10.1111/j.1365-2869.1992.tb00013.x

Borghini, G., Astolfi, L., Vecchiato, G., Mattia, D., Babiloni, F., 2014. Measuring neurophysiological signals in aircraft pilots and car drivers for the assessment of mental workload, fatigue and drowsiness. Neuroscience & Biobehavioral Reviews, Applied Neuroscience: Models, methods, theories, reviews. A Society of Applied Neuroscience (SAN) special issue. 44, 58–75. https://doi.org/10.1016/j.neubiorev.2012.10.003

Boulanger, T., Pigeon, P., Crawford, S., 2024. Diagnostic challenges and burden of idiopathic hypersomnia: a systematic literature review. SLEEP Advances 5, zpae059. https://doi.org/10.1093/sleepadvances/zpae059

Bové, A., Culebras, A., Moore, J.T., Westlake, R.E., 1994. Relationship between sleep spindles and hypersomnia. Sleep 17, 449–455. https://doi.org/10.1093/sleep/17.5.449

Braley, T.J., Chervin, R.D., 2010. Fatigue in Multiple Sclerosis: Mechanisms, Evaluation, and Treatment. Sleep 33, 1061–1067. https://doi.org/10.1093/sleep/33.8.1061

Bréant, B.J.B., Mengual, J.P., Hoerder-Suabedissen, A., Patel, J., Bannerman, D.M., Sharp, T., Vyazovskiy, V.V., 2024. Sleep-like state during wakefulness induced by psychedelic 5-MeO-DMT in mice. https://doi.org/10.1101/2022.12.11.519886

Brooks, D.C., 1975. The effect of LSD upon sponstaneous PGO wave activity and REM sleep in the cat. Neuropharmacology 14, 847–857. https://doi.org/10.1016/0028-3908(75)90113-6

Cairns, A., Bogan, R., 2019. Comparison of the macro and microstructure of sleep in a sample of sleep clinic hypersomnia cases. Neurobiology of Sleep and Circadian Rhythms 6, 62–69. https://doi.org/10.1016/j.nbscr.2019.02.001

Canguilhem, G., 2013. Le normal et le pathologique. https://doi.org/10.3917/puf.cangu.2013.01

Cavanagh, J.F., Frank, M.J., 2014. Frontal theta as a mechanism for cognitive control. Trends Cogn Sci 18, 414–421. https://doi.org/10.1016/j.tics.2014.04.012

Champetier, P., André, C., Weber, F.D., Rehel, S., Ourry, V., Laniepce, A., Lutz, A., Bertran, F., Cabé, N., Pitel, A.-L., Poisnel, G., de la Sayette, V., Vivien, D., Chételat, G., Rauchs, G., on behalf of the Medit-Ageing Research Group, 2023. Age-related changes in fast spindle clustering during non-rapid eye movement sleep and their relevance for memory consolidation. Sleep 46, zsac282. https://doi.org/10.1093/sleep/zsac282

Chauvette, S., Crochet, S., Volgushev, M., Timofeev, I., 2011. Properties of slow oscillation during slow-wave sleep and anesthesia in cats. J Neurosci 31, 14998–15008. https://doi.org/10.1523/JNEUROSCI.2339-11.2011

Chen, T., Guestrin, C., 2016. XGBoost: A Scalable Tree Boosting System, in: Proceedings of the 22nd ACM SIGKDD International Conference on Knowledge Discovery and Data Mining. Presented at the KDD '16: The 22nd ACM SIGKDD International Conference on Knowledge Discovery and Data Mining, ACM, San Francisco California USA, pp. 785–794. https://doi.org/10.1145/2939672.2939785

Christoff, K., Irving, Z.C., Fox, K.C.R., Spreng, R.N., Andrews-Hanna, J.R., 2016. Mind-wandering as spontaneous thought: a dynamic framework. Nat Rev Neurosci 17, 718–731. https://doi.org/10.1038/nrn.2016.113

Cirelli, C., Tononi, G., 2008. Is sleep essential? PLoS Biol 6, e216. https://doi.org/10.1371/journal.pbio.0060216

Compton, R.J., Gearinger, D., Wild, H., 2019. The wandering mind oscillates: EEG alpha power is enhanced during moments of mind-wandering. Cogn Affect Behav Neurosci 19, 1184–1191. https://doi.org/10.3758/s13415-019-00745-9

Conrad, C., Newman, A., 2021. Measuring Mind Wandering During Online Lectures Assessed With EEG. Front Hum Neurosci 15, 697532. https://doi.org/10.3389/fnhum.2021.697532

Cori, J.M., Anderson, C., Shekari Soleimanloo, S., Jackson, M.L., Howard, M.E., 2019. Narrative review: Do spontaneous eye blink parameters provide a useful assessment of state drowsiness? Sleep Medicine Reviews 45, 95–104. https://doi.org/10.1016/j.smrv.2019.03.004

Cover, T.M., Thomas, J.A., 2005. ELEMENTS OF INFORMATION THEORY.

Curcio, G., Casagrande, M., Bertini, M., 2001. Sleepiness: evaluating and quantifying methods. International Journal of Psychophysiology, Abstracts of the 13th Conference on Event-Related Potentials of the Brain, EPIC XIII 41, 251–263. https://doi.org/10.1016/S0167-8760(01)00138-6

Dang-Vu, T.T., McKinney, S.M., Buxton, O.M., Solet, J.M., Ellenbogen, J.M., 2010. Spontaneous brain rhythms predict sleep stability in the face of noise. Curr Biol 20, R626-627. https://doi.org/10.1016/j.cub.2010.06.032

De Gennaro, L., Ferrara, M., 2003. Sleep spindles: an overview. Sleep Med Rev 7, 423–440. https://doi.org/10.1053/smrv.2002.0252

De Gennaro, L., Ferrara, M., Curcio, G., Cristiani, R., 2001. Antero-posterior EEG changes during the wakefulness–sleep transition. Clinical Neurophysiology 112, 1901–1911. https://doi.org/10.1016/S1388-2457(01)00649-6

Dehaene, S., Sergent, C., Changeux, J.-P., 2003. A neuronal network model linking subjective reports and objective physiological data during conscious perception. Proceedings of the National Academy of Sciences 100, 8520–8525. https://doi.org/10.1073/pnas.1332574100

Delrosso, L.M., Chesson, A.L., Hoque, R., 2014. Manual characterization of sleep spindle index in patients with narcolepsy and idiopathic hypersomnia. Sleep Disord 2014, 271802. https://doi.org/10.1155/2014/271802

Ding, C., Peng, H., 2003. Minimum redundancy feature selection from microarray gene expression data, in: Computational Systems Bioinformatics. CSB2003. Proceedings of the 2003 IEEE Bioinformatics Conference. CSB2003. Presented at the Computational Systems Bioinformatics. CSB2003. Proceedings of the 2003 IEEE Bioinformatics Conference. CSB2003, pp. 523–528. https://doi.org/10.1109/CSB.2003.1227396

Dinges, D.F., Powell, J.W., 1985. Microcomputer analyses of performance on a portable, simple visual RT task during sustained operations. Behavior Research Methods, Instruments, & Computers 17, 652–655. https://doi.org/10.3758/BF03200977

Dirik, H.B., Darendeli, A., Ertan, H., 2023. The new wireless EEG device Mentalab Explore is a valid and reliable system for the measurement of resting state EEG spectral features. Brain Research 1798, 148164. https://doi.org/10.1016/j.brainres.2022.148164

Dodet, P., Chavez, M., Leu-Semenescu, S., Golmard, J.-L., Arnulf, I., 2015. Lucid Dreaming in Narcolepsy. Sleep 38, 487–497. https://doi.org/10.5665/sleep.4516

Dongen, H.V.V., Maislin, G., Dinges, D., 2004. Dealing with inter-individual differences in the temporal dynamics of fatigue and performance: importance and techniques. Aviation, space, and environmental medicine.

Donoghue, T., Haller, M., Peterson, E.J., Varma, P., Sebastian, P., Gao, R., Noto, T., Lara, A.H., Wallis, J.D., Knight, R.T., Shestyuk, A., Voytek, B., 2020. Parameterizing neural power spectra into periodic and aperiodic components. Nat Neurosci 23, 1655–1665. https://doi.org/10.1038/s41593-020-00744-x

Drummond, S.P.A., Bischoff-Grethe, A., Dinges, D.F., Ayalon, L., Mednick, S.C., Meloy, M.J., 2005. The neural basis of the psychomotor vigilance task. Sleep 28, 1059–1068.

El-Kanbi, K., Lavilléon, G. de, Bagur, S., Lacroix, M., Benchenane, K., 2022. Distinction between slow waves and delta waves sheds light to sleep homeostasis and their association to hippocampal sharp waves ripples. https://doi.org/10.1101/2022.12.27.522034

Ellis, H., 1917. The Laws of Relative Fatigue. (Psychol. Rev., March, 1917.) Dodge, R. Journal of Mental Science 63, 594–595. https://doi.org/10.1192/bjp.63.263.594

Epstein, M.A., Duchowny, M., Jayakar, P., Resnick, T.J., Alvarez, L.A., 1994. Altered responsiveness during hyperventilation-induced EEG slowing: a non-epileptic phenomenon in normal children. Epilepsia 35, 1204–1207. https://doi.org/10.1111/j.1528-1157.1994.tb01790.x

Esposito, F., Otto, T., Zijlstra, F.R.H., Goebel, R., 2014. Spatially Distributed Effects of Mental Exhaustion on Resting-State FMRI Networks. PLOS ONE 9, e94222. https://doi.org/10.1371/journal.pone.0094222

Evangelista, E., Lopez, R., Barateau, L., Chenini, S., Bosco, A., Jaussent, I., Dauvilliers, Y., 2018. Alternative diagnostic criteria for idiopathic hypersomnia: A 32-hour protocol. Ann Neurol 83, 235–247. https://doi.org/10.1002/ana.25141

Faber, L.G., Maurits, N.M., Lorist, M.M., 2012. Mental Fatigue Affects Visual Selective Attention. PLoS ONE 7, e48073. https://doi.org/10.1371/journal.pone.0048073

Fabiani, M., Gratton, G., Karis, D., Donchin, E., 1987. Definition, Identification, and Reliability of Measurement of the P300 Component of the Event-Related Brain Potential. Advances in Psychophysiology 2, 1–78.

Facque, V., Wiehler, A., Volle, E., Mandonnet, E., Pessiglione, M., 2022. Present bias in economic choice demonstrates increased cognitive fatigability of glioma patients. Cortex 151, 281–293. https://doi.org/10.1016/j.cortex.2022.02.015

Fell, J., 2022. What is mind blanking: A conceptual clarification. European Journal of Neuroscience 56, 4837–4842. https://doi.org/10.1111/ejn.15782

Ferentinos, P., Kontaxakis, V., Havaki-Kontaxaki, B., Dikeos, D., Papadimitriou, G., 2010. The Fatigue Questionnaire: Standardization in patients with major depression. Psychiatry Res 177, 114–119. https://doi.org/10.1016/j.psychres.2009.01.029

Fernandez, L.M.J., Lüthi, A., 2020. Sleep Spindles: Mechanisms and Functions. Physiological Reviews 100, 805–868. https://doi.org/10.1152/physrev.00042.2018

Ferrarelli, F., 2021. Sleep abnormalities in Schizophrenia (SCZ): state of the art and next steps. Am J Psychiatry 178, 903–913. https://doi.org/10.1176/appi.ajp.2020.20070968

Finelli, L.A., Baumann, H., Borbély, A.A., Achermann, P., 2000. Dual electroencephalogram markers of human sleep homeostasis: correlation between theta activity in waking and slow-wave activity in sleep. Neuroscience 101, 523–529. https://doi.org/10.1016/s0306-4522(00)00409-7

Foustoukos, G., Lüthi, A., 2025. Monoaminergic signaling during mammalian NREM sleep - Recent insights and next-level questions. Current Opinion in Neurobiology 92, 103025. https://doi.org/10.1016/j.conb.2025.103025

Fox, K., Nijeboer, S., Solomonova, E., Domhoff, G.W., Christoff, K., 2013. Dreaming as mind wandering: evidence from functional neuroimaging and first-person content reports. Frontiers in Human Neuroscience 7, 412. https://doi.org/10.3389/fnhum.2013.00412

Frauscher, B., von Ellenrieder, N., Dolezalova, I., Bouhadoun, S., Gotman, J., Peter-Derex, L., 2020. Rapid Eye Movement Sleep Sawtooth Waves Are Associated with Widespread Cortical Activations. J Neurosci 40, 8900–8912. https://doi.org/10.1523/JNEUROSCI.1586-20.2020

Friedman, J.H., Brown, R.G., Comella, C., Garber, C.E., Krupp, L.B., Lou, J.-S., Marsh, L., Nail, L., Shulman, L., Taylor, C.B., Working Group on Fatigue in Parkinson's Disease, 2007. Fatigue in Parkinson's disease: a review. Mov Disord 22, 297–308. https://doi.org/10.1002/mds.21240

Fronczek, R., Arnulf, I., Baumann, C.R., Maski, K., Pizza, F., Trotti, L.M., 2020. To split or to lump? Classifying the central disorders of hypersomnolence. Sleep 43, zsaa044. https://doi.org/10.1093/sleep/zsaa044

Fultz, N.E., Bonmassar, G., Setsompop, K., Stickgold, R.A., Rosen, B.R., Polimeni, J.R., Lewis, L.D., 2019. Coupled electrophysiological, hemodynamic, and cerebrospinal fluid oscillations in human sleep. Science 366, 628–631. https://doi.org/10.1126/science.aax5440

Garbarino, S., Lino, N., Beelke, M., Carli, F.D., Ferrillo, F., 2001. The Contributing Role of Sleepiness in Highway Vehicle Accidents. Sleep 24, 201–206. https://doi.org/10.1093/sleep/24.2.201

Giambra, L.M., Grodsky, A., 1989. Task-Unrelated Images and Thoughts While Reading, in: Shorr, J.E., Robin, P., Connella, J.A., Wolpin, M. (Eds.), Imagery: Current Perspectives. Springer US, Boston, MA, pp. 27–31. https://doi.org/10.1007/978-1-4899-0876-6_3

Girn, M., Mills, C., Roseman, L., Carhart-Harris, R.L., Christoff, K., 2020. Updating the dynamic framework of thought: Creativity and psychedelics. NeuroImage 213, 116726. https://doi.org/10.1016/j.neuroimage.2020.116726

Goode, J.H., 2003. Are pilots at risk of accidents due to fatigue? Journal of Safety Research 34, 309–313. https://doi.org/10.1016/S0022-4375(03)00033-1

Goodwin, D.W., Rosenthal, R., 1971. Clinical Significance of Hallucinations in Psychiatric Disorders: A Study of 116 Hallucinatory Patients. Archives of General Psychiatry 24, 76–80. https://doi.org/10.1001/archpsyc.1971.01750070078011

Gool, J.K., Zhang, Z., Oei, M.S.S.L., Mathias, S., Dauvilliers, Y., Mayer, G., Plazzi, G., Del Rio-Villegas, R., Cano, J.S., Šonka, K., Partinen, M., Overeem, S., Peraita-Adrados, R., Heinzer, R., Martins da Silva, A., Högl, B., Wierzbicka, A., Heidbreder, A., Feketeova, E., Manconi, M., Bušková, J., Canellas, F., Bassetti, C.L., Barateau, L., Pizza, F., Schmidt, M.H., Fronczek, R., Khatami, R., Lammers, G.J., 2022. Data-Driven Phenotyping of Central Disorders of Hypersomnolence With Unsupervised Clustering. Neurology 98, e2387–e2400. https://doi.org/10.1212/WNL.0000000000200519

Gott, J.A., Liley, D.T.J., Hobson, J.A., 2017. Towards a Functional Understanding of PGO Waves. Front Hum Neurosci 11, 89. https://doi.org/10.3389/fnhum.2017.00089

Gramfort, A., Luessi, M., Larson, E., Engemann, D.A., Strohmeier, D., Brodbeck, C., Goj, R., Jas, M., Brooks, T., Parkkonen, L., Hämäläinen, M., 2013. MEG and EEG data analysis with MNE-Python. Front Neurosci 7, 267. https://doi.org/10.3389/fnins.2013.00267

Guillard, M., Beauchamps, V., Pontiggia, A., Dondaine, T., Buchillet, G., Quiquempoix, M., Rabat, A., Touron, J., Arhel, B., Galarme, D., Honfroy, A., Sauvet, F., Leger, D., Chennaoui, M., 2025. Performances aux tests de tir laser au cours d'une période de privation totale de sommeil. Médecine du Sommeil, Le Congrès du Sommeil® Lille, 20-22 novembre 2024 22, 78. https://doi.org/10.1016/j.msom.2025.01.120

Hanif, U., Aloulou, A., Crosbie, F., Bouchequet, P., Chennaoui, M., Andrillon, T., Leger, D., n.d. Deciphering Insomnia: Benchmarking Automated Sleep Staging Algorithms for Complex Sleep Disorders. Journal of Sleep Research n/a, e70048. https://doi.org/10.1111/jsr.70048

He, J., Becic, E., Lee, Y.-C., McCarley, J.S., 2011. Mind wandering behind the wheel: performance and oculomotor correlates. Hum Factors 53, 13–21. https://doi.org/10.1177/0018720810391530

Heerema, R., Carrillo, P., Daunizeau, J., Vinckier, F., Pessiglione, M., 2023. Mood fluctuations shift cost–benefit tradeoffs in economic decisions. Sci Rep 13, 18173. https://doi.org/10.1038/s41598-023-45217-w

Heerema, R., Pessiglione, M., 2025. How mood-related physiological states bias economic decisions. Commun Psychol 3, 55. https://doi.org/10.1038/s44271-025-00241-6

Helfrich, R.F., Knight, R.T., 2016. Oscillatory Dynamics of Prefrontal Cognitive Control. Trends in Cognitive Sciences 20, 916–930. https://doi.org/10.1016/j.tics.2016.09.007

Herd, J.A., 1991. Cardiovascular response to stress. Physiological Reviews 71, 305–330. https://doi.org/10.1152/physrev.1991.71.1.305

Herzog, R., Crosbie, F., Aloulou, A., Hanif, U., Chennaoui, M., Léger, D., Andrillon, T., 2025. A continuous approach to explain insomnia and subjective-objective sleep discrepancy. Commun Biol 8, 1–14. https://doi.org/10.1038/s42003-025-07794-6

Herzog, R., Crosbie, F., Aloulou, A., Hanif, U., Chennaoui, M., Léger, D., Andrillon, T., 2024. Sleep and wake intrusions: A continuous approach to explain insomnia and sleep state misperception. https://doi.org/10.21203/rs.3.rs-4924650/v1

Hobson, J.A., Friston, K.J., 2012. Waking and dreaming consciousness: neurobiological and functional considerations. Prog Neurobiol 98, 82–98. https://doi.org/10.1016/j.pneurobio.2012.05.003

Hockey, G.R.J., 2011. A motivational control theory of cognitive fatigue, in: Cognitive Fatigue: Multidisciplinary Perspectives on Current Research and Future Applications, Decade of Behavior/Science Conference. American Psychological Association, Washington, DC, US, pp. 167–187. https://doi.org/10.1037/12343-008

Hoilett, O.S., Twibell, A.M., Srivastava, R., Linnes, J.C., 2018. Kick LL: A Smartwatch for Monitoring Respiration and Heart Rate using Photoplethysmography, in: 2018 40th Annual International Conference of the IEEE Engineering in Medicine and Biology Society (EMBC). Presented at the 2018 40th Annual International Conference of the IEEE Engineering in Medicine and Biology Society (EMBC), pp. 3821–3824. https://doi.org/10.1109/EMBC.2018.8513356

Horne, J.A., Reyner, L.A., 1995. Sleep related vehicle accidents. BMJ 310, 565–567. https://doi.org/10.1136/bmj.310.6979.565

Huang, M.-K., Chang, K.-S., Kao, W.-F., Li, L.-H., How, C.-K., Wang, S.-H., Lin, Y.-K., Hwang, Y.-S., Chien, D.-K., Chiu, Y.-H., 2021. Visual hallucinations in 246-km mountain ultra-marathoners: An observational study. Chin J Physiol 64, 225–231. https://doi.org/10.4103/cjp.cjp_57_21

Huijben, I.A.M., Hermans, L.W.A., Rossi, A.C., Overeem, S., van Gilst, M.M., van Sloun, R.J.G., 2023. Interpretation and further development of the hypnodensity representation of sleep structure. Physiol. Meas. 44, 015002. https://doi.org/10.1088/1361-6579/aca641

Humphrey, D.G., Kramer, A.F., Stanny, R.R., 1994. Influence of extended wakefulness on automatic and nonautomatic processing. Hum Factors 36, 652–669. https://doi.org/10.1177/001872089403600407

Hung, C.-S., Sarasso, S., Ferrarelli, F., Riedner, B., Ghilardi, M.F., Cirelli, C., Tononi, G., 2013. Local Experience-Dependent Changes in the Wake EEG after Prolonged Wakefulness. Sleep 36, 59–72. https://doi.org/10.5665/sleep.2302

Hurdiel, R., Monaca, C., Mauvieux, B., Mccauley, P., Pa Van Dongen, H., Theunynck, D., 2012. Field study of sleep and functional impairments in solo sailing races. Sleep Biol. Rhythms 10, 270–277. https://doi.org/10.1111/j.1479-8425.2012.00570.x

Hurdiel, R., Pezé, T., Daugherty, J., Girard, J., Poussel, M., Poletti, L., Basset, P., Theunynck, D., 2015. Combined effects of sleep deprivation and strenuous exercise on cognitive performances during The North Face® Ultra Trail du Mont Blanc® (UTMB®). J Sports Sci 33, 670–674. https://doi.org/10.1080/02640414.2014.960883

Hutchison, I.C., Rathore, S., 2015. The role of REM sleep theta activity in emotional memory. Front. Psychol. 6. https://doi.org/10.3389/fpsyg.2015.01439

Inzlicht, M., Schmeichel, B.J., Macrae, C.N., 2014. Why self-control seems (but may not be) limited. Trends Cogn Sci 18, 127–133. https://doi.org/10.1016/j.tics.2013.12.009

Jas, M., Engemann, D., Raimondo, F., Bekhti, Y., Gramfort, A., 2016. Automated rejection and repair of bad trials in MEG/EEG, in: 6th International Workshop on Pattern Recognition in Neuroimaging (PRNI). Trento, Italy.

Johns, M.W., 1991. A new method for measuring daytime sleepiness: the Epworth sleepiness scale. Sleep 14, 540–545. https://doi.org/10.1093/sleep/14.6.540

Jones, C.B., Dorrian, J., Jay, S.M., Lamond, N., Ferguson, S., Dawson, D., 2006. Self-Awareness of Impairment and the Decision to Drive after an Extended Period of Wakefulness. Chronobiology International 23, 1253–1263. https://doi.org/10.1080/07420520601083391

Jong, M. de, Bonvanie, A.M., Jolij, J., Lorist, M.M., 2020. Dynamics in typewriting performance reflect mental fatigue during real-life office work. PLOS ONE 15, e0239984. https://doi.org/10.1371/journal.pone.0239984

Jong, M., Jolij, J., Pimenta, A., Lorist, M.M., 2018. Age Modulates the Effects of Mental Fatigue on Typewriting. Front. Psychol. 9. https://doi.org/10.3389/fpsyg.2018.01113

Jouvet, M., Michel, F., Courjon, J., 1959. [Electric activity of the rhinencephalon during sleep in cats]. C R Seances Soc Biol Fil 153, 101–105.

Jouvet, M., Michel, F., Mounier, D., 1960. [Comparative electroencephalographic analysis of physiological sleep in the cat and in man]. Rev Neurol (Paris) 103, 189–205.

Kam, J.W.Y., Rahnuma, T., Park, Y.E., Hart, C.M., 2022. Electrophysiological markers of mind wandering: A systematic review. NeuroImage 258, 119372. https://doi.org/10.1016/j.neuroimage.2022.119372

Kane, M.J., Brown, L.H., McVay, J.C., Silvia, P.J., Myin-Germeys, I., Kwapil, T.R., 2007. For Whom the Mind Wanders, and When: An Experience-Sampling Study of Working Memory and Executive Control in Daily Life. Psychol Sci 18, 614–621. https://doi.org/10.1111/j.1467-9280.2007.01948.x

Kane, M.J., Gross, G.M., Chun, C.A., Smeekens, B.A., Meier, M.E., Silvia, P.J., Kwapil, T.R., 2017. For Whom the Mind Wanders, and When, Varies Across Laboratory and Daily-Life Settings. Psychol Sci 28, 1271–1289. https://doi.org/10.1177/0956797617706086

Karashima, A., Nakao, M., Katayama, N., Honda, K., 2005. Instantaneous acceleration and amplification of hippocampal theta wave coincident with phasic pontine activities during REM sleep. Brain Research 1051, 50–56. https://doi.org/10.1016/j.brainres.2005.05.055

Kawashima, I., Hinuma, T., Tanaka, S.C., 2023. Ecological momentary assessment of mind-wandering: meta-analysis and systematic review. Sci Rep 13, 2873. https://doi.org/10.1038/s41598-023-29854-9

Killgore, W.D.S., Vanuk, J.R., Knight, S.A., Markowski, S.M., Pisner, D., Shane, B., Fridman, A., Alkozei, A., 2015. Daytime sleepiness is associated with altered resting thalamocortical connectivity. Neuroreport 26, 779–784. https://doi.org/10.1097/WNR.0000000000000418

Killingsworth, M.A., Gilbert, D.T., 2010. A wandering mind is an unhappy mind. Science 330, 932. https://doi.org/10.1126/science.1192439

Kleiner, M., Brainard, D., Pelli, D., Ingling, A., Murray, R., Broussard, C., 2007. What's new in psychtoolbox-3. Perception 36, 1–16.

Kluger, B.M., Herlofson, K., Chou, K.L., Lou, J.-S., Goetz, C.G., Lang, A.E., Weintraub, D., Friedman, J., 2016. Parkinson's Disease-related Fatigue: A Case Definition and Recommendations for Clinical Research. Mov Disord 31, 625–631. https://doi.org/10.1002/mds.26511

Koshino, Y., Nishio, M., Murata, T., Omori, M., Murata, I., Sakamoto, M., Isaki, K., 1993. The Influence of Light Drowsiness on the Latency and Amplitude of P300. Clinical Electroencephalography 24, 110–113. https://doi.org/10.1177/155005949302400307

Krueger, J.M., Nguyen, J.T., Dykstra-Aiello, C.J., Taishi, P., 2019. Local sleep. Sleep Medicine Reviews 43, 14–21. https://doi.org/10.1016/j.smrv.2018.10.001

Kurzban, R., Duckworth, A., Kable, J.W., Myers, J., 2013. An opportunity cost model of subjective effort and task performance. Behav Brain Sci 36, 661–679. https://doi.org/10.1017/S0140525X12003196

Kuznetsova, A., Brockhoff, P.B., Christensen, R.H.B., 2017. lmerTest Package: Tests in Linear Mixed Effects Models. Journal of Statistical Software 82, 1–26. https://doi.org/10.18637/jss.v082.i13

Lacaux, C., Izabelle, C., Santantonio, G., De Villèle, L., Frain, J., Lubart, T., Pizza, F., Plazzi, G., Arnulf, I., Oudiette, D., 2019. Increased creative thinking in narcolepsy. Brain 142, 1988–1999. https://doi.org/10.1093/brain/awz137

Lal, S.K.L., Craig, A., 2002. Driver fatigue: Electroencephalography and psychological assessment. Psychophysiology 39, 313–321. https://doi.org/10.1017/S0048577201393095

Lecci, S., Fernandez, L.M.J., Weber, F.D., Cardis, R., Chatton, J.-Y., Born, J., Lüthi, A., 2017. Coordinated infraslow neural and cardiac oscillations mark fragility and offline periods in mammalian sleep. Science Advances 3, e1602026. https://doi.org/10.1126/sciadv.1602026

Lee, T.W., Girolami, M., Sejnowski, T.J., 1999. Independent component analysis using an extended infomax algorithm for mixed subgaussian and supergaussian sources. Neural Comput 11, 417–441. https://doi.org/10.1162/089976699300016719

Lemercier, C., Pêcher, C., Berthié, G., Valéry, B., Vidal, V., Paubel, P.-V., Cour, M., Fort, A., Galéra, C., Gabaude, C., Lagarde, E., Maury, B., 2014. Inattention behind the wheel: How factual internal thoughts impact attentional control while driving. Safety Science 62, 279–285. https://doi.org/10.1016/j.ssci.2013.08.011

Lenth, R.V., Banfai, B., Bolker, B., Buerkner, P., Giné-Vázquez, I., Herve, M., Jung, M., Love, J., Miguez, F., Piaskowski, J., Riebl, H., Singmann, H., 2025. emmeans: Estimated Marginal Means, aka Least-Squares Means.

Leu-Semenescu, S., De Cock, V.C., Le Masson, V.D., Debs, R., Lavault, S., Roze, E., Vidailhet, M., Arnulf, I., 2011. Hallucinations in narcolepsy with and without cataplexy: contrasts with Parkinson's disease. Sleep Med 12, 497–504. https://doi.org/10.1016/j.sleep.2011.03.006

Likar, M., Becz, B., Simor, P., 2023. Circadian Fluctuations in Mind-wandering: The Temporal Orientation and the Affective Tone of Thoughts. Proceedings of the MEi:CogSci Conference 17.

Linz, R., Pauly, R., Smallwood, J., Engert, V., 2021. Mind-wandering content differentially translates from lab to daily life and relates to subjective stress experience. Psychological Research 85, 649–659. https://doi.org/10.1007/s00426-019-01275-2

Lippert, J., Halfter, H., Heidbreder, A., Röhr, D., Gess, B., Boentert, M., Osada, N., Young, P., 2014. Altered dynamics in the circadian oscillation of clock genes in dermal fibroblasts of patients suffering from idiopathic hypersomnia. PLoS One 9, e85255. https://doi.org/10.1371/journal.pone.0085255

Lloyd, G.E.R., 1983. Hippocrates, the sacred disease, aphorisms, and prognosis. Hippocratic Writings. Boston: Penguin 206–251.

Lorist, M.M., Klein, M., Nieuwenhuis, S., De Jong, R., Mulder, G., Meijman, T.F., 2000. Mental fatigue and task control: planning and preparation. Psychophysiology 37, 614–625.

Lundqvist, M., Miller, E.K., Nordmark, J., Liljefors, J., Herman, P., 2024. Beta: bursts of cognition. Trends Cogn Sci 28, 662–676. https://doi.org/10.1016/j.tics.2024.03.010

Mackworth, N.H., 1948. The breakdown of vigilance during prolonged visual search. Quarterly Journal of Experimental Psychology. https://doi.org/10.1080/17470214808416738

Malow, B.A., 2004. Sleep Deprivation and Epilepsy. Epilepsy Curr 4, 193–195. https://doi.org/10.1111/j.1535-7597.2004.04509.x

Marcus, J.H., Rosekind, M.R., 2017. Fatigue in transportation: NTSB investigations and safety recommendations. Inj Prev 23, 232–238. https://doi.org/10.1136/injuryprev-2015-041791

Maris, E., Oostenveld, R., 2007. Nonparametric statistical testing of EEG- and MEG-data. J Neurosci Methods 164, 177–190. https://doi.org/10.1016/j.jneumeth.2007.03.024

Martel, A., Bruno, N., Robertson, I.H., Dockree, P.M., Sitt, J.D., Valero-Cabré, A., 2023. Distinct Electrophysiological Signatures of Intentional and Unintentional Mind-Wandering Revealed by Low-Frequency EEG Markers. https://doi.org/10.1101/2023.03.21.533634

Maski, K.P., Colclasure, A., Little, E., Steinhart, E., Scammell, T.E., Navidi, W., Diniz Behn, C., 2021. Stability of nocturnal wake and sleep stages defines central nervous system disorders of hypersomnolence. Sleep 44, zsab021. https://doi.org/10.1093/sleep/zsab021

Massimini, M., Corbetta, M., Sanchez-Vives, M.V., Andrillon, T., Deco, G., Rosanova, M., Sarasso, S., 2024. Sleep-like cortical dynamics during wakefulness and their network effects following brain injury. Nat Commun 15, 7207. https://doi.org/10.1038/s41467-024-51586-1

Materna, L., Halfter, H., Heidbreder, A., Boentert, M., Lippert, J., Koch, R., Young, P., 2018. Idiopathic Hypersomnia Patients Revealed Longer Circadian Period Length in Peripheral Skin Fibroblasts. Front Neurol 9, 424. https://doi.org/10.3389/fneur.2018.00424

Mauvieux, B., Hingrand, C., Drigny, J., Hodzic, A., Baron, P., Hurdiel, R., Jouffroy, R., Vauthier, J.-C., Pessiglione, M., Wiehler, A., Degache, F., Pavailler, S., Heyman, E., Plard, M., Noirez, P., Dubois, B., Esculier, J.F., Nguyen, A.P., Van Cant, J., Roy Baillargeon, O., Pairot de Fontenay, B., Delaunay, P.L., Besnard, S., 2022. Study of the Kinetics of the Determinants of Performance During a Mountain Ultramarathon: Multidisciplinary Protocol of the First Trail Scientifique de Clécy 2021. JMIR Res Protoc 11, e38027. https://doi.org/10.2196/38027

Miyauchi, S., Misaki, M., Kan, S., Fukunaga, T., Koike, T., 2009. Human brain activity time-locked to rapid eye movements during REM sleep. Exp Brain Res 192, 657–667. https://doi.org/10.1007/s00221-008-1579-2

Morris, A.M., So, Y., Lee, K.A., Lash, A.A., Becker, C.E., 1992. The P300 event-related potential. The effects of sleep deprivation. J Occup Med 34, 1143–1152.

Mortaheb, S., Klados, M.A., Calster, L.V., Boulakis, P.A., Georgoula, K., Majerus, S., Demertzi, A., 2021. Mind blanking is associated with a rigid spatio-temporal profile in typical wakefulness. https://doi.org/10.1101/2021.05.10.443428

Munoz-Musat, E., Coz, A.L., Corcoran, A.W., Belloli, L., Naccache, L., Andrillon, T., 2025. Mind the blank: behavioral, experiential, and physiological signatures of absent-mindedness. https://doi.org/10.1101/2024.02.11.579845

Murray, B.J., 2017. Subjective and Objective Assessment of Hypersomnolence. Sleep Med Clin 12, 313–322. https://doi.org/10.1016/j.jsmc.2017.03.007

Muscio, B., 1921. FEELING-TONE IN INDUSTRY: A Report to the Industrial Fatigue Research Board. British Journal of Psychology. General Section 12, 150–162. https://doi.org/10.1111/j.2044-8295.1921.tb00047.x

Nierenberg, A.A., Keefe, B.R., Leslie, V.C., Alpert, J.E., Pava, J.A., Worthington, J.J., Rosenbaum, J.F., Fava, M., 1999. Residual symptoms in depressed patients who respond acutely to fluoxetine. J Clin Psychiatry 60, 221–225. https://doi.org/10.4088/jcp.v60n0403

Nikkonen, S., Somaskandhan, P., Korkalainen, H., Kainulainen, S., Terrill, P.I., Gretarsdottir, H., Sigurdardottir, S., Olafsdottir, K.A., Islind, A.S., Óskarsdóttir, M., Arnardóttir, E.S., Leppänen, T., 2024. Multicentre sleep-stage scoring agreement in the Sleep Revolution project. Journal of Sleep Research 33, e13956. https://doi.org/10.1111/jsr.13956

Norman, R.G., Pal, I., Stewart, C., Walsleben, J.A., Rapoport, D.M., 2000. Interobserver Agreement Among Sleep Scorers From Different Centers in a Large Dataset. Sleep 23, 1–8. https://doi.org/10.1093/sleep/23.7.1e

Ordali, E., Marcos-Prieto, P., Avvenuti, G., Ricciardi, E., Boncinelli, L., Pietrini, P., Bernardi, G., Bilancini, E., 2024. Prolonged exertion of self-control causes increased sleep-like frontal brain activity and changes in aggressivity and punishment. Proceedings of the National Academy of Sciences 121, e2404213121. https://doi.org/10.1073/pnas.2404213121

Osorio-Forero, A., Cardis, R., Vantomme, G., Guillaume-Gentil, A., Katsioudi, G., Devenoges, C., Fernandez, L.M.J., Lüthi, A., 2021. Noradrenergic circuit control of non-REM sleep substates. Current Biology 31, 5009-5023.e7. https://doi.org/10.1016/j.cub.2021.09.041

Osorio-Forero, A., Foustoukos, G., Cardis, R., Cherrad, N., Devenoges, C., Fernandez, L.M.J., Lüthi, A., 2025. Infraslow noradrenergic locus coeruleus activity fluctuations are gatekeepers of the NREM–REM sleep cycle. Nat Neurosci 28, 84–96. https://doi.org/10.1038/s41593-024-01822-0

Pallesen, S., Olsen, O.K., Eide, E.M., Nortvedt, B., Grønli, J., Larøi, F., Nordmo, M., Glomlien, F.E., 2018. Sleep deprivation and hallucinations. A qualitative study of military personnel. Military Psychology 30, 430–436. https://doi.org/10.1080/08995605.2018.1478561

Pedregosa, F., Varoquaux, G., Gramfort, A., Michel, V., Thirion, B., Grisel, O., Blondel, M., Prettenhofer, P., Weiss, R., Dubourg, V., Vanderplas, J., Passos, A., Cournapeau, D., 2011. Scikit-learn: Machine Learning in Python. MACHINE LEARNING IN PYTHON.

Peirce, J.W., 2007. PsychoPy--Psychophysics software in Python. J Neurosci Methods 162, 8–13. https://doi.org/10.1016/j.jneumeth.2006.11.017

Perrin, F., Bertrand, O., Pernier, J., 1987. Scalp current density mapping: value and estimation from potential data. IEEE Trans Biomed Eng 34, 283–288. https://doi.org/10.1109/tbme.1987.326089

Pessiglione, M., Blain, B., Wiehler, A., Naik, S., 2025. Origins and consequences of cognitive fatigue. Trends in Cognitive Sciences. https://doi.org/10.1016/j.tics.2025.02.005

Philip, P., Sagaspe, P., Taillard, J., Valtat, C., Moore, N., Åkerstedt, T., Charles, A., Bioulac, B., 2005. Fatigue, Sleepiness, and Performance in Simulated Versus Real Driving Conditions. Sleep 28, 1511–1516. https://doi.org/10.1093/sleep/28.12.1511

Pigarev, I.N., Nothdurft, H.C., Kastner, S., 1997. Evidence for asynchronous development of sleep in cortical areas. Neuroreport 8, 2557–2560. https://doi.org/10.1097/00001756-199707280-00027

Pimenta, A., Carneiro, D., Novais, P., Neves, J., 2014. Analysis of Human Performance as a Measure of Mental Fatigue, in: Polycarpou, M., de Carvalho, A.C.P.L.F., Pan, J.-S., Woźniak, M., Quintian, H., Corchado, E. (Eds.), Hybrid Artificial Intelligence Systems. Springer International Publishing, Cham, pp. 389–401. https://doi.org/10.1007/978-3-319-07617-1_35

Pinggal, E., Dockree, P.M., O'Connell, R.G., Bellgrove, M.A., Andrillon, T., 2022. Pharmacological manipulations of physiological arousal and sleep-like slow waves modulate sustained attention. J. Neurosci. https://doi.org/10.1523/JNEUROSCI.0836-22.2022

Pinggal, E., Jackson, J., Kusztor, A., Chapman, D., Windt, J., Drummond, S., Silk, T., Bellgrove, M.A., Andrillon, T., 2025. Sleep-like Slow Waves During Wakefulness Mediate Attention and Vigilance

Difficulties in Adult Attention-Deficit/Hyperactivity Disorder. https://doi.org/10.1101/2025.07.27.666103

Pion-Tonachini, L., Kreutz-Delgado, K., Makeig, S., 2019. ICLabel: An automated electroencephalographic independent component classifier, dataset, and website. Neuroimage 198, 181–197. https://doi.org/10.1016/j.neuroimage.2019.05.026

Pizza, F., Ferri, R., Poli, F., Vandi, S., Cosentino, F.I.I., Plazzi, G., 2013. Polysomnographic study of nocturnal sleep in idiopathic hypersomnia without long sleep time. J Sleep Res 22, 185–196. https://doi.org/10.1111/j.1365-2869.2012.01061.x

Plante, D.T., 2018. Nocturnal sleep architecture in idiopathic hypersomnia: a systematic review and meta-analysis. Sleep Medicine 45, 17–24. https://doi.org/10.1016/j.sleep.2017.10.005

Plante, D.T., Cook, J.D., Barbosa, L.S., Goldstein, M.R., Prairie, M.L., Smith, R.F., Riedner, B.A., 2019. Establishing the objective sleep phenotype in hypersomnolence disorder with and without comorbid major depression. Sleep 42, zsz060. https://doi.org/10.1093/sleep/zsz060

Plante, D.T., Hagen, E.W., Barnet, J.H., Mignot, E., Peppard, P.E., 2024. Prevalence and Course of Idiopathic Hypersomnia in the Wisconsin Sleep Cohort Study. Neurology 102, e207994. https://doi.org/10.1212/WNL.0000000000207994

Poh, J.-H., Chong, P.L.H., Chee, M.W.L., 2016. Sleepless night, restless mind: Effects of sleep deprivation on mind wandering. J Exp Psychol Gen 145, 1312–1318. https://doi.org/10.1037/xge0000207

Rabat, A., Van Cutsem, J., Marcora, S.M., Lambert, A., Markwald, R., Kubala, A.G., Friedl, K.E., 2025. Fatigue and management of warfighter mental endurance. BMJ Mil Health military-2025-002963. https://doi.org/10.1136/military-2025-002963

Riedner, B.A., Vyazovskiy, V.V., Huber, R., Massimini, M., Esser, S., Murphy, M., Tononi, G., 2007. Sleep Homeostasis and Cortical Synchronization: III. A High-Density EEG Study of Sleep Slow Waves in Humans. Sleep 30, 1643–1657.

Robertson, I.H., Manly, T., Andrade, J., Baddeley, B.T., Yiend, J., 1997. “Oops!”: performance correlates of everyday attentional failures in traumatic brain injured and normal subjects. Neuropsychologia 35, 747–758. https://doi.org/10.1016/s0028-3932(97)00015-8

Rolland, B., Jardri, R., Amad, A., Thomas, P., Cottencin, O., Bordet, R., 2014. Pharmacology of Hallucinations: Several Mechanisms for One Single Symptom? BioMed Research International 2014, 307106. https://doi.org/10.1155/2014/307106

Rye, D.B., Bliwise, D.L., Parker, K., Trotti, L.M., Saini, P., Fairley, J., Freeman, A., Garcia, P.S., Owens, M.J., Ritchie, J.C., Jenkins, A., 2012. Modulation of vigilance in the primary hypersomnias by endogenous enhancement of GABAA receptors. Sci Transl Med 4, 161ra151. https://doi.org/10.1126/scitranslmed.3004685

Santamaria, J., Chiappa, K.H., 1987. The EEG of Drowsiness in Normal Adults. Journal of Clinical Neurophysiology 4, 327.

Sapra, A., Bhandari, P., 2025. Chronic Fatigue Syndrome, in: StatPearls. StatPearls Publishing, Treasure Island (FL).

Sara, S.J., 2009. The locus coeruleus and noradrenergic modulation of cognition. Nat Rev Neurosci 10, 211–223. https://doi.org/10.1038/nrn2573

Sateia, M.J., 2014. International Classification of Sleep Disorders-Third Edition. Chest 146, 1387–1394. https://doi.org/10.1378/chest.14-0970

Sauvain, C., Ventos, V., Sackur, J., 2024. Beyond broad and narrow: Intermediate level traits in the personality of bridge players. PLOS ONE 19, e0305985. https://doi.org/10.1371/journal.pone.0305985

Seabold, S., Perktold, J., 2010. Statsmodels: Econometric and Statistical Modeling with Python. scipy. https://doi.org/10.25080/Majora-92bf1922-011

Seli, P., Kane, M.J., Smallwood, J., Schacter, D.L., Maillet, D., Schooler, J.W., Smilek, D., 2018. Mind-Wandering as a Natural Kind: A Family-Resemblances View. Trends Cogn Sci 22, 479–490. https://doi.org/10.1016/j.tics.2018.03.010

Seli, P., Risko, E.F., Smilek, D., Schacter, D.L., 2016. Mind-Wandering With and Without Intention. Trends Cogn Sci 20, 605–617. https://doi.org/10.1016/j.tics.2016.05.010

Sforza, E., Gaudreau, H., Petit, D., Montplaisir, J., 2000. Homeostatic sleep regulation in patients with idiopathic hypersomnia. Clinical Neurophysiology 111, 277–282. https://doi.org/10.1016/S1388-2457(99)00242-4

Sforza, E., Roche, F., Barthélémy, J.C., Pichot, V., 2016. Diurnal and nocturnal cardiovascular variability and heart rate arousal response in idiopathic hypersomnia. Sleep Medicine 24, 131–136. https://doi.org/10.1016/j.sleep.2016.07.012

Shahid, A., Wilkinson, K., Marcu, S., Shapiro, C.M., 2012. Karolinska Sleepiness Scale (KSS), in: Shahid, A., Wilkinson, K., Marcu, S., Shapiro, C.M. (Eds.), STOP, THAT and One Hundred Other Sleep Scales. Springer, New York, NY, pp. 209–210. https://doi.org/10.1007/978-1-4419-9893-4_47

Sheybani, L., Vivekananda, U., Rodionov, R., Diehl, B., Chowdhury, F.A., McEvoy, A.W., Miserocchi, A., Bisby, J.A., Bush, D., Burgess, N., Walker, M.C., 2023. Wake slow waves in focal human epilepsy impact network activity and cognition. Nat Commun 14, 7397. https://doi.org/10.1038/s41467-023-42971-3

Siclari, F., Baird, B., Perogamvros, L., Bernardi, G., LaRocque, J.J., Riedner, B., Boly, M., Postle, B.R., Tononi, G., 2017. The neural correlates of dreaming. Nat Neurosci 20, 872–878. https://doi.org/10.1038/nn.4545

Siclari, F., Tononi, G., 2017. Local aspects of sleep and wakefulness. Current Opinion in Neurobiology, Neurobiology of Sleep 44, 222–227. https://doi.org/10.1016/j.conb.2017.05.008

Smallwood, J., Schooler, J.W., 2015. The Science of Mind Wandering: Empirically Navigating the Stream of Consciousness. Annual Review of Psychology 66, 487–518. https://doi.org/10.1146/annurev-psych-010814-015331

Smallwood, J., Schooler, J.W., 2006. The restless mind. Psychol Bull 132, 946–958. https://doi.org/10.1037/0033-2909.132.6.946

Smallwood, J.M., Baracaia, S.F., Lowe, M., Obonsawin, M., 2003. Task unrelated thought whilst encoding information. Consciousness and Cognition 12, 452–484. https://doi.org/10.1016/S1053-8100(03)00018-7

Smilek, D., Carriere, J.S.A., Cheyne, J.A., 2010. Failures of sustained attention in life, lab, and brain: Ecological validity of the SART. Neuropsychologia 48, 2564–2570. https://doi.org/10.1016/j.neuropsychologia.2010.05.002

Smith, M.R., Zeuwts, L., Lenoir, M., Hens, N., De Jong, L.M.S., Coutts, A.J., 2016. Mental fatigue impairs soccer-specific decision-making skill. Journal of Sports Sciences 34, 1297–1304. https://doi.org/10.1080/02640414.2016.1156241

Snipes, S., Krugliakova, E., Meier, E., Huber, R., 2022. The theta paradox: 4-8 Hz EEG oscillations reflect both sleep pressure and cognitive control. J. Neurosci. https://doi.org/10.1523/JNEUROSCI.1063-22.2022

Song, X., Wang, X., 2012. Mind Wandering in Chinese Daily Lives – An Experience Sampling Study. PLOS ONE 7, e44423. https://doi.org/10.1371/journal.pone.0044423

Šonka, K., Šusta, M., Billiard, M., 2015. Narcolepsy with and without cataplexy, idiopathic hypersomnia with and without long sleep time: a cluster analysis. Sleep Med 16, 225–231. https://doi.org/10.1016/j.sleep.2014.09.016

Stephan, A.M., Siclari, F., 2023. Reconsidering sleep perception in insomnia: from misperception to mismeasurement. J Sleep Res 32, e14028. https://doi.org/10.1111/jsr.14028

Stephansen, J.B., Olesen, A.N., Olsen, M., Ambati, A., Leary, E.B., Moore, H.E., Carrillo, O., Lin, L., Han, F., Yan, H., Sun, Y.L., Dauvilliers, Y., Scholz, S., Barateau, L., Hogl, B., Stefani, A., Hong, S.C., Kim, T.W., Pizza, F., Plazzi, G., Vandi, S., Antelmi, E., Perrin, D., Kuna, S.T., Schweitzer, P.K., Kushida, C., Peppard, P.E., Sorensen, H.B.D., Jennum, P., Mignot, E., 2018. Neural network analysis of sleep stages enables efficient diagnosis of narcolepsy. Nat Commun 9, 5229. https://doi.org/10.1038/s41467-018-07229-3

Thoret, E., Andrillon, T., Gauriau, C., Léger, D., Pressnitzer, D., 2024. Sleep deprivation detected by voice analysis. PLOS Computational Biology 20, e1011849. https://doi.org/10.1371/journal.pcbi.1011849

Thorndike, E., 1900. Mental fatigue. I. Psychological Review 7, 466–482. https://doi.org/10.1037/h0069440

Tononi, G., Cirelli, C., 2014. Sleep and the price of plasticity: from synaptic and cellular homeostasis to memory consolidation and integration. Neuron 81, 12–34. https://doi.org/10.1016/j.neuron.2013.12.025

Tononi, G., Cirelli, C., 2006. Sleep function and synaptic homeostasis. Sleep Med Rev 10, 49–62. https://doi.org/10.1016/j.smrv.2005.05.002

Tononi, G., Massimini, M., 2008. Why does consciousness fade in early sleep? Ann N Y Acad Sci 1129, 330–334. https://doi.org/10.1196/annals.1417.024

Torsvall, L., åAkerstedt, T., 1987. Sleepiness on the job: continuously measured EEG changes in train drivers. Electroencephalography and Clinical Neurophysiology 66, 502–511. https://doi.org/10.1016/0013-4694(87)90096-4

Tran, Y., Craig, A., Craig, R., Chai, R., Nguyen, H., 2020. The influence of mental fatigue on brain activity: Evidence from a systematic review with meta-analyses. Psychophysiology 57, e13554. https://doi.org/10.1111/psyp.13554

Trimpop, J., Schenk, H., Bieber, G., Lämmel, F., Burggraf, P., 2017. Smartwatch based Respiratory Rate and Breathing Pattern Recognition in an End-consumer Environment, in: Proceedings of the 4th International Workshop on Sensor-Based Activity Recognition and Interaction, iWOAR '17. Association for Computing Machinery, New York, NY, USA, pp. 1–5. https://doi.org/10.1145/3134230.3134235

Troester, M.M., Quan, S.F., Medicine, A.A. of S., Berry, R.B., 2023. The AASM Manual for the Scoring of Sleep and Associated Events, Version 3. American Academy Of Sleep Medicine.

Trotti, L.M., 2017. Waking up is the hardest thing I do all day: Sleep inertia and sleep drunkenness. Sleep Med Rev 35, 76–84. https://doi.org/10.1016/j.smrv.2016.08.005

Unsworth, N., McMillan, B.D., 2013. Mind wandering and reading comprehension: Examining the roles of working memory capacity, interest, motivation, and topic experience. Journal of Experimental Psychology: Learning, Memory, and Cognition 39, 832–842. https://doi.org/10.1037/a0029669

Vallat, R., Walker, M.P., 2021. An open-source, high-performance tool for automated sleep staging. Elife 10, e70092. https://doi.org/10.7554/eLife.70092

Van den Driessche, C., Bastian, M., Peyre, H., Stordeur, C., Acquaviva, É., Bahadori, S., Delorme, R., Sackur, J., 2017. Attentional Lapses in Attention-Deficit/Hyperactivity Disorder: Blank Rather Than Wandering Thoughts. Psychol Sci 28, 1375–1386. https://doi.org/10.1177/0956797617708234

Van den Driessche, C., Chappé, C., Konishi, M., Cleeremans, A., Sackur, J., 2025. States of mind: Towards a common classification of mental states. Consciousness and Cognition 129, 103828. https://doi.org/10.1016/j.concog.2025.103828

van der Wel, P., van Steenbergen, H., 2018. Pupil dilation as an index of effort in cognitive control tasks: A review. Psychon Bull Rev 25, 2005–2015. https://doi.org/10.3758/s13423-018-1432-y

Vanková, J., Nevsímalová, S., Sonka, K., Spacková, N., Svejdová-Blazejová, K., 2001. Increased REM density in narcolepsy-cataplexy and the polysymptomatic form of idiopathic hypersomnia. Sleep 24, 707–711. https://doi.org/10.1093/sleep/24.6.707

Varao-Sousa, T.L., Smilek, D., Kingstone, A., 2018. In the lab and in the wild: How distraction and mind wandering affect attention and memory. Cognitive Research: Principles and Implications 3, 42. https://doi.org/10.1186/s41235-018-0137-0

Vernet, C., Arnulf, I., 2009. Idiopathic Hypersomnia with and without Long Sleep Time: A Controlled Series of 75 Patients. Sleep 32, 753–759. https://doi.org/10.1093/sleep/32.6.753

Vgontzas, A.N., Bixler, E.O., Kales, A., Criley, C., Vela-Bueno, A., 2000. Differences in nocturnal and daytime sleep between primary and psychiatric hypersomnia: diagnostic and treatment implications. Psychosom Med 62, 220–226. https://doi.org/10.1097/00006842-200003000-00013

Virtanen, P., Gommers, R., Oliphant, T.E., Haberland, M., Reddy, T., Cournapeau, D., Burovski, E., Peterson, P., Weckesser, W., Bright, J., van der Walt, S.J., Brett, M., Wilson, J., Millman, K.J., Mayorov, N., Nelson, A.R.J., Jones, E., Kern, R., Larson, E., Carey, C.J., Polat, İ., Feng, Y., Moore, E.W., VanderPlas, J., Laxalde, D., Perktold, J., Cimrman, R., Henriksen, I., Quintero, E.A., Harris, C.R., Archibald, A.M., Ribeiro, A.H., Pedregosa, F., van Mulbregt, P., 2020. SciPy 1.0: fundamental algorithms for scientific computing in Python. Nat Methods 17, 261–272. https://doi.org/10.1038/s41592-019-0686-2

Vyazovskiy, V.V., Andrillon, T., 2025. Local Sleep, in: ResearchGate.

Vyazovskiy, V.V., Harris, K.D., 2013. Sleep and the single neuron: the role of global slow oscillations in individual cell rest. Nature Reviews Neuroscience 14, 443–451. https://doi.org/10.1038/nrn3494

Vyazovskiy, V.V., Olcese, U., Hanlon, E.C., Nir, Y., Cirelli, C., Tononi, G., 2011. Local sleep in awake rats. Nature 472, 443–447. https://doi.org/10.1038/nature10009

Walacik-Ufnal, E., Piotrowska, A.J., Wołyńczyk-Gmaj, D., Januszko, P., Gmaj, B., Ufnal, M., Kabat, M., Wojnar, M., 2017. Narcolepsy type 1 and hypersomnia associated with a psychiatric disorder show different slow wave activity dynamics. Acta Neurobiol Exp (Wars) 77, 147–156. https://doi.org/10.21307/ane-2017-047

Walker, H.E.K., Trick, L.M., 2018. Mind-wandering while driving: The impact of fatigue, task length, and sustained attention abilities. Transportation Research Part F: Traffic Psychology and Behaviour 59, 81–97. https://doi.org/10.1016/j.trf.2018.08.009

Wammes, J.D., Seli, P., Cheyne, J.A., Boucher, P.O., Smilek, D., 2016. Mind wandering during lectures II: Relation to academic performance. Scholarship of Teaching and Learning in Psychology 2, 33–48. https://doi.org/10.1037/stl0000055

Wang, H., Dragomir, A., Abbasi, N.I., Li, J., Thakor, N.V., Bezerianos, A., 2018. A novel real-time driving fatigue detection system based on wireless dry EEG. Cogn Neurodyn 12, 365–376. https://doi.org/10.1007/s11571-018-9481-5

Ward, A., Wegner, D., 2013. Mind-blanking: when the mind goes away. Frontiers in Psychology 4, 650. https://doi.org/10.3389/fpsyg.2013.00650

Ward, A.F., Wegner, D.M., 2013. Mind-blanking: When the mind goes away. Frontiers in Psychology 4. https://doi.org/10.3389/fpsyg.2013.00650

Wascher, E., Heppner, H., Kobald, S.O., Arnau, S., Getzmann, S., Möckel, T., 2016. Age-Sensitive Effects of Enduring Work with Alternating Cognitive and Physical Load. A Study Applying Mobile EEG in a Real Life Working Scenario. Front. Hum. Neurosci. 9. https://doi.org/10.3389/fnhum.2015.00711

Waters, F., Chiu, V., Atkinson, A., Blom, J.D., 2018. Severe Sleep Deprivation Causes Hallucinations and a Gradual Progression Toward Psychosis With Increasing Time Awake. Front Psychiatry 9, 303. https://doi.org/10.3389/fpsyt.2018.00303

Wiehler, A., Branzoli, F., Adanyeguh, I., Mochel, F., Pessiglione, M., 2022. A neuro-metabolic account of why daylong cognitive work alters the control of economic decisions. Current Biology 32, 3564-3575.e5. https://doi.org/10.1016/j.cub.2022.07.010

Williamson, A., Lombardi, D.A., Folkard, S., Stutts, J., Courtney, T.K., Connor, J.L., 2011. The link between fatigue and safety. Accident Analysis & Prevention, Advancing Fatigue and Safety Research 43, 498–515. https://doi.org/10.1016/j.aap.2009.11.011

Wright, R.A., Stewart, C.C., Barnett, B.R., 2008. Mental fatigue influence on effort-related cardiovascular response: Extension across the regulatory (inhibitory)/non-regulatory performance dimension. International Journal of Psychophysiology 69, 127–133. https://doi.org/10.1016/j.ijpsycho.2008.04.002

Xie, L., Kang, H., Xu, Q., Chen, M.J., Liao, Y., Thiyagarajan, M., O'Donnell, J., Christensen, D.J., Nicholson, C., Iliff, J.J., Takano, T., Deane, R., Nedergaard, M., 2013. Sleep Drives Metabolite Clearance from the Adult Brain. Science 342, 373–377. https://doi.org/10.1126/science.1241224

Yang, Z., Williams, S.D., Beldzik, E., Anakwe, S., Schimmelpfennig, E., Lewis, L.D., 2024. Attentional failures after sleep deprivation represent moments of cerebrospinal fluid flow. https://doi.org/10.1101/2024.11.15.623271

Zanoli, C., Villani, V., Picone, M., 2023. The Road to Industry 5.0: The Challenges of Human Fatigue Modeling 4797–4804. https://doi.org/10.1109/smc53992.2023.10394500

Zhao, C., Zhao, M., Liu, J., Zheng, C., 2012. Electroencephalogram and electrocardiograph assessment of mental fatigue in a driving simulator. Accident Analysis & Prevention 45, 83–90. https://doi.org/10.1016/j.aap.2011.11.019

Supplementary Appendix

Note on contribution:

In supplementary studies 1 and 2, Esteban M.M and Andrew W. C. re-analyzed the data collected by Thomas A. during his postdoc at Monash University (Melbourne, Australia, n = 32 participants). I organized the replication of the study with Thomas A. at the Paris Brain Institute (Paris, France, n = 36 participants). In supplemental appendix 3, Yannis I. under the supervision of Delphine O. collected and analyzed the data. I was a blind scorer of 364 video clips displaying parasomnia episode.

Supplementary Appendix 1: Mind the blank: behavioral, experiential, and physiological signatures of absent-mindedness

bioRxiv preprint doi: https://doi.org/10.1101/2024.02.11.579845; this version posted April 22, 2025. The copyright holder for this preprint (which was not certified by peer review) is the author/funder, who has granted bioRxiv a license to display the preprint in perpetuity. It is made available under aCC-BY-NC-ND 4.0 International license.

Title: Mind the blank: behavioral, experiential, and physiological signatures of absent-mindedness

Authors: Esteban Munoz-Musat[1,2], Arthur Le Coz[1,5], Andrew W. Corcoran[3], Laouen Belloli[1], Lionel Naccache[1,4], Thomas Andrillon[1,3,5*]

Affiliations:

[1] Sorbonne Université, Institut du Cerveau - Paris Brain Institute - ICM, Inserm, CNRS, APHP, Hôpital de la Pitié Salpêtrière, Paris, France
[2] Université Paris-Cité/Service de Neurologie Cognitive, hôpital Lariboisière-Fernand Widal. IHU reConnect, Paris, France.
[3] Monash Centre for Consciousness and Contemplative Studies, Faculty of Arts, Monash University, Melbourne, Australia
[4] Service de Neurophysiologie, Hôpital Pitié Salpêtrière, Paris, France
[5] Service des Pathologies du Sommeil, Hôpital Pitié Salpêtrière, Paris, France

*Corresponding author. Email: thomas.andrillon@icm-institute.org.

ABSTRACT:

Does being awake necessarily mean being conscious of something? This study investigates the phenomenon of Mind Blanking (MB), characterized by an "emptiness of mind", comparing it with Mind Wandering (MW) and On-task (ON) states. Using a sustained attention task and electroencephalogram monitoring, behavioral and neurophysiological signatures of MB were examined in 62 participants. MB exhibited a specific pattern of behavioral lapses, as well as decreased fast oscillatory activity and complexity over posterior electrodes compared to MW. Functional connectivity analyses revealed decreased long-range inter-areal connectivity during MB, compared to both ON and MW states. Event-related potentials with source reconstruction and temporal decoding techniques indicated a significant disruption in visual processing during MB, starting from 200 ms post stimulus and echoing into the late-stage of visual processing, suggesting a disruption of conscious access to sensory information during MB. EEG-based neural features enabled trial-level prediction of mental states, furnishing estimates of the fine-grained dynamics of consciousness beyond subjective reports. Overall, these findings challenge the notion of the wakeful conscious mind as inherently content-oriented, suggesting that MB reflects genuine gaps in the stream of conscious thoughts, arising from disruptions in the generation or accessibility of thought content

bioRxiv preprint doi: https://doi.org/10.1101/2024.02.11.579845; this version posted April 22, 2025. The copyright holder for this preprint (which was not certified by peer review) is the author/funder, who has granted bioRxiv a license to display the preprint in perpetuity. It is made available under aCC-BY-NC-ND 4.0 International license.

SIGNIFICANCE STATEMENT:

Employing cutting-edge neurophysiological techniques on high-density electroencephalographic recordings, our study unveils unique neurophysiological markers of mind blanking, a phenomenon characterized by lapses in conscious content amidst the flow of wakeful consciousness. Distinguished from content-oriented states such as on-task and mind-wandering, mind blanking appears to be a distinct mental state. Furthermore, we demonstrate the feasibility of decoding consciousness dynamics solely from EEG features, transcending the limitations of intermittent subjective reports. Our findings thus not only provide a novel framework for investigating the stream of consciousness but also challenge the conventional notion that wakefulness invariably signifies being conscious of something.

Keywords: Mind Blanking, Mind Wandering, EEG, Neurophysiology, Consciousness, Attention.

bioRxiv preprint doi: https://doi.org/10.1101/2024.02.11.579845; this version posted April 22, 2025. The copyright holder for this preprint (which was not certified by peer review) is the author/funder, who has granted bioRxiv a license to display the preprint in perpetuity. It is made available under aCC-BY-NC-ND 4.0 International license.

INTRODUCTION

> *"Consciousness, then, does not appear to itself chopped up in bits. Such words as 'chain' or 'train' do not describe it fitly as it presents itself in the first instance. It is nothing jointed; it flows. A 'river' or a 'stream' are the metaphors by which it is most naturally described. In talking of it hereafter let us call it the stream of thought, of consciousness, or of subjective life"* (William James, 1890).

In the former quote, William James pointed to two very intuitive aspects of our conscious experience[1]. First, consciousness seems *continuous* during wakefulness, without any "pauses" or breaks in the flow of contents of experience. Second, our conscious experience is dynamic and the origin of conscious content changes very frequently. Indeed, the stream of experiences can quickly shift between different external sources of information, but also turn inward towards internally generated task-unrelated thoughts, a phenomenon usually referred to as mind wandering (MW)[2,3]. Extensive research has shown that, in the brain, the transitions between task-related focus and MW involve modulations of activity of the Default-mode network (DMN)[4] as well as changes in cortical dynamics with modulations of alpha activity[5,6] and increases in slower rhythms[7]. MW research has also investigated the distinctions between different MW subtypes, stressing the importance of considering the meta-awareness or voluntariness dimensions of MW[8].

More recently, a third "mind state" has been described, challenging the idea of a continuous stream of conscious contents during wakefulness: the state of mind blanking (MB). MB is described as a waking state that is either spontaneous or intentional, during which a subject does not report any mental content, but rather the feeling of an empty mind[9]. Previous studies have shown that MB is reported about 14-18% of times during focused tasks[9,10] and about 6% of times during resting[11]. Furthermore, MB has been associated with a specific behavioral signature, distinct from both MW and task-focused states[7]. The exact nature of mind blanking is still a matter of debate[12,13] and only a few studies have attempted to investigate its neural correlates[14]. Some have reported a widespread deactivation of thalamic and cortical brain regions during spontaneous MB[15] and a more focal deactivation of the superior and inferior frontal gyri and hippocampus during intentional MB, whereas anterior cingulate cortex activation seemed to increase[16]. Others have reported an increase of functional connectivity, as measured by phase coherence metrics, during MB[17]. Finally, MB has been linked to the occurrence of sleep-like slow waves in scalp EEG[7].

bioRxiv preprint doi: https://doi.org/10.1101/2024.02.11.579845; this version posted April 22, 2025. The copyright holder for this preprint (which was not certified by peer review) is the author/funder, who has granted bioRxiv a license to display the preprint in perpetuity. It is made available under aCC-BY-NC-ND 4.0 International license.

Two pressing questions regarding MB remain. First, it remains unclear whether MW and MB correspond indeed to different subjective and neurophysiological states[18,19] or if they can be traced back to common underlying physiological causes expressed in varying degrees[20]. Recent evidence suggests that both MW and MB could be explained by local sleep phenomena in the brain, but with different regional distributions[7]. Other accounts suggest that MB could arise from a specific pattern of neural (de)activations or functional connectivity, distinguishable from both task-focused and MW states[15,17]. To better understand the true nature of MB in respect to both task-focused and MW states, the neural distinctions of these mind states, if any, need to be further investigated[21,22].

Second, the place of MB in the hierarchy of consciousness states needs to be clarified. Traditionally, a clear distinction was made between states of unconsciousness (e.g., coma, deep N3 sleep) and states of consciousness (e.g., normal Wakefulness, REM sleep). States of consciousness (i.e., being conscious) classically imply the existence of conscious contents (i.e., being conscious of something) whereas states of unconsciousness imply the absence of such contents. Recent work suggests that the frontier between conscious and unconscious states is not as clear-cut. Indeed, conscious experiences (dreams) are often reported during consolidated non-REM sleep[23,24]; and transient behavioral as well as electrophysiological signs of conscious processing have been recently reported during sleep including N3 sleep[25–27]. These results suggest an intriguing possibility: could the reverse phenomenon - transient absence of conscious content during wakefulness- exist[21]? If so, could MB be a potential candidate for such a particular state?

Some theoretical accounts of consciousness align with the possibility of gaps in the stream of conscious contents. For example, the Global Neuronal Workspace Theory of Consciousness (GNWT)[28,29] suggests that conscious access (and hence, reportability) to a given representation depends on the late, sustained and global ‘ignition’ of fronto-parietal associative areas. According to this view, consciousness is a discrete phenomenon, and windows of unconsciousness during Wakefulness could result from a gap between two ignitions. The Integration Information Theory (IIT) posits that consciousness would dissolve whenever the brain’s capacity to integrate information breaks down[30]. Changes in cortical dynamics towards less integration may correspond to gaps in the stream of consciousness, much like the mirror phenomenon, local activations within sleep, is linked to dreaming[24]. The parallel with sleep and dreaming research is particularly inspiring, since extensive research has shown that (macro) unconscious states (N3 sleep, deep anesthesia, coma, the vegetative state) are characterized by : i) a decrease in neural complexity and fast neural oscillations[31–34]; ii) a breakdown of information sharing between distant cortical areas[35–38], particularly in the

bioRxiv preprint doi: https://doi.org/10.1101/2024.02.11.579845; this version posted April 22, 2025. The copyright holder for this preprint (which was not certified by peer review) is the author/funder, who has granted bioRxiv a license to display the preprint in perpetuity. It is made available under aCC-BY-NC-ND 4.0 International license.

delta and theta frequency bands[39,40] ; iii) impaired neural responses and representations to external stimuli, particularly during the late-stage of information processing (>300ms post-stimulus)[33,41–45]. These previous research provide candidate EEG markers to explore the signature of MB.

Here, we present compelling evidence that MB is a separate mental state, distinct from MW and task-focused states at the phenomenological, behavioral and neurophysiological levels. To provide an exhaustive characterization of the neurophysiological fingerprint of MB, we relied on previous work exploring consciousness states and contents[46]. In particular we capitalized on the use of markers tracking both background neural dynamics (complexity, information sharing) and the processing of external information (ERPs, temporal decoding) in the sensor and source space. Based on these signatures, we argue that MB could represent a failure of conscious access mechanisms, resulting in a genuine gap in the stream of conscious contents.

bioRxiv preprint doi: https://doi.org/10.1101/2024.02.11.579845; this version posted April 22, 2025. The copyright holder for this preprint (which was not certified by peer review) is the author/funder, who has granted bioRxiv a license to display the preprint in perpetuity. It is made available under aCC-BY-NC-ND 4.0 International license.

RESULTS

Different behavioral signatures between Mind Blanking and Mind Wandering

In these two studies, 62 healthy participants performed a modified sustained attention to response task (SART), with digits and faces as stimuli presented in separate blocks, while high-density electro-encephalogram (hdEEG) was recorded continuously. After each stimulus presentation, participants had to press a button (Go trials), or refrain from doing so whenever a "3" or a smiling face was presented (No Go trials; 1 out of 9). Stimulus onset asynchrony (SOA) varied randomly (from 750-1250ms) with a null inter-stimulus interval, and participants' mental state was probed at random intervals (every 40-70s, uniform random jitter). Participants were instructed to report their attentional focus 'just before the interruption' by selecting one of four options: (1) 'task-focused' (ON), (2) 'off-task' (mind-wandering, MW), (3) 'mind-blanking' (MB), or (4) 'don't remember'. Since the fourth option accounted for only 2.6% of all probes (i.e., less than two probes per participant on average) and given that previous studies did not consistently distinguish between these options[47], we merged third and fourth options as MB in all analyses (Figure 1A-B).

Participants performed this task with a high accuracy (mean accuracy of 86.5 ± 0.5% (SEM)) and with a relatively low rate of Misses (i.e., errors in Go trials, 10.4 ± 0.5%). Errors in No Go trials (False alarms [FA]) were frequent (36.7 ± 1.5%). At the subjective level, participants reported being focused on the task (ON) in only 52 ± 2.7% of the probes and otherwise reported MW (35 ± 2.3%) or MB (16 ± 1.8%) (Figure 1C). The distribution of the ON, MW and MB mind-states was not uniform across participants (see Figure 1C), with large inter-individual differences: in particular 9 participants (14.5%) did not report any MB experience.

In order to detect fine-grained modulations of behavioral performance according to the participant's mind-state, we labeled all trials presented up to 5 seconds before each probe as corresponding to the probed state (e.g., after an 'ON' response, all previous trials that occurred during the previous 5 seconds were labeled as 'ON' trials). As previously reported in a smaller subgroup of participants (40% of the present cohort)[7], we found a significant main effect of *mind-state* on FA, misses and RTs (see Table S1). Crucially, pairwise comparisons between mind-states revealed different behavioral profiles for MW and MB: while both were characterized by more FA and misses than during ON, FA were equally frequent during MW and MB (with a non-significant trend for more FA during MW trials) and misses were more frequent during MB (i.e. MB>MW>ON) (see Table S1 and Figure 1D). Response times (RTs) were *slower* for MB (compared to both ON and MW), and *faster* for MW (compared to MB and

bioRxiv preprint doi: https://doi.org/10.1101/2024.02.11.579845; this version posted April 22, 2025. The copyright holder for this preprint (which was not certified by peer review) is the author/funder, who has granted bioRxiv a license to display the preprint in perpetuity. It is made available under aCC-BY-NC-ND 4.0 International license.

ON; significant difference for MW vs MB and statistical trend (FDR corrected p-value 0.1) for MW vs ON) (see Table S1 and figure 1D). In sum, while MW seemed characterized by an "impulsive profile" (more FA and faster RTs), MB presented with an "absent profile" (more misses and slower RTs), which confirms our previous findings obtained in one of the two datasets.

'Front-Back' dissociation between Mind Blanking and Mind Wandering

We next investigated neurophysiological correlates of the mind-states (ON, MW and MB) from EEG recorded during the 5s preceding each probe onset. We computed three classes of neural markers: 1) spectral markers (normalized power spectral densities (PSD) in the delta, theta, alpha, beta and gamma bands); 2) complexity markers[33,48] (Kolmogorov Complexity (KC) and Sample Entropy (SE)) and 3) connectivity markers *(weighted symbolic mutual information*[39] (wSMI) in the delta, theta and alpha bands). These markers (and other similar measures) have been previously shown to track modifications of cognitive and consciousness state in a large range of conditions, including disorders of consciousness (DoC)[33,39,49], sleep[40,50,51], hypnosis[52] and meditation[53].

All studied neural markers were modulated by the participants' mind-state. A significant main effect of *mind-state* and of *electrode location* was found for the wSMI in the delta and theta frequency bands, and a significant effect of these two main factors and their interaction was found for all other markers (linear mixed models with mind-state, electrode location and their interaction as main factors; subject ID and dataset (see Methods) were introduced as random intercepts) (see Table S2).

Spectral and complexity measures revealed different profiles for MW and MB: compared to ON, MW was associated with both an increase in fast oscillatory activity and complexity over central electrodes, and with a decrease of these metrics over fronto-polar and posterior electrodes. As for MB, compared to ON, it was associated with an increase in fast oscillatory activity and complexity over frontal and fronto-central electrodes, and with a decrease in these metrics over centro-posterior and posterior electrodes. The direct contrast between MB and MW revealed a front vs. back dissociation: while frontal and fronto-central electrodes showed faster oscillatory activity and higher complexity in MB than in MW, centro-posterior and posterior electrodes showed an opposite difference (see Figure 2A,C).

Mind-state can be modulated by arousal, with MW and MB frequency increasing in moments of hypovigilance[7,54]. Therefore, some of the observed changes in neural markers could be

bioRxiv preprint doi: https://doi.org/10.1101/2024.02.11.579845; this version posted April 22, 2025. The copyright holder for this preprint (which was not certified by peer review) is the author/funder, who has granted bioRxiv a license to display the preprint in perpetuity. It is made available under aCC-BY-NC-ND 4.0 International license.

explained by a decrease in alertness. To ensure that our results couldn't be *exclusively* explained by this arousal factor, we conducted a verification analysis, by including in our statistical model the vigilance score as a covariate (4-point scale, 1 = Extremely Sleepy, 4 = Extremely Alert), as well as the interaction between electrode location and vigilance score. The observed results for spectral and complexity measures were nearly identical to those previously presented, with the persistence of a clear front-back dissociation between MW and MB. See supplementary Figure S1A,C.

Breakdown of long-range information sharing during Mind Blanking.

Functional connectivity analyses revealed a significant modulation by *mind-state* of the wSMI metric in frequency bands of interest (delta, theta and alpha) (see Table S2). Post-hoc topographical analyses in sensor space revealed a progressive breakdown of connectivity from ON to MW, and then from MW to MB, particularly in the alpha band (see Figure 2B). As for spectral and complexity measures, the inclusion of vigilance score as a covariate in statistical models resulted in very similar results (see Figure S1B). To better characterize these connectivity modulations in function of mind state, we reconstructed the cortical sources of the EEG signal (N=68 cortical sources) at the trial level and computed the information metric wSMI (at different frequency bands) between each pair of sources (n=2278 connections). These sources were further grouped in 10 pairs (right and left) of 5 ROIs, according to the Desikan-Killiany atlas (frontal, limbic, temporal, parietal and occipital), obtaining thus 45 averaged connections between ROIs. Since previous studies reported modifications of coherence-based metrics during MB, we also computed in source space the Phase Locking Value (PLV), for comparison. The statistical analysis revealed a main effect of *mind-state* for all computed connectivity metrics (linear mixed model with mind-state, connection and their interaction as main factors; subject ID and dataset were introduced as random intercepts; see Table S3). As reported in a previous study[17], the coherence-based metric PLV showed an increase in inter-areal connectivity during MB, compared to both MW and ON states (see Figure 3, top panel). By contrast, the information-based metric wSMI showed the reverse pattern: for all computed frequency bands (delta, theta and alpha), a significant reduction in inter-areal connectivity was observed during MB, compared to both ON and MW (except for the connectivity in the delta band between right frontal and right occipital areas, which increased) (see Figure 3). This disruption of inter-areal connectivity during MB concerned mainly parietal areas, and in particular fronto-parietal connectivity.

The inclusion of the vigilance score in the statistical models led to results largely consistent with those previously presented for the PLV and the wSMI in the theta and alpha bands; for

bioRxiv preprint doi: https://doi.org/10.1101/2024.02.11.579845; this version posted April 22, 2025. The copyright holder for this preprint (which was not certified by peer review) is the author/funder, who has granted bioRxiv a license to display the preprint in perpetuity. It is made available under aCC-BY-NC-ND 4.0 International license.

the wSMI in the delta band, the results were more nuanced, revealing both increases and decreases of long-range connectivity during MB (see Figure S2).

As it will be discussed later, the contrast between the PLV and the wSMI results could reflect the relative implication of linear vs. non-linear interactions between cortical regions during these different mind states, non-linear interactions being best captured by the wSMI (see discussion).

As an interim conclusion, these neurophysiological findings confirmed and extended our behavioral results, by showing that MB is associated with a specific brain state distinct from MW. In addition, the significant disruption of long-range connectivity revealed by the wSMI metric during MB suggests a marked impairment of information sharing between cortical areas during this mind-state, as systematically observed during unconscious states.

Disruption of the brain processing of external stimuli during Mind Blanking

The processing of external information is very dependent upon the background brain activity and associated mind state, and foremost the state of consciousness. Previous research has shown that early and intermediate cortical processing is preserved in classically unconscious states such as non-REM sleep[44,55–59] or coma[60–62] (having a prognostic value in this last case). By contrast, late cortical processing seems to be associated with conscious states[25,41,42,44] and conscious processing of external information[63–66]. With this in mind, we decided to probe the differential neural fate of the presented visual stimuli according to the reported mind-state.

First, we conducted a single-trial multi-level analysis of event-related potentials (ERPs) in sensor space (see Methods for details and Table S4 for the results of the statistical model). Early processing of visual stimuli was extremely similar across ON, MW and MB mind-states. In particular, a similar posterior positivity peaking around 100-150 ms after stimulus presentation, and corresponding to the P1 component[67], was present in all 3 conditions (see Figure 4A). Visually, this P1 component seemed more pronounced in ON and MW states than in MB, but very few electrodes showed a significant effect (≤3). No significant differences were observed between MW and ON during the early time-window (see Figure 4B). Crucially, stimulus processing diverged massively as a function of mind-state during the late time-window (>350ms). In ON trials, a classical P3b component (central positivity) spanned roughly from 400 to 650 ms after stimulus onset. In MW trials, this P3b pattern was still observable, but with a longer latency, a reduced maximal amplitude and a shorter duration. Finally, in this late time-window, no clear P3b response was observable in MB trials; amplitudes of MB ERPs

bioRxiv preprint doi: https://doi.org/10.1101/2024.02.11.579845; this version posted April 22, 2025. The copyright holder for this preprint (which was not certified by peer review) is the author/funder, who has granted bioRxiv a license to display the preprint in perpetuity. It is made available under aCC-BY-NC-ND 4.0 International license.

were significantly decreased as compared to ON and MW, with only a reduced and left-lateralized response, possibly related to motor responses (Figure 4A-B). As a control, we also conducted the previously described analysis independently for each stimulus type (faces vs digits). ERP profiles show differences in the timing of early and late components yet, for digits and faces, MB trials were characterised by a disruption of late components compared to ON trials (see Figure S3).

While univariate methods such as ERPs provide with important information about the amplitude and timing of cortical activations in response to external stimuli, multivariate decoding methods allow for a more subtle analysis, and provide information at the level of neural representations. We wanted to answer the following question: does brain activity encode relevant information about the presented stimuli, and how these neural representations vary as a function of the reported mind-state? To do so, we tested whether we could decode stimulus type (Faces vs. Digits) from brain responses using multivariate pattern analysis (MPVA), with the Temporal Decoding method[43,68]. Briefly, this type of analysis consists in using a subset of the data to train a linear classifier at each time-point to differentiate trials where a *Face* was presented from trials where a *Digit* was presented, and then testing its performance, independently at each time-point, in a different subset of the data. We ensured a comparable number of trials between mind-states by randomly subsampling trials from each mind-state. Then, we applied the Temporal Decoding method independently for each mind state, and statistically compared the obtained performance scores (ROC AUC) with a dummy random distribution centered around 0.5 (chance level performance). Results can be found in Figure 4C. For ON trials, we found several time-windows with significant decoding compared to chance level performance. The first one, around 200ms, coincided with a sharp decoding peak (AUC>0.65). The other ones, spanning from 250ms to 580ms, corresponded to a sustained period of decoding. For MW trials, we found a similar initial peak around 200ms; however, later time-windows with significant decoding were sparser, with a period around 350ms, and then a few significant time-points after 400ms. Crucially, we didn't observe any statistically significant decoding for MB trials.

Given these results, we reconstructed the cortical sources of the EEG signals at trial level, and compared the post-stimulus activations (time-window: 0-700ms) to the activations during the baseline period (-250 - 0 ms). For both ON and MW trials, we observed a significant activation of bilateral occipital visual regions (around 200-300 ms post-stimulus), followed by an activation of regions along the ventral and dorsal visual streams (300-600ms), reaching some frontal areas (around 500ms post stimulus). Responses in MW trials were smaller, delayed and less spatially extended compared to ON. Importantly, for MB trials, we observed

bioRxiv preprint doi: https://doi.org/10.1101/2024.02.11.579845; this version posted April 22, 2025. The copyright holder for this preprint (which was not certified by peer review) is the author/funder, who has granted bioRxiv a license to display the preprint in perpetuity. It is made available under aCC-BY-NC-ND 4.0 International license.

only sparse activations, mostly left-sided (contralateral to motor responses), with no clear involvement of the dorsal or ventral visual streams (see Figure 5).

In sum, while the essential processing steps of visual information seem preserved during MW compared to ON-task, these processes appear significantly disrupted during MB, particularly the late responses usually associated with conscious access.

Trial-by-trial prediction of mind-state based on EEG neural features.

The exploration of the dynamics of consciousness is limited by the reliance on the discrete sampling of experience through mind probes and subjective reports. To circumvent this snapshot approach, we set out to predict participants' mind-states on a trial-by-trial basis using neural features. We gathered all the previously presented EEG markers from stimulus-centered epochs (-0.25 to 0.75 s relative to stimulus onset), for all trials. We then trained and cross-validated, independently for each subject, machine learning classifiers (Random Forest), using exclusively trials within the 5 seconds preceding probe onsets (since we can label these trials as "ground truth" based on subjective reports). Importantly, during the cross-validation procedure, we grouped trials by experimental block (6 blocks for each participant) to avoid overfitting due to temporal proximity between trials (see Methods for more details). In multiclass classification (ON vs MW vs MB), the median classifier's balanced accuracy score across participants was of 46%, significantly above chance level performance (median chance level (500 permutations): 37%, FDR corrected p-value=9.10^{-6}, Wilcoxon rank-sum test, see Methods for more details) (Figure 6A; Table S5 and S6). Classifiers' performances varied sharply between participants with classification scores above 60% for some participants, while for other participant's the classifier presented with chance-level performance.

We then used our trained classifiers to estimate the mind-state in non-labeled trials (>5s before probe onsets). To estimate the reliability of these single-trial predictions, we computed metrics of behavioral performance in these trials for each predicted state ($\widehat{ON}$, $\widehat{MW}$, $\widehat{MB}$). Indeed, as shown previously, ON, MW and MB have different behavioral signatures so we can use behavior to check if these signatures are consistent with our predictions. And indeed, behavioral patterns of predicted states were very similar to the corresponding labeled states: we observed more misses in (predicted) $\widehat{MB}$ trials than in $\widehat{ON}$ and $\widehat{MW}$ trials, as well as longer RTs in $\widehat{MB}$ as compared to $\widehat{MW}$ and $\widehat{ON}$ trials (see Table S7 and Figure 6B). We also observed more FA in $\widehat{MW}$ compared to $\widehat{ON}$ trials but RT were significantly slower and not faster (see

bioRxiv preprint doi: https://doi.org/10.1101/2024.02.11.579845; this version posted April 22, 2025. The copyright holder for this preprint (which was not certified by peer review) is the author/funder, who has granted bioRxiv a license to display the preprint in perpetuity. It is made available under aCC-BY-NC-ND 4.0 International license.

Figure 1). This pattern of results suggest that our classifiers were able to retrieve the behavioral signatures on ON, MW and MB states for unprobed trials.

bioRxiv preprint doi: https://doi.org/10.1101/2024.02.11.579845; this version posted April 22, 2025. The copyright holder for this preprint (which was not certified by peer review) is the author/funder, who has granted bioRxiv a license to display the preprint in perpetuity. It is made available under aCC-BY-NC-ND 4.0 International license.

DISCUSSION

Mind Blanking corresponds to a specific brain state, different from Mind Wandering

In this study replicating and extending a previously published study[7], we examined the behavioral and neural correlates of MB, compared to those of MW and ON states. During a sustained attention task, we confirmed our previous findings[7] showing that MB corresponds to a distinct mental state, characterized by a specific behavioral profile and by specific neural signatures. At a behavioral level, MB was characterized by response slowing and higher rate of misses, compatible with participants' subjective report of having been "absent minded" during those moments. This behavioral profile was different from the one observed during MW that was characterized by an acceleration of responses and more false alarms, suggestive of an 'impulsive' pattern of behavior. These differences in behavioral outcomes between MW and MB were previously reported in different tasks (e.g., reading)[69] or even task-free resting state (RT computed on probe responses)[54]. At the neural level, both state markers (spectral, complexity and connectivity measures) and brain responses to external stimuli differentiate MB from MW and ON states. This complements previous findings in fMRI associating spontaneous MB with a pattern of whole-brain hyper-connectivity and de-activation[15,17]. A multivariate combination of these neural metrics allowed for higher than chance prediction of mind-state on a trial-by-trial basis, further supporting the idea that MB, MW and ON states correspond to different mental and neurophysiological states. Taken together, these multimodal results reaffirm the specificity of MB as a distinct mental state[22].

These results face the intrinsic limitations of the validity and reliability of self-reports during experience sampling[70]. Since we used a probe-catching method where subjective reports were assessed every 1 min or so, we cannot exclude the possibility of mental contents/states happening during the interprobe intervals that participants could not report. Moreover, the experience sampling method does not allow to determine precisely the time window that corresponds to a given mind-state. As a first step towards addressing this limitation in the future, we tried to predict the participant's mind-state without reports using multivariate classifiers trained with neural metrics during those trials. Finally, our criterion for considering trials as belonging to a particular mind state (5 seconds) was motivated by technical reasons (see Methods), and not hypothesis or data-driven.

bioRxiv preprint doi: https://doi.org/10.1101/2024.02.11.579845; this version posted April 22, 2025. The copyright holder for this preprint (which was not certified by peer review) is the author/funder, who has granted bioRxiv a license to display the preprint in perpetuity. It is made available under aCC-BY-NC-ND 4.0 International license.

Front vs Back dissociation between Mind Blanking and Mind Wandering

We found that spectral and complexity markers display opposite topographical profiles for MW and MB: whereas MB was characterized by an increase of both complexity and fast oscillatory activity over frontal electrodes (compared to MW), it was also characterized by a decrease in these same metrics over posterior electrodes. These results are in line with previous analyses in a subset of our dataset (40% of the current data)[7], that found evidence for sleep-like slow-waves in both MW and MB, but with different regional localizations: while MW was associated with the presence of wake slow-waves over frontal scalp regions, MB was associated with their extension to posterior regions. Two previous fMRI studies showed that spontaneous MB is associated with an extensive cortical and thalamic de-activation as well as a widespread positive phase-coupling between brain regions[15,17]. Interestingly, chemogenetic inhibition of the mouse prefrontal cortex can result in (i) a decrease in neuronal firing, (ii) the presence of slow oscillations, (iii) an increase in functional connectivity[71], which suggests that the different neural correlates of MB (slow waves, deactivation and hyper-connectivity) could reflect the same neural mechanisms.

These results contrast with another study in fMRI focusing this time on *voluntary* MB, which showed its association with a deactivation of lateral prefrontal regions and hippocampus, but an activation of anterior cingulate cortex[16]. While our spectral and complexity measures were computed in sensor space, and therefore lack precise anatomical information, the observed increase in fast oscillatory activity and neural complexity over centro-anterior electrodes during MB could also be related to ACC activation. These findings are also in line with studies contrasting episodes of MW in which participants are aware or unaware of their own MW. When caught unaware, participants exhibited more activation in frontal areas (dorsal Anterior Cingulate Cortex and ventral Pre Frontal Cortex)[72], which could be related to the increase in fast oscillations we observed in MB, possibly suggesting a continuum between MB and unaware MW. Overall these results highlight the necessity to refine the phenomenological characterization of MB in order to better apprehend its neural correlates[12,13]. It further enriches the literature on spontaneous thoughts and experiences, which previously focused on MW but stressed the importance of considering phenomenal dimensions of MW such as meta-awareness, voluntariness or emotional valence. With MB, we emphasise that the continuous presence of experiential contents should not be taken for granted.

bioRxiv preprint doi: https://doi.org/10.1101/2024.02.11.579845; this version posted April 22, 2025. The copyright holder for this preprint (which was not certified by peer review) is the author/funder, who has granted bioRxiv a license to display the preprint in perpetuity. It is made available under aCC-BY-NC-ND 4.0 International license.

Increased phase synchrony with decreased information sharing between distant brain regions during Mind Blanking

To date, previous studies have reported mixed results regarding functional connectivity during MB. A previous study using fMRI[16] revealed lower functional connectivity between the default mode network and frontal, visual, and salience networks during voluntary MB as compared to MW. By contrast, using a coherence-based measure, a recent study[17] found a pattern of global positive connectivity during spontaneous MB. Beyond potential differences between voluntary and spontaneous MB, it is important to consider that functional connectivity results depend very much on the type of measure being computed. In the present study, we computed two different metrics: the PLV[73], a classical coherence-based measure that captures strictly linear correlations, and the wSMI, an information theory based measure which favors non-linear correlations over purely linear ones[39]. While the PLV showed an increase of inter-areal connectivity in MB as compared to both ON and MW (in line with the previously mentioned study), the wSMI revealed the inverse pattern, with reduced inter-areal (and more specifically, fronto-parietal) connectivity. Dissociations between coherence-based measures and the wSMI have already been reported, for example when contrasting Wakefulness and N3 sleep, where the whole-brain wSMI was significantly decreased in N3 sleep compared to wakefulness, whereas the wPLI (weighted Phase Lag Index) was not[74]. Our results could reflect a dissociation between increased phase-synchrony with decreased information sharing in MB, which could be caused by the occurrence of synchronous episodes of slow waves and neural silencing over associative cortices[75,76]. This model stresses the influence of episodes of hypo-arousal in the occurrence of MB but does not exclude that MB could also occur in states of hyper-arousal as suggested elsewhere[54].

Disrupted neural representations of external stimuli during MB.

Stimulus-induced activity analyses (ERPs, source reconstruction and temporal decoding) revealed similar patterns of processing of task stimuli during ON-task and MW states, significantly different from those observed during MB.

The most obvious difference between mind-states concerned the P3b component. A P3b response (central positivity between 400 and 600 ms post-stimulus) was clearly present during ON-task, was reduced but still observable during MW and seemed to lack during MB trials. While the neural correlates and signatures of the conscious processing of external information remain highly debated[77,78], previous studies[41,64,65] have proposed the P3b component as an EEG signature of conscious access. This interpretation remains debated, since some authors have claimed that the P3b relates more to post-perceptual processes associated with

bioRxiv preprint doi: https://doi.org/10.1101/2024.02.11.579845; this version posted April 22, 2025. The copyright holder for this preprint (which was not certified by peer review) is the author/funder, who has granted bioRxiv a license to display the preprint in perpetuity. It is made available under aCC-BY-NC-ND 4.0 International license.

(external) report than to conscious awareness *per se*[79,80]. The reduction of the P3b observed in MW (shorter duration and decreased amplitude compared to ON-task) is in line with previous findings showing the impact of top-down attention on the P3b[81]. This reduction suggests the superposition of stimulus-unrelated processes during the time-window of the P3b response during MW. This last interpretation is in agreement with a recent study[63], which demonstrated that the P3b can be modulated by participants' attentional focus but conscious perception is always associated with a P3b-like activation of a broad set of associative cortical areas (frontal, parietal and temporal) even in the absence of report. When participants were paying attention and reported on the stimuli, additional cortical areas becoming involved during the same time window lead to a full-fledged P3b. Our source localization results align with this model with a similar activation of the dorsal and ventral visual streams during the late time-window for both ON and MW conditions, reaching some frontal areas in both conditions, but with a less spatially extended response during MW. Crucially, MB showed here a very different ERP signature at the sensor and source level. The relative absence of a P3b response as well as the absence of clear activation of the ventral/dorsal visual streams strongly suggests the absence of conscious access to external visual stimuli in MB trials in contrast with both ON and MW trials.

We also observed differences at the level of early visual processing between the different mind states. While no major differences were observable in sensor-space ERPs during the early time-window (<300ms post-stimulus), our temporal decoding analysis revealed the emergence of distinct visual neural representations around 150-200ms post-stimulus for both ON and MW trials (significant decoding against chance level performance of stimulus category), while this was not the case for MB trials (despite the fact that the number of trials were balanced across conditions). The absence of a significant encoding of visual stimuli over occipital areas around 200ms could suggest a disruption of the actualization of visual representations during MB. This aligns with the pattern of global cortical deactivations reported during MB[15]. It further suggests that the lack of late potentials observed during MB could be due to a weaker or absent sensory activation, failing to ignite the cascade of activations observed in ON and MW, albeit with decreased amplitude for the latter.

Probing mind-state without external reports

The stream of conscious experiences is private and probing for its contents and dynamic is only possible with a sparse and disruptive sampling approach. We attempted here to bypass these reports by leveraging our new correlates of MW and MB. We showed first that we could predict above chance the mind-state category of trials just before a probe (using the mind-state reported following the probe as a ground truth) using a multivariate combination of

bioRxiv preprint doi: https://doi.org/10.1101/2024.02.11.579845; this version posted April 22, 2025. The copyright holder for this preprint (which was not certified by peer review) is the author/funder, who has granted bioRxiv a license to display the preprint in perpetuity. It is made available under aCC-BY-NC-ND 4.0 International license.

different neural markers. Second, we applied the same algorithm to predict mind-states for trials away from the probes, so during moments where we do not have participant's mind-state reports. We could retrieve the behavioral signatures of these states, which suggests that this MVPA approach partially captures a similar dynamics of conscious experience as evidenced in trials in which participants reported on their mental state. While the accuracy of our classifier approach remains very limited, this proof of concept provides an interesting new approach to estimate the second-by-second dynamics of mental states beyond the classical minute-by-minute sampling of subjective experience, paving the way for a fine-grained exploration of the dynamics of consciousness, without under-sampling or interfering with these dynamics by requiring a verbal report.

Conclusion: is Mind Blanking a state without conscious content during wakefulness?

In the introduction of this paper, we presented the predicted neural correlates of a potential contentless conscious state during wakefulness, based on theoretical[28,29,82] and empirical[25,33,39,40,63] considerations. We showed here that the state of MB, a phenomenological, behavioral and neurophysiological distinct state from MW, fulfils these predictions. First, as predicted, the sharing of information between distant cortical areas was disrupted during MB, in particular in the delta and theta frequency bands. Second, the neural representations of external stimuli were significantly disrupted during MB, starting from early periods of processing and echoing into late processing, usually associated with conscious access, with a lack of the usual signatures of conscious access during this mind-state. Finally, spectral, complexity and coherence based connectivity metrics point towards the hypothesis of neural silencing of posterior associative cortices, a key node for consciousness according to most theoretical accounts[29,83]. Since we studied MB in a specific context and task-design, it is possible that some of the markers obtained here would not generalise to other instances of MB. Yet, some of the markers evidenced in this study are compatible with those obtained using a different neuroimaging technique (fMRI) and without a task[15,17].

The presence or absence of internally generated representations during this mind-state remains an open question, and the impression of an "empty mind" reported by the participants during MB could be accounted for by different mechanisms (i.e., lack of metacognitive awareness, lack of memory encoding, language limitations) other than a lack of conscious experience altogether[13]. Still, based on the above presented results, we argue in favour of the more radical interpretation of MB as a "content-free" mind state. This would challenge our intuition of a continuous conscious content during wakefulness. In this view, conscious experience would be a discrete phenomenon, with discrete temporal islets with conscious

bioRxiv preprint doi: https://doi.org/10.1101/2024.02.11.579845; this version posted April 22, 2025. The copyright holder for this preprint (which was not certified by peer review) is the author/funder, who has granted bioRxiv a license to display the preprint in perpetuity. It is made available under aCC-BY-NC-ND 4.0 International license.

content, separated by brief contentless periods[82]. While puzzling, this perspective would bring even more value to those precious moments of conscious experience.

bioRxiv preprint doi: https://doi.org/10.1101/2024.02.11.579845; this version posted April 22, 2025. The copyright holder for this preprint (which was not certified by peer review) is the author/funder, who has granted bioRxiv a license to display the preprint in perpetuity. It is made available under aCC-BY-NC-ND 4.0 International license.

METHODS

Experimental procedure and data collection

Participants

A total of sixty-eight (N = 68) healthy adult subjects were enrolled in this study. Thirty-two (N=32) were recorded at the Monash University (Melbourne, Australia), between June 2018 and February 2019. An additional set of thirty-six (N=36) subjects were recorded at the Paris Brain Institute (Paris, France) from June 2024 to September 2024. The original experiment (Monash) was conducted in English, and instructions were translated in French for the Paris experiment. All other materials and procedures (including the EEG equipment) were similar for the two groups. Due to technical complications during the recording process or suboptimal physiological recording quality identified via retrospective visual examination of the data, six individuals were excluded from subsequent analysis. The final study group, comprising 62 participants (age: 27.9 ± 0.7 years, mean ± standard deviation (age missing for one individual); 31 females), was included in all analyses. Prior to study involvement, participants submitted written informed consent. Both sites Human Research Ethics Committees approved the study protocol (Monash University Human Research Ethics Committee, Project ID: 10994 ; and Comité d'Éthique de la Recherche (CER) de Sorbonne Université, Project ID: CER-2023-DEGRAVE-MW_Respi)

Experimental design and stimuli

Participants were positioned in a dimly lit room, seated approximately 60 cm away from a computer screen with their chin supported. Task instructions, stimuli presentation, and button response collection were executed using the Psychtoolbox extension for Matlab (Mathworks, Natick, MA, USA).

The experimental design involved two adapted SARTs, where participants were instructed to focus on a series of human face images during Face SART blocks and on digits during Digit SART blocks. The sequence of Face and Digit blocks was pseudo-randomized for each participant. Each block lasted for roughly 12-15 minutes, with rest periods permitted between blocks. Participants completed three Face SART and three Digit SART blocks, totalling a duration of 86.7 ± 1.2 minutes (mean ± standard deviation) for the SART, and 108.4 ± 3.4 minutes for the entire recording session. Prior to each type of Face and Digit SART, participants underwent a brief training session (27 trials) with performance feedback on correct trials and average reaction times (RTs). Participants were urged to prioritize accuracy over speed.

bioRxiv preprint doi: https://doi.org/10.1101/2024.02.11.579845; this version posted April 22, 2025. The copyright holder for this preprint (which was not certified by peer review) is the author/funder, who has granted bioRxiv a license to display the preprint in perpetuity. It is made available under aCC-BY-NC-ND 4.0 International license.

Face and digit stimuli were displayed continuously, with each stimulus shown for 750-1250 ms (uniform random jitter). Face stimuli were derived from the Radboud Face Database[84], consisting of eight neutral faces (four females, four males) and one smiling female face. Digits ranging from 1 to 9 were displayed in a fixed font size. For Face SART, participants pressed a button for all neutral faces (Go trials) and refrained from pressing the button for the smiling face (No Go trials). The face order was pseudo-randomized throughout the task (presentation order permuted every nine stimuli, without immediate repetition). For Digit SART, participants pressed a button for all digits except digit 3 (No Go trials), with the digit order pseudo-randomized similarly.

During the SART, stimulus presentation was halted at random intervals (every 40-70 s, uniform random jitter) accompanied by a sound and the word "STOP" on the screen. These interruptions allowed for the assessment of participants' mental states using a series of eight questions. Participants were notably instructed to report their attentional focus "just before the interruption" by selecting one of four options: (1) "task-focused" (ON), (2) "off-task" (mind-wandering, MW), (3) "mind-blanking" (MB), or (4) "don't remember." Since the fourth option accounted for only 2.6% of all probes (less than 2 probes per participant on average) and previous studies do not consistently distinguish between these options[47], we combined the third and fourth options as MB in all analyses. Whenever participants chose the off-task option, they were prompted to indicate the origin of their thoughts or experiences: (1) the environment (distractions), (2) the task (interferences), or (3) internally generated contents. Participants also rated their vigilance levels over the past few trials on a 4-point scale (1 = Extremely Sleepy, 4 = Extremely Alert). Each 12-15 minute SART block contained ten interruptions (30 interruptions per SART task, 60 interruptions per participant). Participants were briefed on the interruptions and question types prior to the experiment. The mental state categories (ON, MW, and MB) were explained both orally and in writing to participants.

Physiological recordings

High-density scalp EEG data were obtained utilizing an EasyCap (Monash) or actiCap Snap (Paris) with 63 active electrodes, connected to a BrainAmp system (Brain Products GmbH). A ground electrode was positioned frontally (Fpz in the 10-20 system), while electrodes were referenced online to a frontal electrode (AFz). Additional electrodes were placed above and below the left and right canthi to record ocular movements (electrooculogram, EOG). Two electrodes were placed over the deltoid muscles to capture electrocardiographic (ECG) activity. EEG, EOG, and ECG signals were sampled at a rate of 500 Hz. Eye movements and pupil size from one eye were recorded using an EyeLink 1000 system (SR Research) but not analyzed here. In the Paris dataset, participants were also equipped with a respiratory belt.

bioRxiv preprint doi: https://doi.org/10.1101/2024.02.11.579845; this version posted April 22, 2025. The copyright holder for this preprint (which was not certified by peer review) is the author/funder, who has granted bioRxiv a license to display the preprint in perpetuity. It is made available under aCC-BY-NC-ND 4.0 International license.

Behavioral analyses

Go trials were deemed incorrect (Miss) if no response was registered between the onset of the stimulus and the subsequent stimulus onset. In contrast, No-Go trials were classified as incorrect (false alarm; FA) if a response was detected within the same time frame. Reaction times (RTs) were calculated from the onset of stimulus presentation. Behavioral performances for each probe were computed using trials within 5 seconds from probe onset. The choice of a 5 second window allowed the inclusion of sufficient No-Go trials for analysis (in average one No-Go trial every two probes), while focusing on trials very close from probe onset and subsequent subjective reports.

EEG preprocessing and analysis

Preprocessing

The raw EEG signal was first high-pass filtered >1 Hz, using a linear-phase, zero-phase FIR (finite impulse response) filter to remove low-frequency drifts which could negatively affect the quality of the ICA fit (see below). A notch filter was then applied (stopbands: [49, 51], [99,101] Hz, FIR filter) to remove line noise. Electrodes that were visually identified as noisy throughout the recording were removed and interpolated using neighbouring electrodes. The EEG signal was then decomposed using independent component analysis (ICA), and the components containing ocular artifacts or electrocardiogram (ECG) artifacts were removed prior to signal reconstruction.

The ICA-cleaned EEG signal was then down-sampled to 250 Hz, and low-pass filtered <60 Hz. An average reference was applied to all EEG electrodes. Finally, the continuous EEG data were segmented in two different manners, so as to obtain two sets of epochs for different analyses: from -5 to 0 seconds relative to the probe onsets (“Probe epochs”), and from -0.25 to 0.75 seconds relative to the stimuli onsets (“Target epochs”). Probe epochs were labelled according to the mind state reported by the participant at probe onset. Target epochs in the 5 second period prior to the probes were labelled according to the subjective report, all other Target epochs were considered non-labelled (unknown mind state).

Sensor space analyses

Calculation of electroencephalographic markers tracking cognitive fluctuations

Previous work has shown that cognitive and consciousness state modifications can be tracked using different spectral, complexity or connectivity measures derived from the scalp or

bioRxiv preprint doi: https://doi.org/10.1101/2024.02.11.579845; this version posted April 22, 2025. The copyright holder for this preprint (which was not certified by peer review) is the author/funder, who has granted bioRxiv a license to display the preprint in perpetuity. It is made available under aCC-BY-NC-ND 4.0 International license.

intracranial electroencephalographic recording. By combining these markers, it is possible to distinguish conscious participants, patients in a minimal consciousness state and patients with unresponsive wakefulness syndrome[33,34,39]. These measures can also differentiate sleep stages[40,51,74] and track cognitive and consciousness modifications related to psychedelics or meditation[53]. In our study, we computed these different measures to try to describe the neural correlates of the different mind states (ON, MW and MB). We therefore computed these measures on a trial-by-trial basis on "Probe epochs" (from -5s to 0s relative to probe onsets), the 5 second time-window allowing for both a sufficient time-period for correct maker computation and for (very) close proximity to the subjective reports.

Prior to marker computation, we performed a spatial Laplacian transformation of the EEG signal (also known as Current Source Density (CSD) estimate)[85]. We applied a spherical spline surface Laplacian transformation, with 50 Legendre terms, a stiffness of the spline of value 4 and a regularization parameter (lambda 2) of 1e-5.

Spectral markers

We computed the normalized power spectral densities (PSD) in delta (1-4 Hz), theta (4-8 Hz), alpha (8-12 Hz), beta (12-30 Hz) and gamma (30-60) frequency bands, using Welch's method. The length of each Welch segment (windowed with a Hamming window) was set to be equal to the length of the FFT (fast Fourier transform) and equal to 256 samples (1024 ms). The obtained segments were then averaged, in order to obtain a single value per epoch, channel and frequency. To obtain the normalized PSDs in each frequency band of interest, we: 1) added the raw power of all the frequencies in each frequency band of interest; and 2) computed for each trial and each electrode the normalized PSD by normalizing the raw frequency band PSD by the total power of the electrode.

Complexity markers

We computed two different complexity measures: the Kolmogorov Complexity (KC) and the Sample Entropy (SE). Although they differ in their method of calculation, both measure the level of predictability and regularity of the EEG signal: the more the signal is unpredictable, the more it's algorithmic complexity is important (more information is needed to describe the signal), and the more the complexity of the local neural processing captured by the EEG sensor is assumed to be important.

We computed these two complexity measures for each trial and each EEG electrode (n= 64). See Supplementary material of Sitt et. al (2014)[33] for a detailed description of KC, as well as

bioRxiv preprint doi: https://doi.org/10.1101/2024.02.11.579845; this version posted April 22, 2025. The copyright holder for this preprint (which was not certified by peer review) is the author/funder, who has granted bioRxiv a license to display the preprint in perpetuity. It is made available under aCC-BY-NC-ND 4.0 International license.

its computation. Details regarding the SE measure can be found in Richman & Moorman (2000)[48].

Connectivity markers

Weighted symbolic mutual information

We focused on the *weighted symbolic mutual information* (wSMI), a functional connectivity measure capturing linear and non-linear coupling between sensors, which relies on the symbolic transformation of the EEG signal. The wSMI assesses the degree to which two EEG sensors exhibit non-random joint fluctuations, implying information sharing. The time series X and Y in all EEG channels are initially converted into discrete symbol sequences (X^, Y^). These symbols are encoded based on the trends in amplitudes in a predetermined number of consecutive time points. The symbols are therefore defined by two parameters: the number of time points considered (k) and the temporal separation between the time points that constitute a symbol ($\boldsymbol{\tau}$). Following previous work, we chose the parameter k to be 3, implying that the symbols are constituted of three elements, leading to 3! = 6 different potential symbols in total. The parameter $\boldsymbol{\tau}$ sets the broad frequency-specific window of sensitivity of this connectivity measure, allowing to compute the wSMI in the delta ($\boldsymbol{\tau}$= 64ms), theta ($\boldsymbol{\tau}$= 32ms) and alpha ($\boldsymbol{\tau}$= 16ms) bands. For each frequency band, the joint probability of each pair of symbols co-occurring in two different time series is computed to estimate the *symbolic mutual information* (SMI) shared across two signals. To minimise volume conduction, the *weighted* symbolic mutual information disregards co-occurrences of identical or opposite-sign signals.

The wSMI between two EEG sensors is computed, after symbolic transformation, according to the following formula:

$$\mathrm{wSMI}(\widehat{X},\widehat{Y}) = \frac{1}{log(k!)} \sum_{\hat{x}\epsilon\widehat{X}} \sum_{\hat{y}\epsilon\widehat{Y}} w(\hat{x},\hat{y}) p(\hat{x},\hat{y}) log \frac{p(\hat{x},\hat{y})}{p(\hat{x})p(\hat{y})}$$

where w(x,y) is the weight matrix and p(x,y) is the joint probability of co-occurrence of symbol x in signal X and symbol y in signal Y. Finally p(x) and p(y) are the probabilities of those symbols in each signal.

We computed, in each frequency band, and for each trial, the wSMI between each pair of electrodes (N pairs=2016). To obtain the topographical maps shown in Supplementary Figure S1, we computed, for each sensor, its median connectivity with all other sensors, obtaining a single value per channel per trial.

bioRxiv preprint doi: https://doi.org/10.1101/2024.02.11.579845; this version posted April 22, 2025. The copyright holder for this preprint (which was not certified by peer review) is the author/funder, who has granted bioRxiv a license to display the preprint in perpetuity. It is made available under aCC-BY-NC-ND 4.0 International license.

Phase Locking Value (PLV)

We also computed a more classical spectral connectivity measure, the Phase Locking Value (PLV), on a trial-by-trial basis. For each channel i, we extracted the instantaneous phase $\phi i^a(t)$ of the analytical signal $xi^a(t)$ of the time series $xi\,(t)$. Then, for each pair (i,j) of channels, we computed the modulus of the time averaged phase difference mapped onto the unit circle:

$$PLV_{ij} = \left| \frac{1}{T} \sum_t e^{i(\phi_i^a(t) - \phi_j^a(t))} \right|$$

As with wSMI, we computed the PLV at trial level for each pair of electrodes, and then, for topographical representation, we computed the median PLV per EEG channel per trial.

Event-related potentials (ERPs) elicited by visual stimuli during the task

In order to study the neural fate of visual stimuli (digits and faces) during the SART task as a function of mind state, we conducted an event-related potential analysis on “Target epochs” (-0.25 to 0.75 s relative to stimulus onset). We first applied a baseline correction relative to the -0.25 to 0s time interval. Given the unbalanced nature of our dataset (important variability of the distribution of mind states across participants), we performed a single-trial multi-level analysis of ERPs responses[86] (see Statistics section for more details about this analysis). Before statistical analysis, to reduce inter-subject variability and to better fit the statistical model, we normalized channel voltages independently for each subject, by subtracting to each point of the *channel x time* matrix the mean *m* and dividing the result by the standard deviation *s*, with *m* and *s* being computed across all points of the *channel x time* matrix. Given that trials follow one another in close succession, it is normal for the baseline activity to be influenced by the activity of the previous trials as seen in Figure 4.

As a control, we also conducted the previously described analysis for each stimulus type (Faces vs. Digits) separately (see Figure S3).

Temporal decoding of stimulus type

To further study the neural fate of the visual stimuli as a function of mind state, we assessed whether we could decode stimulus type (Faces vs. Digits) from brain responses using multivariate pattern analysis (MVPA), with temporal decoding methods[43,68,87]. Briefly, this type of analysis consists in using a subset of the data to train a linear classifier at each time-point to differentiate trials where a *Face* was presented from trials where a *Digit* was presented, and then testing its performance, independently at each time-point, in a different subset of the data.

bioRxiv preprint doi: https://doi.org/10.1101/2024.02.11.579845; this version posted April 22, 2025. The copyright holder for this preprint (which was not certified by peer review) is the author/funder, who has granted bioRxiv a license to display the preprint in perpetuity. It is made available under aCC-BY-NC-ND 4.0 International license.

This method provides statistics tracking the temporal dynamics of mental representations. In the present study, we were interested in the differential profile of the temporal dynamics of mental representations related to external stimuli, as a function of the subject's mind-states (ON,MW and MB).

First, to avoid potential biases related to an unbalanced number of trials between mind-states (example: significantly more trials belonging to the ON mind state would induce better classifier performance in this condition than in the MB condition, independently of differential neural stimulus processing between conditions), we randomly downsampled, for each subject, the number of trials, so each mind state was equally represented. Then, independently for each reported mind-state (ON, MW, MB), we standardized the data at the subject level to suppress interindividual variability. At each time sample, and independently for each channel, channel voltages were standardized across trials sampled from the same participant, by removing the mean and scaling to unit variance. We then trained a linear classifier to decode Digits vs. Faces, using an L2-regularized (C=1) logistic regression, in a 10-fold cross-validation procedure. In each fold, all the trials were shuffled in a pseudo-randomized manner and split into a training set (9/10 of the trials) and a testing set (1/10 of the trials). The classifier's features were the standardized channel amplitudes. This training procedure was applied at each time step independently. Following the temporal decoding approach, the model trained at each time step was then tested at the same time-step on the testing set trials, at each cross-validation fold. The classifier performance at each testing time was evaluated by the area under the receiver operating curve (AUC) at each cross-validation fold. Global performance for each condition and at each time point was obtained by averaging the AUCs across folds. At each time point, performance against chance level was computed (see Statistics section). For visualization purposes, performance curves in function of time were smoothed using a gaussian filter, this filter wasn't applied for statistical analysis.

Decoding of mind-state using dimensionality reduction and a Random Forest classifier

Training and testing the classifier on labeled trials

We set out to determine if the participant's mind state could be predicted based on brain activity, on a trial-by-trial basis, using machine learning classifiers. We first focused on "Labeled Target" epochs, where the participant's mind state was considered as known (trials in the 5 seconds before subjective reports). From these epochs, we extracted the previously described EEG metrics (spectral, complexity, and connectivity, see "Calculation of electroencephalographic markers tracking cognitive modifications" section). We also added

bioRxiv preprint doi: https://doi.org/10.1101/2024.02.11.579845; this version posted April 22, 2025. The copyright holder for this preprint (which was not certified by peer review) is the author/funder, who has granted bioRxiv a license to display the preprint in perpetuity. It is made available under aCC-BY-NC-ND 4.0 International license.

two supplementary features, the mean channel voltages during the early time-period (100 ms to 300ms relative to trial onset) and the mean channel voltages during the late time-period (400-600ms relative to trial onset). For all the previously mentioned markers, we extracted for each trial the values of these markers for each EEG channel (obtaining thus 14 x 64 = 896 features). Given the very high dimensionality of our feature space, we implemented a dimensionality reduction technique prior to classification, using a non-linear (kernel) Principal Component Analysis (PCA)[88]. Classification was performed afterwards using Random Forest Classifiers. To take into account individual variability in neural metrics, we trained and tested a PCA/Random Forest classifier independently per participant, the hyperparameters of the PCA (Kernel type, number of components) and of the Random Forest (number of estimators, criterion, maximum depth) being fitted independently for each participant (see below). Importantly, to ensure an appropriate number of components/number of features ratio, the number of PCA components was chosen in the interval [2,25], corresponding therefore to a ratio of 1 component/10 trials or less, and hence avoiding overfitting. Kernel type was chosen from a list including the following Kernels: Linear, Polynomial, RBF and Sigmoid.

To find the best hyperparameters for our PCA/Random Forest pipeline, while also avoiding overfitting, we adopted a “Randomized Grid Search/Cross-validation procedure”, using 100 iterations. We performed this procedure for each participant. In each iteration, a combination of parameter settings was randomly sampled from all specified possible values of each parameter, then the PCA/Random Forest classifier was trained and tested by cross-validation (see below). At the end of all iterations, the set of hyperparameters that obtained the best cross-validated score (balanced accuracy, see below) was selected for further analyses. Comparison to chance level performance was obtained using a 500-permutation procedure, independently for each participant. First, the true classifier’s score was obtained by training and testing the best model (best set of hyperparameters) by cross validation. Then, at each permutation, trial labels were randomly shuffled, and the entire cross-validation procedure was repeated. We thus obtained a distribution of chance-level scores, for each participant. For each participant, we estimated the individual significance against chance by computing a p-value (by counting the number of permutation scores equal or higher to the true score and dividing it by the number of permutations plus one). Group-level significance against chance was also computed, by comparing the distribution of the classifiers' true scores across participants to the distribution of the mean permutation scores across participants (see Statistics section).

Cross-validation was performed using a 5-stratified group fold strategy. In each fold, 4/5 segments of the data were used to train the classifier and the remaining segment was used to

bioRxiv preprint doi: https://doi.org/10.1101/2024.02.11.579845; this version posted April 22, 2025. The copyright holder for this preprint (which was not certified by peer review) is the author/funder, who has granted bioRxiv a license to display the preprint in perpetuity. It is made available under aCC-BY-NC-ND 4.0 International license.

test the classifier (computation of the balanced accuracy score, see below). Note that class distributions (proportion of ON, MW, and MB trials) were preserved across partitions of the data. Note also that folds were grouped by experimental block (6 block per participant): the blocks that served for the training were not used for the testing. This was done to avoid overfitting linked to temporal proximity of epochs (trials) situated in the same experimental blocks. Note also that this group parameter (experimental block) was also used during the permutation procedure (labels were shuffled inside each block), to avoid over-estimation of significance against chance. At the end of the cross-validation procedure, mean performance scores were obtained by averaging the values obtained in each fold.

We computed a performance score adapted to unbalanced datasets such as ours (unbalanced number of ON, MW, and MB trials): the balanced accuracy score. The balanced accuracy is defined, in multi-class classification, as the average sensitivity Se ("How many relevant items are retrieved?") for each class. The sensitivity is computed as the number of true positives, divided by the number of true positives plus false negatives. Hence, the balanced accuracy (BA) was computed in our dataset according to the following formula:

$$_{BA} = \frac{Se_{ON} + Se_{MW} + Se_{MB}}{3}$$
$$= \frac{(TP/TP+FN)_{ON} + (TP/TP+FN)_{MW} + (TP/TP+FN)_{MB}}{3}$$

Note again that all the previously presented steps were performed using the Labeled Target epochs, where the participant's mind state was considered as known (trials in the 5 second period before subjective reports).

We also computed other very used classification metrics, at subject level and for each class: the Se (also called recall), the precision (TP/TP+FP) and the F1-score ((precision x recall)/(precision + recall)).

Predicting behavioral performances in non-labeled trials

To further test the performances of our classifier, trained on labeled trials, we predicted the mind state in non-labeled trials (more than 5 seconds before probe onsets). Practicaly speaking, we first fitted individual models with labeled data, and then predicted the mind state in non-labeled trials. Given the very high number of non-labeled trials (n=182,970) and its associated computational cost, we randomly subsampled, independently for each subject, 10% of non-labeled trials, resulting in a total of 18,293 trials included in this analysis. To assess the accuracy of this prediction, we once again computed behavioral performances, but this time only on non-labeled trials, and compared the behavioral profile as a function of the mind-

bioRxiv preprint doi: https://doi.org/10.1101/2024.02.11.579845; this version posted April 22, 2025. The copyright holder for this preprint (which was not certified by peer review) is the author/funder, who has granted bioRxiv a license to display the preprint in perpetuity. It is made available under aCC-BY-NC-ND 4.0 International license.

state in non-labeled trials (according to the classifier's prediction), to the behavioral profile in labeled trials.

Source space analyses

Forward Model and Source Modeling

We used a constrained distributed model consisting of 15,000 current dipoles, constrained to the cortical mantle of a generic brain model obtained from the BrainStorm software package. EEG forward modeling was computed using a symmetric Boundary Element Method (BEM) head model. Current density maps were computed using a minimum norm imaging method[89].

Computation of wSMI and PLV at source level

We estimated the cortical sources of our "Probe epochs". We then extracted trial-to-trial source activity time series of a set of 68 cortical regions, according to a standard anatomical atlas (Desikan-Killiany[90]). Using the same method described for sensor space analysis, we computed the wSMI and the PLV between each pair of cortical regions (n=2278). Finally, to reduce the number of multiple comparisons and ease the interpretation of this analysis, we computed the median wSMI between pairs of regions of interest (ROIs). To do so, we grouped the 68 cortical regions in 5 pairs of ROIs, according to the Desikan-Killiany atlas (frontal, limbic, temporal, parietal and occipital). The wSMI/PLV between two ROIs was computed as the median across all the connections shared by the two ROIs. We hence computed a wSMI or PLV value for each pair of ROIs (n=45 connections) and each trial, at each frequency band for the wSMI (delta, theta, alpha, beta and gamma).

Source estimation of stimulus evoked activity

We also estimated the cortical sources of our "Target epochs". Independently for each condition (mind state), we compared the stimulus evoked activity to baseline activity (at source level) using a t-test against the baseline period (see Statistics section).

Statistics

Analyses are listed by order of apparition in the results section

bioRxiv preprint doi: https://doi.org/10.1101/2024.02.11.579845; this version posted April 22, 2025. The copyright holder for this preprint (which was not certified by peer review) is the author/funder, who has granted bioRxiv a license to display the preprint in perpetuity. It is made available under aCC-BY-NC-ND 4.0 International license.

Behavior

We compared the rate of Misses and FA between mind states at trial level using binomial generalized linear mixed models, with mind state as the explanatory factor and with two random factors (random intercepts): **subject ID and dataset (Monash dataset and Paris Brain Institute dataset**). For each behavioral measure and each mind state, response probability and confidence intervals (95%) were back-transformed from the logit scale. For RTs, we used a (gaussian) linear mixed model with mind state as the explanatory factor and s**ubject ID and dataset as random intercepts.** Subject ID is nested within dataset as each subject belongs to only one dataset. Estimated marginal means and confidence intervals (95%) of RTs for each mind state were extracted from the model. All p-values were corrected for multiple comparisons using a *False Discovery Rate* (FDR) procedure, with an alpha level at 0.05 (5%) (for n= 24 comparisons) .

Sensor space EEG markers

For each previously described EEG marker, we compared the three mind states (ON, MW, MB) using linear mixed models at trial level, with mind state, EEG sensor (n=64) and their interaction as explanatory factors, and two random factors (random intercepts), subject identity and dataset (Monash dataset and Paris Brain Institute dataset). Marker values were standardized (z-scored) across all trials before statistical analysis to better fit the linear mixed models. ANOVA tables were computed from the models. We computed post-hoc contrasts between mind states (model estimates and statistical comparisons) at each EEG sensor. During this post-hoc analysis, to reduce the effect of possibly spurious outliers, we applied a winsorizing procedure to all contrast estimates and uncorrected p-values, were the contrast minima and maxima, as well as the p-value minima were limited to values between -5 and +5 T-values. All p-values were corrected for multiple comparisons using an FDR procedure. Main factor's p-values were corrected across the number of factors and the total number of EEG statistical models (n_factors x n_models= 3x (10 state markers + 4 source space connectivity measured + 10 ERPs time windows = 3 x 24 = 72 comparisons, alpha level = 0.05). Post-hoc p-values for each EEG marker were corrected after winsorization across the number of EEG sensors and the number of conditions (correction for n_sensors x n_conditions= 64 x 3=192 comparisons, alpha level = 0.05) .

As a control analysis, we also computed statistical models including the vigilance score, and its interaction with electrode location, as covariates, all other factors and parameters being kept identical as previously described.

bioRxiv preprint doi: https://doi.org/10.1101/2024.02.11.579845; this version posted April 22, 2025. The copyright holder for this preprint (which was not certified by peer review) is the author/funder, who has granted bioRxiv a license to display the preprint in perpetuity. It is made available under aCC-BY-NC-ND 4.0 International license.

Source space wSMI

For each frequency band, we performed a linear mixed model at trial level, with mind state, connection id (ROI1-ROI2) (n=45) and their interaction as explanatory factors, and the same random intercepts (subject identity and dataset). As before, we computed ANOVA tables and post-hoc contrasts between mind-states for each pair of source ROIs, correcting all p-values for multiple comparisons using an FDR procedure, as described above (correction for 72 comparisons for models' main factors, and for n_conditions x n_connections = 3 x 45 = 135 comparisons for each connectivity metric post-hoc p-values)

As a control analysis, we also computed statistical models including the vigilance score, and its interaction with connection identity, as covariates, all other factors and parameters being kept identical as previously described

Sensor space ERPs

We performed a mass-univariate (across time and space dimensions) single-trial multi-level analysis of ERPs responses. We initially intended to add both *EEG channel* and *time* (in addition to *mind state*) as factors to the same mixed linear model, but this was not feasible for computational reasons. We therefore subsampled our time dimension (-250 to 750 ms relative to stimuli onsets) by using a -25 to +25ms sliding time-window, with 75ms steps, resulting in a set of 10 time-windows of interest. We then performed a linear mixed model for each time-window, with *channel amplitude* as the dependent factor; *mind state*, *EEG sensor* and their interaction as explanatory factors; and subject ID and dataset as a random factors (random intercepts). Models' main factors' p-values were corrected for the total number of EEG statistical models x number of factors = 72 comparisons (FDR procedure, alpha level= 0.05). For each time-window, voltage estimates for each mind state, and their statistical comparisons, were computed for each EEG sensor. All obtained p-values were corrected for multiple comparisons using an FDR procedure (for n_sensors x n_conditions x n_times = 64 x 3 x 10 = 1920 comparisons, alpha level = 0.05).

Temporal decoding

For each mind-state, classification performance at each time point was tested against chance level performance using a two-sided non-parametric test (Mann-Whitney) across validation folds (distribution of scores across folds compared to a dummy beta distribution centered around 0.5, with alpha = beta= 20). These statistics were then corrected for multiple comparisons using an FDR procedure (for n_times X n_conditions= 251 x 3= 753 comparisons, alpha level = 0.05).

bioRxiv preprint doi: https://doi.org/10.1101/2024.02.11.579845; this version posted April 22, 2025. The copyright holder for this preprint (which was not certified by peer review) is the author/funder, who has granted bioRxiv a license to display the preprint in perpetuity. It is made available under aCC-BY-NC-ND 4.0 International license.

Source estimation of stimulus evoked activity

We performed a t-test against baseline at each time sample and each cortical source, and corrected for multiple comparisons across time, space and frequency dimensions using an FDR procedure (alpha=0.0001).

Comparison to chance level performance of the classifier trained to distinguish different mind states

As already explained in the previous sections, we compared our classifiers' performances to chance level using a 500-permutation procedure. We performed this procedure for each participant. At each permutation, trial labels were randomly shuffled (grouped by experimental blocks), then the entire training/testing cross-validation procedure was repeated, using the hyperparameters previously selected during the grid search procedure. We thus obtained a distribution of chance-level scores, for each participant. To calculate the individual p-value, we counted the number of permutation scores equal or higher to our true score and divided it by the number of permutations plus one. To assess group level statistical significance against chance, we performed a two-tailed Wilcoxon rank sum test, where we compared the distribution of true classification scores across participants (non permuted data), to the distribution of mean permutation scores (permuted data) across participants.

Software

Most analyses were performed in Python 3.9.13 , using the following packages:

- MNE (v 1.4.2) (https://mne.tools/stable/index.html): preprocessing and manipulation of EEG data
- MNE-features (v 0.2.1) (https://mne.tools/mne-features/) and nice-tools (https://github.com/nice-tools/nice): computation of EEG neural markers
- Pymer4 (v 0.8.0) (https://eshinjolly.com/pymer4/) and pingouin (v 0.5.3) (https://pingouin-stats.org/build/html/index.html) : statistical analysis
- Scikit-learn (v 1.3) (https://scikit-learn.org/stable/) : machine learning analyses

Binomial mixed models (for behavioral analyses) were performed in R using the *lme4* and *emmeans* libraries.

Source reconstruction analyses were performed in Matlab using the Brainstorm package (https://neuroimage.usc.edu/brainstorm/Introduction)

bioRxiv preprint doi: https://doi.org/10.1101/2024.02.11.579845; this version posted April 22, 2025. The copyright holder for this preprint (which was not certified by peer review) is the author/funder, who has granted bioRxiv a license to display the preprint in perpetuity. It is made available under aCC-BY-NC-ND 4.0 International license.

For the Monash dataset, initial preprocessing of raw EEG files using ICA was performed in Matlab using EEGlab 2021.1 and FieldTrip-20210807.

bioRxiv preprint doi: https://doi.org/10.1101/2024.02.11.579845; this version posted April 22, 2025. The copyright holder for this preprint (which was not certified by peer review) is the author/funder, who has granted bioRxiv a license to display the preprint in perpetuity. It is made available under aCC-BY-NC-ND 4.0 International license.

REFERENCES

1. James, W. *The Principles of Psychology*. (Henry Holt and Company, New York, 1890).

2. Smallwood, J., Obonsawin, M. & Heim, D. Task unrelated thought: the role of distributed processing. *Conscious Cogn* **12**, 169–189 (2003).

3. Smallwood, J. & Schooler, J. W. The Science of Mind Wandering: Empirically Navigating the Stream of Consciousness. *Annual Review of Psychology* **66**, 487–518 (2015).

4. Gruberger, M., Simon, E., Levkovitz, Y., Zangen, A. & Hendler, T. Towards a Neuroscience of Mind-Wandering. *Frontiers in Human Neuroscience* **5**, (2011).

5. Compton, R. J., Gearinger, D. & Wild, H. The wandering mind oscillates: EEG alpha power is enhanced during moments of mind-wandering. *Cogn Affect Behav Neurosci* **19**, 1184–1191 (2019).

6. Braboszcz, C. & Delorme, A. Lost in thoughts: neural markers of low alertness during mind wandering. *Neuroimage* **54**, 3040–3047 (2011).

7. Andrillon, T., Burns, A., Mackay, T., Windt, J. & Tsuchiya, N. Predicting lapses of attention with sleep-like slow waves. *Nat Commun* **12**, 3657 (2021).

8. Schooler, J. W. *et al.* Meta-awareness, perceptual decoupling and the wandering mind. *Trends in Cognitive Sciences* **15**, 319–326 (2011).

9. Ward, A. & Wegner, D. Mind-blanking: when the mind goes away. *Frontiers in Psychology* **4**, (2013).

10. Schooler, J. W., Reichle, E. D. & Halpern, D. V. Zoning Out while Reading: Evidence for Dissociations between Experience and Metaconsciousness. in *Thinking and seeing: Visual metacognition in adults and children* 203–226 (MIT Press, Cambridge, MA, US, 2004).

bioRxiv preprint doi: https://doi.org/10.1101/2024.02.11.579845; this version posted April 22, 2025. The copyright holder for this preprint (which was not certified by peer review) is the author/funder, who has granted bioRxiv a license to display the preprint in perpetuity. It is made available under aCC-BY-NC-ND 4.0 International license.

11. Van Calster, L., D'Argembeau, A., Salmon, E., Peters, F. & Majerus, S. Fluctuations of Attentional Networks and Default Mode Network during the Resting State Reflect Variations in Cognitive States: Evidence from a Novel Resting-state Experience Sampling Method. *Journal of Cognitive Neuroscience* **29**, 95–113 (2017).

12. Kaufmann, A., Parmigiani, S., Kawagoe, T., Zabaroff, E. & Wells, B. Two models of mind blanking. *Eur J of Neuroscience* ejn.16164 (2023) doi:10.1111/ejn.16164.

13. Fell, J. What is mind blanking: A conceptual clarification. *Eur J of Neuroscience* **56**, 4837–4842 (2022).

14. Boulakis, P. A. & Demertzi, A. Relating mind-blanking to the content and dynamics of spontaneous thinking. *Current Opinion in Behavioral Sciences* **61**, 101481 (2025).

15. Boulakis, P. A., Mortaheb, S., Van Calster, L., Majerus, S. & Demertzi, A. Whole-Brain Deactivations Precede Uninduced Mind-Blanking Reports. *J. Neurosci.* **43**, 6807–6815 (2023).

16. Kawagoe, T., Onoda, K. & Yamaguchi, S. The neural correlates of "mind blanking": When the mind goes away. *Human Brain Mapping* **40**, 4934–4940 (2019).

17. Mortaheb, S. *et al.* Mind blanking is a distinct mental state linked to a recurrent brain profile of globally positive connectivity during ongoing mentation. *Proceedings of the National Academy of Sciences* **119**, e2200511119 (2022).

18. Mittner, M., Hawkins, G. E., Boekel, W. & Forstmann, B. U. A Neural Model of Mind Wandering. *Trends in Cognitive Sciences* **20**, 570–578 (2016).

19. Unsworth, N. & Robison, M. K. Tracking arousal state and mind wandering with pupillometry. *Cogn Affect Behav Neurosci* **18**, 638–664 (2018).

bioRxiv preprint doi: https://doi.org/10.1101/2024.02.11.579845; this version posted April 22, 2025. The copyright holder for this preprint (which was not certified by peer review) is the author/funder, who has granted bioRxiv a license to display the preprint in perpetuity. It is made available under aCC-BY-NC-ND 4.0 International license.

20. Andrillon, T. *et al.* Does the Mind Wander When the Brain Takes a Break? Local Sleep in Wakefulness, Attentional Lapses and Mind-Wandering. *Frontiers in Neuroscience* **13**, (2019).

21. Andrillon, T., Lutz, A., Windt, J. & Demertzi, A. Where is my Mind?: A Neurocognitive Investigation of Mind Blanking. Preprint at https://doi.org/10.31234/osf.io/xmtga (2024).

22. Boulakis, P. A. & Demertzi, A. Relating mind-blanking to the content and dynamics of spontaneous thinking. *Current Opinion in Behavioral Sciences* **61**, 101481 (2025).

23. Siclari, F., LaRocque, J., Postle, B. & Tononi, G. Assessing sleep consciousness within subjects using a serial awakening paradigm. *Frontiers in Psychology* **4**, (2013).

24. Siclari, F. *et al.* The neural correlates of dreaming. *Nature Neuroscience* **20**, 872–878 (2017).

25. Türker, B. *et al.* Behavioral and brain responses to verbal stimuli reveal transient periods of cognitive integration of the external world during sleep. *Nat Neurosci* **26**, 1981–1993 (2023).

26. Mazza, S. *et al.* Asleep but aware? *Brain and Cognition* **87**, 7–15 (2014).

27. Andrillon, T. & Kouider, S. The vigilant sleeper: neural mechanisms of sensory (de)coupling during sleep. *Current Opinion in Physiology* **15**, 47–59 (2020).

28. Dehaene, S. Towards a cognitive neuroscience of consciousness: basic evidence and a workspace framework. *Cognition* **79**, 1–37 (2001).

29. Mashour, G. A., Roelfsema, P., Changeux, J.-P. & Dehaene, S. Conscious Processing and the Global Neuronal Workspace Hypothesis. *Neuron* **105**, 776–798 (2020).

30. Tononi, G. & Massimini, M. Why does consciousness fade in early sleep? *Ann N Y Acad Sci* **1129**, 330–334 (2008).

bioRxiv preprint doi: https://doi.org/10.1101/2024.02.11.579845; this version posted April 22, 2025. The copyright holder for this preprint (which was not certified by peer review) is the author/funder, who has granted bioRxiv a license to display the preprint in perpetuity. It is made available under aCC-BY-NC-ND 4.0 International license.

31. Casali, A. G. *et al.* A Theoretically Based Index of Consciousness Independent of Sensory Processing and Behavior. *Science Translational Medicine* **5**, 198ra105-198ra105 (2013).

32. Casarotto, S. *et al.* Exploring the Neurophysiological Correlates of Loss and Recovery of Consciousness: Perturbational Complexity. in *Brain Function and Responsiveness in Disorders of Consciousness* (eds. Monti, M. M. & Sannita, W. G.) 93–104 (Springer International Publishing, Cham, 2016). doi:10.1007/978-3-319-21425-2_8.

33. Sitt, J. D. *et al.* Large scale screening of neural signatures of consciousness in patients in a vegetative or minimally conscious state. *Brain* **137**, 2258–2270 (2014).

34. Engemann, D. A. *et al.* Robust EEG-based cross-site and cross-protocol classification of states of consciousness. *Brain* **141**, 3179–3192 (2018).

35. Boveroux, P. *et al.* Breakdown of within- and between-network resting state functional magnetic resonance imaging connectivity during propofol-induced loss of consciousness. *Anesthesiology* **113**, 1038–1053 (2010).

36. Ranft, A. *et al.* Neural Correlates of Sevoflurane-induced Unconsciousness Identified by Simultaneous Functional Magnetic Resonance Imaging and Electroencephalography. *Anesthesiology* **125**, 861–872 (2016).

37. Horovitz, S. G. *et al.* Decoupling of the brain's default mode network during deep sleep. *Proc Natl Acad Sci U S A* **106**, 11376–11381 (2009).

38. Spoormaker, V. I. *et al.* Development of a large-scale functional brain network during human non-rapid eye movement sleep. *J Neurosci* **30**, 11379–11387 (2010).

39. King, J.-R. *et al.* Information Sharing in the Brain Indexes Consciousness in Noncommunicative Patients. *Current Biology* **23**, 1914–1919 (2013).

bioRxiv preprint doi: https://doi.org/10.1101/2024.02.11.579845; this version posted April 22, 2025. The copyright holder for this preprint (which was not certified by peer review) is the author/funder, who has granted bioRxiv a license to display the preprint in perpetuity. It is made available under aCC-BY-NC-ND 4.0 International license.

40. Bourdillon, P. *et al.* Brain-scale cortico-cortical functional connectivity in the delta-theta band is a robust signature of conscious states: an intracranial and scalp EEG study. *Scientific Reports* **10**, 1–13 (2020).

41. Bekinschtein, T. A. *et al.* Neural signature of the conscious processing of auditory regularities. *PNAS* **106**, 1672–1677 (2009).

42. Perez, P. *et al.* Auditory Event-Related "Global Effect" Predicts Recovery of Overt Consciousness. *Frontiers in Neurology* **11**, (2021).

43. King, J.-R., Gramfort, A., Schurger, A., Naccache, L. & Dehaene, S. Two Distinct Dynamic Modes Subtend the Detection of Unexpected Sounds. *PLoS ONE* **9**, e85791 (2014).

44. Strauss, M. *et al.* Disruption of hierarchical predictive coding during sleep. *Proceedings of the National Academy of Sciences* **112**, E1353–E1362 (2015).

45. Hayat, H. *et al.* Reduced neural feedback signaling despite robust neuron and gamma auditory responses during human sleep. *Nat Neurosci* **25**, 935–943 (2022).

46. Pérez, P. *et al.* Content–state dimensions characterize different types of neuronal markers of consciousness. *Neuroscience of Consciousness* **2024**, niae027 (2024).

47. Van den Driessche, C. *et al.* Attentional Lapses in Attention-Deficit/Hyperactivity Disorder: Blank Rather Than Wandering Thoughts. *Psychol Sci* **28**, 1375–1386 (2017).

48. Richman, J. S. & Moorman, J. R. Physiological time-series analysis using approximate entropy and sample entropy. *American Journal of Physiology-Heart and Circulatory Physiology* **278**, H2039–H2049 (2000).

49. Engemann, D. A. *et al.* Robust EEG-based cross-site and cross-protocol classification of states of consciousness. *Brain* **141**, 3179–3192 (2018).

50. Schartner, M. M. *et al.* Global and local complexity of intracranial EEG decreases during NREM sleep. *Neuroscience of Consciousness* **2017**, (2017).

bioRxiv preprint doi: https://doi.org/10.1101/2024.02.11.579845; this version posted April 22, 2025. The copyright holder for this preprint (which was not certified by peer review) is the author/funder, who has granted bioRxiv a license to display the preprint in perpetuity. It is made available under aCC-BY-NC-ND 4.0 International license.

51. Türker, B. *et al.* Behavioral and brain responses to verbal stimuli reveal transient periods of cognitive integration of external world in all sleep stages. 2022.05.04.490484 Preprint at https://doi.org/10.1101/2022.05.04.490484 (2022).

52. Munoz Musat, E., Rohaut, B., Sangare, A., Benhaiem, J.-M. & Naccache, L. Hypnotic Induction of Deafness to Elementary Sounds: An Electroencephalography Case-Study and a Proposed Cognitive and Neural Scenario. *Frontiers in Neuroscience* **16**, (2022).

53. Martínez Vivot, R., Pallavicini, C., Zamberlan, F., Vigo, D. & Tagliazucchi, E. Meditation Increases the Entropy of Brain Oscillatory Activity. *Neuroscience* **431**, 40–51 (2020).

54. Boulakis, P. A. *et al.* Variations of autonomic arousal mediate the reportability of mind blanking occurrences. *Sci Rep* **15**, 4956 (2025).

55. Bastuji, H. & García-Larrea, L. Evoked potentials as a tool for the investigation of human sleep. *Sleep Med Rev* **3**, 23–45 (1999).

56. Ruby, P., Caclin, A., Boulet, S., Delpuech, C. & Morlet, D. Odd sound processing in the sleeping brain. *J Cogn Neurosci* **20**, 296–311 (2008).

57. Nir, Y., Vyazovskiy, V. V., Cirelli, C., Banks, M. I. & Tononi, G. Auditory responses and stimulus-specific adaptation in rat auditory cortex are preserved across NREM and REM sleep. *Cereb Cortex* **25**, 1362–1378 (2015).

58. Kouider, S., Andrillon, T., Barbosa, L. S., Goupil, L. & Bekinschtein, T. A. Inducing Task-Relevant Responses to Speech in the Sleeping Brain. *Current Biology* **24**, 2208–2214 (2014).

59. Andrillon, T., Poulsen, A. T., Hansen, L. K., Léger, D. & Kouider, S. Neural Markers of Responsiveness to the Environment in Human Sleep. *J. Neurosci.* **36**, 6583–6596 (2016).

60. Fischer, C. *et al.* Mismatch negativity and late auditory evoked potentials in comatose patients. *Clinical Neurophysiology* **110**, 1601–1610 (1999).

bioRxiv preprint doi: https://doi.org/10.1101/2024.02.11.579845; this version posted April 22, 2025. The copyright holder for this preprint (which was not certified by peer review) is the author/funder, who has granted bioRxiv a license to display the preprint in perpetuity. It is made available under aCC-BY-NC-ND 4.0 International license.

61. Fischer, C., Luauté, J., Adeleine, P. & Morlet, D. Predictive value of sensory and cognitive evoked potentials for awakening from coma. *Neurology* **63**, 669–673 (2004).

62. Robinson, L. R., Micklesen, P. J., Tirschwell, D. L. & Lew, H. L. Predictive value of somatosensory evoked potentials for awakening from coma*. *Critical Care Medicine* **31**, 960 (2003).

63. Sergent, C. *et al.* Bifurcation in brain dynamics reveals a signature of conscious processing independent of report. *Nat Commun* **12**, 1149 (2021).

64. Sergent, C., Baillet, S. & Dehaene, S. Timing of the brain events underlying access to consciousness during the attentional blink. *Nature Neuroscience* **8**, 1391–1400 (2005).

65. Del Cul, A., Baillet, S. & Dehaene, S. Brain Dynamics Underlying the Nonlinear Threshold for Access to Consciousness. *PLoS Biol* **5**, (2007).

66. Gaillard, R. *et al.* Converging Intracranial Markers of Conscious Access. *PLoS Biol* **7**, (2009).

67. Spehlmann, R. The averaged electrical responses to diffuse and to patterned light in the human. *Electroencephalogr Clin Neurophysiol* **19**, 560–569 (1965).

68. King, J.-R. *et al.* Encoding and Decoding Neuronal Dynamics: Methodological Framework to Uncover the Algorithms of Cognition. (2018).

69. Ward, A. F. & Wegner, D. M. Mind-blanking: when the mind goes away. *Front Psychol* **4**, 650 (2013).

70. Nisbett, R. E. & Wilson, T. D. Telling more than we can know: Verbal reports on mental processes. *Psychological Review* **84**, 231–259 (1977).

71. Rocchi, F. *et al.* Increased fMRI connectivity upon chemogenetic inhibition of the mouse prefrontal cortex. *Nat Commun* **13**, 1056 (2022).

bioRxiv preprint doi: https://doi.org/10.1101/2024.02.11.579845; this version posted April 22, 2025. The copyright holder for this preprint (which was not certified by peer review) is the author/funder, who has granted bioRxiv a license to display the preprint in perpetuity. It is made available under aCC-BY-NC-ND 4.0 International license.

72. Christoff, K., Gordon, A. M., Smallwood, J., Smith, R. & Schooler, J. W. Experience sampling during fMRI reveals default network and executive system contributions to mind wandering. *Proceedings of the National Academy of Sciences of the United States of America* **106**, 8719–8724 (2009).

73. Aydore, S., Pantazis, D. & Leahy, R. M. A note on the phase locking value and its properties. *NeuroImage* **74**, 231–244 (2013).

74. Imperatori, L. S. *et al.* EEG functional connectivity metrics wPLI and wSMI account for distinct types of brain functional interactions. *Sci Rep* **9**, 8894 (2019).

75. Aedo-Jury, F., Schwalm, M., Hamzehpour, L. & Stroh, A. Brain states govern the spatio-temporal dynamics of resting-state functional connectivity. *eLife* **9**, e53186 (2020).

76. El-Baba, M. *et al.* Functional connectivity dynamics slow with descent from wakefulness to sleep. *PLOS ONE* **14**, e0224669 (2019).

77. Aru, J., Bachmann, T., Singer, W. & Melloni, L. Distilling the neural correlates of consciousness. *Neuroscience & Biobehavioral Reviews* **36**, 737–746 (2012).

78. Tsuchiya, N., Wilke, M., Frässle, S. & Lamme, V. A. F. No-Report Paradigms: Extracting the True Neural Correlates of Consciousness. *Trends in Cognitive Sciences* **19**, 757–770 (2015).

79. Cohen, M. A., Ortego, K., Kyroudis, A. & Pitts, M. Distinguishing the Neural Correlates of Perceptual Awareness and Postperceptual Processing. *J. Neurosci.* **40**, 4925–4935 (2020).

80. Pitts, M. A., Metzler, S. & Hillyard, S. A. Isolating neural correlates of conscious perception from neural correlates of reporting one's perception. *Front Psychol* **5**, 1078 (2014).

81. Polich, J. Updating P300: An integrative theory of P3a and P3b. *Clinical Neurophysiology* **118**, 2128–2148 (2007).

bioRxiv preprint doi: https://doi.org/10.1101/2024.02.11.579845; this version posted April 22, 2025. The copyright holder for this preprint (which was not certified by peer review) is the author/funder, who has granted bioRxiv a license to display the preprint in perpetuity. It is made available under aCC-BY-NC-ND 4.0 International license.

82. Naccache, L. Why and how access consciousness can account for phenomenal consciousness. *Philosophical Transactions of the Royal Society B: Biological Sciences* **373**, 20170357 (2018).

83. Tononi, G. The Integrated Information Theory of Consciousness: An Updated Account. *Archives Italiennes de Biologie* **150**, 56–90 (2012).

84. Langner, O. *et al.* Presentation and validation of the Radboud Faces Database. *Cognition & Emotion* **24**, 1377–1388 (2010).

85. Kayser, J. & Tenke, C. E. Principal components analysis of Laplacian waveforms as a generic method for identifying ERP generator patterns: II. Adequacy of low-density estimates. *Clinical Neurophysiology* **117**, 369–380 (2006).

86. Volpert-Esmond, H. I., Merkle, E. C., Levsen, M. P., Ito, T. A. & Bartholow, B. D. Using Trial-Level Data and Multilevel Modeling to Investigate Within-Task Change in Event-Related Potentials. *Psychophysiology* **55**, e13044 (2018).

87. King, J.-R. & Dehaene, S. Characterizing the dynamics of mental representations: the temporal generalization method. *Trends in Cognitive Sciences* **18**, 203–210 (2014).

88. Weston, J., Schölkopf, B. & Bakir, G. Learning to Find Pre-Images. in *Advances in Neural Information Processing Systems* vol. 16 (MIT Press, 2003).

89. Baillet, S., Mosher, J. C. & Leahy, R. M. Electromagnetic brain mapping. *IEEE Signal Processing Magazine* **18**, 14–30 (2001).

90. Desikan, R. S. *et al.* An automated labeling system for subdividing the human cerebral cortex on MRI scans into gyral based regions of interest. *NeuroImage* **31**, 968–980 (2006).

bioRxiv preprint doi: https://doi.org/10.1101/2024.02.11.579845; this version posted April 22, 2025. The copyright holder for this preprint (which was not certified by peer review) is the author/funder, who has granted bioRxiv a license to display the preprint in perpetuity. It is made available under aCC-BY-NC-ND 4.0 International license.

bioRxiv preprint doi: https://doi.org/10.1101/2024.02.11.579845; this version posted April 22, 2025. The copyright holder for this preprint (which was not certified by peer review) is the author/funder, who has granted bioRxiv a license to display the preprint in perpetuity. It is made available under aCC-BY-NC-ND 4.0 International license.

Acknowledgments:

AWC acknowledges the support of the Three Springs Foundation. The research leading to these results has received funding from the national program “Investissements d’avenir” ANR-10- IAIHU-0006. Part of this work was carried out in the CENIR of ICM. We gratefully acknowledge Laurent Hugueville and Amandine Carrie for their contribution to data collection at the Paris Brain Institute. We thank Teigane Mackay for data collection at Monash University, Naotsugu Tsuchiya, and Jennifer Windt for their support to TA at the inception of this line of research, and Jakob Howhy, Delphine Oudiette and Jacobo Sitt for the discussion about the nature and dynamics of consciousness.

Funding:

European Research Council ERC-StG SleepingAwake 101116748 (TA)

Agence Nationale de la Recherche ANR-22-CE37–0006-01 (TA)

Human Frontiers Science Program LT000362/2018-L (TA)

Author contributions:

Conceptualization: EMM, AWC, LN, TA

Data acquisition: ALC, TA

Methodology: EMM, AWC, LB, LN, TA

Investigation: EMM, TA

Visualization: EMM, TA

Funding acquisition: LN, TA

Supervision: LN, TA

Writing – original draft: EMM

Writing – review & editing: EMM, ALC, AWC, LB, LN, TA

Competing interests:

Authors declare that they have no competing interests.

bioRxiv preprint doi: https://doi.org/10.1101/2024.02.11.579845; this version posted April 22, 2025. The copyright holder for this preprint (which was not certified by peer review) is the author/funder, who has granted bioRxiv a license to display the preprint in perpetuity. It is made available under aCC-BY-NC-ND 4.0 International license.

Data and materials availability:

All data, code, and materials used in the analysis will be freely available upon publication.

FIGURES

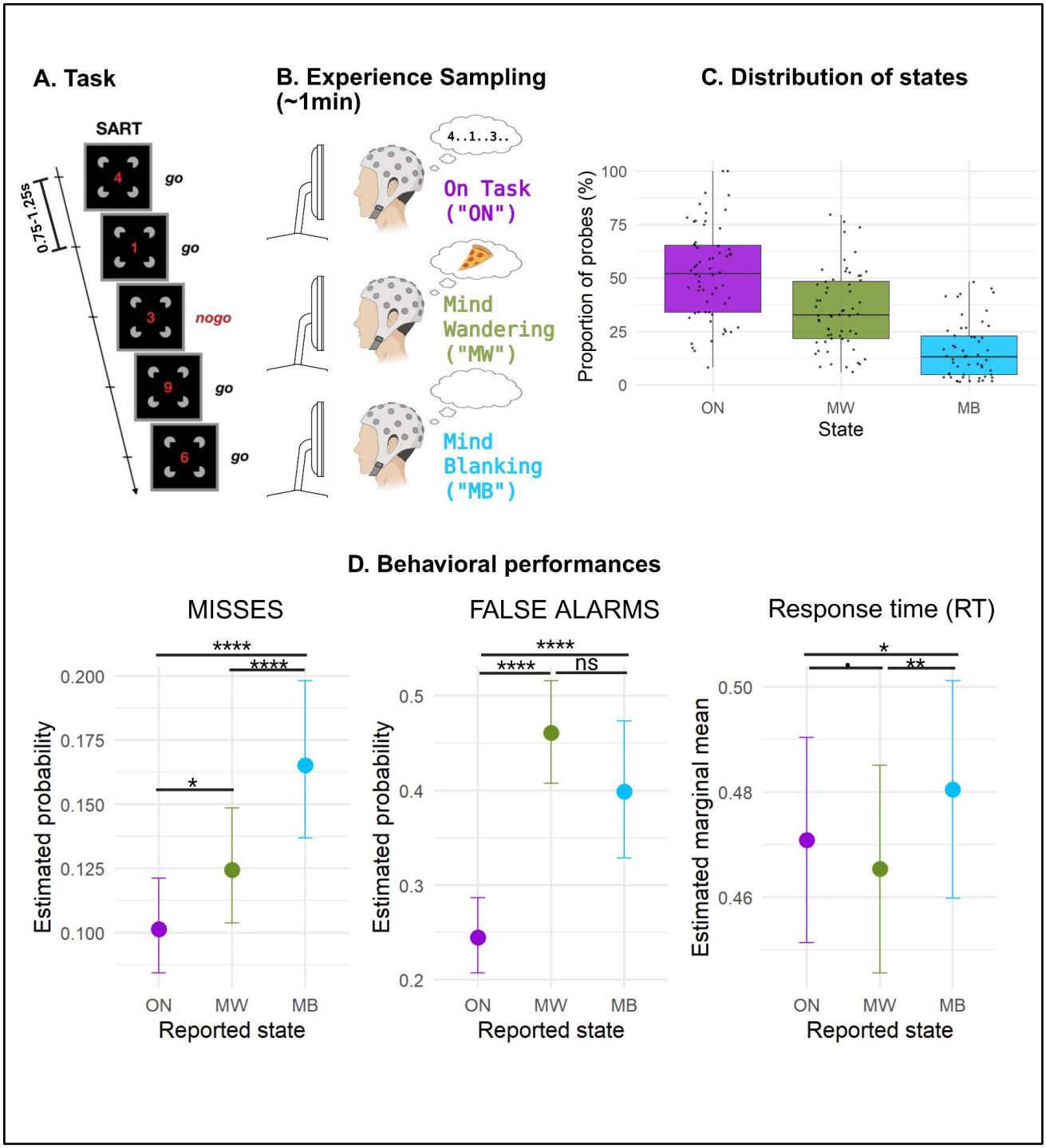

bioRxiv preprint doi: https://doi.org/10.1101/2024.02.11.579845; this version posted April 22, 2025. The copyright holder for this preprint (which was not certified by peer review) is the author/funder, who has granted bioRxiv a license to display the preprint in perpetuity. It is made available under aCC-BY-NC-ND 4.0 International license.

Figure 1: Experimental paradigm and behavioral results. Panels A and B: Experimental paradigm. 62 healthy participants performed a sustained attention to response task (SART), with digits and faces as stimuli, while high-density electro-encephalogram (EEG) was recorded continuously. After each stimulus presentation, participants had to press a button (Go trials), or refrain from doing so, whenever a "3" or a smiling face was presented (No Go trials; 1 out of 9). SOA varied randomly (750-1250ms) with a null ISI (panel A). Participants' mental state was probed at random intervals (every 40-70s, uniform random jitter). They had to report their attentional focus by selecting one of four options: (1) 'task-focused' (ON), (2) 'off-task' (mind-wandering, MW), (3) 'mind-blanking' (MB) (panel B). Panel C: proportion of probes in function of the reported mind-state. Proportions were computed at subject level (individual dots) and the distributions at group level are represented by a boxplot (the boundaries of the boxes represent first and third quartiles (Q1 and Q3 respectively), mid-line represents the medium and the whiskers depict Q1-1.5*IQR and Q3*1.5*IQR). Panel D: Behavioral performances in function of the reported mind-state. Misses, False Alarms and Response Times (RT) were computed for the trials between the 5s before probe-onsets. (Binomial) linear mixed models were computed with *mind-state* as the main explanatory factor, and subject ID/dataset as a random intercepts. We found fine-grained modulations of performance in function of mind-state, with distinct behavioral profiles for MW (faster RTs) and MB (slower RTs, more misses). The statistical bars and stars represent the pairwise comparisons between mind-states (FDR corrected). The detailed statistical results can be found on Table 1.

****: FDR corrected p-value<0.0001

**: FDR corrected p-value<0.01

*: FDR corrected p-value<0.05

. : FDR corrected p-value<0.1

n.s. FDR corrected p-value>0.1

bioRxiv preprint doi: https://doi.org/10.1101/2024.02.11.579845; this version posted April 22, 2025. The copyright holder for this preprint (which was not certified by peer review) is the author/funder, who has granted bioRxiv a license to display the preprint in perpetuity. It is made available under aCC-BY-NC-ND 4.0 International license.

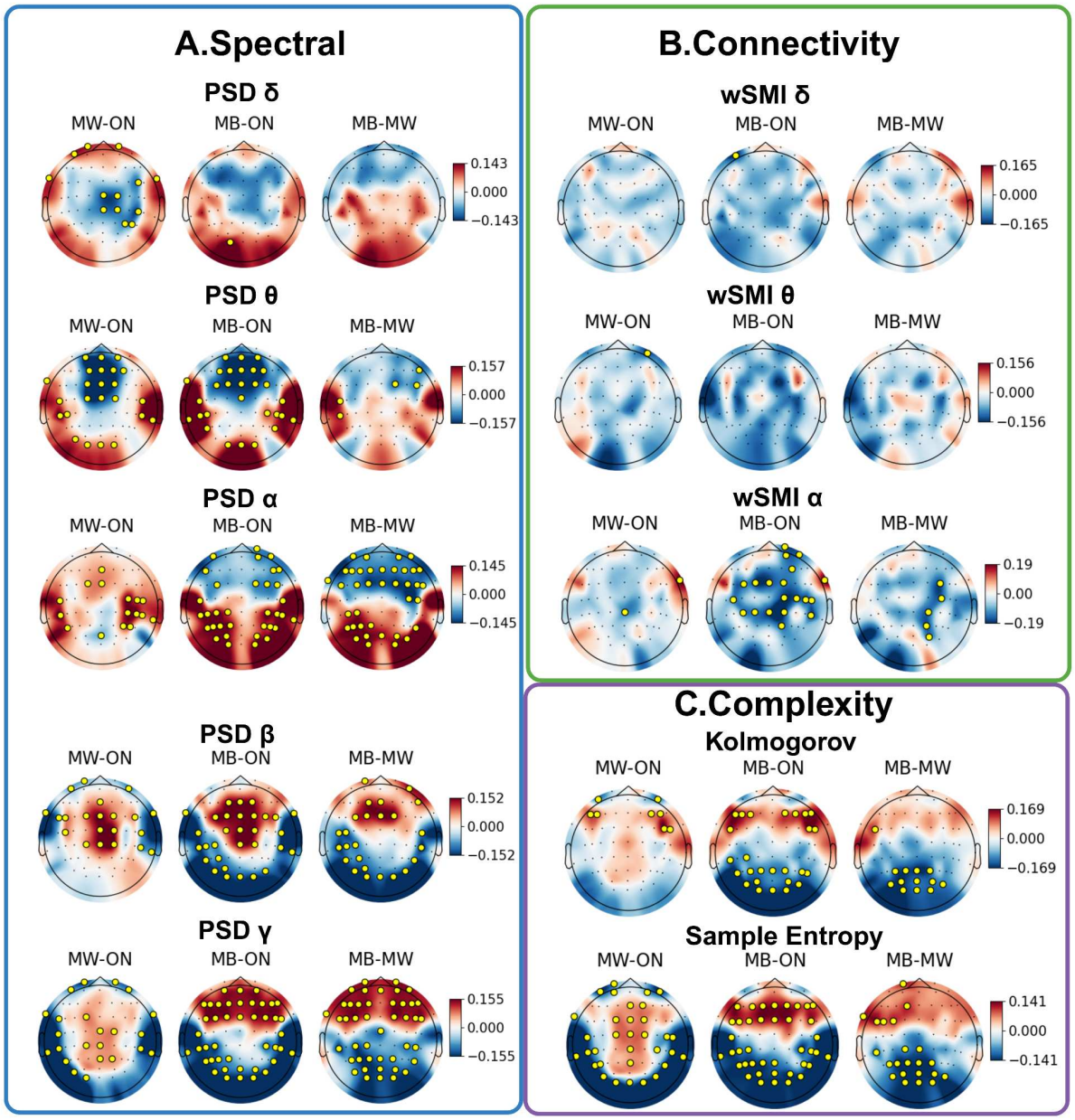

Figure 2: EEG-based neurophysiological markers differentiate MB from ON and MW. Spectral (A), Connectivity (B) and Complexity (C) results. Each subplot represents the pairwise statistical contrast between two states (left: MW - ON; middle: MB - ON; right: MB - MW), at sensor level (topographical representation of the scalp). Model estimates for the contrast between states were computed for each electrode, and locations with statistically significant differences (FDR corrected p-value<0.05) are depicted with a golden circle. We observed a front-back dissociation between MW and MB for spectral and complexity measures, and a progressive breakdown of functional connectivity going from ON to MB (ON>MW>MB). The ANOVA tables summarizing the main factor's effects (linear mixed models with mind-state, electrode/connection and their interaction as main factors, and subject ID/dataset as a random intercepts) for each EEG metric can be found in Table 2.

bioRxiv preprint doi: https://doi.org/10.1101/2024.02.11.579845; this version posted April 22, 2025. The copyright holder for this preprint (which was not certified by peer review) is the author/funder, who has granted bioRxiv a license to display the preprint in perpetuity. It is made available under aCC-BY-NC-ND 4.0 International license.

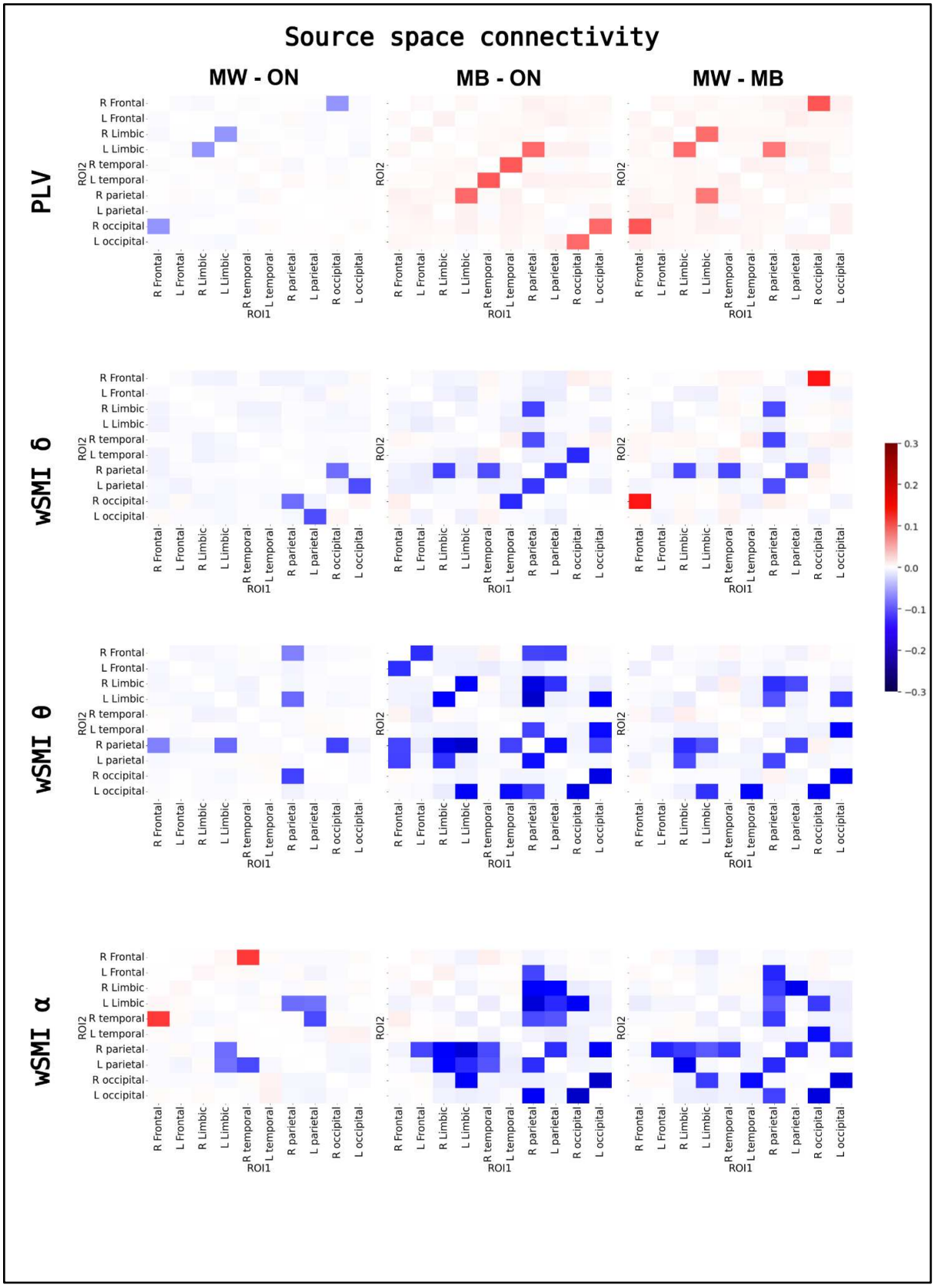

bioRxiv preprint doi: https://doi.org/10.1101/2024.02.11.579845; this version posted April 22, 2025. The copyright holder for this preprint (which was not certified by peer review) is the author/funder, who has granted bioRxiv a license to display the preprint in perpetuity. It is made available under aCC-BY-NC-ND 4.0 International license.

Figure 3: Increased phase synchrony with reduced information sharing during MB. The PLV (top) and the wSMI in different frequency bands were computed at the source level. Each square-matrix represents the contrast in connectivity, computed in source space, between two mind-states, for each pair of regions of interest (ROIs). Only significantly different connections (FDR corrected p-value<0.05) are highlighted, the other ones are masked. ANOVA tables for the statistical models can be found in Table 3. We observed a dissociation between the PLV and wSMI, with increased PLV (phase synchrony) and decreased wSMI (information sharing) between distant cortical areas (in particular fronta-parietal) during MB, as compared to ON and MW.

δ: delta band; θ: theta band; α: alpha band
wSMI: weighted symbolic mutual information
PLV: Phase Locking Value
R: right; L: left

bioRxiv preprint doi: https://doi.org/10.1101/2024.02.11.579845; this version posted April 22, 2025. The copyright holder for this preprint (which was not certified by peer review) is the author/funder, who has granted bioRxiv a license to display the preprint in perpetuity. It is made available under aCC-BY-NC-ND 4.0 International license.

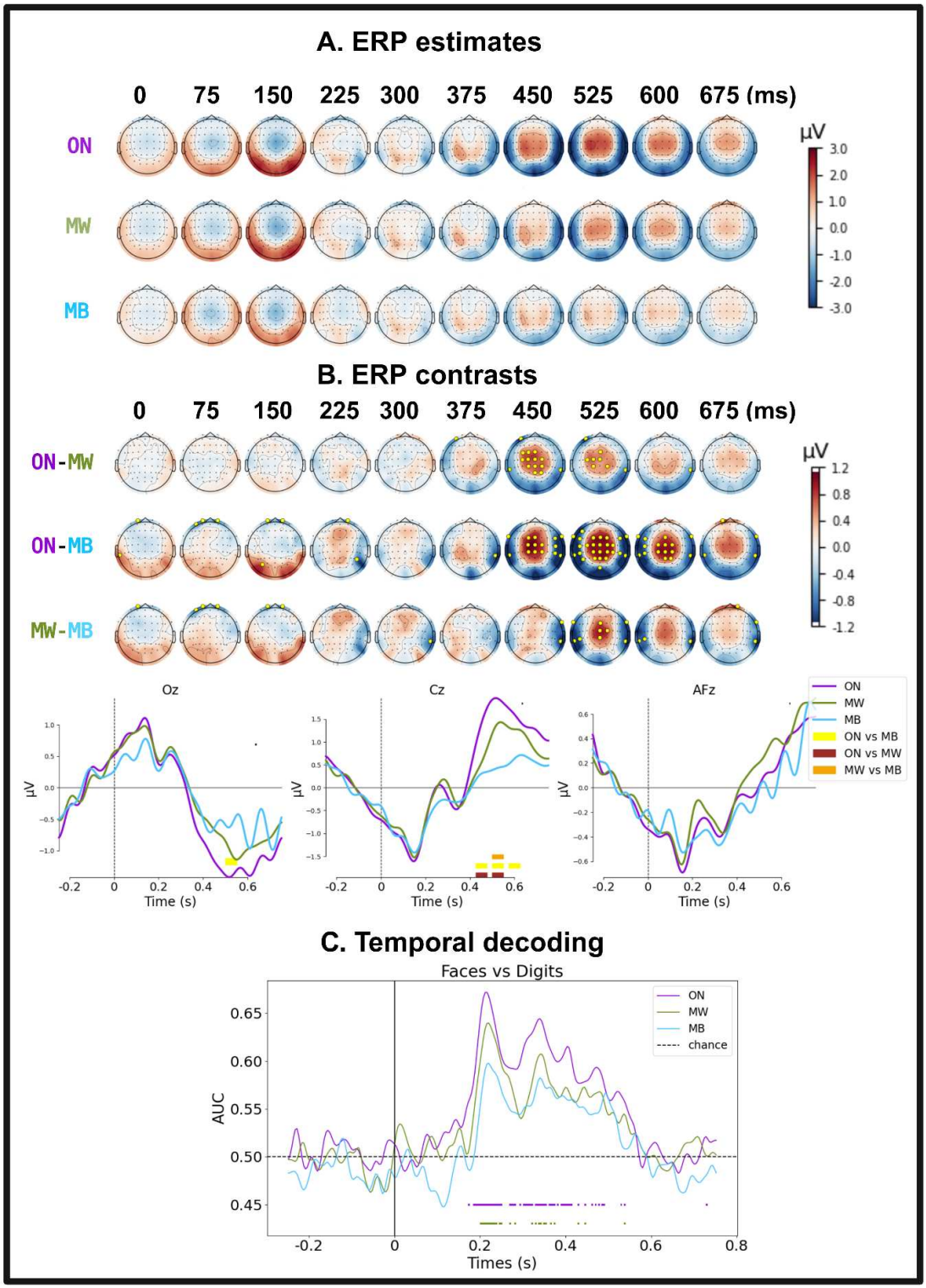

bioRxiv preprint doi: https://doi.org/10.1101/2024.02.11.579845; this version posted April 22, 2025. The copyright holder for this preprint (which was not certified by peer review) is the author/funder, who has granted bioRxiv a license to display the preprint in perpetuity. It is made available under aCC-BY-NC-ND 4.0 International license.

Figure 4: Stimulus-induced activity analyses. Panels A and B: Topographical scalp representation of the ERP estimates for each mind state (A) and ERP contrasts between mind-states (B), derived from the statistical model (single-trial multi-level analysis with mind-state, EEG channel and their interaction as main factors, and subject ID/dataset as random intercepts). Marked electrodes in panel B (golden circles) are the ones presenting a statistically significant difference between conditions (FDR corrected p-value<0.05). Panel B bottom presents the grand-average ERP time-series for each mind-state (ON: violet; MW: green; MB: blue) for 3 electrodes of interest (Oz, Cz and AFz). Time-points with statistically significant differences between conditions (FDR corrected p-value<0.05) are highlighted (ON vs MW: brown; ON vs MB: yellow; MW vs MB: orange). Given that trials follow one another in close succession, it is normal for the baseline activity to be influenced by the activity of the previous trials. Panel C: Temporal decoding of stimulus category. A linear classifier was trained and then tested (via cross validation) at each time point to distinguish stimulus category (Faces vs Digits), allowing the tracking of the temporal dynamics of neural representations, independently for each mind-state. Note that the number of trials were identical between mind-states for this analysis. Classifiers' performances were compared to chance-level performance (see Methods), independently for each mind-state, and statistically significant time-points were represented by colored horizontal bars. While both early (<300ms) and late (>300ms) time-points with significant decoding were observed for ON and MW, no significant decoding was observed for MB trials.

bioRxiv preprint doi: https://doi.org/10.1101/2024.02.11.579845; this version posted April 22, 2025. The copyright holder for this preprint (which was not certified by peer review) is the author/funder, who has granted bioRxiv a license to display the preprint in perpetuity. It is made available under aCC-BY-NC-ND 4.0 International license.

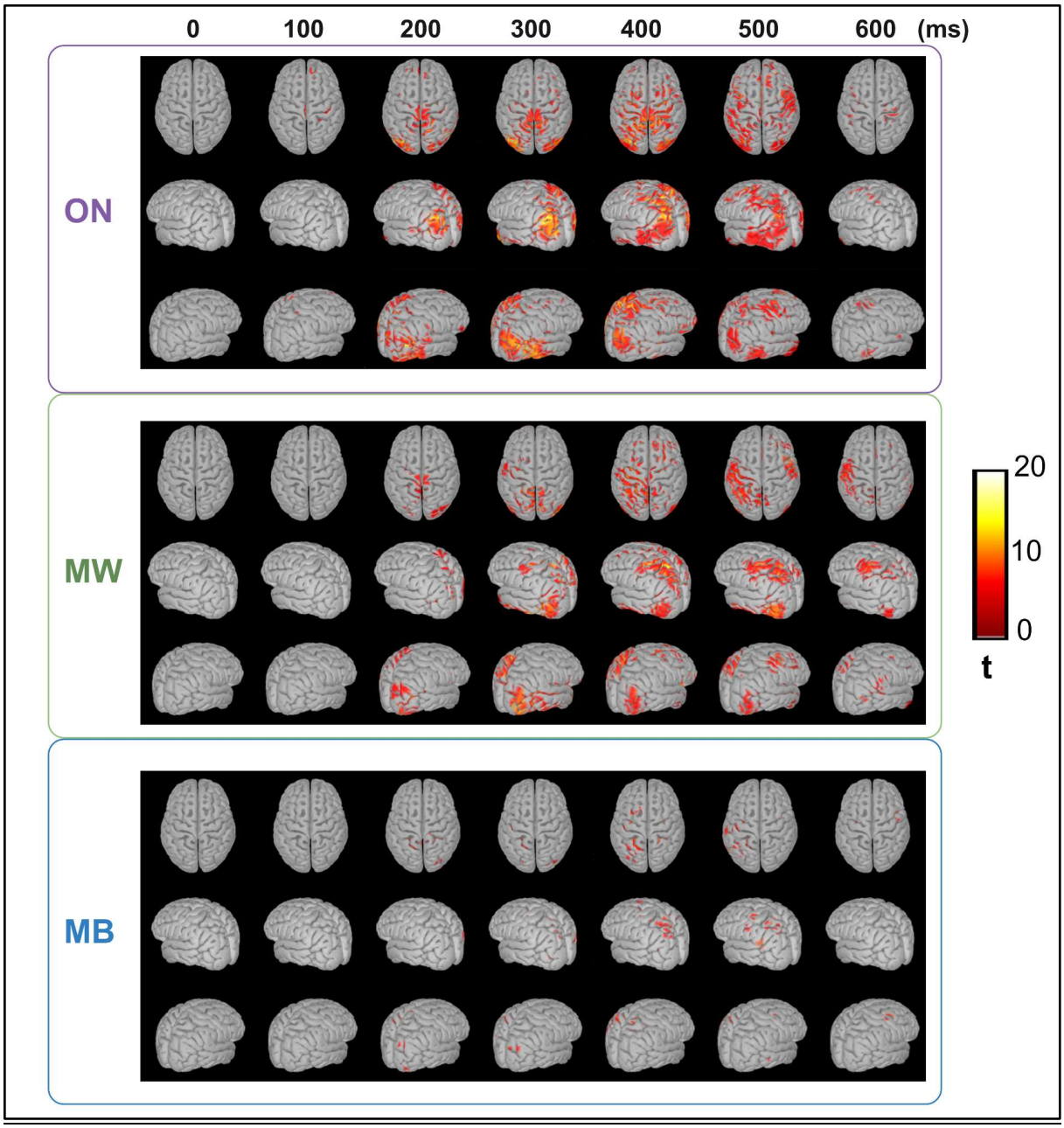

Figure 5: Source reconstruction of stimulus-induced activity. Source reconstruction at trial level was performed independently for each mind state, and a t-test against the baseline (-0.25 to 0s relative to stimulus onset) was performed. Only statistically significant modulations of activity compared to the baseline (FDR corrected p-value<0.05, corrected for multiple comparisons across time, space and frequencies) are highlighted. While significant activations of visual streams (dorsal and ventral) were observable for both ON and MW conditions, starting from 200ms post-stimulus, this was not observed during MB trials.

bioRxiv preprint doi: https://doi.org/10.1101/2024.02.11.579845; this version posted April 22, 2025. The copyright holder for this preprint (which was not certified by peer review) is the author/funder, who has granted bioRxiv a license to display the preprint in perpetuity. It is made available under aCC-BY-NC-ND 4.0 International license.

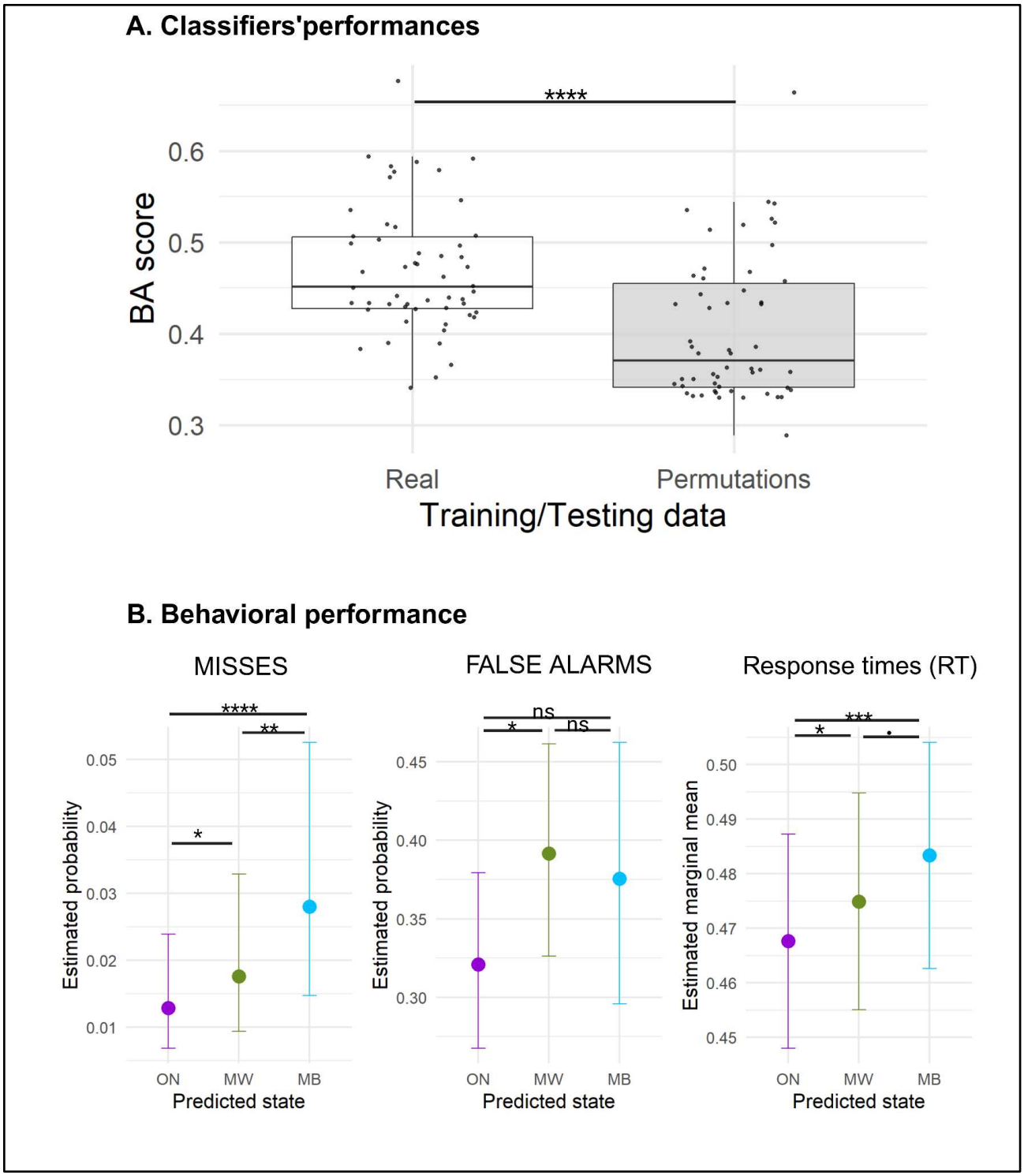

Figure 6: Trial-by-trial prediction of mind-state using a multivariate combination of neural markers. Panel A: Distribution of performances (balanced accuracy) of subject-level classifiers, both for true data and permuted data (mean score of 500 labels permutations). The classifier was trained and tested by cross-validation using labeled trials (<5 seconds before probe onsets). Spectral, complexity, connectivity, and ERP markers were used as raw features, followed by a dimensionality reduction by (non-linear) PCA. Only subjects presenting

bioRxiv preprint doi: https://doi.org/10.1101/2024.02.11.579845; this version posted April 22, 2025. The copyright holder for this preprint (which was not certified by peer review) is the author/funder, who has granted bioRxiv a license to display the preprint in perpetuity. It is made available under aCC-BY-NC-ND 4.0 International license.

with the 3 mind-states were included in this analysis. Panel B: Behavioral markers as a function of the predicted mind state in non-labeled trials (>5s before probe onsets). (Binomial) linear mixed models were computed with predicted mind-state as the main explanatory factor, and subject ID/dataset as random intercepts. Statistical bars represent pairwise statistical comparisons between states. We found very similar behavioral patterns for predicted trials as compared to reported (labeled) trials.

The detailed statistical results can be found in Table S6.
****: FDR corrected p-value<0.0001
***: FDR corrected p-value<0.001
**: FDR corrected p-value<0.01
*: FDR corrected p-value<0.05
▪ : FDR corrected p-value<0.1
n.s.: FDR corrected p-value>0.1

bioRxiv preprint doi: https://doi.org/10.1101/2024.02.11.579845; this version posted April 22, 2025. The copyright holder for this preprint (which was not certified by peer review) is the author/funder, who has granted bioRxiv a license to display the preprint in perpetuity. It is made available under aCC-BY-NC-ND 4.0 International license.

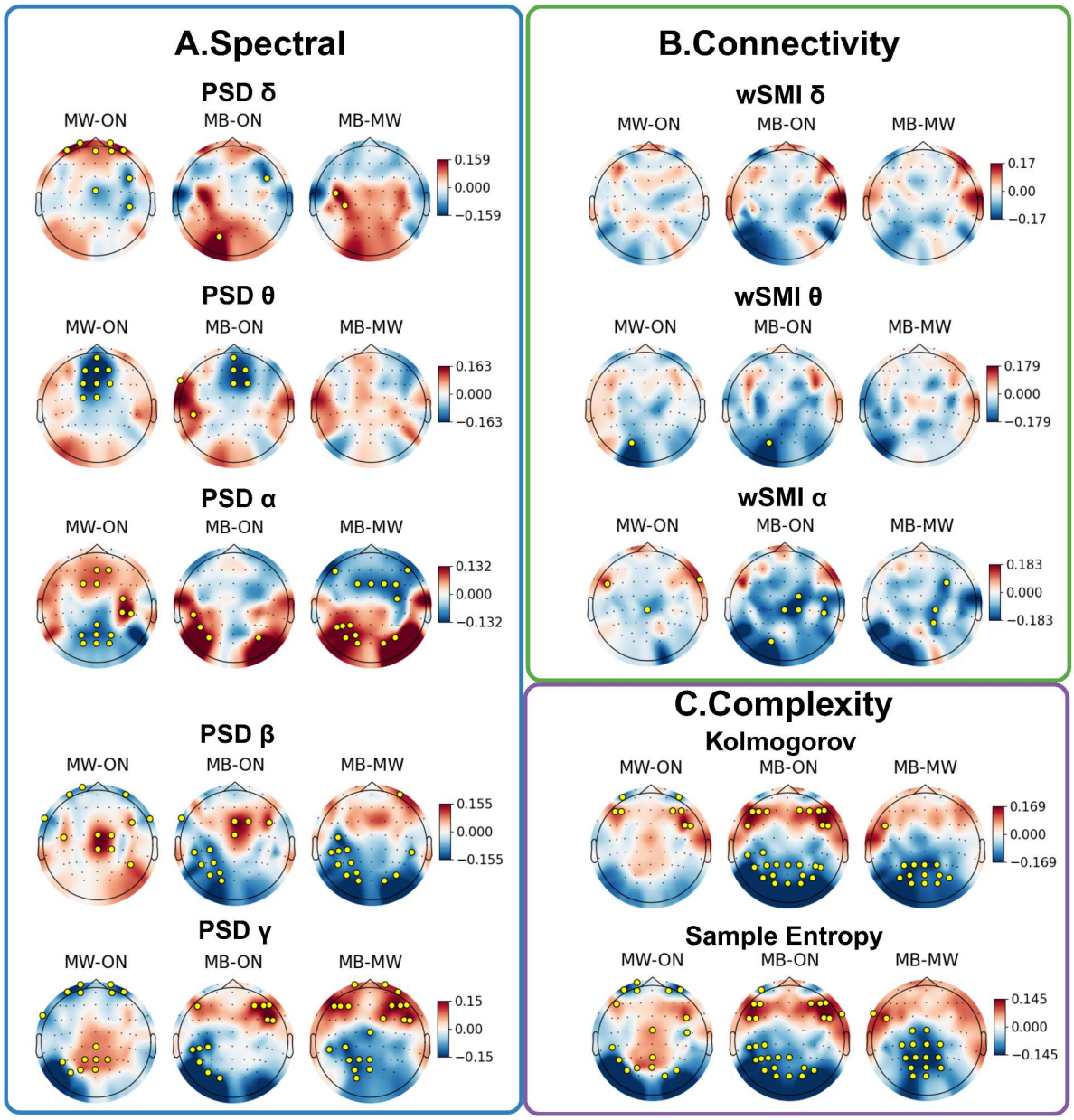

Figure S1: Modulation of EEG markers by mind-state corrected for vigilance modifications. Spectral (A), Connectivity (B) and Complexity (C) results. Each subplot represents the pairwise statistical contrast between two states (left: MW - ON; middle: MB - ON; right: MB - MW), at sensor level. Statistical models included the main effect of mind -state, electrode location and vigilance score (4-point scale, 1 = Extremely Sleepy, 4 = Extremely Alert), as well as the interactions mind-state/electrode location and vigilance score/electrode location. Subject ID and dataset were included as random intercepts. Model estimates for the contrast between states were computed for each electrode, and locations with statistically significant differences (FDR corrected p-value<0.05) are depicted with a golden circle. The observed results reproduced closely the results obtained with models not including vigilance score as a covariate (see main Figure 2).

bioRxiv preprint doi: https://doi.org/10.1101/2024.02.11.579845; this version posted April 22, 2025. The copyright holder for this preprint (which was not certified by peer review) is the author/funder, who has granted bioRxiv a license to display the preprint in perpetuity. It is made available under aCC-BY-NC-ND 4.0 International license.

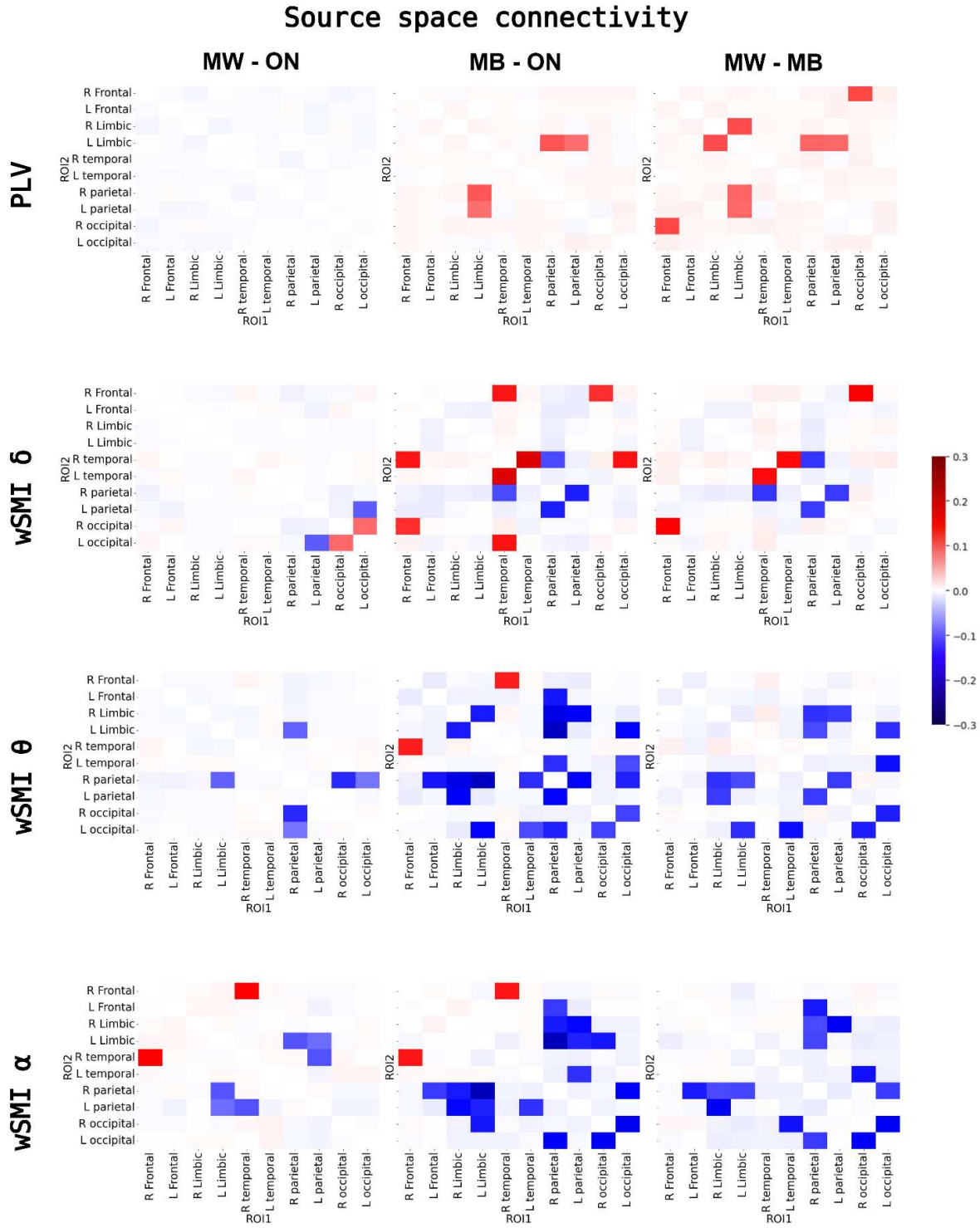

Figure S2: Modulation of source space connectivity by mind-state corrected for vigilance modifications. The PLV (top) and the wSMI in different frequency bands were computed at the source level. Each square-matrix represents the contrast in connectivity,

bioRxiv preprint doi: https://doi.org/10.1101/2024.02.11.579845; this version posted April 22, 2025. The copyright holder for this preprint (which was not certified by peer review) is the author/funder, who has granted bioRxiv a license to display the preprint in perpetuity. It is made available under aCC-BY-NC-ND 4.0 International license.

computed in source space, between two mind-states, for each pair of regions of interest (ROIs). Only significantly different connections (FDR corrected p-value<0.05) are highlighted, the other ones are masked. Statistical models included the main effect of mind -state, electrode location and vigilance score (4-point scale, 1 = Extremely Sleepy, 4 = Extremely Alert), as well as the interactions mind-state/electrode location and vigilance score/electrode location. Subject ID and dataset were included as random intercepts We observed a dissociation between the PLV and wSMI, with increased PLV (phase synchrony) and decreased wSMI (information sharing) between distant cortical areas, in particular in the theta and alpha bands, during MB, as compared to ON and MW. These results are similar to those obtained without including the vigilance score in the statistical models (see Figure 3).

δ: delta band; θ: theta band; α: alpha band
wSMI: weighted symbolic mutual information
PLV: Phase Locking Value
R: right; L: left

bioRxiv preprint doi: https://doi.org/10.1101/2024.02.11.579845; this version posted April 22, 2025. The copyright holder for this preprint (which was not certified by peer review) is the author/funder, who has granted bioRxiv a license to display the preprint in perpetuity. It is made available under aCC-BY-NC-ND 4.0 International license.

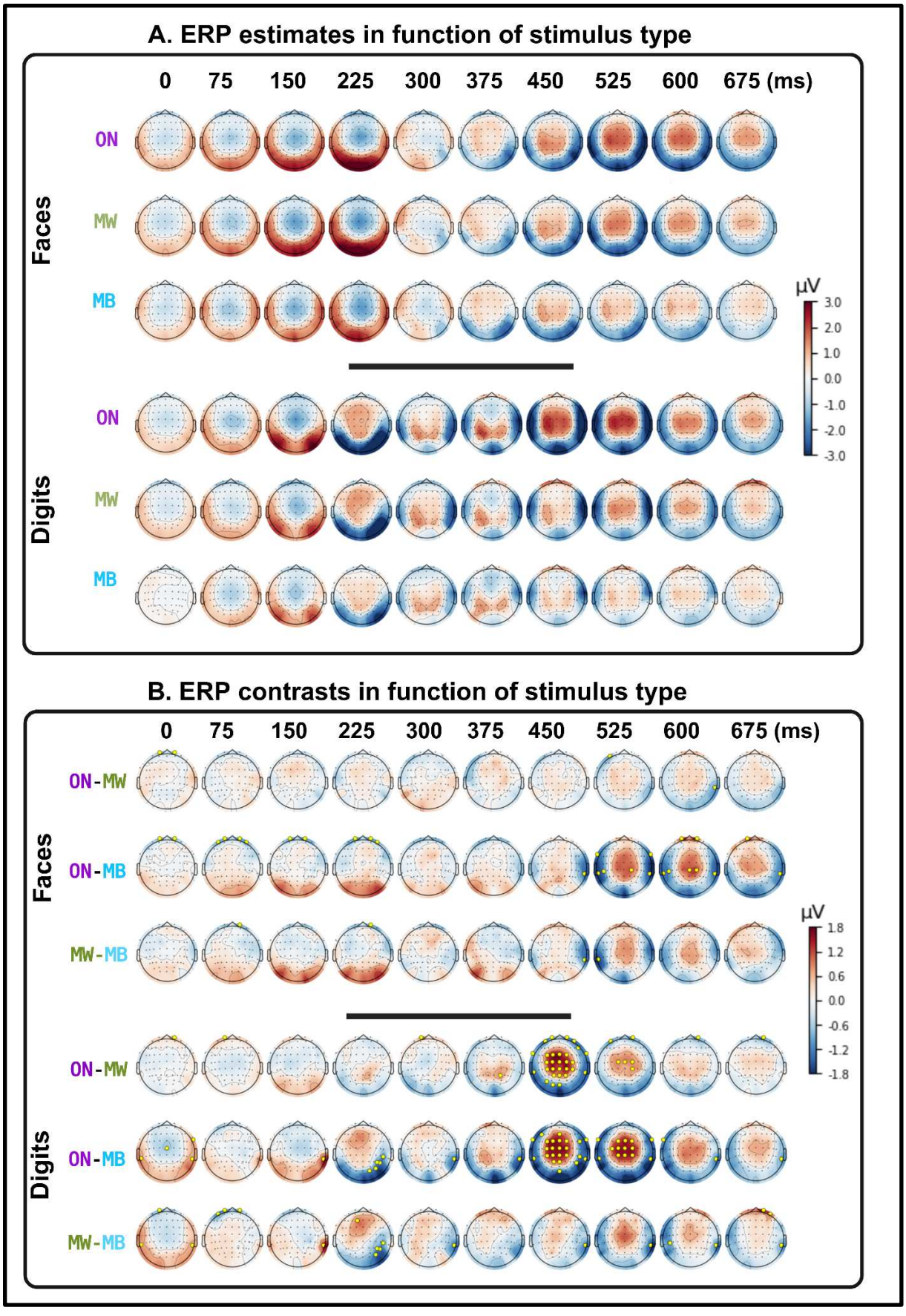

bioRxiv preprint doi: https://doi.org/10.1101/2024.02.11.579845; this version posted April 22, 2025. The copyright holder for this preprint (which was not certified by peer review) is the author/funder, who has granted bioRxiv a license to display the preprint in perpetuity. It is made available under aCC-BY-NC-ND 4.0 International license.

Figure S3: ERP results independently for faces and digits. Panels A and B: Topographical scalp representation of the ERP estimates for each mind state (A) and ERP contrasts between mind-states (B), derived from the statistical model (single-trial multi-level analysis with mind-state, EEG channel and their interaction as main factors, and subject ID/dataset as random intercepts). Marked electrodes in panel B (golden circles) are the ones presenting a statistically significant difference between conditions (FDR corrected p-value<0.05). As seen in the figure, the analysis was conducted independently for faces and digits. ERPs ' profiles in function of the reported mind-state were consistent across stimuli types.

bioRxiv preprint doi: https://doi.org/10.1101/2024.02.11.579845; this version posted April 22, 2025. The copyright holder for this preprint (which was not certified by peer review) is the author/funder, who has granted bioRxiv a license to display the preprint in perpetuity. It is made available under aCC-BY-NC-ND 4.0 International license.

SUPPLEMENTARY RESULTS

TABLES

Mental state	FA (%)	Misses (%)	RTs (ms)
ON	24.5 ± 2.0	10.1 ± 0.9	471 ± 10
MW	46.1 ± 2.7	12.4 ± 1.1	465 ± 10
MB	39.9 ± 3.7	16.5 ± 1.6	480 ± 11

Behavioral measure	Main effect of mind state		Pairwise contrasts
	χ²	***FDR corrected p-value***	
FA	χ^2 (2)=69.8	$8.3 * 10^{-15}$	MW *vs* ON : z-ratio=8.2, p-value= $5.0 * 10^{-15}$ MB *vs* ON: z-ratio=4.5, p-value= $2.5 * 10^{-5}$ MB vs MW: z-ratio=-1.6 p-value=0.12
Misses	χ^2 (2)=64.0	$7.6 * 10^{-14}$	MW *vs* ON : z-ratio=3.9, p-value= $2.4 * 10^{-4}$ MB *vs* ON: z-ratio=8.0, p-value= $1.8 * 10^{-14}$ MB vs MW: z-ratio=4.6 p-value=$1.7 * 10^{-5}$

bioRxiv preprint doi: https://doi.org/10.1101/2024.02.11.579845; this version posted April 22, 2025. The copyright holder for this preprint (which was not certified by peer review) is the author/funder, who has granted bioRxiv a license to display the preprint in perpetuity. It is made available under aCC-BY-NC-ND 4.0 International license.

RT	F (2)=5.2	$9.4 * 10^{-3}$	MW *vs* ON : z-ratio=-1.67, p-value= 0.1 MB *vs* ON: z-ratio=2.1, p-value= 0.043 MB vs MW: z-ratio=3.2 p-value=$2.6 * 10^{-3}$

Table S1: Behavioral results in labeled trials. Results of the linear mixed models with mind-state as a main factor and subject ID/dataset as random intercepts, for false alarms (FA), misses and response times (RT). The table presents the model estimates for each mind-state (top) and the statistical contrasts (bottom). All p-values were corrected for multiple comparisons using an FDR procedure.

bioRxiv preprint doi: https://doi.org/10.1101/2024.02.11.579845; this version posted April 22, 2025. The copyright holder for this preprint (which was not certified by peer review) is the author/funder, who has granted bioRxiv a license to display the preprint in perpetuity. It is made available under aCC-BY-NC-ND 4.0 International license.

EEG metric	Mind -state		Channel location		Mind-state:Channel	
	F (2)	p-value	F (63)	p-value	F (126)	p -value
Kolmogorov	19.8	3.78E-09	356.7	0	6.3	1.5E-97
Sample Entropy	46.7	9.49E-21	747.3	0	9.6	2.5E-175
normalized PSD delta	5.9	0.003542	99.6	0	3.1	3.5E-28
normalized PSD theta	8.34	0.00031	503.1	0	9.3	4.0E-169
normalized PSD alpha	62.3	1.73E-27	1335.2	0	6.5	4.3E-101
normalized PSD beta	8.3	0.000318	235.9	0	7.0	1.6E-113
normalized PSD gamma	9.4	0.000109	1180.2	0	10.0	1.5E-186
wSMI delta	37.4	1.03E-16	50.6	0	0.9	0.7
wSMI theta	57.9	1.37E-25	51.8	0	1.0	0.4
wSMI alpha	77.5	4.74E-34	69.3	0	1.9	1.1E-08

Table S2: Neural markers results (sensor space). ANOVA tables of the statistical models computed for each neural marker in sensor space (linear mixed models with mind state, electrode location and their interaction as main factors, and subject ID/dataset as a random intercepts). P-values were corrected for multiple comparisons using an FDR procedure.

bioRxiv preprint doi: https://doi.org/10.1101/2024.02.11.579845; this version posted April 22, 2025. The copyright holder for this preprint (which was not certified by peer review) is the author/funder, who has granted bioRxiv a license to display the preprint in perpetuity. It is made available under aCC-BY-NC-ND 4.0 International license.

Connectivity metric	Mind-state		Connection		Mind-state:Connection	
	F (2)	p-value	F (44)	p-value	F (88)	p-value
wSMI alpha	32.9	8.52E-15	352.5	0	1.7	0.0001
wSMI theta	42.9	3.95E-19	213.3	0	1.1	0.2
wSMI delta	24.8	2.9E-11	203.8	0	1.2	0.1

Table S3: Source-level connectivity. ANOVA tables of the statistical models computed for each connectivity measure in source space (linear mixed models with mind state, connection ID and their interaction as main factors, and subject ID/dataset as random intercepts). P-values were corrected for multiple comparisons using an FDR procedure.

bioRxiv preprint doi: https://doi.org/10.1101/2024.02.11.579845; this version posted April 22, 2025. The copyright holder for this preprint (which was not certified by peer review) is the author/funder, who has granted bioRxiv a license to display the preprint in perpetuity. It is made available under aCC-BY-NC-ND 4.0 International license.

Time-window (-/+ 25ms)	Mind-state		Channel location		Mind-state:Channel location	
	F (2)	p-value	F (63)	p-value	F (126)	p-value
0 ms	0.3	0.8	48.9	0	1.9	5.3E-10
75 ms	0.5	0.7	83.2	0	1.9	8.0E-10
150 ms	0.3	0.8	138.9	0	1.5	0.0003
225 ms	0.2	0.9	32.0	0	1.8	3.1E-07
300 ms	0.2	0.9	34.5	0	1.1	0.4
375 ms	0.07	0.9	38.9	0	1.8	3.4E-08
450 ms	0.2	0.9	91.9	0	6.6	8.6E-103
525 ms	0.5	0.7	119.9	0	7.7	2.1E-130
600 ms	0.6	0.6	83.8	0	4.4	1.6E-55
675 ms	0.3	0.8	52.4	0	2.7	1.5E-21

bioRxiv preprint doi: https://doi.org/10.1101/2024.02.11.579845; this version posted April 22, 2025. The copyright holder for this preprint (which was not certified by peer review) is the author/funder, who has granted bioRxiv a license to display the preprint in perpetuity. It is made available under aCC-BY-NC-ND 4.0 International license.

Table S4 : Event related potentials (ERPs). ANOVA tables of the statistical models computed at each time window (linear mixed models with mind state, electrode location and their interaction as main factors, and subject ID/dataset as random intercepts). P-values were corrected for multiple comparisons using an FDR procedure.

bioRxiv preprint doi: https://doi.org/10.1101/2024.02.11.579845; this version posted April 22, 2025. The copyright holder for this preprint (which was not certified by peer review) is the author/funder, who has granted bioRxiv a license to display the preprint in perpetuity. It is made available under aCC-BY-NC-ND 4.0 International license.

	ON	MW	MB
Precision	0.598	0.498	0.278
Recall	0.631	0.516	0.309
F1-score	0.605	0.498	0.289

Table S5: Weighted-average performance of individual's classifiers (PCA/Random Forest classifier) for each mind-state. The metrics (precision, recall, f1-score) are computed as the weighted mean across subjects, where each subject's contribution is weighted by the number of trials (support) for the respective class.

Subject	MB			MW			ON			Balanced accuracy/permutation test		
	Pr	Re	F1	Pr	Re	F1	Pr	Re	F1	Observed	Perm mean	p-value
Monash 001	NA	NA	NA	0.562	0.551	0.557	0.745	0.753	0.749	0.6805	0.5035	0.0040
Monash 002	NA	NA	NA	0.316	0.200	0.245	0.913	0.951	0.931	0.7321	0.6503	0.0200
Monash 003	**0.403**	**0.475**	**0.436**	**0.200**	**0.162**	**0.179**	**0.299**	**0.277**	**0.287**	**0.3524**	**0.3301**	**0.6387**
Monash 004	**0.392**	**0.305**	**0.343**	**0.237**	**0.136**	**0.173**	**0.475**	**0.656**	**0.551**	**0.4325**	**0.3340**	**0.0080**
Monash 005	**0.075**	**0.167**	**0.103**	**0.218**	**0.449**	**0.294**	**0.700**	**0.295**	**0.415**	**0.4505**	**0.3451**	**0.1018**

bioRxiv preprint doi: https://doi.org/10.1101/2024.02.11.579845; this version posted April 22, 2025. The copyright holder for this preprint (which was not certified by peer review) is the author/funder, who has granted bioRxiv a license to display the preprint in perpetuity. It is made available under aCC-BY-NC-ND 4.0 International license.

Monash 006	NA	NA	NA	0.794	0.992	0.882	0.000	0.000	0.000	0.5943	0.5961	0.8563
Monash 007	**0.133**	**0.053**	**0.075**	**0.511**	**0.627**	**0.563**	**0.291**	**0.255**	**0.272**	**0.4134**	**0.3917**	**0.8822**
Monash 008	**0.115**	**0.111**	**0.113**	**0.486**	**0.493**	**0.490**	**0.427**	**0.424**	**0.426**	**0.4336**	**0.3583**	**0.1058**
Monash 009	**0.432**	**0.488**	**0.458**	**0.476**	**0.291**	**0.361**	**0.155**	**0.391**	**0.222**	**0.4272**	**0.3503**	**0.0259**
Monash 010	**0.244**	**0.270**	**0.256**	**0.450**	**0.386**	**0.415**	**0.426**	**0.433**	**0.430**	**0.4103**	**0.3322**	**0.0758**
Monash 011	NA	NA	NA	0.000	0.000	0.000	0.845	0.992	0.912	0.6955	0.6986	0.9082
Monash 012	**0.264**	**0.383**	**0.313**	**0.569**	**0.412**	**0.478**	**0.298**	**0.364**	**0.327**	**0.4037**	**0.3387**	**0.3353**
Monash 013	NA	NA	NA	NA	NA	NA	1.000	1.000	1.000	1.000	1.000	1.0
Monash 014	**0.000**	**0.000**	**0.000**	**0.174**	**0.043**	**0.069**	**0.634**	**0.899**	**0.744**	**0.5769**	**0.5442**	**0.2255**
Monash 015	**0.000**	**0.000**	**0.000**	**0.531**	**0.673**	**0.594**	**0.423**	**0.275**	**0.333**	**0.4281**	**0.3855**	**0.6327**
Monash 016	**0.232**	**0.333**	**0.274**	**0.429**	**0.368**	**0.396**	**0.282**	**0.296**	**0.289**	**0.3891**	**0.3428**	**0.4471**
Monash 017	**0.059**	**0.046**	**0.052**	**0.298**	**0.330**	**0.313**	**0.533**	**0.550**	**0.541**	**0.3408**	**0.3408**	**0.6248**
Monash 018	**0.000**	**0.000**	**0.000**	**0.678**	**0.775**	**0.723**	**0.100**	**0.070**	**0.083**	**0.4963**	**0.4604**	**0.6906**
Monash 019	**0.503**	**0.593**	**0.545**	**0.239**	**0.145**	**0.180**	**0.323**	**0.352**	**0.337**	**0.4368**	**0.3373**	**0.2076**
Monash 020	**0.000**	**0.000**	**0.000**	**0.135**	**0.086**	**0.105**	**0.757**	**0.864**	**0.807**	**0.4522**	**0.4338**	**0.4691**
Monash 021	**0.000**	**0.000**	**0.000**	**0.086**	**0.049**	**0.062**	**0.710**	**0.850**	**0.774**	**0.5463**	**0.5257**	**0.8204**

bioRxiv preprint doi: https://doi.org/10.1101/2024.02.11.579845; this version posted April 22, 2025. The copyright holder for this preprint (which was not certified by peer review) is the author/funder, who has granted bioRxiv a license to display the preprint in perpetuity. It is made available under aCC-BY-NC-ND 4.0 International license.

Monash 022	**0.000**	**0.000**	**0.000**	**0.547**	**0.611**	**0.577**	**0.552**	**0.540**	**0.546**	**0.5877**	**0.4632**	**0.2056**
Monash 023	**0.000**	**0.000**	**0.000**	**0.423**	**0.294**	**0.347**	**0.642**	**0.782**	**0.705**	**0.5031**	**0.4343**	**0.0878**
Monash 024	**0.000**	**0.000**	**0.000**	**0.359**	**0.137**	**0.199**	**0.540**	**0.859**	**0.663**	**0.3831**	**0.3305**	**0.0399**
Monash 025	NA	NA	NA	0.783	0.864	0.822	0.348	0.232	0.278	0.6912	0.5992	0.0259
Monash 026	**0.000**	**0.000**	**0.000**	**0.778**	**0.871**	**0.822**	**0.420**	**0.300**	**0.350**	**0.5712**	**0.5423**	**0.1677**
Paris 001	**0.211**	**0.154**	**0.178**	**0.521**	**0.656**	**0.580**	**0.393**	**0.276**	**0.324**	**0.4264**	**0.3355**	**0.0299**
Paris 002	**0.480**	**0.571**	**0.522**	**0.316**	**0.276**	**0.294**	**0.385**	**0.321**	**0.350**	**0.4377**	**0.3528**	**0.3154**
Paris 003	**0.389**	**0.323**	**0.353**	**0.637**	**0.745**	**0.687**	**0.148**	**0.085**	**0.108**	**0.4181**	**0.3615**	**0.1617**
Paris 004	**0.130**	**0.062**	**0.085**	**0.366**	**0.293**	**0.325**	**0.400**	**0.540**	**0.460**	**0.4414**	**0.3783**	**0.4511**
Paris 005	**0.358**	**0.375**	**0.366**	**0.463**	**0.452**	**0.458**	**0.398**	**0.398**	**0.398**	**0.4325**	**0.3374**	**0.0200**
Paris 006	**0.000**	**0.000**	**0.000**	**0.382**	**0.366**	**0.374**	**0.647**	**0.776**	**0.706**	**0.4394**	**0.3603**	**0.0479**
Paris 007	**0.000**	**0.000**	**0.000**	**0.520**	**0.552**	**0.536**	**0.700**	**0.684**	**0.692**	**0.5831**	**0.4713**	**0.0160**
Paris 008	**0.161**	**0.310**	**0.212**	**0.388**	**0.392**	**0.390**	**0.655**	**0.547**	**0.596**	**0.5069**	**0.3629**	**0.0020**
Paris 009	**0.309**	**0.630**	**0.415**	**0.312**	**0.164**	**0.215**	**0.721**	**0.613**	**0.663**	**0.4295**	**0.3346**	**0.0060**
Paris 010	**0.200**	**0.222**	**0.211**	**0.443**	**0.360**	**0.397**	**0.678**	**0.729**	**0.703**	**0.4759**	**0.3574**	**0.0020**
Paris 011	**0.000**	**0.000**	**0.000**	**0.125**	**0.017**	**0.030**	**0.629**	**0.914**	**0.745**	**0.5198**	**0.5191**	**0.7066**

bioRxiv preprint doi: https://doi.org/10.1101/2024.02.11.579845; this version posted April 22, 2025. The copyright holder for this preprint (which was not certified by peer review) is the author/funder, who has granted bioRxiv a license to display the preprint in perpetuity. It is made available under aCC-BY-NC-ND 4.0 International license.

Paris 012	**0.333**	**0.419**	**0.371**	**0.511**	**0.463**	**0.486**	**0.146**	**0.125**	**0.135**	**0.4235**	**0.3422**	**0.0958**
Paris 013	**0.461**	**0.519**	**0.488**	**0.000**	**0.000**	**0.000**	**0.611**	**0.725**	**0.663**	**0.4728**	**0.3503**	**0.0060**
Paris 014	**0.125**	**0.256**	**0.168**	**0.106**	**0.292**	**0.156**	**0.853**	**0.540**	**0.661**	**0.4463**	**0.3560**	**0.2774**
Paris 015	**0.000**	**0.000**	**0.000**	**0.351**	**0.283**	**0.313**	**0.837**	**0.884**	**0.860**	**0.5066**	**0.4472**	**0.0080**
Paris 016	**0.000**	**0.000**	**0.000**	**0.444**	**0.330**	**0.379**	**0.709**	**0.814**	**0.758**	**0.5167**	**0.4674**	**0.1198**
Paris 017	**0.354**	**0.347**	**0.350**	**0.118**	**0.095**	**0.105**	**0.589**	**0.628**	**0.608**	**0.4727**	**0.3302**	**0.0100**
Paris 018	**0.000**	**0.000**	**0.000**	**0.000**	**0.000**	**0.000**	**0.887**	**1.000**	**0.940**	**0.6767**	**0.6642**	**0.0359**
Paris 019	**0.000**	**0.000**	**0.000**	**0.000**	**0.000**	**0.000**	**0.746**	**0.946**	**0.834**	**0.4836**	**0.4969**	**1.0**
Paris 020	**0.000**	**0.000**	**0.000**	**0.250**	**0.328**	**0.284**	**0.783**	**0.731**	**0.756**	**0.5917**	**0.5353**	**0.1796**
Paris 021	NA	NA	NA	0.269	0.206	0.233	0.773	0.829	0.800	0.5267	0.4979	0.4311
Paris 022	**0.036**	**0.071**	**0.048**	**0.497**	**0.657**	**0.566**	**0.375**	**0.206**	**0.266**	**0.4624**	**0.3788**	**0.1876**
Paris 023	**0.000**	**0.000**	**0.000**	**0.000**	**0.000**	**0.000**	**0.600**	**0.907**	**0.722**	**0.4985**	**0.5135**	**0.7485**
Paris 024	**0.550**	**0.484**	**0.515**	**0.000**	**0.000**	**0.000**	**0.611**	**0.739**	**0.669**	**0.5353**	**0.4324**	**0.0160**
Paris 025	**0.447**	**0.273**	**0.339**	**0.350**	**0.500**	**0.412**	**0.377**	**0.460**	**0.414**	**0.4773**	**0.3320**	**0.0020**
Paris 026	**0.000**	**0.000**	**0.000**	**0.000**	**0.000**	**0.000**	**0.817**	**0.992**	**0.896**	**0.4333**	**0.4324**	**0.6567**
Paris 027	**0.000**	**0.000**	**0.000**	**0.579**	**0.596**	**0.587**	**0.627**	**0.631**	**0.629**	**0.5789**	**0.4578**	**0.0020**

bioRxiv preprint doi: https://doi.org/10.1101/2024.02.11.579845; this version posted April 22, 2025. The copyright holder for this preprint (which was not certified by peer review) is the author/funder, who has granted bioRxiv a license to display the preprint in perpetuity. It is made available under aCC-BY-NC-ND 4.0 International license.

Paris 028	**0.382**	**0.317**	**0.347**	**0.465**	**0.444**	**0.454**	**0.500**	**0.555**	**0.526**	**0.4328**	**0.3821**	**0.3253**
Paris 029	**0.000**	**0.000**	**0.000**	**0.590**	**0.727**	**0.651**	**0.432**	**0.312**	**0.363**	**0.4850**	**0.4429**	**0.0978**
Paris 030	**0.218**	**0.250**	**0.233**	**0.472**	**0.402**	**0.434**	**0.431**	**0.470**	**0.450**	**0.4202**	**0.2885**	**0.0020**
Paris 031	**0.091**	**0.042**	**0.057**	**0.270**	**0.233**	**0.250**	**0.687**	**0.768**	**0.725**	**0.4677**	**0.3857**	**0.0240**
Paris 032	NA	NA	NA	NA	NA	NA	1.000	1.000	1.000	1.000	1.000	1.0
Paris 033	**0.273**	**0.284**	**0.278**	**0.233**	**0.206**	**0.219**	**0.538**	**0.556**	**0.547**	**0.3660**	**0.3457**	**0.2176**
Paris 034	**0.000**	**0.000**	**0.000**	**0.462**	**0.362**	**0.406**	**0.621**	**0.728**	**0.670**	**0.5940**	**0.5215**	**0.1178**
Paris 035	**0.000**	**0.000**	**0.000**	**0.500**	**0.667**	**0.571**	**0.415**	**0.300**	**0.348**	**0.4877**	**0.4284**	**0.2475**
Paris 036	**0.222**	**0.229**	**0.225**	**0.315**	**0.299**	**0.307**	**0.560**	**0.574**	**0.567**	**0.3897**	**0.3309**	**0.0060**

Table S6: Detailed results of subject level classifiers. For each subject and each class, precision (Pr), recall (Re) and F-1 score are presented. For each subject, the observed balanced accuracy score, the mean balanced accuracy of the permutation test and the p-value of the permutation test are presented. Highlighted subjects (in bold) present with the 3 classes (3 mind states) and were included in the group analysis (Figure 6, n= 54/62)

bioRxiv preprint doi: https://doi.org/10.1101/2024.02.11.579845; this version posted April 22, 2025. The copyright holder for this preprint (which was not certified by peer review) is the author/funder, who has granted bioRxiv a license to display the preprint in perpetuity. It is made available under aCC-BY-NC-ND 4.0 International license.

Predicted Mental state	**FA (%)**	**Misses (%)**	**RTs (ms)**
ON	32.1 ± 2.9	1.3 ± 0.4	468 ± 10
MW	39.2 ± 3.5	1.8 ± 0.6	475 ± 10
MB	37.6 ± 4.2	2.8 ± 0.9	483 ± 11

Behavioral measure	**Main effect of mind state**		**Pairwise contrasts**
	χ²	***FDR corrected p-value***	
FA	χ^2 (2)=6.8	0.04	MW *vs* ON : z-ratio=2.5, p-value= 0.02 MB *vs* ON: z-ratio=1.5, p-value= 0.1 MB vs MW: z-ratio=-0.4, p-value=0.7
Misses	χ^2 (2)=31.5	$5.7 * 10^{-7}$	MW *vs* ON : z-ratio=2.4, p-value= 0.02 MB *vs* ON: z-ratio=5.6, p-value=$9.6 * 10^{-8}$ MB vs MW: z-ratio=3.3, p-value=0.002
RT	F (2)=7.4	$1.4 * 10^{-3}$	MW *vs* ON : z-ratio=2.3, p-value= 0.03 MB *vs* ON: z-ratio=3.6, p-value= $7.5 * 10^{-4}$ MB vs MW: z-ratio=1.8 p-value=0.08

Table S7: Behavioral results in non-labeled trials in function of the predicted mind-state. Results of the linear mixed models with predicted mind-state as a main factor and subject ID/dataset as random intercepts, for false alarms (FA), misses and response times (RT). The table presents the model estimates for each mind -state (top) and the statistical contrasts (bottom). P-values were corrected for multiple comparisons using an FDR procedure.

Supplementary Appendix 2: When your heart isn't in it anymore: Cardiac correlates of task disengagement

bioRxiv preprint doi: https://doi.org/10.1101/2024.06.21.599851; this version posted May 17, 2025. The copyright holder for this preprint (which was not certified by peer review) is the author/funder, who has granted bioRxiv a license to display the preprint in perpetuity. It is made available under aCC-BY-NC 4.0 International license.

When your heart isn't in it anymore: Cardiac correlates of task disengagement

Andrew W. Corcoran

Monash Centre for Consciousness & Contemplative Studies, Monash University, Melbourne, Victoria, VIC 3800, Australia

https://orcid.org/0000-0002-0449-4883

Arthur Le Coz

Sorbonne Université, Institut du Cerveau - Paris Brain Institute - ICM, Inserm, CNRS, 75013 Paris, France

https://orcid.org/0009-0007-4464-1570

Jakob Hohwy

Monash Centre for Consciousness & Contemplative Studies, Monash University, Melbourne, Victoria, VIC 3800, Australia

https://orcid.org/0000-0003-3906-3060

Thomas Andrillon

Sorbonne Université, Institut du Cerveau - Paris Brain Institute - ICM, Inserm, CNRS, 75013 Paris, France

Monash Centre for Consciousness & Contemplative Studies, Monash University, Melbourne, Victoria, VIC 3800, Australia

https://orcid.org/0000-0003-2794-8494

Corresponding author email address: andrew.corcoran@monash.edu

Conflict of interest statement: The authors declare no conflict of interest.

bioRxiv preprint doi: https://doi.org/10.1101/2024.06.21.599851; this version posted May 17, 2025. The copyright holder for this preprint (which was not certified by peer review) is the author/funder, who has granted bioRxiv a license to display the preprint in perpetuity. It is made available under aCC-BY-NC 4.0 International license.

Abstract

Neuroscience is beginning to uncover the role of interoceptive feedback in perception, learning, and decision-making; however, the relation between spontaneous visceral and cognitive dynamics has received surprisingly little scrutiny. Here, we investigate how subjective, physiological, and behavioural indicators of arousal and attentional state vary in relation to ongoing cardiac activity and brain-heart coupling. Electroencephalogram, electrocardiogram, and pupillometric records were obtained from 65 adults during the performance of a sustained attention to response task (SART). Thought probes were intermittently administered during the SART to collect subjective reports of attentional state (i.e., on-task, mind-wandering, mind-blanking) and vigilance level (i.e., alertness vs. sleepiness). Mind-wandering and mind-blanking reports increased in frequency with time-on-task and were accompanied by decreases in alertness and pupil-linked arousal, but evinced distinct psychophysiological and behavioural profiles. While mind-wandering was associated with greater heart-rate variability and late modulation of the heartbeat-evoked potential, mind-blanking was characterised by greater decreases in heart-rate, pupil size, and brain-heart coupling. Lower heart-rate predicted decreased vigilance and pupil size, in addition to slower, less-biased responses; increased heart-rate variability predicted more impulsive behaviour and pupil dilation. Together, these findings reveal that cardiac and brain-heart connectivity measures afford complementary information about arousal states and attentional dynamics during task performance.

Keywords: Arousal; Attention; Brain-body interaction; Heartbeat-evoked potential; Heart-rate variability; Mind-blanking; Mind-wandering; Pupillometry; SART; Vigilance

bioRxiv preprint doi: https://doi.org/10.1101/2024.06.21.599851; this version posted May 17, 2025. The copyright holder for this preprint (which was not certified by peer review) is the author/funder, who has granted bioRxiv a license to display the preprint in perpetuity. It is made available under aCC-BY-NC 4.0 International license.

Introduction

Neural monitoring of internal bodily states (interoception) is essential for homeostasis, and conditions the way we perceive and act in the world [1–5]. For example, visceral afferent signals generated by the heartbeat modulate the sensation [6–11], learning, and memory of external stimuli [12–14], coincide with the initiation of voluntary actions [15–17], and are adaptively regulated to optimise perceptual decision-making [18]. Moreover, cortical processing of cardiac-related interoceptive signals predicts stimulus detection [19–21], interoceptive attention [22–24], and decision-making [25] in healthy individuals, and may harbour diagnostic information in disorders of consciousness [26,27]. While this growing body of work demonstrates the involvement of cardio-afferent signals in shaping conscious experience and behaviour, very little is known about the way cardiac activity relates to ongoing cognitive dynamics, such as the spontaneous vacillation between task-focused attention and task disengagement.

Arousal state and attentional engagement have long been associated with cardiac regulation [28–32]. For instance, phasic heart-rate responses to salient events vary depending on stimulus attributes such as intensity [33,34] and content [35,36], while prevailing heart-rate is reliably modulated by task demands (e.g., attentive listening vs. mental arithmetic) [37,38] and situational properties (e.g., uncertainty, incentivisation) [39]. Early studies of heart-rate variability (HRV) – i.e., fluctuations in the duration separating each heartbeat [40–42] – also revealed sensitivity to task performance, with transient heart-rate decelerations indexing both anticipatory [43,44] and error-related processing [45] (for recent reviews, see Skora and colleagues [5] and Di Gregorio and colleagues [46]). HRV has since been extensively studied as a biomarker of the capacity to regulate one's arousal, attention, and behaviour [47–51], and would therefore seem to present a promising psychophysiological candidate for tracking the spontaneous evolution of cognitive dynamics.

Alterations in cardiac parameters such as heart-rate (or its reciprocal, heart period) and HRV are primarily driven by the central modulation of sympathetic and parasympathetic outflows [52–55]. Such parameters thus afford information about the way integrated cortical and subcortical networks co-ordinate physiological and behavioural responses to evolving conditions [56–61]. Effective regulation depends on the neural monitoring of visceral afferent feedback generated by autonomic activity [62–64]; the heartbeat-evoked potential (HEP [65,66]) has been widely interpreted as a neurophysiological index of such interoceptive processing [67,68]. Intriguingly, this evoked response is modulated by attentional focus – attending to heartbeat sensations amplifies the HEP compared to when attention is directed towards external stimuli [22–24,69–72].

bioRxiv preprint doi: https://doi.org/10.1101/2024.06.21.599851; this version posted May 17, 2025. The copyright holder for this preprint (which was not certified by peer review) is the author/funder, who has granted bioRxiv a license to display the preprint in perpetuity. It is made available under aCC-BY-NC 4.0 International license.

Altered heartbeat-evoked responses have also been reported in the context of self-related spontaneous cognition [73,74] and mental imagery [75], indicating that HEP amplitude is sensitive to the content of thought independent of cardiac dynamics.

A more recent development in the psychophysiology and neuroscience of brain-heart integration is the use of frequency-domain coupling measures to assess how cortical and cardiac rhythms co-evolve through time [76]. While the HEP tracks how neural responses to the heartbeat unfold over the course of a few hundred milliseconds, coupling measures can be deployed to summarise dependencies between time-series on the order of seconds or minutes. Signal processing and modelling techniques may also be used to infer whether fluctuations in coupling strength are primarily driven by one signal or another (i.e., whether changes in brain-heart connectivity reflect a relative shift towards top-down autonomic regulation or bottom-up interoceptive processing). For example, a recent study reported a predominantly bottom-up pattern of brain-heart coupling under (task-free) resting-state conditions, whereby spontaneous neural oscillations were modulated by the phase of the HRV time-series [77]. Brain-heart coupling has also been found to differ across levels of arousal (e.g., sleep stage [78,79], physiological [80,81] or mental challenge [82,83], emotion induction [84–86]). However, we are unaware of any previous attempts to evaluate whether brain-heart coupling systematically varies as a function of attentional state dynamics.

In this study, we investigate whether cardiac parameters encode information distinguishing subjective reports of task-focused attention ('on-task' state) from spontaneous episodes of task disengagement. We distinguished between two modes of task disengagement – task-unrelated thought ('mind-wandering') and the absence of thought ('mind-blanking') – because of their distinct signatures in terms of behaviour and arousal, with mind-blanking being associated with lower levels of arousal and more sluggish responding than mind-wandering [87,88]. Notably, mind-wandering has previously been linked with increased heart-rate during the performance of laboratory-based tasks [89–92]. However, this association was not evident in a 24-hr experience sampling study [93,94]. Short-term HRV has also been identified as a potential biomarker of mind-wandering, although differences in HRV have thus far only been reported for perseverative, negatively-valenced thoughts [89,93,94]. We are unaware of any attempt to characterise the expression of cardiac dynamics during mind-blanking, although recent work suggests cardiac features may be informative for distinguishing mind-blanking from other states [88]. Beyond the mind-wandering and mind-blanking literature, subjective disengagement from challenging tasks has been associated with blunted increases in heart-rate relative to resting-state [95,96], indicating that cardiac dynamics afford information about one's willingness to invest effort in task performance.

bioRxiv preprint doi: https://doi.org/10.1101/2024.06.21.599851; this version posted May 17, 2025. The copyright holder for this preprint (which was not certified by peer review) is the author/funder, who has granted bioRxiv a license to display the preprint in perpetuity. It is made available under aCC-BY-NC 4.0 International license.

Given the paucity of data on the relation between cardiac activity and spontaneous cognition (in contrast to the rich literature linking mind-wandering and pupillometry [87,97–101]) – and extending beyond recent studies investigating brain-heart interaction under task-free resting-state conditions [77,88,102] and arousal state manipulations [80–86] – we sought to identify the cardiac signatures of task (dis)engagement during the performance of a Go/NoGo paradigm known as the sustained attention to response task (SART [103,104]). We evaluated how cardiac parameters varied as a function of participants' focus of attention (on-task, mind-wandering, mind-blanking) while performing the SART, and how these profiles compared with established indices of arousal and task (dis)engagement (i.e., subjective alertness/fatigue, pupil size, behavioural performance). Finally, we computed two complementary measures of interoceptive processing – the well-established HEP [67,68] and a more-recently proposed method for quantifying cerebro-peripheral signal coupling [105,106] – to assess whether attentional states are characterised by distinctive patterns of brain-heart interaction.

Materials and Methods

Participants

We analysed data collected from 26 adults as part of a previously published study conducted in Melbourne, Australia [107], and from 41 adults who participated in a replication of the original experiment in Paris, France. Both datasets featured electroencephalogram (EEG), electrocardiogram (ECG), and pupillometric recordings (except for two participants) obtained during performance of the SART. One participant from each dataset was excluded from analysis due to a faulty ECG. The remaining sample consisted of 36 males and 29 females aged 20 to 39 years (M = 27.3, S.D. = 5.3; age of one participant missing). All individuals provided written informed consent prior to participating in the study. The study protocol was approved by the Monash University Human Research Ethics Committee (Project ID: 10994) and Comité d'Éthique de la Recherche (CER) de Sorbonne Université (Project ID: CER-2023-DEGRAVE-MW_Respi).

Stimuli and experimental design

Task instructions and stimuli were presented using the Psychophysics Toolbox (Melbourne: v3.0.14; Paris: v3.0.18 [108]) for MATLAB (The MathWorks Inc., Natick, MA, USA; Melbourne: R2018b, Paris: 2022b). Participants viewed task stimuli while seated in a dimly-lit room with their head stabilised on a support positioned approximately 60 cm from the computer screen.

bioRxiv preprint doi: https://doi.org/10.1101/2024.06.21.599851; this version posted May 17, 2025. The copyright holder for this preprint (which was not certified by peer review) is the author/funder, who has granted bioRxiv a license to display the preprint in perpetuity. It is made available under aCC-BY-NC 4.0 International license.

Participants performed two versions of a modified SART: one featuring face stimuli, another featuring numerical digits (Figure 1). Face stimuli were sampled from the Radboud Face Database [109]. Eight faces (4 female) featuring a neutral expression were selected as Go stimuli; one image of a smiling female served as the NoGo stimulus. Stimuli for the Digit SART were computer-generated integers ranging from 1 to 9, with "3" serving as the NoGo stimulus. All digits were presented at a uniform font size.

In order to induce steady-state visual evoked potentials (SSVEPs) in the EEG, the left and right halves of each presented face stimulus were flickered at different frequencies (12 and 15 Hz; laterality counterbalanced across blocks). Digit stimuli were embedded within a Kanizsa illusory square, the left and right parts of which were likewise flickered. Analysis of this component of the experimental design is postponed to future work. Please note, flicker frequencies were sufficiently high that participants did not report any impact on their capacity to perform the SART.

Stimuli were presented continuously at the centre of the screen, with successive trial onsets occurring at intervals of 750 to 1250 ms (randomly sampled from a uniform distribution). All 9 stimuli within the stimulus set were present once in a pseudo-randomised order, before the set was randomly permuted for the next 9 trials (with the constraint that the same stimulus never appeared twice in succession). The probability of a NoGo trial was thus fixed at $p = .11$. Participants were instructed to pay attention to each presented stimulus and respond via button-press each time a Go stimulus appeared. Conversely, they were told to withhold their response whenever a NoGo stimulus was presented. Participants were advised to prioritise accuracy over speed of response, in line with evidence that this strategy improves the precision of SART errors as an index of attentional lapses [110].

The SART was intermittently interrupted by the presentation of the word "STOP", followed by a set of 7 or 8 thought probes. Our analysis focuses on participants' subjective reports of the content of their attentional focus "just before the interruption". Participants responded to this probe by selecting one of the following options: (1) "task-focused" (i.e., on-task), (2) "off-task" (i.e., focused on something other than the SART; mind-wandering), (3) "mind-blanking" (i.e., focused on nothing), (4) "don't remember". In the analyses that follow, responses (3) and (4) were collapsed into a single "mind-blanking" category. Data from the final probe of each set, which asked participants to rate their level of vigilance "over the past few trials" on a 4-point Likert scale (1 = "Extremely Sleepy"; 4 = "Extremely Alert"), are also reported. In addition, participants were also asked to answer the following questions, which were not analysed here: (1) "Were you looking at the screen?" (response: yes / no); (2) "How aware were you of your

bioRxiv preprint doi: https://doi.org/10.1101/2024.06.21.599851; this version posted May 17, 2025. The copyright holder for this preprint (which was not certified by peer review) is the author/funder, who has granted bioRxiv a license to display the preprint in perpetuity. It is made available under aCC-BY-NC 4.0 International license.

focus?" (response: from 1, I was fully aware, to 4, I was not aware at all); (3) "Was your state of mind intentional?" (response: from 1, entirely intentional, to 4, entirely unintentional); (6) "How engaging were your thoughts?" (response: from 1, not engaging, to 4, very engaging); (7) "How well do you think you have been performing?" (response: from 1, not good, to 4, very good).

Prior to commencing the experiment, participants performed two blocks of practice trials (1 block of 27 trials for each variant of the SART). Performance feedback (proportion of correct responses, average response time) was provided at the end of each practice block. Participants then performed 3 blocks of each SART (block order randomly permuted per participant) for a total of 6 blocks. Blocks comprised between 459 and 616 trials (median = 540), lasted approximately 12–15 min, and were separated by self-paced breaks (total duration: M = 95.1 min, S.D. = 10.4). Each block comprised 10 sets of thought probes separated by intervals ranging from 40 to 70 s (randomly sampled from a uniform distribution).

bioRxiv preprint doi: https://doi.org/10.1101/2024.06.21.599851; this version posted May 17, 2025. The copyright holder for this preprint (which was not certified by peer review) is the author/funder, who has granted bioRxiv a license to display the preprint in perpetuity. It is made available under aCC-BY-NC 4.0 International license.

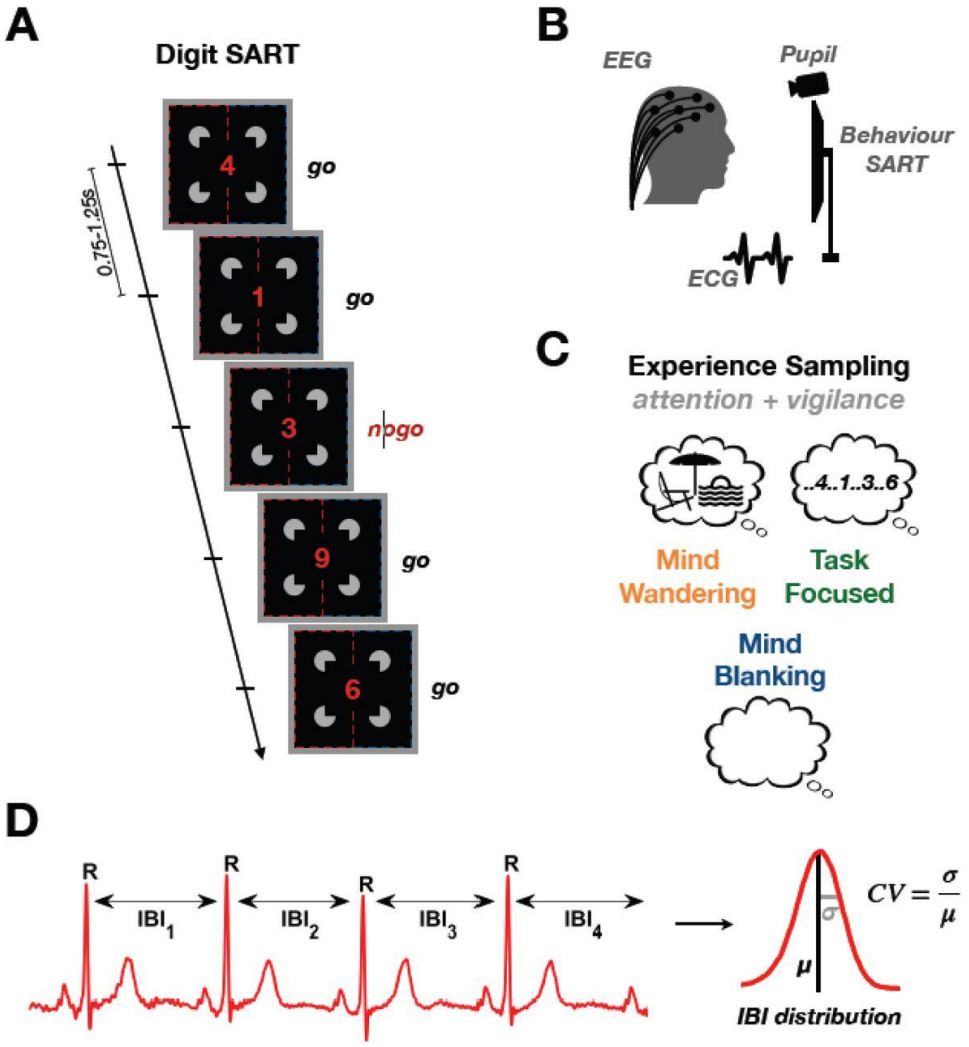

Figure 1: Tracking the neural and cardiac correlates of task disengagement

A: Participants were instructed to perform a modified version of the Sustained Attention to Response Task (SART), a Go/NoGo task involving either face or digit stimuli (block design). Participants had to respond to all stimuli (Go trials) except when presented with a specific target stimulus (smiling face or digit '3'; NoGo trials). B: For each participant, EEG and ECG signals, pupil size, and behavioural data on the SART were continuously recorded. C: Participants were interrupted every 40-70 s (10 times per block) and asked to report their attentional state (on-task, mind-wandering, or mind-blanking) and vigilance level (alertness). D: In ECG recordings, we automatically detected R-peaks and computed the duration of successive interbeat intervals (IBIs) during SART performance. The IBI time-series was used to calculate the IBI distribution from which we derived the mean IBI duration (i.e., average heart period; inverse heart-rate) and coefficient of variation (CV; i.e., heart-rate variability) during epochs preceding thought probes.

bioRxiv preprint doi: https://doi.org/10.1101/2024.06.21.599851; this version posted May 17, 2025. The copyright holder for this preprint (which was not certified by peer review) is the author/funder, who has granted bioRxiv a license to display the preprint in perpetuity. It is made available under aCC-BY-NC 4.0 International license.

Psychophysiological signal acquisition and preprocessing

Electroencephalography and electrocardiography

For the Melbourne dataset, high-density EEG was acquired using 63 EasyCap-mounted active electrodes. A ground electrode was placed over FPz; AFz served as the online reference. The ECG was acquired from electrodes placed on either shoulder; the electro-oculogram (EOG) was recorded from electrodes placed above and below the left and right canthi. All signals were sampled at 500 Hz using a BrainAmp system (Brain Products GmbH) in conjunction with BrainVision Recorder (v1.21.0402; Brain Products GmbH).

For the Paris dataset, EEG records were acquired via 63 actiCap Snap-mounted active electrodes. AFz was again used as the ground electrode, while FCz served as the online reference. The ECG was recorded from an electrode placed below the right shoulder and one placed above the left hip. Horizontal and vertical EOG were acquired from electrodes positioned above and below the dominant eye, and on the left and right outer canthi. All additional electrodes to the EEG (HEOG, VEOG, ECG) were referenced to a ground positioned behind the right shoulder. All signals were sampled at 1000 Hz using BrainVision Recorder (v1.24.0001; Brain Products GmbH).

Offline preprocessing of the raw EEG and ECG was performed in MATLAB R2022a (v9.12.0.1884302) in conjunction with the EEGLAB toolbox (v2024.2.1 [111]). Data collected in Paris were initially downsampled to 500 Hz to match the online sampling rate in Melbourne. EEG signals were re-referenced to the common average so that the online reference could be reintroduced into the array, and then re-referenced to the average of TP9 and TP10 (in lieu of linked mastoids). The following 62 channels were included in the analysis: Fp1, Fp2, AF7, AF3, AFz, AF4, AF8, F7, F5, F3, F1, Fz, F2, F4, F6, F8, FT9, FT7, FC5, FC3, FC1, FCz, FC2, FC4, FC6, FT8, FT10, T7, C5, C3, C1, Cz, C2, C4, C6, T8, TP7, CP5, CP3, CP1, CPz, CP2, CP4, CP6, TP8, P7, P5, P3, P1, Pz, P2, P4, P6, P8, PO7, PO3, POz, PO4, PO8, O1, Oz, O2.

EEG and ECG records were high-pass filtered (passband edge = 0.5 Hz, transition width = 0.5 Hz) via the ‘pop_eegfiltnew’ function of the ‘firfilt’ plugin (v2.8). Line noise was suppressed at 50 and 100 Hz via the ‘cleanLineNoise’ function from the ‘PrepPipeline’ plugin (v0.55.4 [112]). The data were then low-pass filtered via ‘pop_eegfiltnew’ (passband edge = 40 Hz, transition width = 10 Hz) and segments between trial blocks excluded. Automated bad channel detection (flatline criterion = 5 s; channel criterion = .8; median number of rejected channels = 0; range = [0, 6]) and artifact subspace reconstruction (burst criterion = 20 [113]) routines were applied to

bioRxiv preprint doi: https://doi.org/10.1101/2024.06.21.599851; this version posted May 17, 2025. The copyright holder for this preprint (which was not certified by peer review) is the author/funder, who has granted bioRxiv a license to display the preprint in perpetuity. It is made available under aCC-BY-NC 4.0 International license.

the EEG via the 'clean_rawdata' plugin (v2.91 [114]). The ECG was z-normalised and R-wave peaks automatically identified using the QRS beat-detection algorithm implemented by the 'ConvertRawDataToRRIntervals' function of the PhysioNet Cardiovascular Signal Toolbox (v1.0 [115]). R-peak annotations were visually inspected (and where necessary, manually corrected) with the aid of the HEPLAB plugin (v1.0.1 [116]). The ECG signal was then reunited with the EEG and R-peak latency information appended to the event structure.

EEG and ECG data were downsampled to 250 Hz and subjected to independent component analysis (ICA; extended infomax algorithm [117]). Components were automatically classified using ICLabel (v1.6 [118]); those classed as ocular, cardiac, or channel noise artefacts with > .90 probability were subtracted from the dataset (median number of rejected components = 4; range = [1, 11]). Data were then subjected to a second round of ICA specifically designed to mitigate the impact of the cardiac field artefact. EEG records were epoched [-200, 200] ms relative to each R-peak and decomposed via ICA. Component and ECG time-series were then low-pass filtered below 25 Hz using a 2-pass, 2nd-order Butterworth filter and Hilbert-transformed to obtain instantaneous phase estimates. Coherence of each component with the ECG signal was calculated as the mean difference between each pair of component-ECG phase angles [119,120]. Components scoring > 3 S.D. above the subject-level mean coherence were marked as cardiac in nature and subtracted from the full EEG dataset. This procedure was repeated until a maximum of 3 components were excluded, or until no remaining coherence values exceeded the rejection threshold (which was recalculated on each iteration; median number of rejected components = 2; range = [0, 3]). For similar approaches, see Banellis and Cruse [121] and Buot and colleagues [122].

Pupillometry

Eye-movements and pupil size of one eye were sampled at 1000 Hz via an EyeLink 1000 eye-tracking system (SR Research Ltd., Mississauga, Canada). The eye-tracker was calibrated at the beginning of each experimental session using the EyeLink acquisition software. EyeLink 1000 Edf files were imported into MATLAB via the Edf2Mat Toolbox (v1.21.0 [123]) and preprocessed using custom-built functions based on procedures previously reported by van Kempen and colleagues [124] and Corcoran and colleagues [125]. Blink timings (automatically identified by the EyeLink acquisition software) were corrected via linear interpolation over the blink interval. The start and end points of the interpolated segment were calculated by taking the average pupil size spanning [-200, -100] ms before and [100, 200] ms after the blink period, respectively. The corrected signal was then low-pass filtered below 6 Hz using a 2-pass, 4th-

bioRxiv preprint doi: https://doi.org/10.1101/2024.06.21.599851; this version posted May 17, 2025. The copyright holder for this preprint (which was not certified by peer review) is the author/funder, who has granted bioRxiv a license to display the preprint in perpetuity. It is made available under aCC-BY-NC 4.0 International license.

order Butterworth filter. Blinks exceeding 2000 ms were marked as missing data, as were data points spanning 100 ms before and after the blink period.

Data analysis

Signal detection theoretic measures

Responses on Go trials were classed as 'hits'; failures to respond (errors of omission) were classed as 'misses'. Responses during NoGo trials (errors of commission) were classed as 'false alarms'; withheld responses were classed as 'correct rejections'. Hit rate was calculated as the proportion of Go trials that elicited a response within the 10 s time window preceding the onset of experience sampling ('preprobe epoch'); false alarm rate was analogously calculated as the proportion of NoGo trials that elicited a response (loglinear correction for extreme values applied following Hautus [126]). Please note, correct rejections preceded and followed by misses were excluded from analysis on the basis that sustained lack of responding across Go-NoGo-Go trial sequences is indicative of a period of task disengagement (rather than selective response inhibition).

Sensitivity to trial type (Go vs. NoGo) was quantified with the discriminability index *d'*, which was obtained by subtracting z-scored false alarm rates from corresponding z-scored hit rates. A *d'* of 0 indicates chance-level discrimination of Go trials from NoGo trials; more positive values indicate increasing sensitivity. Response bias (decision criterion) was quantified as *c*, the mean of z-scored hit and false alarm rates. A *c* of 0 indicates no bias towards either stimulus category; more positive values indicate greater bias towards issuing a response (i.e., liberal criterion), while more negative values indicate greater bias towards withholding a response (i.e., conservative criterion).

Response speed

Response speed estimates were calculated by inverting response times obtained from Go trials (response speed was favoured on account of rendering a more Gaussian-distributed set of observations than response time). Responses registered within 300 ms of trial onset were discarded, since they conflate fast responses to the present trial with (very) slow responses to the preceding trial (see, e.g., Cheyne and colleagues [127]). Mean response speed ($RS\mu$) was obtained by averaging response speed estimates within each preprobe epoch per participant. A minimum of 5 valid responses was required to estimate $RS\mu$ for a given epoch (median number of rejected epochs = 3; range = [0, 39]). Response speed time-series were then linearly interpolated to impute missing or withheld trial responses, and the coefficient of

bioRxiv preprint doi: https://doi.org/10.1101/2024.06.21.599851; this version posted May 17, 2025. The copyright holder for this preprint (which was not certified by peer review) is the author/funder, who has granted bioRxiv a license to display the preprint in perpetuity. It is made available under aCC-BY-NC 4.0 International license.

variation (RSc_v) for each preprobe epoch obtained by dividing the standard deviation of the interpolated series (RSσ) by the corresponding mean (RSμ):

$$RSc_v = \frac{RS\sigma}{RS\mu} .$$

Pupil size

Preprocessed pupil size estimates from each set of trials were z-transformed on the subject-level. Estimates spanning the 10 s interval immediately preceding each set of thought probes were averaged to yield preprobe estimates of mean pupil size. Preprobe epochs containing < 5 s of pupil size data were excluded from analysis (median number of rejected epochs = 0; range = [0, 24]).

Cardiac parameters

Interbeat intervals (IBIs) – an estimator of cardiac cycle duration (i.e., heart period) – were calculated as the difference between successive R-peaks. IBIs < 300 ms or > 2000 ms in duration were excluded as physiologically implausible. IBIs were z-transformed on the subject-level, and scores exceeding +\- 5 z.u. excluded from analysis (on the basis such extreme outliers were likely artifacts due to missing or spurious R-peak annotations; median number of rejected IBIs = 2; range = [0, 30]). The corrected IBI time-series (i.e., tachogram) was then upsampled to 5 Hz and cubic-spline interpolated. Analogous to the reaction speed analysis, mean IBI (IBIμ) and coefficient of variation (IBIc_v) estimates were calculated for each preprobe epoch. IBIc_v was natural log-transformed as follows:

$$IBIc_v = ln(\frac{IBI\sigma}{IBI\mu}) .$$

Heartbeat-evoked potentials

Heartbeat-evoked potentials (HEPs) were extracted by first applying lowpass filters to the ICA-corrected EEG and ECG signals (passband edge = 20 Hz, transition width = 5 Hz) and segmenting [-0.3, 0.9] s around each R-peak resolved in the 10 s preprobe epoch. R-peaks followed by IBI durations < 600 ms were discarded, and a minimum of 5 R-peaks was required to estimate the HEP for each individual epoch (these criteria resulted in the exclusion of 8 preprobe epochs from one participant and 1 preprobe epoch from another). Epoched data were not 'baseline-corrected', since this procedure may contaminate HEP estimates with fluctuations deriving from the preceding cardiac cycle [1,68].

bioRxiv preprint doi: https://doi.org/10.1101/2024.06.21.599851; this version posted May 17, 2025. The copyright holder for this preprint (which was not certified by peer review) is the author/funder, who has granted bioRxiv a license to display the preprint in perpetuity. It is made available under aCC-BY-NC 4.0 International license.

Mutual information between cardiac and brain signals

Coupling between the EEG and ECG time-series was quantified using mutual information (MI), an information-theoretic measure of the statistical relationship between two random variables [128,129]. MI was estimated using the Gaussian-Copula technique (see Ince and colleagues [106]) as implemented via v0.4 of the open-source MATLAB code available from https://github.com/robince/gcmi.

ICA-corrected EEG-ECG records were downsampled to 50 Hz and epoched [-16, 2] s relative to the onset of each set of probes. We then used the Nonlinear Mode Decomposition (NMD) toolbox (v2.00 [130]) to calculate the wavelet transform of the ECG signal between the frequencies [0.5, 2.0] Hz, from which the dominant oscillatory component (i.e., instantaneous heart frequency – a time-resolved representation of HRV) was extracted [18,131]. EEG signals were bandpass filtered into the following 8 log-spaced low-frequency bands: [0.8, 1.2], [1.2, 1.8], [1.8, 2.6], [2.6, 3.9], [3.9, 5.8], [5.8, 8.6], [8.6, 12.8], and [12.7, 19.0] Hz. Each filtered time-series was Hilbert-transformed to obtain its analytic signal, the real and imaginary components of which were scaled by their corresponding absolute values prior to copula-normalisation ('copnorm' function). Normalised time-series were then segmented into 10 s epochs according to the scheme outlined below and the MI between each EEG-ECG channel pair estimated via the 'mi_gg' function.

To assess the extent to which coupling dynamics were driven by top-down (brain-to-heart) or bottom-up (heart-to-brain) connectivity, paired signals were offset from one another such that one signal corresponded to the 10 s preprobe epoch while the other preceded this period by some arbitrary time constant. For brain-to-heart coupling, cardiac phase estimates lagged the EEG phase series by the following 12 log-spaced intervals: 159 ms, 204 ms, 262 ms, 337 ms, 433 ms, 557 ms, 715 ms, 920 ms, 1182 ms, 1520 ms, 1954 ms, 2512 ms. For heart-to-brain coupling, EEG phase estimates lagged the cardiac phase series by the following 12 log-spaced intervals: 100 ms, 126 ms, 159 ms, 200 ms, 251 ms, 316 ms, 398 ms, 501 ms, 631 ms, 794 ms, 1000 ms, 1259 ms. Longer latencies were favoured when estimating fluctuations in brain-to-heart coupling due to time delays in the modulation of cardiac pacing incurred at the sino-atrial node [132]. MI statistics were averaged across time-lags to provide an estimate of brain-to-heart ($MI_{BRAIN-HEART}$) and heart-to-brain ($MI_{HEART-BRAIN}$) coupling for each channel x frequency combination in each preprobe epoch.

bioRxiv preprint doi: https://doi.org/10.1101/2024.06.21.599851; this version posted May 17, 2025. The copyright holder for this preprint (which was not certified by peer review) is the author/funder, who has granted bioRxiv a license to display the preprint in perpetuity. It is made available under aCC-BY-NC 4.0 International license.

Statistical analysis

Statistical analysis of behavioural, pupillometric, and cardiac parameters was performed in *R* (v4.2.1 [2022-06-23 ucrt] [133]) using the *RStudio Desktop* IDE (v2022.07.2+576 [134]) in conjunction with the 'tidyverse' package (v1.3.2 [135]). These analyses were conducted under a generalised additive mixed-effects model framework (a semiparametric extension of linear mixed-effects modelling) implemented via the 'mcgv' package (v1.8-40 [136,137]). Model diagnostics were assessed using functions from the 'itsadug' (v2.4.1 [138]) and 'mgcViz' (v0.1.9 [139]) packages; model visualisation was accomplished with the aid of 'cowplot' (v1.1.1 [140]), 'emmeans' (v1.7.5 [141]), 'ggeffects' (v1.1.2 [142]), and 'ggh4x' (v0.2.8 [143]).

All models were fitted using restricted maximum likelihood via the 'gam' function. Attentional state reports were modelled as unordered categorical data using multinomial logistic regression; vigilance reports were modelled as ordered categorical data. Hit and false alarm rates were modelled using the logit-linked beta distribution; response speed variability was modelled using the log-linked tweedie distribution. All other models assumed Gaussian-distributed errors. Dependent variables were regressed onto a covariate encoding stimulus type (Digit vs. Face) and the independent variable of interest (except in the case of IBIμ and IBIc_v, which were included together as orthogonal predictors). When models were fitted to data from Melbourne and Paris, site of data collection was included as an additional covariate. Models were additionally equipped with a by-participant factor smooth on probe number to control for time-on-task and reduce the temporal autocorrelation of residuals (see Baayen and colleagues [144]).

Brain-heart connectivity measures were analysed in MATLAB R2022a (v9.12.0.1884302) using a mass linear mixed-effects modelling approach [145]. Linear mixed-effects models including fixed effects of attentional state or vigilance level, covariates for stimulus type and site, and random intercepts for participant identity, were fitted to HEP or MI estimates using maximum likelihood estimation ('fitlme'). HEP models additionally included covariates for IBIμ and IBIc_v. Marginal estimates for each channel x time-point (HEP) or channel x frequency-band (MI) combination were extracted for subsequent mass univariate linear regression analysis ('lmeEEG_regress'). T-values obtained from these regression models were then compared against those generated from 1000 random permutations of the design matrix ('lmeEEG_permutations') using threshold-free cluster enhancement [146,147] (TFCE; implemented via 'lmeEEG_TFCE'). For the HEP analysis, the time-window of interest ranged [200, 600] ms post R-peak.

bioRxiv preprint doi: https://doi.org/10.1101/2024.06.21.599851; this version posted May 17, 2025. The copyright holder for this preprint (which was not certified by peer review) is the author/funder, who has granted bioRxiv a license to display the preprint in perpetuity. It is made available under aCC-BY-NC 4.0 International license.

As a further precaution against the possibility of spurious results marring our HEP analysis, t-values from significant clusters resolved using TFCE were compared to those generated by replicating the mass univariate analysis on surrogate R-peaks [73,148]. We created surrogate R-peaks by randomly permuting each IBI time-series within the 40 s period preceding each set of thought probes and time-locking our HEP analysis to the latencies implied by the reordered IBIs. This procedure was repeated 100 times to build a null distribution of surrogate t-values that reflected differences in EEG fluctuations that were not systematically related to the heartbeat (since the temporal dependence between EEG responses and cardiac systole had been broken) [149]. Observed t-values that failed to exceed the permutation threshold defining a Monte Carlo p-value < .05 (two-tailed) were masked as non-significant.

Data and code availability

The datasets analysed in this report can be accessed from the Open Science Framework platform (Melbourne: https://osf.io/ey3ca/ [150]; Paris: https://osf.io/v9xsw/ [151]). The code used to perform these analyses is available on GitHub: https://github.com/corcorana/WIM_HB [152].

Results

Prevalence of disengaged states and impact on behavioural performance

Similar to the original analysis reported by Andrillon and colleagues [107], participants tested in Melbourne declared being on-task an average 49% of times probed; mind-wandering and mind-blanking were reported an average 39% and 13% of the time, respectively. A comparable profile of responses was observed in the Paris dataset (ON: 56% probes; MW: 30% probes; MB: 14% probes). These findings are broadly consistent with previous experience-sampling research examining on-task vs. disengaged states [153]. One participant in the Melbourne dataset and three in the Paris dataset reported being on-task throughout the session; hence, these individuals were excluded from analyses involving attentional state reports (but were retained otherwise).

Mind-wandering and mind-blanking states were reported more frequently with time-on-task in both datasets (MW_{MEL}: $\beta = 0.46$, s.e. = 0.06, $z = 7.16$, $p < .001$; MW_{PAR}: $\beta = 0.32$, s.e. = 0.05, $z = 6.33$, $p < .001$; MB_{MEL}: $\beta = 0.35$, s.e. = 0.09, $z = 3.79$, $p < .001$; MB_{PAR}: $\beta = 0.15$, s.e. = 0.07, $z = 2.27$, $p = .024$). They were also associated with lower vigilance ratings (MW_{MEL}: $\beta =$

bioRxiv preprint doi: https://doi.org/10.1101/2024.06.21.599851; this version posted May 17, 2025. The copyright holder for this preprint (which was not certified by peer review) is the author/funder, who has granted bioRxiv a license to display the preprint in perpetuity. It is made available under aCC-BY-NC 4.0 International license.

-0.87, s.e. = 0.11, z = 7.64, p < .001; MW_{PAR}: β = -0.83, s.e. = 0.08, z = 10.95, p < .001; MB_{MEL}: β = -1.28, s.e. = 0.17, z = 7.66, p < .001; MB_{PAR}: β = -1.36, s.e. = 0.11, z = 12.28, p < .001) and smaller pupil size (MW_{MEL}: β= -0.34, s.e. = 0.11, z = 3.24,, p = .001; MW_{PAR}: β= -0.25, s.e. = 0.08, z = 3.16., p = .002; MB_{MEL}: β = -0.54, s.e. = 0.14, z = 3.79, p < .001; MB_{PAR}: β = -0.50, s.e. = 0.11, z = 4.61, p < .001), than on-task reports.

Using signal detection theory [154,155], we calculated measures of sensitivity (*d'*) and response bias (*c*) in 10 s trial epochs preceding thought probes. Sensitivity was significantly decreased in epochs preceding off-task reports (MW_{MEL}: β = -0.26, s.e. = 0.04, t = 5.92, p < .001; MW_{PAR}: β= -0.34, s.e. = 0.04, z = 8.94., p < .001; MB_{MEL}: β = -0.32, s.e. = 0.06, t = 5.13, p < .001; MB_{PAR}: β = -0.46, s.e. = 0.05, z = 9.27, p < .001) as compared to on-task reports. Bias was significantly increased (i.e., increased tendency to produce false alarms) in epochs preceding mind-wandering (MW_{MEL}: β = 0.09, s.e. = 0.02, t = 4.21, p < .001; MW_{PAR}: β = 0.06, s.e. = 0.02, t = 3.29, p = .001), but not mind-blanking (MB_{MEL}: β = 0.02, s.e. = 0.03, t = 0.65, p = .516; MB_{PAR}: β = 0, s.e. = 0.02, t = 0.02, p = .982).

Mean response speed (1/Response Time; RSμ) on Go trials preceding mind-wandering reports did not significantly differ from on-task reports (MW_{MEL}: β = 0, s.e. = 0.01, t = 0.03, p = .977; MW_{PAR}: β = -0.02, s.e. = 0.02, t = 1.03, p = .304). However, mind-blanking was associated with significant response slowing (MB_{MEL}: β = -0.05, s.e. = 0.02, t = 2.63, p = .009; MB_{PAR}: β = -0.04, s.e. = 0.02, t = 2.00, p = .046). Response speed variability (RSc_v) was significantly increased prior to both mind-wandering (MW_{MEL}: β = 0.06, s.e. = 0.02, t = 2.25, p = .025; MW_{PAR}: β = 0.05, s.e. = 0.02, t = 2.03, p = .021) and mind-blanking (MB_{MEL}: β = 0.11, s.e. = 0.04, t = 3.02, p = .003; MB_{PAR}: β = 0.10, s.e. = 0.03, t = 3.35, p < .001) relative to on-task epochs. See Table 1 for summary statistics.

Overall, these results confirm previous reports from overlapping and different datasets [87,88,101,156] showing distinct signatures of mind-wandering and mind-blanking on cognitive performance. Given the remarkable consistency of the findings observed across the Melbourne and Paris datasets, the remainder of this report focuses on a single set of results obtained from analysis of the combined dataset (please note, site of data collection was included as a covariate within each model).

bioRxiv preprint doi: https://doi.org/10.1101/2024.06.21.599851; this version posted May 17, 2025. The copyright holder for this preprint (which was not certified by peer review) is the author/funder, who has granted bioRxiv a license to display the preprint in perpetuity. It is made available under aCC-BY-NC 4.0 International license.

Site	Melbourne			Paris		
State	ON	MW	MB	ON	MW	MB
d'	1.67 (0.66)	1.44 (0.76)	1.36 (0.84)	1.52 (0.75)	1.15 (0.82)	0.99 (0.88)
c	0.52 (0.34)	0.60 (0.36)	0.52 (0.34)	0.51 (0.34)	0.57 (0.40)	0.48 (0.47)
RSμ	1.86 (0.31)	1.93 (0.33)	1.82 (0.30)	2.27 (0.35)	2.29 (0.35)	2.20 (0.36)
RSc_v	0.17 (0.08)	0.18 (0.09)	0.20 (0.09)	0.17 (0.07)	0.18 (0.08)	0.20 (0.08)

Table 1. Summary statistics for behavioural measures calculated under each attentional state for both datasets.

Mean (standard deviation) for sensitivity (d'), bias (c), response speed (RSμ) and coefficient of variation (RSc_v) measures calculated within each attentional state response category for both the Melbourne and Paris datasets. ON = on-task; MW = mind-wandering; MB = mind-blanking.

Cardiac measures afford complementary information about arousal, attentional, and behavioural states

Having confirmed the expected differences in behavioural and pupillometric measures across attentional and vigilance state reports, we next sought to examine whether cardiac parameters derived from epochs preceding thought probes predict attentional and arousal states and their behavioural correlates.

Mixed-effects modelling revealed a positive association between mean interbeat interval (IBIμ) and off-task attentional states: increased IBIμ (i.e., lower heart-rate) significantly increased the propensity to report both mind-wandering ($\beta = 0.31$, s.e. = 0.07, $z = 4.22$, $p < .001$) and mind-blanking ($\beta = 0.70$, s.e. = 0.10, $z = 7.08$, $p < .001$). Moreover, increased IBIμ was associated with lower alertness ratings ($\beta = -0.35$, s.e. = 0.07, $z = 4.89$, $p < .001$) and smaller pupil size ($\beta = -0.21$, s.e. = 0.02, $z = 11.42$, $p < .001$), consistent with a global shift towards parasympathetic dominance and hypoarousal [157,158]. HRV (interbeat interval coefficient of variation; IBIc_v) did not significantly predict mind-blanking ($\beta = 0.12$, s.e. = 0.08, $z = 1.57$, $p = .117$) nor vigilance level ($\beta = -0.05$, s.e. = 0.05, $z = 0.95$, $p = .035$), but did predict increases

bioRxiv preprint doi: https://doi.org/10.1101/2024.06.21.599851; this version posted May 17, 2025. The copyright holder for this preprint (which was not certified by peer review) is the author/funder, who has granted bioRxiv a license to display the preprint in perpetuity. It is made available under aCC-BY-NC 4.0 International license.

in mind-wandering (β = 0.10, s.e. = 0.05, z = 1.99, p = .046) and pupil dilation (β = 0.07, s.e. = 0.01, z = 5.64, p < .001; see Figure 2).

Turning next to behavioural performance during the SART, a negative association was observed between IBIμ and *d'* (β = -0.05, s.e. = 0.02, t = 2.40, p = .027). This effect was driven by a reduction in hit rate as IBIμ increased (β = -0.16, s.e. = 0.02, t = 8.30, p < .001). Increased IBIμ was also associated with decreased *c* (β = -0.06, s.e. = 0.01, z = 6.03, p < .001), RSμ (β = -0.02, s.e. = 0.01, z = 3.11, p = .002), and increased RSc_v (β = 0.04, s.e. = 0.01, z = 3.59, p < .001), but did not predict false alarm rate (β = -0.03, s.e. = 0.02, z = 1.57, p = .117). IBIc_v was likewise negatively associated with *d'* (β = -0.06, s.e. = 0.02, t = 3.84, p < .001); however, this effect was driven by an increase in false alarm rate (β = 0.07, s.e. = 0.02, z = 4.05, p < .001). IBIc_v also predicted increases in *c* (β = 0.02, s.e. = 0.01, t = 2.82, p = .005) and RSμ (β = 0.01, s.e. = 0.01, t = 2.46, p = .014), but not hit rate (β = 0, s.e. = 0.01, z = 0.11, p = .910) or RSc_v (β = 0.01, s.e. = 0.01, z = 0.58, p = .559).

bioRxiv preprint doi: https://doi.org/10.1101/2024.06.21.599851; this version posted May 17, 2025. The copyright holder for this preprint (which was not certified by peer review) is the author/funder, who has granted bioRxiv a license to display the preprint in perpetuity. It is made available under aCC-BY-NC 4.0 International license.

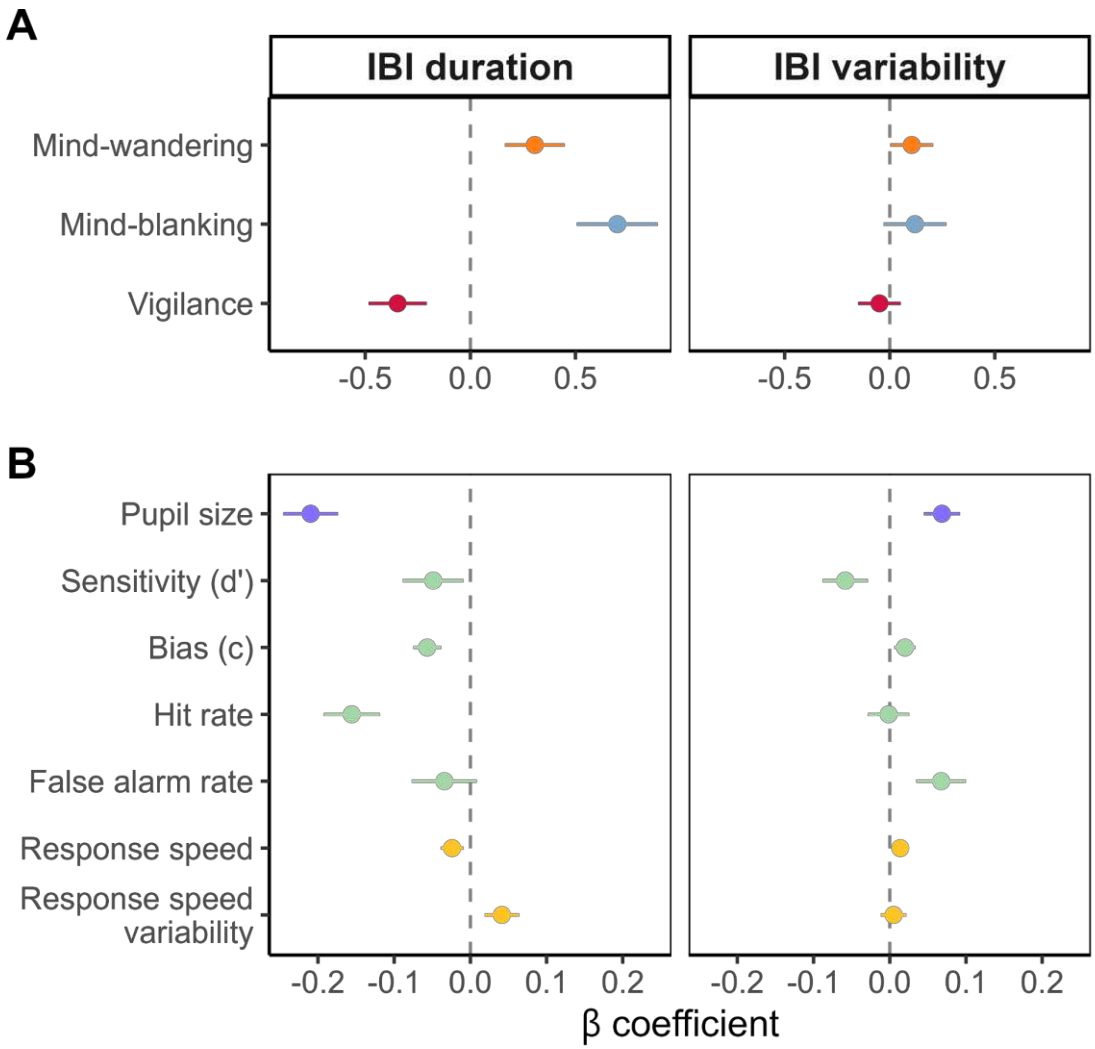

Figure 2: Summary of modelled relationships between cardiac parameters and attentional, arousal, and behavioural state variables

A: Estimated effect of a z-unit increase in mean interbeat interval (IBI) duration (left) and coefficient of variation (right) on subjective reports of attentional state and vigilance level. Mind-wandering and mind-blanking coefficients encode differences relative to the on-task state, where a positive coefficient indicates an increase in the likeliness of reporting mind-wandering/mind-blanking (per z-unit increase in IBI duration/variability). B: Estimated effect of a z-unit increase in mean IBI duration (left) and coefficient of variation (right) on mean pupil size, signal detection theoretic and response speed measures. Error bars represent 95% confidence intervals. All estimates derived from 10 s epochs immediately preceding thought probes.

bioRxiv preprint doi: https://doi.org/10.1101/2024.06.21.599851; this version posted May 17, 2025. The copyright holder for this preprint (which was not certified by peer review) is the author/funder, who has granted bioRxiv a license to display the preprint in perpetuity. It is made available under aCC-BY-NC 4.0 International license.

Error-related cardiac deceleration does not account for differences across attentional states

Since mind-wandering and mind-blanking reports were associated with decrements in SART performance, we considered whether the differences we observed in IBIμ between task-focused and disengaged states could be attributed to increased rates of erroneous responding during periods of task disengagement. IBIs are known to lengthen in response to performance errors even in the absence of explicit feedback [46]; hence, increased false alarm rates might be expected to elicit more frequent bouts of cardiac deceleration, thereby lowering IBIμ.

To assess this possibility, we identified all NoGo trials occurring within each 10 s preprobe epoch and extracted the z-scored duration of the 3 IBIs preceding and following the interval in which the NoGo stimulus was presented (IBIs following the NoGo stimulus were discarded if they were interrupted by thought probes). IBI duration was then regressed onto factors encoding the ordinal position of each IBI relative to NoGo trial onset, behavioural response category (CR vs. FA), and subsequent attentional state report (ON vs. MW vs. MB), along with interactions between these factors. Covariates for stimulus type (Digit vs. Face), site of data collection (Melbourne vs. Paris), and random factor smooths for probe and participant identity were also included, consistent with the models reported in the previous two sections.

Model predictions are visualised in Figure 3. As expected, the main effect of IBI order was significant ($F(6) = 27.82$, $p < .001$); the first IBI following NoGo trial onset was significantly longer than both the preceding interval (IBI_{+1}-$IBI_0 = 0.15$, se = 0.02, $t = 7.57$, $p_{adj} < .001$) and the subsequent interval (IBI_{+1}-$IBI_{+2} = 0.12$, s.e. = 0.02, $t = 5.75$, $p_{adj} < .001$), consistent with the occurrence of a cardiac deceleration response to salient (i.e., rare or task-relevant) stimuli. The main effect of attentional state was also significant ($F(2) = 51.71$, $p < .001$), consistent with the observation that IBIs tend to be longer on average in epochs preceding mind-wandering ($\beta = 0.06$, s.e. = 0.02, $t = 3.85$, $p < .001$) and mind-blanking reports ($\beta = 0.22$, s.e. = 0.02, $t = 10.13$, $p < .001$) than on-task reports. Interestingly, IBIs tended to be longer in sequences spanning a correct rejection ($F(1) = 23.95$, $p < .001$), irrespective of the subsequent attentional state report. This observation is consistent with our finding that increased IBIμ predicted decreased response bias. Moreover, false alarms did not generate more profound cardiac decelerations than those observed when responses to NoGo trials were withheld. Together, these observations indicate that the increase in IBIμ associated

bioRxiv preprint doi: https://doi.org/10.1101/2024.06.21.599851; this version posted May 17, 2025. The copyright holder for this preprint (which was not certified by peer review) is the author/funder, who has granted bioRxiv a license to display the preprint in perpetuity. It is made available under aCC-BY-NC 4.0 International license.

with mind-wandering and mind-blanking was unlikely to be driven by higher error rates of erroneous responding.

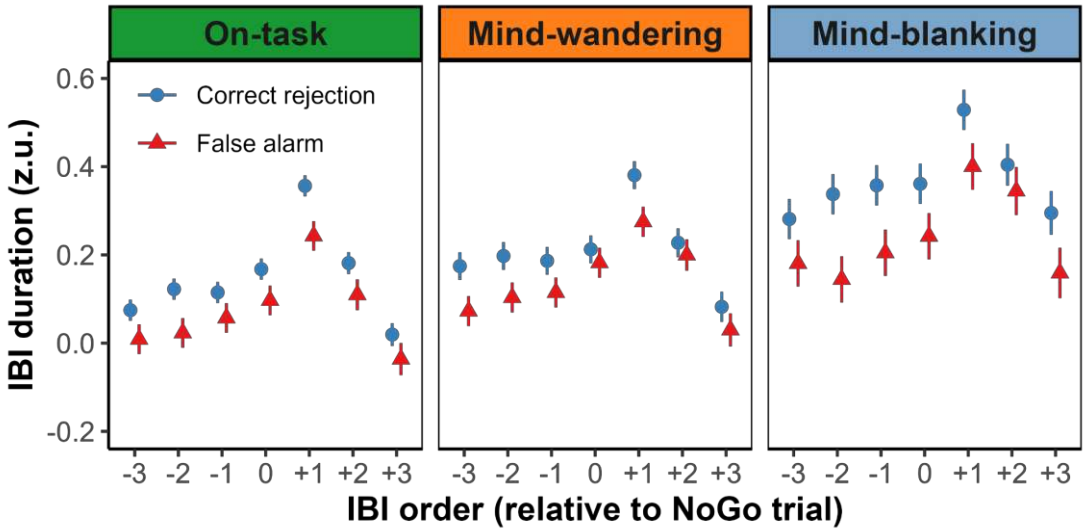

Figure 3: Interbeat intervals show similar NoGo response profiles across attentional states.

Estimated marginal mean IBI duration (z-units) for IBI sequences centred on IBIs containing the onset of NoGo trials within the 10 s preprobe epoch. IBI sequences featuring NoGo trials that elicited correct rejections are denoted as blue circles; those associated with false alarms (errors of commission) are denoted as red triangles. Estimates are further faceted according to the attentional state that was reported following the epoch. Error bars represent the standard error of the mean (SEM).

Heartbeat-evoked potentials are modulated by mind-wandering

To assess whether task-disengagement is accompanied by altered interoceptive processing of cardiac signals, we investigated how neural responses time-locked to the heartbeat (i.e., heartbeat-evoked potentials; HEPs) varied as a function of attentional state and vigilance level reports. HEPs were estimated on the participant-level for R-peaks captured within the 10 s epoch preceding each set of thought probes. ERPs were also computed for the corresponding ECG signal. Linear mixed-effects models were fitted for each channel x time-point combination in order to examine the impact of attentional states and vigilance ratings on the time course of the ECG-ERP (Figure 4A) and HEP (Figure 4B). To correct for multiple comparisons, we

bioRxiv preprint doi: https://doi.org/10.1101/2024.06.21.599851; this version posted May 17, 2025. The copyright holder for this preprint (which was not certified by peer review) is the author/funder, who has granted bioRxiv a license to display the preprint in perpetuity. It is made available under aCC-BY-NC 4.0 International license.

applied a cluster permutation approach across all channels for the time-window of interest (200–600 ms post R-peak). As an additional safeguard against spurious results, t-values from significant clusters were checked against those derived from a set of surrogate R-peak latencies (see Methods for further details).

Following these procedures, we found two significant clusters indicative of modulations of the HEP during epochs associated with mind-wandering (relative to those observed prior to on-task reports). The first cluster spanned [380, 500] ms, and included frontal and left-parietal scalp regions; the second cluster spanned [540, 596] ms, and evinced a more lateralised topography (Figure 4C). These fluctuations were not accompanied by corresponding differences in the time-course of ECG-ERP (Figure 4A), suggesting that late modulation of the HEP during mind-wandering states derived from genuine differences in cortical responses to the heartbeat. No significant clusters were identified when HEPs preceding mind-blanking reports were contrasted with those preceding on-task reports, nor when HEPs were compared across different vigilance levels (see Figure 4B for representative ERPs).

bioRxiv preprint doi: https://doi.org/10.1101/2024.06.21.599851; this version posted May 17, 2025. The copyright holder for this preprint (which was not certified by peer review) is the author/funder, who has granted bioRxiv a license to display the preprint in perpetuity. It is made available under aCC-BY-NC 4.0 International license.

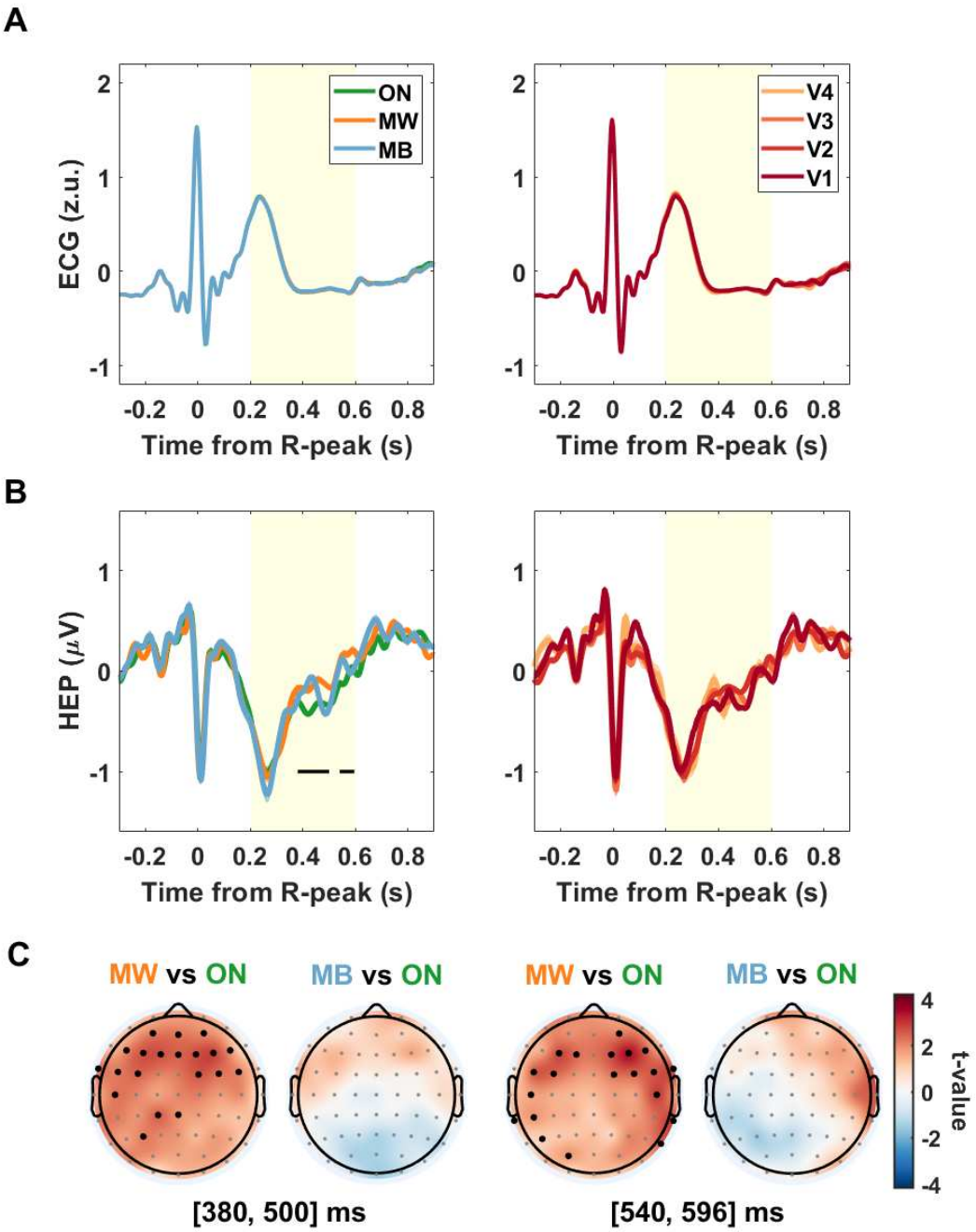

Figure 4: Heartbeat-evoked potentials are modulated by attentional state but not vigilance level.

A: Event-related potential (ERP) of the electrocardiogram (ECG) averaged across individuals for the different attentional states (left; ON = on-task, MW = mind-wandering, MB = mind-blanking) and vigilance levels (right; V1 = extreme sleepiness, V4 = extreme alertness). B: Heartbeat-evoked potential (HEP) for the different attentional states (left) and vigilance levels (right). Each HEP was averaged across the 11 channels that revealed significant differences between mind-wandering and on-task states (MW vs. ON) in both the earlier and later clusters.

bioRxiv preprint doi: https://doi.org/10.1101/2024.06.21.599851; this version posted May 17, 2025. The copyright holder for this preprint (which was not certified by peer review) is the author/funder, who has granted bioRxiv a license to display the preprint in perpetuity. It is made available under aCC-BY-NC 4.0 International license.

For both A and B, shaded areas denote the standard error of the mean (SEM); yellow shading indicates time-window of interest; horizontal black bars indicate the timespan of significant clusters in the MW vs. ON contrast ($p_{cluster}$< 0.05, corrected for surrogate t-values; see Methods). C: Topographic representation of t-values from the attentional state contrasts averaged over the timespan of the two significant clusters marked in B. Black dots indicate electrodes that exceeded both the permutation-test and surrogate t-value thresholds for cluster membership (see Methods).

Brain-heart dynamics decouple with task-disengagement and fatigue

Finally, we sought to complement our analysis of cortical responses to the heartbeat in the time-domain by investigating how the evolution of cardiac and brain activity in the frequency-domain varies across attentional states and vigilance levels. To this end, we estimated the mutual information (MI) shared between the instantaneous phases of the dominant heart frequency and low-frequency EEG signals within each preprobe epoch. Computing this measure at various time-lags enabled us evaluate how MI changed depending on which time-series led the other, whereby changes in coupling strength were assumed to be driven by the earlier-occurring signal (e.g., when the EEG preceded the ECG signal [BRAIN-HEART], increased MI was interpreted as evidence of increased top-down cardiac regulation; when the ECG preceded the EEG signal [HEART-BRAIN], increased MI was interpreted as evidence of increased interoceptive processing of bottom-up input). MI estimates were averaged across time-lags within each set of directionalities, and subjected to a similar mixed-effects modelling and cluster permutation procedure to that employed in our HEP analysis (see Methods for further details).

Very similar profiles of time-averaged MI were resolved across frequencies in both the brain-to-heart and heart-to-brain directionality (Figure 5A). MI tended to be highest for the lowest two EEG frequency bands included in the analysis (0.8–1.8 Hz), which correspond to the lower half of the canonical delta band (1–4 Hz). MI declined by approximately an order of magnitude in the transition from (high) delta (1.8–3.9 Hz) to alpha band activity (8.5–12.8 Hz), and remained low when estimated for the (low) beta band (12.7–19.0 Hz).

bioRxiv preprint doi: https://doi.org/10.1101/2024.06.21.599851; this version posted May 17, 2025. The copyright holder for this preprint (which was not certified by peer review) is the author/funder, who has granted bioRxiv a license to display the preprint in perpetuity. It is made available under aCC-BY-NC 4.0 International license.

Focusing on differences in $MI_{BRAIN-HEART}$ across attentional states (Figure 5B), our analysis revealed no significant changes in brain-to-heart phase coupling between on-task and mind-wandering epochs. By contrast, mind-blanking epochs revealed significant decreases in $MI_{BRAIN-HEART}$ estimates relative to on-task epochs. This effect was evident to varying degrees across all included frequency bins, but most spatially extensive in the bands spanning [1.8, 3.9] Hz. Significant clusters were also resolved at higher frequencies, including a left-temporal and right fronto-parietal cluster in the [5.8, 8.6] Hz band, and a predominantly frontal cluster in the [8.5, 12.8] Hz band. Repeating this analysis on $MI_{HEART-BRAIN}$ contrasts revealed a qualitatively similar pattern of results, albeit with a few additional significant effects. A significant left-parietal cluster was resolved for mind-wandering epochs in the [1.8, 2.6] Hz band. Mind-blanking epochs evinced more extensive left- and right-sided clusters in the [1.2, 1.8] Hz band as compared to the $MI_{BRAIN-HEART}$ contrast for the same band. Large clusters were again resolved in the [1.8, 3.9] Hz range, while broadly similar effects were observed in the higher frequency bands.

Turning next to vigilance reports, we compared how brain-heart phase coupling fluctuated relative to states of ‘extreme alertness’ (V4; Figure 5C). We found no significant effects for either directionality when contrasting MI estimates from epochs preceding V3 reports to those preceding V4; however, lower levels of alertness were associated with significant decreases in brain-to-heart phase coupling. Moderate sleepiness (V2) was associated with significant decreases in $MI_{BRAIN-HEART}$ and $MI_{HEART-BRAIN}$ across 2 frontal channels in the [1.8, 2.6] Hz band; $MI_{HEART-BRAIN}$ was also significantly reduced across a small number of left-parietal channels in the [2.6, 5.8 Hz] range. Extreme sleepiness (V1) was accompanied by more spatially extensive reductions in brain-heart phase coupling, where the largest clusters spanned the [1.2, 3.9] Hz range. Clusters tended to include more frontal electrode channels in the brain-to-heart analysis than the corresponding heart-to-brain contrasts. Unlike the mind-blanking effects, few significant effects were observed for either directionality in frequencies above 5.8 Hz.

bioRxiv preprint doi: https://doi.org/10.1101/2024.06.21.599851; this version posted May 17, 2025. The copyright holder for this preprint (which was not certified by peer review) is the author/funder, who has granted bioRxiv a license to display the preprint in perpetuity. It is made available under aCC-BY-NC 4.0 International license.

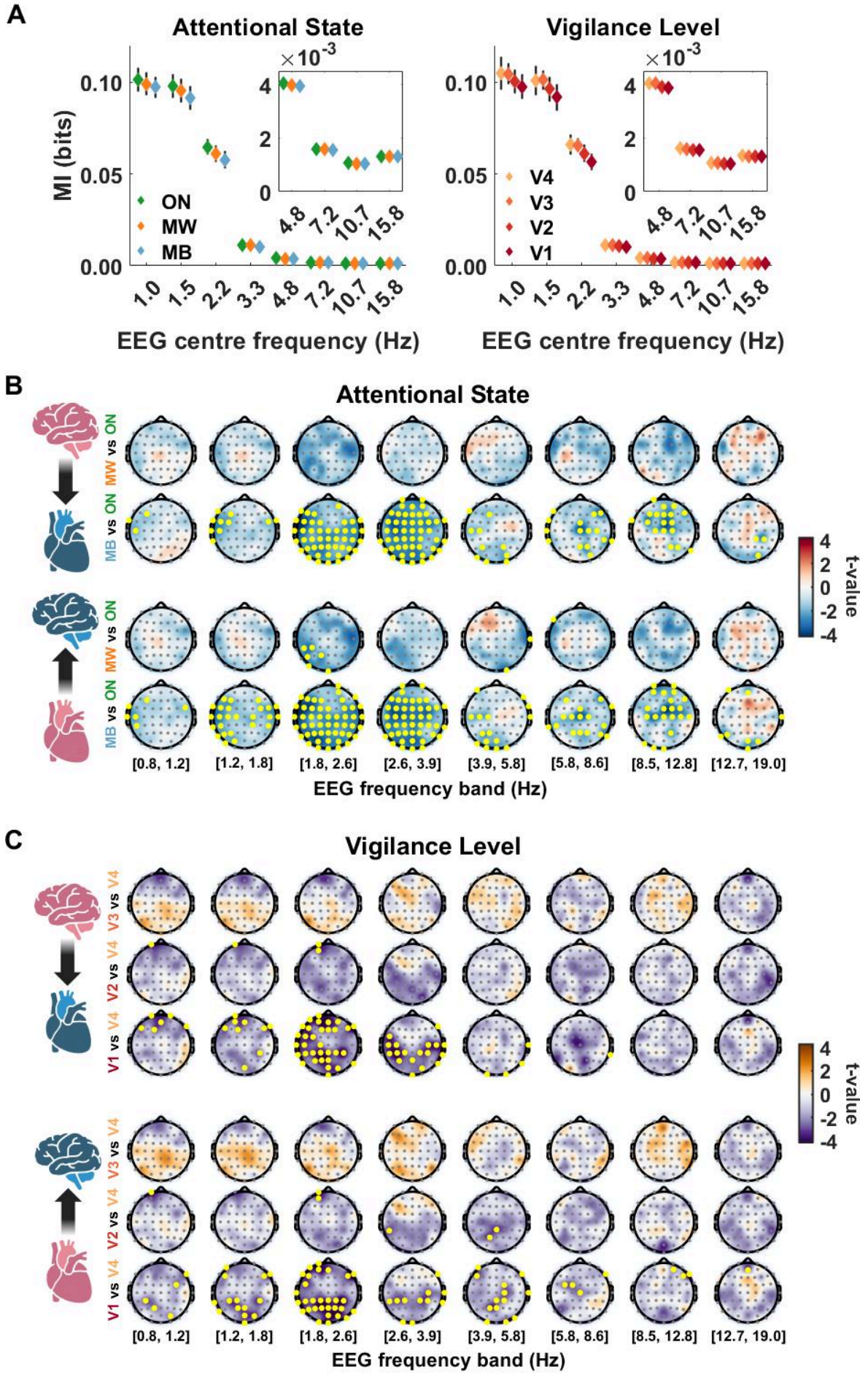

bioRxiv preprint doi: https://doi.org/10.1101/2024.06.21.599851; this version posted May 17, 2025. The copyright holder for this preprint (which was not certified by peer review) is the author/funder, who has granted bioRxiv a license to display the preprint in perpetuity. It is made available under aCC-BY-NC 4.0 International license.

Figure 5: Phase coupling between brain and heart signals decreases with task-disengagement and sleepiness.

A: Mutual information (MI) profiles averaged across channels and directionalities for attentional state (left; ON = on-task, MW = mind-wandering, MB = mind-blanking) and vigilance level (right; V1 = extreme sleepiness, V4 = extreme alertness). Error bars indicate the standard deviation of channel-wise MI estimates. Inset panels depict averaged MI estimates for higher frequency EEG bands at increased magnification. B: Topographic representation of t-values from the attentional state contrasts for each frequency band and directionality (brain-to-heart top; heart-to-brain bottom). Yellow dots indicate electrodes that exceeded the permutation test t-value threshold. C: Topographic representation of t-values from the vigilance level contrasts for each frequency band and directionality (brain-to-heart top; heart-to-brain bottom). Yellow dots indicate electrodes that exceeded the permutation test t-value threshold.

Discussion

This study investigated how spontaneous fluctuations of attention are related to subjective and physiological measures of arousal, with specific focus on the brain-heart axis [60]. In summary, we found that task disengagement (i.e., self-reported episodes of mind-wandering or mind-blanking) was characterised by decreases in autonomic arousal, as indicated by reductions in prevailing heart-rate (increased IBIμ) and smaller pupil size. These physiological effects manifested subjectively as increased sleepiness and behaviourally as reduced sensitivity (*d'*) and increased response speed variability (RSc_v). Notably, mind-blanking states were accompanied by more pronounced reductions in heart-rate and response speed (RSμ) than mind-wandering states, thus suggesting that mind-blanking is more likely to occur in the context of hypoarousal. Mind-wandering, by contrast, was characterised by subtler decreases in arousal that were associated with more stereotypic behaviour (increased response bias (*c*), unchanged response speed) and increased heart-rate variability (HRV; as quantified by IBIc_v). Independent of attentional state, greater HRV predicted increased pupil dilation, response bias, response speed, and false alarm rate, suggesting transient fluctuations in heartbeat dynamics afford unique information pertaining to what appear to be impulsive patterns of behaviour.

Having identified how cardiac parameters vary in relation to subjective and objective indices of task focus and disengagement, we next sought to examine whether such fluctuations are

bioRxiv preprint doi: https://doi.org/10.1101/2024.06.21.599851; this version posted May 17, 2025. The copyright holder for this preprint (which was not certified by peer review) is the author/funder, who has granted bioRxiv a license to display the preprint in perpetuity. It is made available under aCC-BY-NC 4.0 International license.

accompanied by distinctive profiles of brain-heart interaction. We turned first to the heartbeat-evoked potential (HEP), an extensively-studied psychophysiological marker of interoceptive processing that has been associated with the focus of attention [67]. This analysis revealed a late modulation of HEPs obtained in the period preceding mind-wandering reports, relative to those obtained prior to on-task reports. No differences were observed between mind-blanking and on-task states, or amongst vigilance levels. Finally, we used a mutual information (MI) based method to estimate phase coupling between brain and heart signal components. This analysis revealed evidence of decreasing MI as participants transitioned from task-focused to disengaged states (especially mind-blanking), and as vigilance level declined. Together, these findings suggest that more profound states of hypoarousal are accompanied by a generalised decoupling of brain and heart dynamics, paralleling the decoupling from exteroceptive inputs reported elsewhere [159].

Our results add to recent evidence that mind-blanking constitutes a low-arousal state distinct from other forms of task disengagement, such as mind-wandering [87,88,159–161]. Our focus on cardiac parameters and measures of brain-heart coupling complement previous reports on the oscillatory, event-related, and information-theoretic EEG signatures of mind-blanking [87,159], demonstrating that these signatures are accompanied by detectable alterations in peripheral electrophysiology and cerebro-peripheral connectivity. They also cohere with recent evidence that mind-blanking reports elicited during task-free resting-state are more prevalent in the context of low-arousal conditions induced by sleep deprivation [88]. While the latter study indicated that the addition of cardiac parameters to EEG measures helped improve the automated classification of mental state reports, our findings isolate the information afforded by particular cardiac parameters with respect to subjective, neurophysiological, and behavioural measures of arousal and attentional state dynamics.

Mean interbeat interval duration (IBIμ) and pupil size provide complementary psychophysiological indices of arousal state that reflect the balance between sympathetic and parasympathetic tone [157,162–164]. Our findings reveal that mind-wandering and mind-blanking episodes are characterised by a progressive shift towards parasympathetic dominance, as indicated by corresponding decreases in prevailing heart-rate and pupil size. This finding is consonant with the reduction in heart-rate observed during the transition from wakefulness to deep sleep [165–168] – a phenomenon tied to arousal state modulation (not just circadian variability) [169,170]. Notably, the effects we report here were observed after statistically controlling for time-on-task (i.e., by specifying factor-smooths on probe number for each participant), indicating that markers of parasympathetic outflow afford specific information (related to cardiac activity) about the transition from on-task through to mind-blanking states

bioRxiv preprint doi: https://doi.org/10.1101/2024.06.21.599851; this version posted May 17, 2025. The copyright holder for this preprint (which was not certified by peer review) is the author/funder, who has granted bioRxiv a license to display the preprint in perpetuity. It is made available under aCC-BY-NC 4.0 International license.

over and above generic effects pertaining to prolonged task performance (e.g., motivational state, mental fatigue, drowsiness, etc.) [171–175].

Intriguingly, short-term heart-rate variability – which is commonly used to measure phasic fluctuations in parasympathetic activity, and which also typically increases in sleep [176–179] – was positively associated with mean pupil size. While this finding might seem counterintuitive given the aforementioned negative association between IBIμ and pupil size, two points need to be borne in mind: First, increases in HRV need not derive from tonic increases in parasympathetic outflow (or a relative shift towards parasympathetic dominance), but may simply reflect altered phasic patterning of parasympathetic discharge [162]. Second, by taking the coefficient of variation as our estimator of HRV (and by controlling for potential confounding from time-on-task effects), we ensured that our measures of heartbeat activity were orthogonal to one another – thus enabling us to uncover different relations between unique components of cardiac control.

Increased pupil-linked arousal in the context of enhanced HRV may be mechanistically explained by phasic input from ascending parasympathetic pathways into the noradrenergic locus coeruleus [180–183], a major neuromodulatory system responsible for the regulation of arousal and task (dis)engagement [184,185]. Given that IBIc_v was also associated with increases in response bias, speed, and false alarm rate (errors of commission), the positive relation we observed between pupil dilation and HRV may be partially explained by error-related orienting [45,186–189], whereby the unexpected occurrence of an erroneous behavioural action (i.e., responding to a NoGo stimulus) precipitated a transient increase in arousal and the reallocation of attentional resources toward the task at hand [190–194]. In turn, the positive association between IBIc_v and mind-wandering (but not mind-blanking) suggests that mind-wandering is associated with episodes of low but unstable arousal. Accordingly, mind-wandering could represent transitions to or from low levels of arousal, whereas mind-blanking would represent stable periods of hypoarousal.

Our analysis of neural responses time-locked to the heartbeat revealed a late modulation of HEPs derived from epochs preceding mind-wandering reports. Since these epochs were also characterised by increases in IBIc_v, one potential explanation for this finding is that neural responses to afferent feedback generated by the heartbeat were amplified as a consequence of greater uncertainty about the precise timing of successive bursts of interoceptive input. Notice, however, that we included IBIc_v as a covariate in our regression-based HEP analysis; hence, we believe this effect to be specific to the context of mind-wandering per se, rather than a generic consequence of the temporal uncertainty induced by more variable (i.e.,

bioRxiv preprint doi: https://doi.org/10.1101/2024.06.21.599851; this version posted May 17, 2025. The copyright holder for this preprint (which was not certified by peer review) is the author/funder, who has granted bioRxiv a license to display the preprint in perpetuity. It is made available under aCC-BY-NC 4.0 International license.

unpredictable) fluctuations in cardio-afferent feedback. Functional brain imaging has revealed the default mode network as an important neural substrate for both mind-wandering [195–197] and parasympathetic activity [61,198], while self-related cognitive processes typically engaged during episodes of mind-wandering have been linked with altered heartbeat-evoked responses [73–75]. Collectively, these findings suggest that increases in HRV and HEP amplitude reflect changes in central autonomic activity that stem from the enhanced functional integration of brain regions involved in the spontaneous generation of task-unrelated thought.

In contrast to the circumscribed findings of our HEP analysis, our MI analysis revealed that phase coupling between evolving heart dynamics and bandpass-filtered EEG time-series progressively decreased as participants transitioned from higher to lower states of arousal. This effect is congruent with evidence of cardiac and low-frequency EEG decoupling during the transition from wakefulness to sleep [199,200]. We observed more widespread decreases in coupling strength in both sensor and frequency space when participants reported mind-blanking (rather than mind-wandering) and – to a lesser extent – extreme sleepiness (as opposed to mild or moderate decreases in alertness). The qualitative similarity evinced by top-down and bottom-up estimates of brain-heart connectivity suggest a functional decoupling of the dynamics expressed by these two systems, rather than a relative shift towards a more predominantly top-down or bottom-up pattern of information exchange. That is, low arousal states appear to be characterised by more intrinsically-driven patterns of cardiac activity, which in turn exert less influence on the evolving dynamics of low-frequency brain activity.

Previous work has suggested that endogenous fluctuations in attentional focus may reflect transient oscillations between external (exteroceptive) vs. internal (interoceptive) states [19,69,72,201,202]. One might therefore anticipate that task disengagement is associated with stronger brain-heart interactions, on the basis that individuals disengaged from their external environment are consequently more engaged with their internal environment. While this account may hold for certain scenarios, our analysis furnishes evidence against a simple switch-like mechanism whereby reduced attention to the external environment necessarily entails increased interoceptive monitoring and physiological regulation. Indeed, it seems plausible to us that effective task engagement should call for a concerted increase in brain-heart integration in addition to the allocation of attentional resources towards task-relevant stimuli, such that evolving physiological dynamics may be deftly calibrated in accordance with evolving situational demands (e.g., transiently increasing heart-rate to meet the metabolic costs of completing a particularly challenging component of a task). During more quiescent states, by contrast, the brain might take the opportunity to disengage from both its external and internal environments, thereby ‘relaxing’ control over the cardiovascular system (or

bioRxiv preprint doi: https://doi.org/10.1101/2024.06.21.599851; this version posted May 17, 2025. The copyright holder for this preprint (which was not certified by peer review) is the author/funder, who has granted bioRxiv a license to display the preprint in perpetuity. It is made available under aCC-BY-NC 4.0 International license.

delegating control to lower-order networks; e.g., those situated within the brainstem and hypothalamus).

In conclusion, this study adds to the growing body of literature distinguishing mind-wandering and mind-blanking as distinctive attentional states. Our analysis of cardiac dynamics in conjunction with subjective, behavioural, and pupillometric measures provides complementary evidence that mind-wandering and mind-blanking arise as arousal levels progressively decrease, likely mediated by global increases in parasympathetic tone. Late modulation of heartbeat-evoked responses further indicates that mind-wandering is associated with amplified cortical processing of interoceptive signals. The allocation of attentional resources towards interoceptive processes that typically unfold outside of awareness may contribute to the subjective experience of losing track of one's surroundings. Furthermore, decreasing arousal is associated with decoupling of brain and heart dynamics, suggesting task disengagement is accompanied by a concomitant disengagement from the monitoring and regulation of internal bodily states. Finally, the link between heartbeat fluctuations, pupil dilation, and impulsive-like behaviour suggests transient bursts of vagal outflow promote phasic increases of arousal, possibly on account of driving input to the noradrenergic locus coeruleus. Together, these findings highlight how the neural processing and regulation of cardiac activity varies as a function of attentional state, shedding light on the way brain-body interactions shape cognitive and behavioural dynamics subtending multiple timescales.

Acknowledgements

Funded by the European Union (ERC, SleepingAwake, 101116748). The research leading to these results has received funding from the national program "Investissements d'avenir" ANR-10- IAIHU-0006. Part of this work was carried out in the CENIR of ICM. AWC and JH acknowledge the support of the Three Springs Foundation. TA was supported by a National Health Medical Research Council Ideas Project (APP1183280) and a Long-Term Fellowship from the Human Frontier Science Programme (LT000362/2018-L). ALC is supported by a scholarship from the Fondation pour la Recherche Médicale (FDT202404018709). We thank Teigane Mackay and Devangna Tangri for data collection in Melbourne, Marie Degrave, Laurent Hugueville, and Amandine Carrie for data collection at the Paris Brain Institute, Naotsugu Tsuchiya and Jennifer Windt for their support to TA at the inception of this line of research, and three anonymous reviewers for their feedback on a previous version of this manuscript.

bioRxiv preprint doi: https://doi.org/10.1101/2024.06.21.599851; this version posted May 17, 2025. The copyright holder for this preprint (which was not certified by peer review) is the author/funder, who has granted bioRxiv a license to display the preprint in perpetuity. It is made available under aCC-BY-NC 4.0 International license.

References

1. Azzalini, D., Rebollo, I. & Tallon-Baudry, C. Visceral signals shape brain dynamics and cognition. *Trends Cogn. Sci.* **23**, 488–509 (2019).
2. Critchley, H. D. & Garfinkel, S. N. The influence of physiological signals on cognition. *Curr. Opin. Behav. Sci.* **19**, 13–18 (2018).
3. Engelen, T., Solcà, M. & Tallon-Baudry, C. Interoceptive rhythms in the brain. *Nat. Neurosci.* **26**, 1670–1684 (2023).
4. Khalsa, S. S. *et al.* Interoception and mental health: A roadmap. *Biol. Psychiatry Cogn. Neurosci. Neuroimaging* **3**, 501–513 (2018).
5. Skora, L. I., Livermore, J. J. A. & Roelofs, K. The functional role of cardiac activity in perception and action. *Neurosci. Biobehav. Rev.* **137**, 104655 (2022).
6. Edwards, L., Ring, C., McIntyre, D., Winer, J. B. & Martin, U. Sensory detection thresholds are modulated across the cardiac cycle: Evidence that cutaneous sensibility is greatest for systolic stimulation. *Psychophysiology* **46**, 252–256 (2009).
7. Motyka, P. *et al.* Interactions between cardiac activity and conscious somatosensory perception. *Psychophysiology* **56**, e13424 (2019).
8. Sandman, C. A., McCanne, T. R., Kaiser, D. N. & Diamond, B. Heart rate and cardiac phase influences on visual perception. *J. Comp. Physiol. Psychol.* **91**, 189–202 (1977).
9. Saxon, S. A. Detection of near threshold signals during four phases of cardiac cycle. *Ala. J. Med. Sci.* **7**, 427–430 (1970).
10. Wilkinson, M., McIntyre, D. & Edwards, L. Electrocutaneous pain thresholds are higher during systole than diastole. *Biol. Psychol.* **94**, 71–73 (2013).
11. Leupin, V. & Britz, J. Interoceptive signals shape the earliest markers and neural pathway to awareness at the visual threshold. *Proc. Natl. Acad. Sci.* **121**, e2311953121 (2024).
12. Fiacconi, C. M., Peter, E. L., Owais, S. & Köhler, S. Knowing by heart: Visceral feedback shapes recognition memory judgments. *J. Exp. Psychol. Gen.* **145**, 559–572

bioRxiv preprint doi: https://doi.org/10.1101/2024.06.21.599851; this version posted May 17, 2025. The copyright holder for this preprint (which was not certified by peer review) is the author/funder, who has granted bioRxiv a license to display the preprint in perpetuity. It is made available under aCC-BY-NC 4.0 International license.

(2016).

13. Garfinkel, S. N. *et al.* What the heart forgets: Cardiac timing influences memory for words and is modulated by metacognition and interoceptive sensitivity. *Psychophysiology* **50**, 505–512 (2013).
14. Garfinkel, S. N. *et al.* Interoceptive cardiac signals selectively enhance fear memories. *J. Exp. Psychol. Gen.* **150**, 1165–1176 (2021).
15. Galvez-Pol, A., McConnell, R. & Kilner, J. M. Active sampling in visual search is coupled to the cardiac cycle. *Cognition* **196**, 104149 (2020).
16. Kunzendorf, S. *et al.* Active information sampling varies across the cardiac cycle. *Psychophysiology* **56**, e13322 (2019).
17. Palser, E. R., Glass, J., Fotopoulou, A. & Kilner, J. M. Relationship between cardiac cycle and the timing of actions during action execution and observation. *Cognition* **217**, 104907 (2021).
18. Corcoran, A. W., Macefield, V. G. & Hohwy, J. Be still my heart: Cardiac regulation as a mode of uncertainty reduction. *Psychon. Bull. Rev.* **28**, 1211–1223 (2021).
19. Al, E. *et al.* Heart-brain interactions shape somatosensory perception and evoked potentials. *Proc. Natl. Acad. Sci.* **117**, 10575–10584 (2020).
20. Al, E., Iliopoulos, F., Nikulin, V. V. & Villringer, A. Heartbeat and somatosensory perception. *NeuroImage* **238**, 118247 (2021).
21. Park, H.-D., Correia, S., Ducorps, A. & Tallon-Baudry, C. Spontaneous fluctuations in neural responses to heartbeats predict visual detection. *Nat. Neurosci.* **17**, 612–618 (2014).
22. Fló, E. *et al.* Predicting attentional focus: Heartbeat-evoked responses and brain dynamics during interoceptive and exteroceptive processing. *PNAS Nexus* **3**, pgae531 (2024).
23. Petzschner, F. H. *et al.* Focus of attention modulates the heartbeat evoked potential. *NeuroImage* **186**, 595–606 (2019).
24. Zaccaro, A. *et al.* Attention to cardiac sensations enhances the heartbeat-evoked

bioRxiv preprint doi: https://doi.org/10.1101/2024.06.21.599851; this version posted May 17, 2025. The copyright holder for this preprint (which was not certified by peer review) is the author/funder, who has granted bioRxiv a license to display the preprint in perpetuity. It is made available under aCC-BY-NC 4.0 International license.

potential during exhalation. *iScience* **27**, 109586 (2024).

25. Azzalini, D., Buot, A., Palminteri, S. & Tallon-Baudry, C. Responses to heartbeats in ventromedial prefrontal cortex contribute to subjective preference-based decisions. *J. Neurosci.* **41**, 5102–5114 (2021).
26. Candia-Rivera, D. *et al.* Neural responses to heartbeats detect residual signs of consciousness during resting state in postcomatose patients. *J. Neurosci.* **41**, 5251–5262 (2021).
27. Candia-Rivera, D. *et al.* Conscious processing of global and local auditory irregularities causes differentiated heartbeat-evoked responses. *eLife* **12**, e75352 (2023).
28. Porges, S. W. Autonomic regulation and attention. in *Attention and information processing in infants and adults: Perspectives from human and animal research* (eds. Campbell, B. A., Hayne, H. & Richardson, R.) 201–223 (New York and London: Psychology Press, 1992).
29. Jennings, J. R. Bodily changes during attention. in *Psychophysiology: Systems, Processes, and Applications* (eds. Coles, M. G. H., Donchin, E. & Porges, S. W.) 268–289 (New York & London: Guilford Press, 1986).
30. Öhman, A., Hamm, A. & Hugdahl, K. Cognition and the autonomic nervous system: Orienting, anticipation, and conditioning. in *Handbook of psychophysiology* (eds. Cacioppo, J. T., Tassinary, L. G. & Berntson, G. G.) 533–575 (Cambridge: Cambridge University Press, 2000).
31. Darrow, C. W. Differences in the physiological reactions to sensory and ideational stimuli. *Psychol. Bull.* **26**, 185–201 (1929).
32. Malmo, R. B. Activation: A neuropsychological dimension. *Psychol. Rev.* **66**, 367–386 (1959).
33. Graham, F. K. & Clifton, R. K. Heart-rate change as a component of the orienting response. *Psychol. Bull.* **65**, 306–320 (1966).
34. Graham, F. K. Distinguishing among orienting, defense, and startle reflexes. in *The orienting reflex in humans* (eds. Kimmel, H. D., van Olst, E. H. & Orlebeke, J. F.) 137–

bioRxiv preprint doi: https://doi.org/10.1101/2024.06.21.599851; this version posted May 17, 2025. The copyright holder for this preprint (which was not certified by peer review) is the author/funder, who has granted bioRxiv a license to display the preprint in perpetuity. It is made available under aCC-BY-NC 4.0 International license.

167 (Hillsdale, N.J.: Lawrence Erlbaum Associates, 1979).

35. Libby, W. L., Jr., Lacey, B. C. & Lacey, J. I. Pupillary and cardiac activity during visual attention. *Psychophysiology* **10**, 270–294 (1973).

36. Bradley, M. M., Codispoti, M., Cuthbert, B. N. & Lang, P. J. Emotion and motivation I: Defensive and appetitive reactions in picture processing. *Emotion* **1**, 276–298 (2001).

37. Lacey, J. I. Psychophysiological approaches to the evaluation of psychotherapeutic process and outcome. in *Research in Psychotherapy* (eds. Rubinstein, E. A. & Parloff, M. B.) 160–208 (Washington, D.C.: American Psychological Association, 1959).

38. Lacey, J. I., Kagan, J., Lacey, B. C. & Moss, H. A. The visceral level: Situational determinants and behavioral correlates of autonomic response patterns. in *Expression of the emotions in man* (ed. Knapp, P. H.) 161–196 (New York, NY: International Universities Press, 1963).

39. Elliott, R. Tonic heart rate: Experiments on the effects of collative variables lead to a hypothesis about its motivational significance. *J. Pers. Soc. Psychol.* **12**, 211–228 (1969).

40. Shaffer, F., McCraty, R. & Zerr, C. L. A healthy heart is not a metronome: An integrative review of the heart's anatomy and heart rate variability. *Front. Psychol.* **5**, (2014).

41. Berntson, G. G. *et al.* Heart rate variability: Origins, methods, and interpretive caveats. *Psychophysiology* **34**, 623–648 (1997).

42. Ernst, G. Hidden signals — The history and methods of heart rate variability. *Front. Public Health* **5**, 265 (2017).

43. Lang, P. J., Öhman, A. & Simons, R. F. The psychophysiology of anticipation. in *Attention and performance VII* (ed. Requin, J.) 469–485 (Hillsdale, N.J.: Lawrence Erlbaum Associates, 1978).

44. Bohlin, G. & Kjellberg, A. Orienting activity in two stimulus paradigms as reflected in heart rate. in *The orienting reflex in humans* (eds. Kimmel, H. D., van Olst, E. H. & Orlebeke, J. F.) 169–198 (Hillsdale, N.J.: Lawrence Erlbaum Associates, 1979).

45. Danev, S. G. & de Winter, C. R. Heart rate deceleration after erroneous responses: A

bioRxiv preprint doi: https://doi.org/10.1101/2024.06.21.599851; this version posted May 17, 2025. The copyright holder for this preprint (which was not certified by peer review) is the author/funder, who has granted bioRxiv a license to display the preprint in perpetuity. It is made available under aCC-BY-NC 4.0 International license.

phenomenon complicating the use of heart rate variability for assessing mental load. *Psychol. Forsch.* **35**, 27–34 (1971).

46. Di Gregorio, F., Steinhauser, M., Maier, M. E., Thayer, J. F. & Battaglia, S. Error-related cardiac deceleration: Functional interplay between error-related brain activity and autonomic nervous system in performance monitoring. *Neurosci. Biobehav. Rev.* **157**, 105542 (2024).
47. Thayer, J. F., Hansen, A. L., Saus-Rose, E. & Johnsen, B. H. Heart rate variability, prefrontal neural function, and cognitive performance: The neurovisceral integration perspective on self-regulation, adaptation, and health. *Ann. Behav. Med.* **37**, 141–153 (2009).
48. Beauchaine, T. P. & Thayer, J. F. Heart rate variability as a transdiagnostic biomarker of psychopathology. *Int. J. Psychophysiol.* **98**, 338–350 (2015).
49. Mather, M. & Thayer, J. F. How heart rate variability affects emotion regulation brain networks. *Curr. Opin. Behav. Sci.* **19**, 98–104 (2018).
50. Forte, G., Favieri, F. & Casagrande, M. Heart rate variability and cognitive function: A systematic review. *Front. Neurosci.* **13**, 710 (2019).
51. Magnon, V. *et al.* Does heart rate variability predict better executive functioning? A systematic review and meta-analysis. *Cortex* **155**, 218–236 (2022).
52. Silvani, A., Calandra-Buonaura, G., Dampney, R. A. L. & Cortelli, P. Brain–heart interactions: Physiology and clinical implications. *Philos. Trans. R. Soc. Math. Phys. Eng. Sci.* **374**, 20150181 (2016).
53. Elstad, M., O'Callaghan, E. L., Smith, A. J., Ben-Tal, A. & Ramchandra, R. Cardiorespiratory interactions in humans and animals: Rhythms for life. *Am. J. Physiol.-Heart Circ. Physiol.* **315**, H6–H17 (2018).
54. Schwerdtfeger, A. R. *et al.* Heart rate variability (HRV): From brain death to resonance breathing at 6 breaths per minute. *Clin. Neurophysiol.* **131**, 676–693 (2020).
55. Karemaker, J. M. The multibranched nerve: Vagal function beyond heart rate variability. *Biol. Psychol.* **172**, 108378 (2022).

bioRxiv preprint doi: https://doi.org/10.1101/2024.06.21.599851; this version posted May 17, 2025. The copyright holder for this preprint (which was not certified by peer review) is the author/funder, who has granted bioRxiv a license to display the preprint in perpetuity. It is made available under aCC-BY-NC 4.0 International license.

56. Valenza, G., Ciò, F. D., Toschi, N. & Barbieri, R. Sympathetic and parasympathetic central autonomic networks. *Imaging Neurosci.* **2**, 1–17 (2024).

57. Grossman, P. Respiratory sinus arrhythmia (RSA), vagal tone and biobehavioral integration: Beyond parasympathetic function. *Biol. Psychol.* **186**, 108739 (2024).

58. Smith, R., Thayer, J. F., Khalsa, S. S. & Lane, R. D. The hierarchical basis of neurovisceral integration. *Neurosci. Biobehav. Rev.* **75**, 274–296 (2017).

59. Forte, G. & Casagrande, M. The intricate brain–heart connection: The relationship between heart rate variability and cognitive functioning. *Neuroscience* **565**, 369–376 (2025).

60. Valenza, G., Matić, Z. & Catrambone, V. The brain–heart axis: Integrative cooperation of neural, mechanical and biochemical pathways. *Nat. Rev. Cardiol.* (2025) doi:10.1038/s41569-025-01140-3.

61. Thayer, J. F., Ahs, F., Fredrikson, M., Sollers, III., J. J. & Wager, T. D. A meta-analysis of heart rate variability and neuroimaging studies: Implications for heart rate variability as a marker of stress and health. *Neurosci. Biobehav. Rev.* **36**, 747–756 (2012).

62. Quadt, L., Critchley, H. D. & Garfinkel, S. N. The neurobiology of interoception in health and disease. *Ann. N. Y. Acad. Sci.* **1428**, 112–128 (2018).

63. Chen, W. G. *et al.* The emerging science of interoception: Sensing, integrating, interpreting, and regulating signals within the self. *Trends Neurosci.* **44**, 3–16 (2021).

64. Berntson, G. G. & Khalsa, S. S. Neural circuits of interoception. *Trends Neurosci.* **44**, 17–28 (2021).

65. Schandry, R., Sparrer, B. & Weitkunat, R. From the heart to the brain: A study of heartbeat contingent scalp potentials. *Int. J. Neurosci.* **30**, 261–275 (1986).

66. Schandry, R. & Montoya, P. Event-related brain potentials and the processing of cardiac activity. *Biol. Psychol.* **42**, 75–85 (1996).

67. Coll, M.-P., Hobson, H., Bird, G. & Murphy, J. Systematic review and meta-analysis of the relationship between the heartbeat-evoked potential and interoception. *Neurosci. Biobehav. Rev.* **122**, 190–200 (2021).

bioRxiv preprint doi: https://doi.org/10.1101/2024.06.21.599851; this version posted May 17, 2025. The copyright holder for this preprint (which was not certified by peer review) is the author/funder, who has granted bioRxiv a license to display the preprint in perpetuity. It is made available under aCC-BY-NC 4.0 International license.

68. Park, H.-D. & Blanke, O. Heartbeat-evoked cortical responses: Underlying mechanisms, functional roles, and methodological considerations. *NeuroImage* **197**, 502–511 (2019).

69. Villena-González, M. *et al.* Attending to the heart is associated with posterior alpha band increase and a reduction in sensitivity to concurrent visual stimuli. *Psychophysiology* **54**, 1483–1497 (2017).

70. García-Cordero, I. *et al.* Attention, in and out: Scalp-level and intracranial EEG correlates of interoception and exteroception. *Front. Neurosci.* **11**, 411 (2017).

71. Montoya, P., Schandry, R. & Müller, A. Heartbeat evoked potentials (HEP): topography and influence of cardiac awareness and focus of attention. *Electroencephalogr. Clin. Neurophysiol. Potentials Sect.* **88**, 163–172 (1993).

72. Kritzman, L. *et al.* Steady-state visual evoked potentials differentiate between internally and externally directed attention. *NeuroImage* **254**, 119133 (2022).

73. Babo-Rebelo, M., Richter, C. G. & Tallon-Baudry, C. Neural responses to heartbeats in the default network encode the self in spontaneous thoughts. *J. Neurosci.* **36**, 7829–7840 (2016).

74. Babo-Rebelo, M., Wolpert, N., Adam, C., Hasboun, D. & Tallon-Baudry, C. Is the cardiac monitoring function related to the self in both the default network and right anterior insula? *Philos. Trans. R. Soc. B* **371**, 1–13 (2016).

75. Babo-Rebelo, M., Buot, A. & Tallon-Baudry, C. Neural responses to heartbeats distinguish self from other during imagination. *NeuroImage* **191**, 10–20 (2019).

76. Candia-Rivera, D., Faes, L., Fallani, F. D. V. & Chavez, M. Measures and models of brain-heart interactions. *IEEE Rev. Biomed. Eng.* 1–17 (2025) doi:10.1109/RBME.2025.3529363.

77. Sargent, K. S. *et al.* Oscillatory coupling between neural and cardiac rhythms. *Psychol. Sci.* 09567976241235932 (2024) doi:10.1177/09567976241235932.

78. Abdalbari, H. *et al.* Brain and brain-heart Granger causality during wakefulness and sleep. *Front. Neurosci.* **16**, 927111 (2022).

bioRxiv preprint doi: https://doi.org/10.1101/2024.06.21.599851; this version posted May 17, 2025. The copyright holder for this preprint (which was not certified by peer review) is the author/funder, who has granted bioRxiv a license to display the preprint in perpetuity. It is made available under aCC-BY-NC 4.0 International license.

79. Faes, L., Nollo, G., Jurysta, F. & Marinazzo, D. Information dynamics of brain–heart physiological networks during sleep. *New J. Phys.* **16**, 105005 (2014).

80. Candia-Rivera, D., Catrambone, V., Barbieri, R. & Valenza, G. Functional assessment of bidirectional cortical and peripheral neural control on heartbeat dynamics: A brain-heart study on thermal stress. *NeuroImage* **251**, 119023 (2022).

81. Catrambone, V., Candia-Rivera, D. & Valenza, G. Intracortical brain-heart interplay: An EEG model source study of sympathovagal changes. *Hum. Brain Mapp.* **45**, e26677 (2024).

82. Pernice, R. *et al.* Multivariate correlation measures reveal structure and strength of brain–body physiological networks at rest and during mental stress. *Front. Neurosci.* **14**, 602584 (2021).

83. Yu, X., Zhang, C., Su, L., Zhang, J. & Rao, N. Estimation of the cortico-cortical and brain-heart functional coupling with directed transfer function and corrected conditional entropy. *Biomed. Signal Process. Control* **43**, 110–116 (2018).

84. Candia-Rivera, D., Catrambone, V., Thayer, J. F., Gentili, C. & Valenza, G. Cardiac sympathetic-vagal activity initiates a functional brain–body response to emotional arousal. *Proc. Natl. Acad. Sci.* **119**, e2119599119 (2022).

85. Valenza, G. *et al.* Combining electroencephalographic activity and instantaneous heart rate for assessing brain–heart dynamics during visual emotional elicitation in healthy subjects. *Philos. Trans. R. Soc. Math. Phys. Eng. Sci.* **374**, 20150176 (2016).

86. Greco, A. *et al.* Lateralization of directional brain-heart information transfer during visual emotional elicitation. *Am. J. Physiol.-Regul. Integr. Comp. Physiol.* **317**, R25–R38 (2019).

87. Andrillon, T., Burns, A., MacKay, T., Windt, J. & Tsuchiya, N. Predicting lapses of attention with sleep-like slow waves. *Nat. Commun.* (2021) doi:10.1101/2020.06.23.166991.

88. Boulakis, P. A. *et al.* Variations of autonomic arousal mediate the reportability of mind blanking occurrences. *Sci. Rep.* **15**, 4956 (2025).

bioRxiv preprint doi: https://doi.org/10.1101/2024.06.21.599851; this version posted May 17, 2025. The copyright holder for this preprint (which was not certified by peer review) is the author/funder, who has granted bioRxiv a license to display the preprint in perpetuity. It is made available under aCC-BY-NC 4.0 International license.

89. Ottaviani, C., Shapiro, D. & Couyoumdjian, A. Flexibility as the key for somatic health: From mind wandering to perseverative cognition. *Biol. Psychol.* **94**, 38–43 (2013).

90. Smallwood, J. *et al.* Subjective experience and the attentional lapse: Task engagement and disengagement during sustained attention. *Conscious. Cogn.* **13**, 657–690 (2004).

91. Smallwood, J., O'Connor, R. C., Sudbery, M. V. & Obonsawin, M. Mind-wandering and dysphoria. *Cogn. Emot.* **21**, 816–842 (2007).

92. Smallwood, J., O'Connor, R. C., Sudberry, M. V., Haskell, C. & Ballantyne, C. The consequences of encoding information on the maintenance of internally generated images and thoughts: The role of meaning complexes. *Conscious. Cogn.* **13**, 789–820 (2004).

93. Ottaviani, C., Medea, B., Lonigro, A., Tarvainen, M. & Couyoumdjian, A. Cognitive rigidity is mirrored by autonomic inflexibility in daily life perseverative cognition. *Biol. Psychol.* **107**, 24–30 (2015).

94. Ottaviani, C. *et al.* Cognitive, behavioral, and autonomic correlates of mind wandering and perseverative cognition in major depression. *Front. Neurosci.* **8**, 433 (2015).

95. Hase, A., Aan Het Rot, M., De Miranda Azevedo, R. & Freeman, P. Threat-related motivational disengagement: Integrating blunted cardiovascular reactivity to stress into the biopsychosocial model of challenge and threat. *Anxiety Stress Coping* **33**, 355–369 (2020).

96. Behnke, M., Hase, A., Kaczmarek, L. D. & Freeman, P. Blunted cardiovascular reactivity may serve as an index of psychological task disengagement in the motivated performance situations. *Sci. Rep.* **11**, 18083 (2021).

97. Franklin, M. S., Broadway, J. M., Mrazek, M. D., Smallwood, J. & Schooler, J. W. Window to the Wandering Mind: Pupillometry of Spontaneous Thought While Reading. *Q. J. Exp. Psychol.* **66**, 2289–2294 (2013).

98. Mittner, M. *et al.* When the Brain Takes a Break: A Model-Based Analysis of Mind Wandering. *J. Neurosci.* **34**, 16286–16295 (2014).

99. Smallwood, J. *et al.* Pupillometric Evidence for the Decoupling of Attention from

bioRxiv preprint doi: https://doi.org/10.1101/2024.06.21.599851; this version posted May 17, 2025. The copyright holder for this preprint (which was not certified by peer review) is the author/funder, who has granted bioRxiv a license to display the preprint in perpetuity. It is made available under aCC-BY-NC 4.0 International license.

Perceptual Input during Offline Thought. *PLoS ONE* **6**, e18298 (2011).

100. Unsworth, N. & Robison, M. K. Pupillary correlates of lapses of sustained attention. *Cogn. Affect. Behav. Neurosci.* **16**, 601–615 (2016).
101. Unsworth, N. & Robison, M. K. Tracking arousal state and mind wandering with pupillometry. *Cogn. Affect. Behav. Neurosci.* **18**, 638–664 (2018).
102. Patron, E., Mennella, R., Messerotti Benvenuti, S. & Thayer, J. F. The frontal cortex is a heart-brake: Reduction in delta oscillations is associated with heart rate deceleration. *NeuroImage* **188**, 403–410 (2019).
103. Robertson, I. H., Manly, T., Andrade, J., Baddeley, B. T. & Yiend, J. 'Oops!': Performance correlates of everyday attentional failures in traumatic brain injured and normal subjects. *Neuropsychologia* **35**, 747–758 (1997).
104. Manly, T., Robertson, I. H., Galloway, M. & Hawkins, K. The absent mind: Further investigations of sustained attention to response. *Neuropsychologia* **37**, 661–670 (1999).
105. Gross, J. *et al.* Comparison of undirected frequency-domain connectivity measures for cerebro-peripheral analysis. *NeuroImage* **245**, 118660 (2021).
106. Ince, R. A. A. *et al.* A statistical framework for neuroimaging data analysis based on mutual information estimated via a gaussian copula. *Hum. Brain Mapp.* **38**, 1541–1573 (2017).
107. Andrillon, T., Burns, A., Mackay, T., Windt, J. & Tsuchiya, N. Predicting lapses of attention with sleep-like slow waves. *Nat. Commun.* **12**, 3657 (2021).
108. Brainard, D. H. The psychophysics toolbox. *Spat. Vis.* **10**, 433–436 (1997).
109. Langner, O. *et al.* Presentation and validation of the Radboud Faces Database. *Cogn. Emot.* **24**, 1377–1388 (2010).
110. Seli, P., Cheyne, J. A. & Smilek, D. Attention failures versus misplaced diligence: Separating attention lapses from speed-accuracy trade-offs. *Conscious. Cogn.* **21**, 277–291 (2012).
111. Delorme, A. & Makeig, S. EEGLAB: An open source toolbox for analysis of single-trial

bioRxiv preprint doi: https://doi.org/10.1101/2024.06.21.599851; this version posted May 17, 2025. The copyright holder for this preprint (which was not certified by peer review) is the author/funder, who has granted bioRxiv a license to display the preprint in perpetuity. It is made available under aCC-BY-NC 4.0 International license.

EEG dynamics including independent component analysis. *J. Neurosci. Methods* **134**, 9–21 (2004).

112. Bigdely-Shamlo, N., Mullen, T., Kothe, C., Su, K.-M. & Robbins, K. A. The PREP pipeline: Standardized preprocessing for large-scale EEG analysis. *Front. Neuroinformatics* **9**, (2015).
113. Mullen, T. R. *et al.* Real-time neuroimaging and cognitive monitoring using wearable dry EEG. *IEEE Trans. Biomed. Eng.* **62**, 2553–2567 (2015).
114. Kothe, C., Miyakoshi, M. & Delorme, A. clean_rawdata. (2019).
115. Vest, A. N. *et al.* An open source benchmarked toolbox for cardiovascular waveform and interval analysis. *Physiol. Meas.* **39**, 105004 (2018).
116. Perakakis, P. HEPLAB: A Matlab graphical interface for the preprocessing of the heartbeat-evoked potential. Zenodo https://doi.org/10.5281/ZENODO.2649943 (2019).
117. Bell, A. J. & Sejnowski, T. J. An information-maximization approach to blind separation and blind deconvolution. *Neural Comput.* **7**, 1129–1159 (1995).
118. Pion-Tonachini, L., Kreutz-Delgado, K. & Makeig, S. ICLabel: An automated electroencephalographic independent component classifier, dataset, and website. *NeuroImage* **198**, 181–197 (2019).
119. Lachaux, J.-P., Rodriguez, E., Martinerie, J. & Varela, F. J. Measuring phase synchrony in brain signals. *Hum. Brain Mapp.* **8**, 194–208 (1999).
120. Mormann, F., Lehnertz, K., David, P. & E. Elger, C. Mean phase coherence as a measure for phase synchronization and its application to the EEG of epilepsy patients. *Phys. Nonlinear Phenom.* **144**, 358–369 (2000).
121. Banellis, L. & Cruse, D. Heartbeat-evoked potentials during interoceptive-exteroceptive integration are not consistent with precision-weighting. Preprint at https://doi.org/10.1101/2021.02.03.429610 (2021).
122. Buot, A., Azzalini, D., Chaumon, M. & Tallon-Baudry, C. Does stroke volume influence heartbeat evoked responses? *Biol. Psychol.* **165**, 108165 (2021).
123. Etter, A. & Biedermann, M. Edf2Mat© Matlab Toolbox. (2024).

bioRxiv preprint doi: https://doi.org/10.1101/2024.06.21.599851; this version posted May 17, 2025. The copyright holder for this preprint (which was not certified by peer review) is the author/funder, who has granted bioRxiv a license to display the preprint in perpetuity. It is made available under aCC-BY-NC 4.0 International license.

124. Van Kempen, J. *et al.* Behavioural and neural signatures of perceptual decision-making are modulated by pupil-linked arousal. *eLife* **8**, e42541 (2019).

125. Corcoran, A. W. *et al.* Expectations boost the reconstruction of auditory features from electrophysiological responses to noisy speech. *Cereb. Cortex* **33**, 691–708 (2023).

126. Hautus, M. J. Corrections for extreme proportions and their biasing effects on estimated values of *d'*. *Behav. Reseach Methods Instrum. Comput.* **27**, 46–51 (1995).

127. Cheyne, J. A., Solman, G. J. F., Carriere, J. S. A. & Smilek, D. Anatomy of an error: A bidirectional state model of task engagement/disengagement and attention-related errors. *Cognition* **111**, 98–113 (2009).

128. Cover, T. M. & Thomas, J. A. *Elements of Information Theory*. (Wiley, 2005). doi:10.1002/047174882X.

129. Shannon, C. E. A mathematical theory of communication. *Bell Syst. Tech. J.* **27**, 379–423 (1948).

130. Iatsenko, D., McClintock, P. V. E. & Stefanovska, A. Nonlinear mode decomposition: A noise-robust, adaptive decomposition method. *Phys. Rev. E* **92**, 032916 (2015).

131. Iatsenko, D., McClintock, P. V. E. & Stefanovska, A. Extraction of instantaneous frequencies from ridges in time-frequency representations of signals. *Signal Process.* **125**, 290–303 (2016).

132. Berger, R. D., Saul, J. P. & Cohen, R. J. Transfer function analysis of autonomic regulation. I. Canine atrial rate response. *Am. J. Physiol.-Heart Circ. Physiol.* **256**, H142–H152 (1989).

133. R Core Team. *R: A Language and Environment for Statistical Computing*. (Vienna: R Foundation for Statistical Computing, 2019).

134. RStudio Team. *RStudio: Integrated Development for R.* (RStudio, Inc., Boston, MA., 2015).

135. Wickham, H. *et al.* Welcome to the Tidyverse. *J. Open Source Softw.* **4**, 1686 (2019).

136. Wood, S. N. Fast stable restricted maximum likelihood and marginal likelihood estimation of semiparametric generalized linear models. *J. R. Stat. Soc. Ser. B Stat.*

bioRxiv preprint doi: https://doi.org/10.1101/2024.06.21.599851; this version posted May 17, 2025. The copyright holder for this preprint (which was not certified by peer review) is the author/funder, who has granted bioRxiv a license to display the preprint in perpetuity. It is made available under aCC-BY-NC 4.0 International license.

Methodol. **73**, 3–36 (2011).

137. Wood, S. N. *Generalized Additive Models: An Introduction with R*. (Boca Raton, FL.: CRC Press, 2017).
138. van Rij, J., Wieling, M., Baayen, H. R. & van Rijn, H. itsadug: Interpreting time series and autocorrelated data using GAMMs. (2017).
139. Fasiolo, M., Nedellec, R., Goude, Y. & Wood, S. N. Scalable visualization methods for modern generalized additive models. *J. Comput. Graph. Stat.* **29**, 78–86 (2020).
140. Wilke, C. O. cowplot: Streamlined plot theme and plot annotations for `ggplot2'. (2020).
141. Lenth, R. emmeans: Estimated marginal means, aka least-squares means. (2020).
142. Lüdecke, D. ggeffects: Tidy data frames of marginal effects from regression models. *J. Open Source Softw.* **3**, 772 (2018).
143. van den Brand, T. ggh4x: Hacks for 'ggplot2'. (2024).
144. Baayen, H. R., Vasishth, S., Kliegl, R. & Bates, D. The cave of shadows: Addressing the human factor with generalized additive mixed models. *J. Mem. Lang.* **94**, 206–234 (2017).
145. Visalli, A. *et al.* lmeEEG: Mass linear mixed-effects modeling of EEG data with crossed random effects. *J. Neurosci. Methods* **401**, 109991 (2024).
146. Mensen, A. & Khatami, R. Advanced EEG analysis using threshold-free cluster-enhancement and non-parametric statistics. *NeuroImage* **67**, 111–118 (2013).
147. Smith, S. & Nichols, T. Threshold-free cluster enhancement: Addressing problems of smoothing, threshold dependence and localisation in cluster inference. *NeuroImage* **44**, 83–98 (2009).
148. Aprile, F. *et al.* The heartbeat-evoked potential in young and older adults during attention orienting. *Psychophysiology* **62**, e70057 (2025).
149. Steinfath, P. *et al.* Validating genuine changes in Heartbeat Evoked Potentials using Pseudotrials and Surrogate Procedures. Preprint at https://doi.org/10.1101/2024.08.24.609348 (2024).
150. Andrillon, T., Burns, A., MacKay, T., Windt, J. & Tsuchiya, N. Predicting lapses of

bioRxiv preprint doi: https://doi.org/10.1101/2024.06.21.599851; this version posted May 17, 2025. The copyright holder for this preprint (which was not certified by peer review) is the author/funder, who has granted bioRxiv a license to display the preprint in perpetuity. It is made available under aCC-BY-NC 4.0 International license.

attention with sleep-like slow waves. OSF https://doi.org/10.17605/OSF.IO/EY3CA (2020).

151. Corcoran, A., Le Coz, A., Hohwy, J. & Andrillon, T. When your heart isn't in it anymore: Cardiac correlates of task disengagement. OSF https://doi.org/10.17605/OSF.IO/V9XSW (2025).
152. Corcoran, A. W. & Andrillon, T. WIM_HB. (2024).
153. Seli, P., Carriere, J. S. A., Levene, M. & Smilek, D. How few and far between? Examining the effects of probe rate on self-reported mind wandering. *Front. Psychol.* **4**, (2013).
154. Green, D. M. & Swets, J. A. *Signal Detection Theory and Psychophysics*. (New York, NY: Wiley, 1966).
155. Macmillan, N. A. & Creelman, C. D. *Detection Theory: A User's Guide*. (New York, NY: Psychological Press, 2005).
156. Ward, A. F. & Wegner, D. M. Mind-blanking: when the mind goes away. *Front. Psychol.* **4**, (2013).
157. Joshi, S. & Gold, J. I. Pupil size as a window on neural substrates of cognition. *Trends Cogn. Sci.* **24**, 466–480 (2020).
158. Matuz, A. *et al.* Enhanced cardiac vagal tone in mental fatigue: Analysis of heart rate variability in Time-on-Task, recovery, and reactivity. *PLOS ONE* **16**, e0238670 (2021).
159. Musat, E. M., Corcoran, A. W., Belloli, L., Naccache, L. & Andrillon, T. Mind the blank: behavioral, experiential, and physiological signatures of absent-mindedness. Preprint at https://doi.org/10.1101/2024.02.11.579845 (2024).
160. Andrillon, T. *et al.* Does the Mind Wander When the Brain Takes a Break? Local Sleep in Wakefulness, Attentional Lapses and Mind-Wandering. *Front. Neurosci.* **13**, (2019).
161. Boulakis, P. A. & Demertzi, A. Relating mind-blanking to the content and dynamics of spontaneous thinking. *Curr. Opin. Behav. Sci.* **61**, 101481 (2025).
162. Grossman, P. & Taylor, E. W. Toward understanding respiratory sinus arrhythmia: Relations to cardiac vagal tone, evolution and biobehavioral functions. *Biol. Psychol.*

bioRxiv preprint doi: https://doi.org/10.1101/2024.06.21.599851; this version posted May 17, 2025. The copyright holder for this preprint (which was not certified by peer review) is the author/funder, who has granted bioRxiv a license to display the preprint in perpetuity. It is made available under aCC-BY-NC 4.0 International license.

74, 263–285 (2007).

163. Wang, C.-A. *et al.* Arousal effects on pupil size, heart rate, and skin conductance in an emotional face task. *Front. Neurol.* **9**, 1029 (2018).
164. Liu, Y., Narasimhan, S., Schriver, B. J. & Wang, Q. Perceptual behavior depends differently on pupil-linked arousal and heartbeat dynamics-linked arousal in rats performing tactile discrimination tasks. *Front. Syst. Neurosci.* **14**, 614248 (2021).
165. Aldredge, J. L. & Welch, A. J. Variations of heart rate during sleep as a function of the sleep cycle. *Electroencephalogr. Clin. Neurophysiol.* **35**, 193–198 (1973).
166. Snyder, F., Hobson, J. A., Morrison, D. F. & Goldfrank, F. Changes in respiration, heart rate, and systolic blood pressure in human sleep. *J. Appl. Physiol.* **19**, 417–422 (1964).
167. Cajochen, C., Pischke, J., Aeschbach, D. & Borbély, A. A. Heart rate dynamics during human sleep. *Physiol. Behav.* **55**, 769–774 (1994).
168. Somers, V. K., Dyken, M. E., Mark, A. L. & Abboud, F. M. Sympathetic-nerve activity during sleep in normal subjects. *N. Engl. J. Med.* **328**, 303–307 (1993).
169. Cellini, N., Whitehurst, L. N., McDevitt, E. A. & Mednick, S. C. Heart rate variability during daytime naps in healthy adults: Autonomic profile and short-term reliability. *Psychophysiology* **53**, 473–481 (2016).
170. Trinder, J., Waloszek, J., Woods, M. J. & Jordan, A. S. Sleep and cardiovascular regulation. *Pflüg. Arch. - Eur. J. Physiol.* **463**, 161–168 (2012).
171. Pattyn, N., Neyt, X., Henderickx, D. & Soetens, E. Psychophysiological investigation of vigilance decrement: Boredom or cognitive fatigue? *Physiol. Behav.* **93**, 369–378 (2008).
172. Gergelyfi, M., Jacob, B., Olivier, E. & Zénon, A. Dissociation between mental fatigue and motivational state during prolonged mental activity. *Front. Behav. Neurosci.* **9**, (2015).
173. Hopstaken, J. F., Van Der Linden, D., Bakker, A. B. & Kompier, M. A. J. A multifaceted investigation of the link between mental fatigue and task disengagement. *Psychophysiology* **52**, 305–315 (2015).

bioRxiv preprint doi: https://doi.org/10.1101/2024.06.21.599851; this version posted May 17, 2025. The copyright holder for this preprint (which was not certified by peer review) is the author/funder, who has granted bioRxiv a license to display the preprint in perpetuity. It is made available under aCC-BY-NC 4.0 International license.

174. Stawarczyk, D. & D'Argembeau, A. Conjoint influence of mind-wandering and sleepiness on task performance. *J. Exp. Psychol. Hum. Percept. Perform.* **42**, 1587–1600 (2016).

175. Stawarczyk, D., François, C., Wertz, J. & D'Argembeau, A. Drowsiness or mind-wandering? Fluctuations in ocular parameters during attentional lapses. *Biol. Psychol.* **156**, 107950 (2020).

176. Vanoli, E. *et al.* Heart rate variability during specific sleep stages: A comparison of healthy subjects with patients after myocardial infarction. *Circulation* **91**, 1918–1922 (1995).

177. Huikuri, H. V. *et al.* Reproducibility and circadian rhythm of heart rate variability in healthy subjects. *Am. J. Cardiol.* **65**, 391–393 (1990).

178. Jurysta, F. *et al.* A study of the dynamic interactions between sleep EEG and heart rate variability in healthy young men. *Clin. Neurophysiol.* **114**, 2146–2155 (2003).

179. Boudreau, P., Yeh, W.-H., Dumont, G. A. & Boivin, D. B. Circadian variation of heart rate variability across sleep stages. *Sleep* **36**, 1919–1928 (2013).

180. Hulsey, D. R. *et al.* Parametric characterization of neural activity in the locus coeruleus in response to vagus nerve stimulation. *Exp. Neurol.* **289**, 21–30 (2017).

181. Collins, L., Boddington, L., Steffan, P. J. & McCormick, D. Vagus nerve stimulation induces widespread cortical and behavioral activation. *Curr. Biol.* **31**, 2088-2098.e3 (2021).

182. Allen, M. *et al.* Unexpected arousal modulates the influence of sensory noise on confidence. *eLife* **5**, (2016).

183. Munn, B. R., Müller, E. J., Wainstein, G. & Shine, J. M. The ascending arousal system shapes neural dynamics to mediate awareness of cognitive states. *Nat. Commun.* **12**, 6016 (2021).

184. Aston-Jones, G. & Cohen, J. D. An integrative theory of locus coeruleus-norepinephrine function: Adaptive gain and optimal performance. *Annu. Rev. Neurosci.* **28**, 403–450 (2005).

bioRxiv preprint doi: https://doi.org/10.1101/2024.06.21.599851; this version posted May 17, 2025. The copyright holder for this preprint (which was not certified by peer review) is the author/funder, who has granted bioRxiv a license to display the preprint in perpetuity. It is made available under aCC-BY-NC 4.0 International license.

185. Sara, S. J. The locus coeruleus and noradrenergic modulation of cognition. *Nat. Rev. Neurosci.* **10**, 211–223 (2009).

186. Stelmack, R. M. & Siddle, D. A. T. Pupillary dilation as an index of the orienting reflex. *Psychophysiology* **19**, 706–708 (1982).

187. Hajcak, G., McDonald, N. & Simons, R. F. To err is autonomic: Error-related brain potentials, ANS activity, and post-error compensatory behavior. *Psychophysiology* **40**, 895–903 (2003).

188. Notebaert, W. *et al.* Post-error slowing: An orienting account. *Cognition* **111**, 275–279 (2009).

189. Wessel, J. R. An adaptive orienting theory of error processing. *Psychophysiology* **55**, e13041 (2018).

190. Yu, A. J. & Dayan, P. Uncertainty, neuromodulation, and attention. *Neuron* **46**, 681–692 (2005).

191. Sara, S. J. & Bouret, S. Orienting and reorienting: The locus coeruleus mediates cognition through arousal. *Neuron* **76**, 130–141 (2012).

192. Sales, A. C., Friston, K. J., Jones, M. W., Pickering, A. E. & Moran, R. J. Locus Coeruleus tracking of prediction errors optimises cognitive flexibility: An Active Inference model. *PLoS Comput. Biol.* **15**, e1006267 (2019).

193. Strauch, C., Wang, C.-A., Einhäuser, W., Van Der Stigchel, S. & Naber, M. Pupillometry as an integrated readout of distinct attentional networks. *Trends Neurosci.* **45**, 635–647 (2022).

194. Jordan, R. The locus coeruleus as a global model failure system. *Trends Neurosci.* **47**, 92–105 (2024).

195. Christoff, K., Gordon, A. M., Smallwood, J., Smith, R. & Schooler, J. W. Experience sampling during fMRI reveals default network and executive system contributions to mind wandering. *Proc. Natl. Acad. Sci. U. S. A.* **106**, 8719–8724 (2009).

196. Buckner, R. L., Andrews-Hanna, J. R. & Schacter, D. L. The brain's default network: Anatomy, function, and relevance to disease. *Ann. N. Y. Acad. Sci.* **1124**, 1–38 (2008).

bioRxiv preprint doi: https://doi.org/10.1101/2024.06.21.599851; this version posted May 17, 2025. The copyright holder for this preprint (which was not certified by peer review) is the author/funder, who has granted bioRxiv a license to display the preprint in perpetuity. It is made available under aCC-BY-NC 4.0 International license.

197. Andrews-Hanna, J. R., Smallwood, J. & Spreng, R. N. The default network and self-generated thought: Component processes, dynamic control, and clinical relevance. *Ann. N. Y. Acad. Sci.* **1316**, 29–52 (2014).

198. Beissner, F., Meissner, K., Bar, K.-J. & Napadow, V. The autonomic brain: An activation likelihood estimation meta-analysis for central processing of autonomic function. *J. Neurosci.* **33**, 10503–10511 (2013).

199. Lechinger, J., Heib, D. P. J., Gruber, W., Schabus, M. & Klimesch, W. Heartbeat-related EEG amplitude and phase modulations from wakefulness to deep sleep: Interactions with sleep spindles and slow oscillations. *Psychophysiology* **52**, 1441–1450 (2015).

200. Rassi, E., Dorffner, G., Gruber, W., Schabus, M. & Klimesch, W. Coupling and decoupling between brain and body oscillations. *Neurosci. Lett.* **711**, 134401 (2019).

201. Ren, Q., Marshall, A. C., Liu, J. & Schütz-Bosbach, S. Listen to your heart: Trade-off between cardiac interoceptive processing and visual exteroceptive processing. *NeuroImage* **299**, 120808 (2024).

202. Tanaka, Y., Ito, Y., Terasawa, Y. & Umeda, S. Modulation of heartbeat-evoked potential and cardiac cycle effect by auditory stimuli. *Biol. Psychol.* **182**, 108637 (2023).

Supplementary Appendix 3: Talking to sleepwalkers? Response to communication efforts in disorders of arousals

SLEEP, 2025, 48, 1–15
https://doi.org/10.1093/sleep/zsae272
Advance access publication 21 November 2024
Original Article

Original Article

Talking to sleepwalkers? Response to communication efforts in disorders of arousals

Yannis Idir[1], Régis Lopez[2,3], Amélie Barbier[1,4], Sony Saint-Auret[1], Emmanuel Morain[1], Raphaël Vollhardt[1], Inès Ben Haj Kacem[1], Arthur Le Coz[1], Ana Gales,[5] Pauline Dodet[1,5], Smaranda Leu-Semenescu,[5] Yves Dauvilliers[2,3], Isabelle Arnulf[1,5] and Delphine Oudiette[1,5,*]

[1]Institut du Cerveau - Paris Brain Institute - ICM, Inserm, CNRS, APHP, Hôpital de la Pitié Salpêtrière, Sorbonne Université, Paris, France,
[2]Department of Neurology, National Reference Centre for Orphan Diseases, Narcolepsy-Rare Hypersomnias, Sleep Unit, CHU Montpellier, University Montpellier, Montpellier, France,
[3]Institute for Neurosciences of Montpellier INM, University Montpellier, INSERM, Montpellier, France,
[4]Laboratoire d'anthropologie sociale, Collège de France, EHESS, EPHE, CNRS, Université de recherche PSL, Paris, France and
[5]Service des Pathologies du Sommeil, National Reference Centre for Narcolepsy and Rare Hypersomnias, AP-HP, Hôpital Pitié-Salpêtrière, Paris, France

*Corresponding author. Delphine Oudiette, Paris Brain Institute, Hôpital Pitié-Salpêtrière, 47-83 boulevard de l'Hôpital, 75013 Paris, France. Email: delphine.oudiette@icm-institute.org.

Abstract

Study Objectives: Disorders of arousal (DoA) are diagnosed on the basis of clinical criteria, including inappropriate or absent responsiveness to communication attempts. Surprisingly, the ability of patients to interact with others during DoA episodes has not been systematically investigated. To address this gap, we conducted three studies.

Methods: First, we used a retrospective questionnaire to assess verbal responsiveness during episodes in 61 adult patients with DoA (Study 1). Second, we used auditory stimulation during polysomnographically verified N3 sleep to trigger DoA episodes in 14 patients. We then asked questions to test the possibility of verbal interactions during the episodes (Study 2). Third, we assessed the presence and quality of conversations with a bed partner in 364 home video-recorded episodes from 19 patients (Study 3).

Results: In Study 1, most patients (81%) reported occasional conversations during parasomnia episodes. Patients' ongoing mental content influenced both their responses to questions during episodes and their perception of the outside world (including their surroundings and the identity of their interlocutor). In Study 2, auditory stimulation had a limited effect in inducing episodes (7/157 trials). One patient indirectly responded to our verbal prompts in a DoA episode. In Study 3, we found 37 video instances of discussion between patients and their partner.

Conclusions: Overall, our findings suggest that DoA episodes are not a uniform state but may instead encompass varying states of consciousness, characterized by different levels of responsiveness and a complex interplay between internal and external information processing. These results highlight the limitations of current diagnostic criteria for DoA.

Key words: sleepwalking; parasomnia; sleep; dreams; consciousness

Submitted for publication: June 21, 2024; **Revised:** October 18, 2024
© The Author(s) 2024. Published by Oxford University Press on behalf of Sleep Research Society.
This is an Open Access article distributed under the terms of the Creative Commons Attribution-NonCommercial License (http://creativecommons.org/licenses/by-nc/4.0/), which permits non-commercial re-use, distribution, and reproduction in any medium, provided the original work is properly cited. For commercial re-use, please contact reprints@oup.com for reprints and translation rights for reprints. All other permissions can be obtained through our RightsLink service via the Permissions link on the article page on our site—for further information please contact journals.permissions@oup.com.

Graphical Abstract

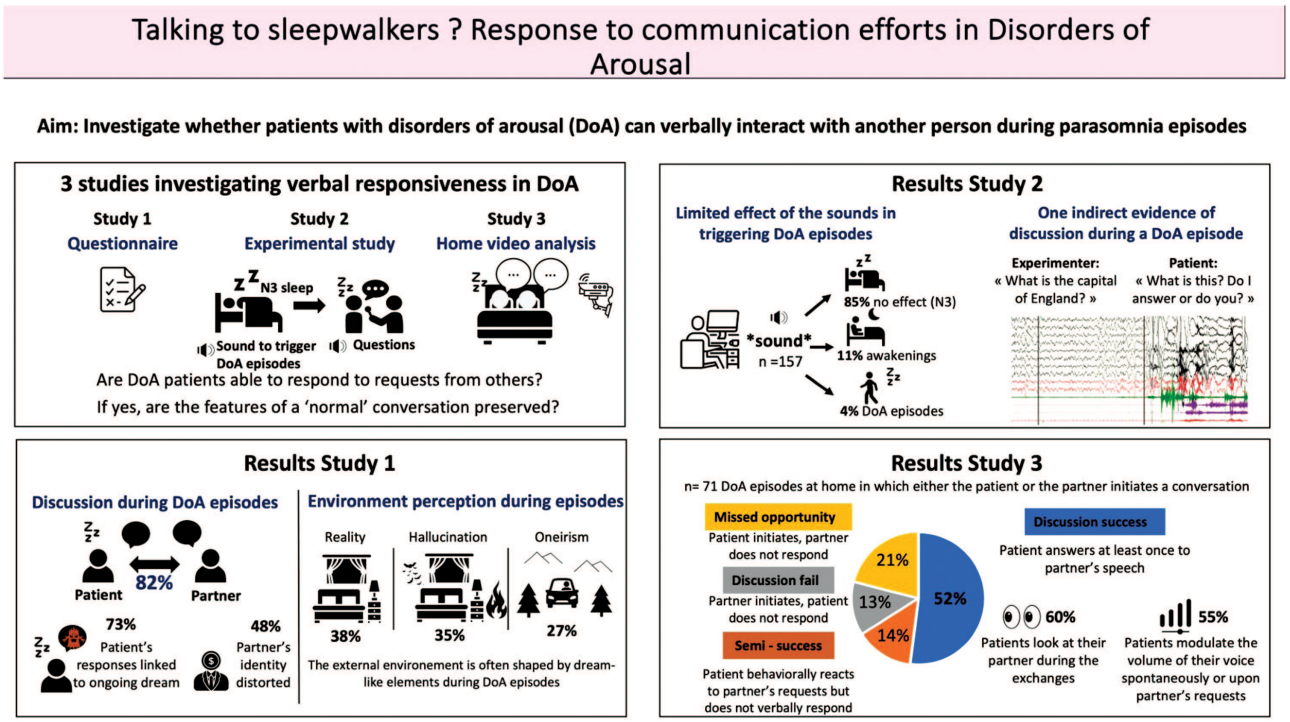

Statement of Significance

Idir et al. show that adult patients with Disorders of Arousal (DoA) can occasionally respond to verbal requests from a partner during an episode. This finding challenges the current diagnostic criteria for DoA.

Introduction

Disorders of arousal (DoA) consist of complex behaviors emerging from NREM sleep (mainly N3 sleep) [1–5]. This family of disorders includes sleepwalking (also called somnambulism), sleep terrors, and confusional arousals. These disorders are relatively widespread in adulthood, ranging from 1.7% to 6.9% of the world's population [6–8]. They are associated with negative consequences, such as daytime sleepiness, psychological distress, and physical injuries to themselves or others [3, 9–13]. Despite their importance, DoA are one of the least studied sleep disorders and remain poorly understood. As there is no consensus on polysomnographic criteria for DoA, the diagnosis still exclusively relies on clinical criteria [4, 12]. In addition to "recurrent episodes of incomplete awakenings from sleep," the international criteria for DoA [14, 15] include inappropriate or absent responsiveness to efforts of others to intervene or redirect the person during the episode, limited (e.g. a single visual scene) or no associated cognition or dream imagery, and partial or complete amnesia of the episode upon awakening. Yet, there is a growing debate [4, 16, 17] as to whether these criteria, based on clinical observations inherited over many years, accurately reflect the cognitive states of DoA patients during the episodes. For example, several studies have questioned the dreamlessness historically associated with DoA [17–30]. However, the extent to which patients can respond to others' queries has been largely overlooked and not formally tested.

Thanks to technological advances in the recent decades, including scalp electroencephalography (EEG) [31, 32], high-density EEG [29, 33–35], intracerebral recordings in epileptic patients [36, 37], or brain scintigraphy [38], the neurophysiological substrates of DoA episodes are better characterized. These studies have revealed that patients are in a dissociated state (a hybrid state between wakefulness and sleep) during the episodes, with some brain regions involved in locomotion and emotional processing (e.g. motor cortex, cingulate cortex, and amygdala) presenting features of wakefulness (e.g. high-frequency EEG activity), while other regions involved in memory and high-order cognitive functions (e.g. associative fronto-parietal cortex and hippocampus) show signs of sleep (e.g. sleep slow waves, spindles, and reduced cerebral blood flow) [39]. Importantly, a recent study [29] showed that such local brain changes are not stereotyped but can vary between and within individuals, or even over the course of a given DoA episode depending on the patients' mental experiences. The authors showed that DoA episodes associated with a mental experience were preceded by an activation of posterior regions and large slow waves in fronto-central regions compared to the episodes without mental experiences. These findings suggest that the brain networks underlying specific cognitive functions may be either restored or abolished during DoA episodes depending on which brain regions show local activations and which remain in slow waves. If true, this hypothesis would imply that the spectrum of cognitive states possible during DoA episodes is broader and more variable than what the current criteria suggest.

The fact that external sounds can trigger episodes [40], and more generally the type of behaviors displayed during DoA

episodes (e.g. navigating through their environment, opening doors, and handling objects [3, 28, 41, 42]), suggest that DoA patients can process visual and auditory stimuli from the outside world. Since they can both perceive input and send "output" (e.g. by talking [43] or by interacting with objects in their environment [44, 45]), patients with DoA should theoretically be able to respond to communication attempts from others. To our knowledge, this possibility has not been systematically investigated. Only a handful of studies, whose primary goals focused on other aspects of DoA, suggest that verbal responsiveness may be possible during DoA episodes. In a study exploring the semiological features of DoA, the authors proposed an "interactive component" (talking with an observer or manipulating nearby objects) as a discriminating factor favoring the diagnosis of DoA over sleep hypermotor epilepsy [46]. In addition, two anecdotal cases of conversations between a patient and another (real) person during a DoA episode have been previously reported [17, 47]; in both cases, the discussion revolved about an imagined threat that the patient was dreaming about (i.e. intruders in the bedroom or power lines).

Here, we seek to formally evaluate the extent to which patients with DoA can interact with another person during parasomnia episodes. To test this question, we used three complementary approaches, including a retrospective questionnaire (Study 1), auditory stimulation applied during polysomnography-verified N3 sleep in the laboratory (Study 2), and an analysis of nocturnal home video recordings of DoA patients sleeping with their partners [48] (Study 3).

Methods

Study 1. Retrospective questionnaire

Participants

Adult patients (N = 105) who had been previously diagnosed with DoA and monitored with video-polysomnography in the Sleep Clinic of Pitié-Salpêtrière University Hospital (Sorbonne University) during 2021–2022 were invited to fill up an online survey after they did not oppose to being contacted for future research. The DoA diagnosis was based on clinical criteria from the International Classification of Sleep Disorders, version 3 (ICSD-3) as well as on video-polysomnography criteria to exclude possible differential diagnoses (e.g. REM sleep behavior disorder and nocturnal seizures). The clinical criteria included recurrent episodes of incomplete awakenings from sleep, not explained by another disorder, medication, or substance abuse. In addition, all patients had the following features on video-polysomnography: (1) at least 1 arousal during N3 associated with an abnormal motor behavior suggesting surprise, confusion, or fear (startling, sitting in the bed, screaming, or looking around surprised); or (2) two or more N3 interruptions containing eye opening [44]. Of note, no patients had parasomnia overlap disorder (DoA + REM sleep behavior disorder) or obvious signs of REM sleep without atonia in the polysomnography. Participants' consent was obtained according to the Declaration of Helsinki. In keeping with French law on research studies, data were pseudonymized, kept, and analyzed following the methodological reference MR003. Participants did not receive any monetary compensation for completing the survey.

Materials and procedure

To investigate the diversity of nocturnal behaviors and associated cognition during the episodes, we created an online questionnaire on LimeSurvey®, a survey tool recommended by the hospital institution "Assistance Publique–Hôpitaux de Paris" (APHP) for ensuring data anonymization and data protection. The questionnaire included general questions about age, gender, occupation, onset of the disease, family history of DoA, potential triggers for the episodes, frequency of episodes in the last year, and current treatment.

The questionnaire was designed to assess the extent to which the international clinical criteria of DoA matched patients' experiences in the past year and included questions about:

- participants' recall of the episodes (free and cued recall).
- the frequency and quality of conversations between the patient and a partner during an episode. When patients reported having had dialogued with a partner, they indicated whether: (1) they perceived their partner's questions as they were enunciated; (2) their responses were coherent; (3) their responses were influenced by ongoing mental content; (4) they correctly identified their interlocutor's identity; (5) they recalled the conversation, and if so, how much.
- participants' dreams, their association with the behaviors exhibited during the episodes, and with the perception of the environment.

The verbatim of the questionnaire and the possible response choices are shown in Supplementary Table S1. Of note, patients were not provided with any definition for the term "dream."

Participants additionally evaluated the frequency of various nocturnal behaviors that could happen during an episode (four-point Likert scale from "never" to "always"). This list of behaviors was chosen based on the literature [9, 18, 19, 21, 24, 27–29] and our clinical experience and included: talking, shouting, laughing, crying, picking up or moving an object, breaking an object/wall/window, jumping/falling out of bed, fighting, opening doors/windows, going to the toilet, eating or preparing food, having sex, hurting/harming oneself, feeling pain, or hurting someone else. Participants were also free to add more actions that were not initially listed. For all the questions above, participants were invited to provide examples detailing the situations (e.g. what they did in reality, what was in their mind at that moment).

Study 2. Prospective polysomnographic study: auditory stimulation during N3 sleep

Participants

We prospectively recruited participants who had been referred to the Sleep Clinic of Pitié-Salpêtrière Hospital for a suspicion of DoA and underwent video-polysomnography during two consecutive nights (the routine procedure for diagnosing DoA and identifying precipitating factors and differential diagnoses in that Sleep Clinic). If the DoA diagnosis was confirmed by the clinician after the first night (same criteria as in Study 1), patients were invited to participate in our research protocol for the second night. A total of 14 participants with DoA (mean age: 25 ± 4 years old; 9 women) were enrolled in this study. The chosen sample size was chosen for pragmatic considerations but was not derived statistically. In that sense, this study should be considered exploratory. None of the participants was taking any treatment that might drastically alter sleep structure (e.g. antidepressants, anxiolytics, etc.). Some patients took melatonin (n = 2), food supplements (n = 1), or antibiotics (for bacterial vaginosis, n = 1). Participants' written consent was obtained according to the Declaration of Helsinki, and the study was approved by an ethics committee (CPP Sud Méditerranée 1). They received no financial compensation for their participation.

Sleep recording and scoring

Participants were continuously monitored with video-polysomnography during the experimental night. The montage included electroencephalography (EEG; eight channels: F1, F2, C3, C4, P3, P4, O1, and O2, referenced to A2), electrooculography (left and right EOG; positioned above the left inferior canthus and right superior epicanthus and referenced each to A2), electromyography (three channels, chin mentalis muscle and right and left tibialis anterior muscles), as well as electrocardiogram (D2 lead), thoracic and abdominal plethysmography to measure respiratory efforts, a nasal cannula, and a pulse oximeter. Nocturnal behaviors were monitored via two infrared cameras and sound recording (one placed on the wall and one next to the bed) synchronized with the neurophysiological sensors. Two speakers, placed close to bed, were used to send auditory stimuli during sleep (see next section).

Sleep stages, arousals, respiratory events, and periodic leg movements were scored by experienced sleep neurologists according to the international criteria [14]. Sleep neurologists screened the video/audio associated with awakenings from N3 sleep and categorized them as either a normal awakening (e.g. in the case of typical comfort arousal actions such as rubbing, yawning, repositioning oneself or the sheets) [44] or a DoA episode when at least one of the following features was present: sudden onset of a behavior including staring or looking around with perplexity, head/trunk raising, sitting, standing up or walking, talking, screaming, touching objects around the bed, or displaying any facial expression of fear, surprise, or confusion.

Experimental procedure

We planned to first induce a DoA episode using auditory stimulation [40], then to ask questions that would allow us to assess the responsiveness of participants during the parasomnia episode. As this study was largely exploratory, we slightly varied the protocol among participants (e.g. the type of sounds, onset time of the first sound, the sound volume, etc.). The general procedure is detailed in Figure 1 and below. Before going to bed, participants were informed that sounds would be played while they slept. If they were awake during the stimulation, participants were instructed to say aloud that they were awake and to verbally report anything that was on their mind before they woke up (e.g. thoughts, sensations, and dreams).

Once participants reached consolidated N3 sleep (at least six consecutive 30-s epochs of N3 sleep), we attempted to induce a DoA episode by delivering an auditory stimulus ("trigger sound," three types, see Material) through a loudspeaker. Following the stimulus, four scenarios were possible: (1) participants could show a DoA episode, (2) wake up, (3) transition to another sleep stage (e.g. N1 or N2), or (4) remain in N3 sleep and show no behavioral reaction to the stimulus. In the first case (induced DoA episode), we immediately asked one of the three prerecorded questions (see Materials), waited 1 min for a response, and woke participants up to collect a dream report. In the second case (normal awakening), we asked participants to report their mental content (if they did not report it spontaneously, as requested before sleep). In the third case (transition to another sleep stage), we did not apply any auditory stimulation and waited for the participants to reach N3 sleep again. In the last case (no reaction), we waited for 10 s and played the trigger sound again, repeating this procedure for up to three trials. If participants still did not show any behavioral response, then we directly asked one of the three prerecorded questions (see Materials) and waited for 1 min. If there was no response, we increased the volume of the auditory stimulus by 10 dB (only when the trigger stimulus was the "pure sound," see Materials) and started a new stimulation cycle until

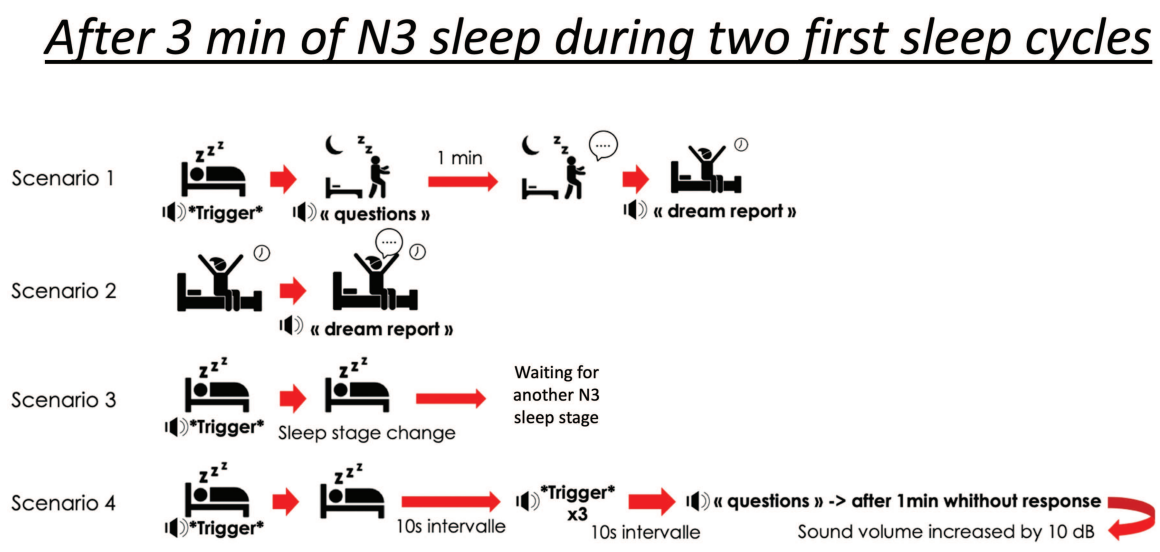

Figure 1. Experimental design aimed at inducing a sleepwalking episode and communicating with the participant during a parasomnia episode. The figure shows the different steps for our four possible experimental scenarios after sending a trigger sound after the participant has been in N3 sleep for three consecutive minutes. In scenario 1, the trigger sound induced a DoA episode; we immediately asked one of the three prerecorded questions, waited 1 min for a response, and woke participants up to collect a dream report. In scenario 2, the trigger sound woke participants; we asked them to report their mental content (if they did not report it spontaneously, as requested before sleep). In scenario 3, the trigger sound induced a transition to another sleep stage; we did not apply any auditory stimulation and waited for the participants to reach N3 sleep again. In scenario 4, participants had no reaction to the trigger sound and remained in N3 sleep; we waited for 10 s and played the trigger sound again, repeating this procedure for up to three trials. If participants still did not show any behavioral response, then we directly asked one of the three prerecorded questions and waited for 1 min. If there was no response, we increased the volume of the auditory stimulus by 10 dB and started a new stimulation cycle until a behavioral response was obtained (a DoA episode or an awakening). We repeated the same procedure several times. Auditory stimuli were played only during the two first sleep cycles.

a behavioral response was obtained (a DoA episode or an awakening). We repeated the same procedure several times. Auditory stimuli were played only during the two first sleep cycles.

In the morning following the experimental night, we asked participants if they thought that they had a parasomnia episode during the night, if they recalled any dreams, and if they heard any questions during the night. Participants also performed an old/new memory test, which includes questions ($N = 12$) that were asked during the night and questions that were not. For each item, they indicated how much it was familiar on a scale from 1 (not familiar at all) to 10 (very familiar).

Materials

We tried various trigger sounds: (1) a short, sharp noise at 50 dB (mimicking a crackling water pipe in the room, as clinicians noticed in several, previous recordings that this sound often precipitated episodes in DoA patients; "crackling sound"; duration: 350 ms; $n = 47$ times), (2) a "pure sound" of 1000 Hz ranging from 40 dB to 80 dB (duration: 3 s; $n = 105$ times), which successfully induced DoA episodes in a previous study [40], or (3) the participant's name uttered at 50 dB ("name sound," $n = 5$ times). After successfully triggering a parasomnia episode or after playing three trigger sounds without behavioral reaction, we used one or several of the three following questions to communicate with participants: "What is the capital of England?," "Where are you?," and "What are you doing?." We chose the first question because there is only one possible correct answer ("London"), making a potential response from participants with DoA easily interpretable as appropriate or not, as opposed to a "yes/no" question, for which an answer could be technically correct even in the absence of a clear understanding of the question. This question allowed us to assess whether participants could access their semantic memory knowledge during the episode. We chose the last two questions because the type of answer could provide clues about the participants' awareness of their state/surrounding (e.g. actual location vs. a dream location; behavior consistent with the actual environment or with hallucinatory elements). The order of the questions was randomized across participants.

We generated the crackling sound and the pure sound using Ableton software. The name sound and questions were prerecorded and spoken by the experimenter's voice (YI). Auditory stimuli were played using an interface developed in C# on Visual Studio software. For each question, the computer microphone, placed close to the participants' bed, recorded the participants' answers.

Study 3. Analysis of verbal interactions recorded by a home infrared camera

Participants

Because complex parasomnia episodes are difficult to capture in the laboratory, we sought to analyze verbal interactions between participants with DoA and their bed partners directly in their home environment, where DoA episodes are often longer and more elaborate [25, 27, 48]. We analyzed 639 home nocturnal video clips from 27 DoA patients (median age 26.5 years, range 21–55; 14 women) who were followed in the Sleep Clinic of the Montpellier University Hospital in France. Some videos of these patients had been analyzed, with a different aim, in a previous study [48]. Inclusion criteria were: (1) diagnosis of DoA according to the ICSD-3 [14], (2) at least one parasomnia episode reported per month, and (3) at least one episode during the last month based on the clinical interview. We also ensured that none of the patients was taking any medication known to influence sleep, breathing, or motor activity for at least 2 weeks prior to the sleep examination. The patients were asked to follow their habitual sleep schedules on weekdays and weekends during the month preceding the evaluation. Participants did not receive any monetary compensation for this study. All procedures performed in this study were in accordance with the ethical standard of the institutional research committee.

Materials and procedure

The procedure for collecting home nocturnal infrared video recordings in patients with DoA was detailed in a previous study [48]. Briefly, participants' nocturnal behaviors at home were recorded with an infrared camera (Minox© DTC 395; triggered by movement), which was placed in front of the bed to see the patient's body and face. Participants kept the camera for at least 5 days. Three experienced sleep clinicians classified nocturnal behaviors as normal awakenings or parasomnia episodes based on video clips only, when the eyes were open and there were one or more atypical behaviors during sleep (facial expression, interaction with the environment, sitting up in bed, wandering out of bed, shouting and talking).

In 364 video clips displaying a parasomnia episode (from 19 participants with DoA), the presence of a bed partner was clearly visible (the camera had a wide enough view to show parts of the partner's body) or easily inferred from auditory or visual cues (e.g. partner's snoring, partner's movements in reaction to the patient's DoA episode). For each of those video clips, three scorers independently evaluated whether patients engaged in a conversation with their bed partner, using the following criteria: (1) the participant talked in the video, (2) the participant's speech seemed to be addressed to someone (e.g. seemed to respect turns of speech, used interjections as if reacting to someone's speech, used interrogative tones, gave orders), (3) the participant's body language and/or gaze direction was, at least sometimes, turned towards the partner or the participants' words were related to what the partner said (e.g. the participant repeated the partners' words), (4) the partner verbally engaged the participant. To further ensure that a true dialogue with a real person was taking place (and that participants with DoA were not just talking with themselves or to a dream character), we used an additional criterion, depending on who—the participant with DoA or the partner—initiated the discussion. Each turn of speech (participant with DoA or partner) counted as 0.5 (half an exchange). In the case where the partner initiated the exchange, we considered that there was a discussion if the total number of speech turns was at least equal to 1 (e.g. partner: "Is everything all right?" [0.5]; participant with DoA: "Yes, everything's all right" [0.5]). In the case where the participant with DoA initiated the exchange, we considered that there was a discussion if the total number of speech turns was equal to 1.5 (e.g. participant with DoA: "Quick, quick, quick" [0.5]; partner: "What?" [0.5]; participant with DoA: "Hurry up, it's going to fall" [0.5], [the participant with DoA looks at their partner and points to an object in the room]).

For each parasomnia episode involving a conversation with the bed partner, three blind scorers evaluated different features of the discussion, including the appropriateness of the participant's responses, the number of exchanges, the time between the question and answer, voice modulation, and the partner's attitude toward the participant (e.g. attempting to stop the behavior or not). The detailed grid of observations is shown in Supplementary Table S2.

When the criteria for conversation were not met, we classified the video clips in one of the following categories: (1) no opportunity, i.e. when the patient did not talk or was seemingly talking alone; (2) semi-success, i.e. when the patient behaviorally reacted to a partner's request (e.g. going back to bed when explicitly asked) but did not verbally respond; (3) missed opportunity, i.e. when the patient initiated a discussion but the partner did not respond; (4) fail, i.e. when the patient did not respond or react to a partner's request.

Results

Study 1. Retrospective questionnaire

Clinical description of the population

In total, 61 (58%) DoA patients responded to the questionnaire (mean age 36.24 ± 9.26 years old; 62% of women) and were included in Study 1. Over the last year, 21.3% of DoA responders had at least 1 episode per night, 44.3% at least 1 episode per week, 23% at least 1 episode per month, and 11.5% less than 1 episode per month. These episodes were regular throughout the year for 41% of participants with DoA, irregular for 29.5%, and clustered per period for the others (29.5%). Forty-nine (80%) responders did not take any psychotropic drug, and twelve (20%) took antiepileptic drugs ($n = 7$, 11%), antidepressants ($n = 4$, 7%), or antihistaminergic drugs ($n = 1$, 2%). Most participants (60.7%) had at least one family member who was also affected by DoA (sleepwalking and/or night terrors). Most participants (83.6%) reported that at least one parasomnia episode during the previous year was associated with a congruent dream (see Supplementary Table S3 for examples of dreams associated with parasomnia episodes).

Patients with DoA can dialogue with another person during an episode

A large majority of participants (50/61, 81.9%) reported having a discussion with their partner at least once during a sleepwalking episode in the past year, and conversations were frequent in 44.1% of the participants (27/61). Examples of discussion between DoA participants and their partners are provided in Table 1.

To investigate whether the conversations that occurred during a parasomnia episode preserved the various components of a normal waking conversation, we examined whether DoA participants perceived their partner's "message" as it was intended (they heard their partner's words as they were enunciated) and by whom. Most (39/48, 81.3%) participants reported that they always or often heard the content of their partner's speech in a way that was true to reality, while 18.7% (9/48) seemed to perceive their partner's words in a distorted way (the patient heard something different than what the partner actually said). Participants perceived their interlocutor as who he/she really was about half of the time (25/48, 52.1%) and as someone different from reality the other half of the time (23/48, 47.8%). When evaluating the appropriateness of their responses to the partner's questions, 44% (22/50) of participants with DoA reported that they often or always responded in a coherent way, while the remaining (28/50, 56%) judged their responses as incoherent. Patients who reported that their responses were incoherent provided examples that could be broadly categorized into three types: (1) the patient's speech is not very intelligible (e.g. "my speech is muddled, not very coherent"), (2) the patient's response does not answer the partner's question (e.g. "I don't respond to what people ask me; I act like I'm handling the situation: 'I'm fine, I'm not in crisis'"), (3) the patient's answer does not reflect what is happening in

Table 1. Examples of reported discussions between patients and their partners during DoA episodes (Study 1)

Patient	Discussion between patient with DoA and their partner during the episodes
S6, M, 34 years old	The person always asks me what's going on; I explain the delusional situation (for example, there's an intruder in the room). The person reassures me, I understand, and I go back to bed.
S11, M, 38 years old	There was an episode when I physically felt a rat biting me in my bed. My parents came into my room and talked to me, and I still felt the sensation of the rat, but it faded in about 1 min. At the same time, I told my parents that there was a rat biting me, and they told me that there was nothing there.
S13, F, 33 years old	Someone asked, "Where are you?." I answered, "In a train."
S23, F, 47 years old	I was afraid I won't be able to pay my banker. But I was actually talking to my husband.
S29, F, 23 years old	I dreamt I was having a telephone conversation with a friend. My sister, who was in the next room, asked me what I was doing. I told her I was on the phone and explained what the conversation was about.
S29, F, 23 years old	I dreamt I had to walk my dog. I wanted to get dressed, but I couldn't find my T-shirt in the dark. My boyfriend asked me what I was doing. I answered rather annoyedly: "I can't find my shirt; it's pissing me off. Too bad, she'll have to wait to go out." And I went back to bed.
S30, F, 20 years old	I walked to my kitchen and asked my mom, "Is my girlfriend home?" My mom said "no." I said "yes" and went back to bed.
S31, F, 27 years old	I was leaving the house in the middle of the night. My parents, standing at the door, said, "What are you doing?." I replied, "Well, I'm sleeping." They asked me to go back to bed, and I headed for the bedroom.
S32, M, 28, years old	My partner asked me what I was doing one night when I was standing at the door. I told her that we had to leave quickly.
S39, F, 19 years old	I was shouting that "everything hurts." My boyfriend said "shh," and I shouted "EVERYTHING" to piss him off. Another time, I said, "the horse" ["le cheval" in French], he said, "What?" I said, "Hor" ["che" in French]" and fell asleep.
S40, F, 51 years old	I was dreaming that I was working in a button factory [not her real job] and "Georges" came to talk to me and bothered me. I was annoyed and tried to stop the machinery by pressing the red emergency stop button. When I pressed it, I found it went limp, and Georges continued to tease me and laugh. That's when I woke up and realized that the red button I thought I was pressing was in fact my boyfriend's nipple. My boyfriend is bald in real life, and "Georges" (not my boyfriend's real name) in my dream had a mustache and a haircut. It was my boyfriend talking to me all along, and his words were translated into my dream through the character of Georges.
S41, F; 33 years old	I was talking about a lighting problem to my brother, who had arrived in the room, while I was standing up to try to solve the problem (which didn't exist).
S43, M, 44 years old	My partner woke me up while I was standing at the open window. I told her I was breathing in the air. She told me to come back to bed. I told her that I would count the stars first. In another episode, I told her to wake up for the movie shooting; she asked me, "Which shooting?" I told her it was "el fanfarino" [the patient was working on a documentary about an Italian movie at the time; "el fanfarino" was not the title of the documentary].

Table 1. Continued

Patient	Discussion between patient with DoA and their partner during the episodes
S44, M, 36 years old	If I'm shouting and my wife tells me to stop, I continue the discussion, whispering.
S45, F, 28 years old	I said, "But didn't you see?," "What?," "I saw the neighbors!" "Nobody is there; get back to sleep."
S47, M, 33 years old	I dreamt I had to save my child and took a cushion instead. My partner asked what I was doing. I replied, "I'm taking my child."
S48, M, 33 years old	I was having a nightmare where there was water on the floor, and I was afraid we were going to get electrocuted. I said: "[Name of his partner], don't touch the ground; you'll get electrocuted"; "No"; "yes, there's electricity."
S57, F, 45 years old	I was trying to turn off a switched-off TV. My mother talked to me to figure out what was going on, and I answered her.

reality; it would sound bizarre/absurd to the partner (e.g. the patient takes a pillow, the partner asks "What are you doing?" and the patient answers "I'm taking my child"). Importantly, this last type of answer could be judged as "coherent" by other patients in the sense that it was congruent with what they had in mind at that moment (e.g. "the person asks me what I'm doing and I am able to explain to them what I think I'm doing and where I think I am," or "I can explain why I was screaming."). In fact, mental content during the episodes seemed to have a major influence on patients' verbal interactions, as most patients (35/48, 72.9%) reported that their responses were more related to the content of their dreams rather than to what was happening in the real world (13/48, 27.1%).

Participants' mental content not only influenced their speech during episodes but also "permeated" their perception of the actual environment in 61.7% (37/60) of the cases (see examples in Supplementary Table S4). In 35% of the cases (21/60), part of the mental content took shape in reality while the rest of the environment remained normal, similar to a dream-like augmented reality (e.g. invisible doors on the walls; fire in the room). In 26.7% (16/60), the environment was completely altered to the point where dream images replaced the reality of the room. In the remaining cases (38.3%, 23/60), the environment was perceived as normal, sometimes with a sense of presence in the room.

Interestingly, 71.2% (37/51) of the sample reported being able to recall their nocturnal discussions during the episodes at least once, but the majority only had the feeling of having discussed without recalling any specific content (19/37, 51.4%). Only 8.1% (3/37) of the DoA participants reported remembering the entire discussion at least once (Table 2).

Spectrum and frequency of behaviors exhibited during DoA episodes

To examine whether discussion with a partner during an episode was a rare or common event within the spectrum of DoA behaviors, participants rated the frequency of various types of behaviors. As shown in Figure 2, talking to a partner was the third most common behavior (81.9%) after talking alone (91.8%) and screaming (90.2%). Other commonly reported behaviors included manipulating and moving objects (67.2%) and falling out of bed (72.1%).

Table 2. Responsiveness of participants with DoA to verbal requests from their partner (Study 1)

Question	Participants with DoA, *N* (%)
Discussion with a real person during DoA episodes	
Never, *n* (%)	11 (18)
Rarely, *n* (%)	23 (37.7)
Often, *n* (%)	24 (39.3)
Always, *n* (%)	3 (4.9)
Coherence of participant's responses	
Never, *n* (%)	8 (16)
Rarely, *n* (%)	20 (40)
Often, *n* (%)	16 (32)
Always, *n* (%)	6 (12)
Perception of the interlocutor's identity (*N* = 48)	
Always corresponds to reality, *n* (%)	12 (25)
Often corresponds to reality, *n* (%)	13 (27.1)
Is most often different, *n* (%)	10 (20.8)
Is always different, *n* (%)	13 (27.1)
Perception of the interlocutor's sentences (*N* = 48)	
Always corresponds to reality, *n* (%)	24 (50)
Often corresponds to reality, *n* (%)	15 (31.3)
Mostly distorted, *n* (%)	6 (12.5)
Always distorted, *n* (%)	3 (6.3)
Content of participant's answer (*N* = 48)	
Always adapted to the real world, *n* (%)	2 (4.2)
Mostly adapted to the real world, *n* (%)	11 (22.9)
Mostly related to a dream, *n* (%)	22 (45.8)
Always related to a dream, *n* (%)	13 (27.1)
Recall of having a discussion during an episode upon awakening	
Never, *n* (%)	14 (26.9)
Rarely, *n* (%)	21 (40.4)
Often, *n* (%)	12 (23.1)
Always, *n* (%)	4 (7.7)
Recall of having a discussion (*N* = 37)	
Feeling of having had a discussion but not remembering the content, *n* (%)	19 (51.4)
Remembering fragments of the discussion, *n* (%)	15 (40.5)
Memory of the entire discussion, *n* (%)	3 (8.1)

Study 2. Verbal response to auditory stimulation during N3 sleep

Description of the clinical population

Study 2 included a subset of 14 participants diagnosed with disorders of arousal (mean age: 25 ± 4, 9 women). None of the participants was on any medication that could alter sleep structure. Two patients took melatonin. The sleep measures of participants during the experimental night are shown in Supplementary Table S5.

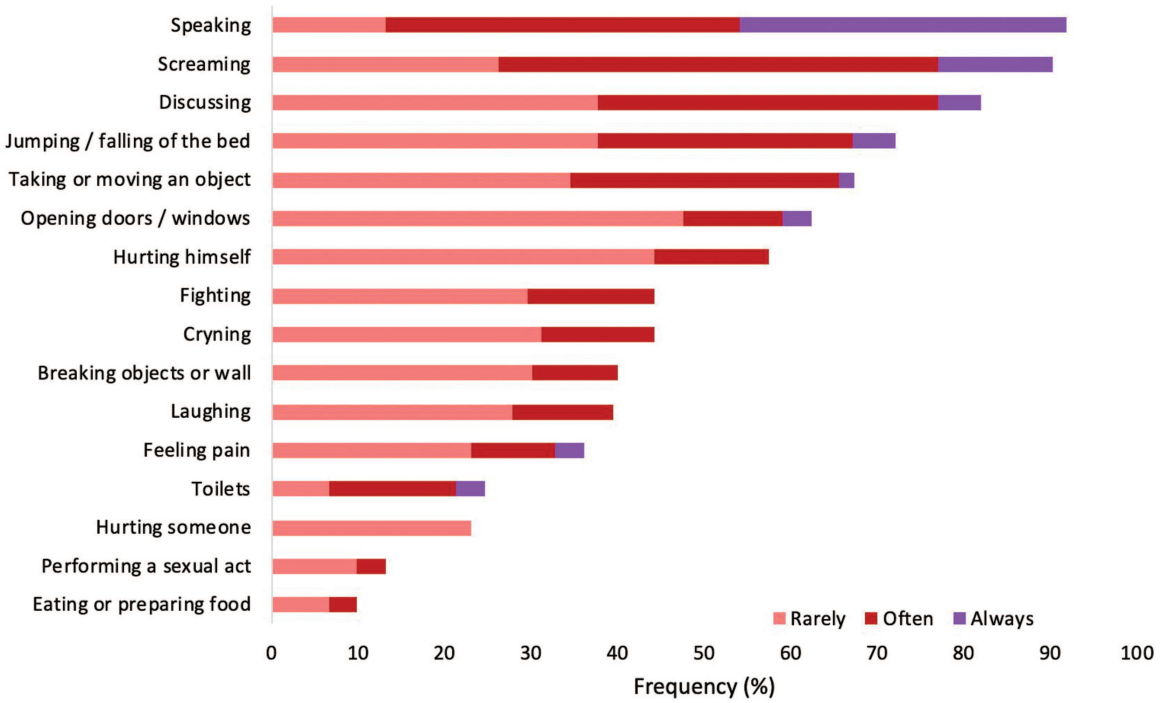

Figure 2. Frequency of behaviors shown during DoA episodes.

Table 3. Effect of auditory stimuli applied during N3 sleep on behavior (Study 2)

Auditory stimuli	Crackling sound	Pure sound	Name sound	Questions
Effect in triggering parasomnia episode				
None, *n* (%)	42 (89.4)	87 (82.9)	4 (80)	27 (84.4)
Awakening, *n* (%)	5 (10.6)	11 (10.4)	1 (20)	5 (15.6)
Episode, *n* (%)	0	7 (4.5)	0	0
Participants' responsiveness to questions asked during sound-induced episodes				
No responses, *n* (%)	-	-	-	10 (91)
Responses while still in an episode, *n* (%)	-	-	-	1 (9)
Correct responses	-	-	-	0

Limited responsiveness to verbal stimulus during parasomnia episodes

The effect of auditory stimuli in inducing parasomnia episodes is summarized in Table 3 (upper part). A total of 157 trigger sounds were applied during N3 sleep in 14 participants (mean number of stimulations per participant: 11.2 ± 13.4). Only 4.5% of the sounds triggered a clear parasomnia episode (in three participants, all women), in which the participants opened their eyes, raised their trunk, and looked around confused or seemingly scared (confusional arousal, no sleepwalking, or sleep terror). In most cases (84.7%), participants remained in N3 sleep and did not react to the sound. They woke up after 10.8% of the auditory stimulations.

When participants did not react to the trigger sounds three times in a row, we directly applied questions during N3 sleep ($n = 32$ questions across 6 participants). In these cases, none of the questions triggered a parasomnia episode. Most (84.4%) participants remained asleep and did not answer questions. In the remaining cases, the verbal questions woke participants, and they responded (in an awake state) to the experimenter.

Of the 12 questions asked directly during a sound-induced parasomnia episode, we observed one indirect response (see Table 3, bottom part). When asked 'What are you doing?', the participant did not react for 27 s, then turned her gaze to a corner of the room [where her boyfriend was standing before the experiment began] and, 13 s later, appeared to address an imaginary person, saying "Are you answering, or am I answering?" (see Supplementary Figure S1 for the polysomnographic recording). The other 11 questions were not answered. In these cases, either the episode was too short for the participant to hear the question in full, the participant went back to sleep, or the participant simply did not answer.

Study 3. Home study of verbal interaction during parasomnia episodes

We performed a retrospective analysis of 364 home video recordings of patients with DoA, during which a bed partner was present in the room. Participants exhibited a behavior without talking in 39% (142/364) of the clips and seemed to talk to themselves or to a dream character—without clear signs indicating a will to interact with their partner—in 41% (151/364) of the episodes. In 20% (71/364) of the episodes, either the patient ($n = 35$) or the partner ($n = 36$) attempted to initiate a conversation. Such an attempt was successful in 52% (37/71) of the cases and failed in 48% (29/71) of the cases. When conversation failed, it was mainly due to the partner being either asleep or not willing to respond to the patient's question (15/35) and, more rarely, because the patient ignored the partner's request (9/36). In the remaining 14% (10/71) of the episodes, the interaction was partially successful as the patient appropriately reacted to the partner's request (e.g. going back to bed) but did not verbally respond. The inter-scorers agreement between the three blind scorers for the categorization of the episodes was high (Fleiss Kappa = 0.66; see Supplementary Table S6).

Overall, if one focuses only on the situations where there was a true opportunity for discussion (the partner was awake and willing; n = 56 episodes corresponding to 13 patients), participants with DoA engaged in a dialogue with their partner in 66% of the cases (37/56 episodes, 13/13 patients), seemed to integrate partners' requests without verbally responding in 18% of the cases (10/56 episodes, 4/13 patients), and completely failed to engage in 16% (9/56 episodes, 3/13 patients). The main results are summarized in Figure 3, and the repartition of the episodes per patient and per night is shown in Figure 4. Examples of discussions are provided in Table 4.

Behavioral characteristics of home parasomnia episodes

Three blind raters evaluated different behavioral features of parasomnia episodes in all 37 video clips that included a discussion. The results are summarized in Table 5, and the inter-scorer agreement for the different discussion features is provided in Supplementary Table S7. In the 37 episodes in which participants with Disorder of Arousal (DoA) engaged in conversations with their bed partner, participants with DoA initiated the exchanges 49% of the time, with an average of 2.1 (±1) exchanges per episode. These interactions occurred around 01:19 am on average (range: 10:55 pm–04:51 am) and lasted 22 (±7) seconds in average. Participants' responses to their bed partner were coherent in 62% of the cases and incoherent in 22% of the cases (the remaining responses were difficult to interpret).

To what extent did the participants modulate their voice appropriately to the context of what they were saying? Interestingly, more than half of the participants (55%) modulated their voice across the course of an episode. They either modulated their voice spontaneously (62%) or at the partner's request (38%), generally by reducing the volume (95%). Of note, most partners (81%)

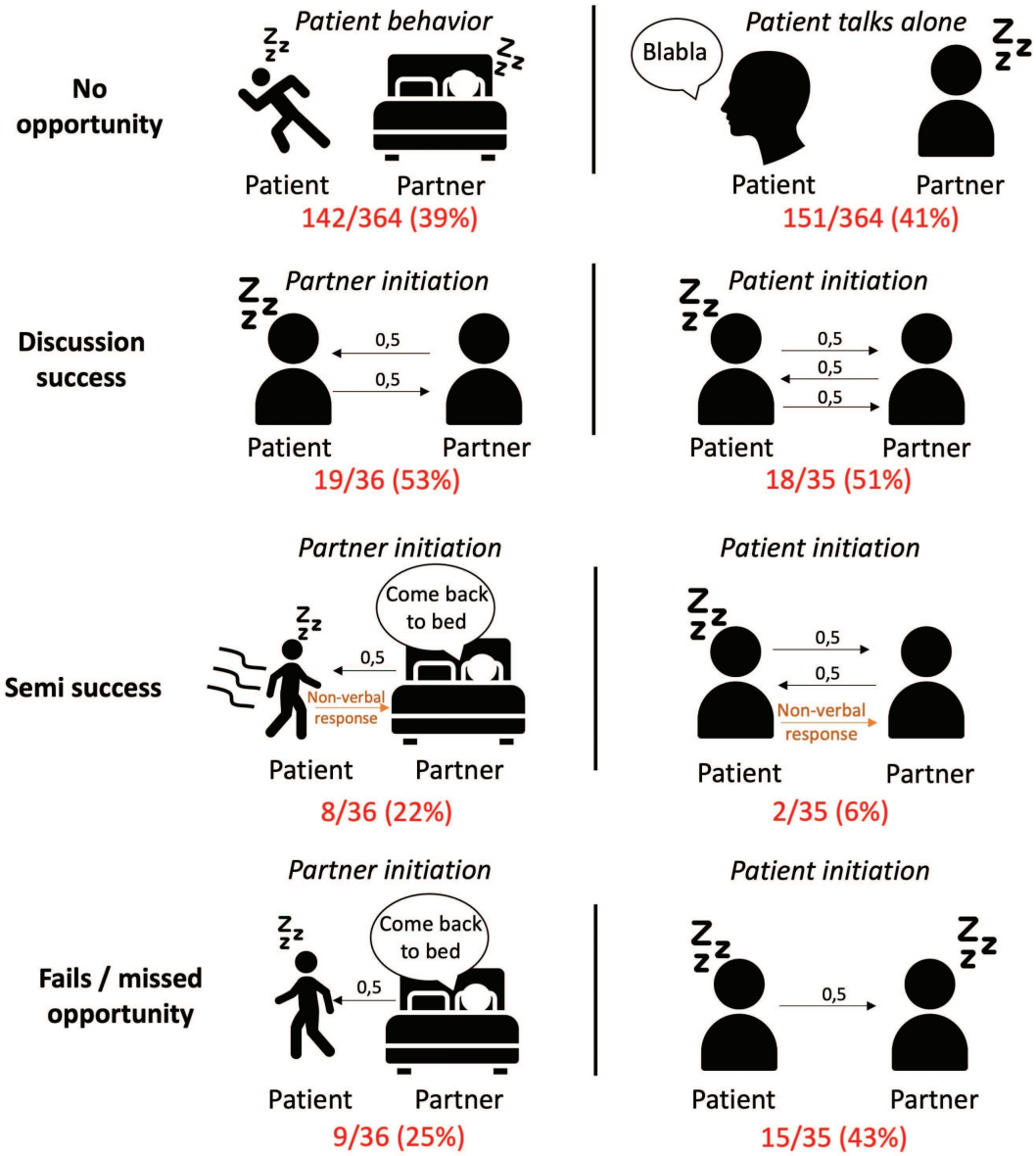

Figure 3. Categorization of verbal interactions in 364 videoclips involving a DoA parasomnia episode during which a bed partner was present. The episodes were categorized as "no opportunity for discussion" when the patient did not talk or seemed to talk alone, without a clear intention to interact with the partner; "discussion success" when the patient spoke at least once after the partner had spoken; "semi-success" when the patient appropriately reacted to a partner's request but without verbally responding; "fail" when the patient did not respond nor react to a partner's request; and "missed opportunity" when the partner ignored the patient's attempt in communicating.

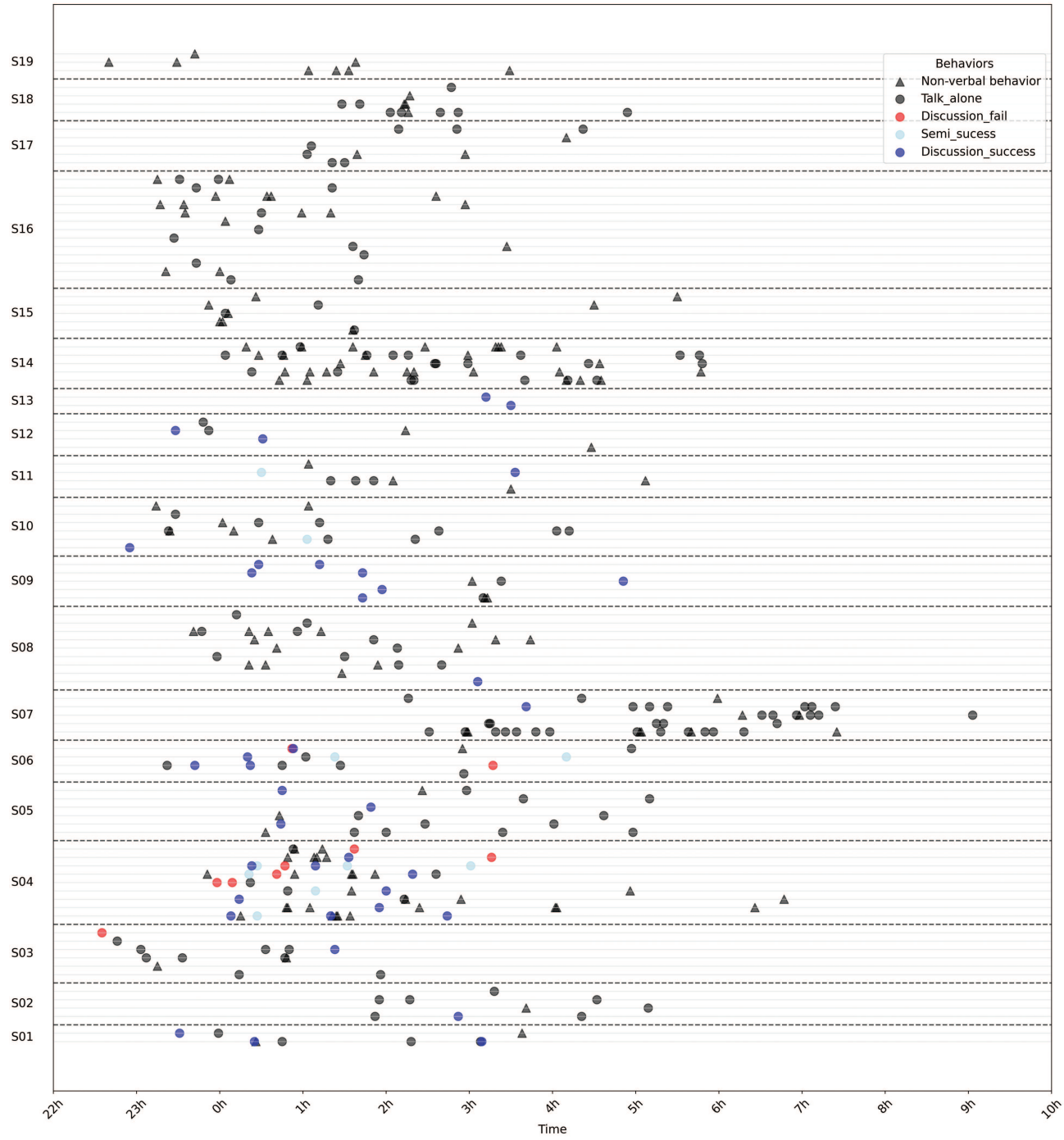

Figure 4. Temporal distribution of the types of behaviors displayed during DoA episodes in the presence of a partner. Each plain line represents one night of a given participant (several nights per participant, separated by the dotted lines). Dark blue circles represent successful discussions between a patient and a partner. Light blue circles represent semi-successful discussions (the patient behaviorally reacted to the partner but did not verbally respond). Orange circles represent discussion failures, when the patient did not react nor verbally respond to a partner's request. Gray circles represent episodes in which patients talk to themselves or to a dream character without clear indication of a willingness to interact with the partner. Gray triangles represent DoA episodes without any verbal behavior.

attempted to stop parasomnia episodes, for example by explicitly asking participants to be quiet or telling them to go back to bed, potentially limiting the duration of the interaction.

Discussion

Our findings, obtained using three complementary methodological approaches, revealed a wide range of behaviors and mental content during parasomnia episodes in adults [14], highlighting variability in cognitive abilities in our sample of patients. Retrospective reports and home video recordings provided proof-of-concept evidence that patients with DoA can, at least sometimes, verbally respond to queries from a partner during an episode. Mental experiences during episodes could influence patients' perception of the external world and the content of verbal interactions with the bed partners. Taken together, these findings challenge the current

Table 4. Examples of patient-partner discussion during parasomnia episodes recorded at home (Study 3)

Patient	Discussion between patient with DoA and their partner during the episodes
S4, F	Partner: "Hush, hush, hush." "What is it?" "Hey, no, easy." "What?," "Hush, easy," "Move it yourself."
	Patient: "No." "Hush, hush, hush, stop, stop! Uh-oh, uh-oh! Hush hush, you're going to fall, you're going to hurt yourself, you're going to hurt yourself!"; "Huh?"; "You're going to hurt yourself, stop"; "What do you mean I'm going to hurt myself? Why do you say that?
	Patient: "Don't tie it up! The hat! Help me! Oh, I'm scared of hats, oh, I'm scared of…"; "Hey, stop!"; "[unintelligible]?"; "What?," "We don't see anything." "Stop, enough! Bedtime."
	Partner: "Are you ok?"; "Yes, I'm ok."
S5, H	Patient: "Whose hand is it? Is it my hand? [unintelligible]; "[unintelligible]"; "Who [unintelligible]? Who does it belong to?" "[unintelligible]"; "Is it yours? And this too?"; "Yes"; "Ok."
	Patient: "Hi!"; "Huh?"; "What?"; "Hello?"; "Hello? Hi!"
	Patient: "What do you see?"; "Huh?"; "You [unintelligible]"; "I'm sleeping"; "I'm scared"; "I'm sleeping"; "Alright."
S6, F	Patient: "Oh fuck! Ask, ask [unintelligible], [scream twice] No, no, no, [unintelligible]"; "Hey!"; "What?"; "Stop"; "What? What? Come on, turn the lights off! Turn the lights off!"; "Argh, come on!"
	Patient: "Quick, quick, quick, quick!"; "What? Oh, come one!"; "Hurry up! [unintelligible] has fallen"; "Oh come on! [sighs] you're pissing me off"; "But, look, you'll see, you don't believe me"; "Hey, speak then, you got a tongue, speak"; "Look! Fuck"; "What thing?": "Gosh!"; "Oh fuck, this one thinks she's on her wedding night"; "Not at all."
S9, H	Patient: [Scream four times] "Go away, go away!"; "Shush sweetheart"; "What 'sweetheart'?" Who is this?"; "It's me"; "Who is this?"; "Turn on the lights"; "How do I turn on the lights?"; "Next to the door, sweetheart"; "I can't see anything." Patient: "[unintelligible]"; "Shush"; "Wait, wait, wait, wait, wait, well, wait, wait, who is going? You or me? Huh?"; "You go"; "Come on. Wait." Patient: "Is someone there?" Yes! Here! Look up! There, there, there!"; "Bedtime, sweetheart"; "I saw [unintelligible]." Patient: "What are you doing? What are you doing? What are you doing? What are you doing? [shout]"; "Shush"; "What is it? [shout]"; "Shush"; "What "Shush" [still shouting]? "; "Sweetheart, stop screaming"; "Why? [whispers]": "You're having a nightmare"; "Yes, but…"
S12, F	Patient: "Granny" [crying]; "What are you doing? Are you ok?"; "I have no light"; "Do you want me to turn on the light? What is going on?"; "I don't know but I have no light"; "Hey, look at me"; "I have no light."
S13; H	Patient: "Fuck, fuck, fuck"; "You're having a nightmare sweetheart"; "Remove your hand"; "Hey, sweetheart, I'm there": "Fuck of fuck of fuck"; "My love?"; "Huh?"; "What is it?"; "Huh [or "nothing"]; "You didn't realize you were saying "fuck?"; "Oh [unintelligible] huh? "; "Nothing."

clinical criteria for DoA, which largely assume a loss of consciousness during episodes [4, 12, 14, 15, 49].

Responding to others' attempts to communicate during parasomnia episodes

Consistent with previous studies [9, 18, 19, 21, 24, 28, 29, 43, 47], we found that verbal behaviors such as talking to a fictional character or shouting are highly prevalent in DoA. Our study goes further by showing that patients with DoA can also respond to questions posed by a real person. Interestingly, the observed dialogs between patients and partners during parasomnia episodes showed both similarities and differences to waking interactions. On the one hand, individuals with DoA seemed to perceive the words from their partners as they were enunciated, appeared to respect turns of speech, and even adapted their communication strategies, such as adjusting their voice volume in response to their partner. On the other hand, patients' responses were usually short, and the number of exchanges was limited. In line with a previous study [17], we found that both participants' responses and their perception of the external environment (including the interlocutor's identity) were often linked to an ongoing dream. Patients' responses could thus be perceived as odd (since they did not reflect what was happening in the real world and would be confusing for the bed partner) or coherent (in the sense that they were logical given the patient's experience at the time). Overall, these results suggest a complex interplay between internal and external information processing during parasomnia episodes.

Effective communication during wakefulness requires many cognitive processes, ranging from selective attention, perception, comprehension, working memory, theory of mind, decision-making and response selection, error monitoring, or emotion regulation. Our work paves the way for future studies testing precisely which ones of these cognitive processes are impaired or preserved during DoA episodes.

Advantages and limitations of our approach

To assess patients' responsiveness during DoA episodes, we used three complementary approaches, each with different advantages and limitations. Retrospective questionnaires allow the inclusion of numerous parasomnia behaviors exhibited over a long period of time (1 year in Study 1), thus increasing the probability of catching putatively rare events. With this approach, we found that most patients (81%) had at least one discussion with a partner over the past year, and 44% reported that such discussions were frequent. However, patients' subjective reports are prone to recall biases, raising the possibility that some instances of reported conversations happened during nighttime wakefulness rather than during parasomnia episodes. Interviewing the bed partners (if any) could be useful to mitigate this bias in future studies.

In contrast, laboratory experiments allow real-time monitoring of sleep and careful control of auditory stimulation, enabling to finely study the prevalence of discussions at the trial (episode) level. However, the potential windows of observation are significantly reduced, as the number of nights is typically limited (one in Study 2) and parasomnia episodes are rarer, less elaborate, and shorter in the laboratory than at home [25, 47, 48]. We attempted to circumvent this limitation by using auditory stimulation to experimentally provoke parasomnia episodes. In a previous study, auditory stimulation induced DoA episodes in 50% of the cases and in 100% of the cases when associated with a 25-h sleep deprivation protocol [40]. In sharp contrast to this previous study, our auditory stimulation was successful in inducing parasomnia episodes in only 7 out of 157 attempts. While the stimuli themselves were similar, we used loudspeakers to deliver the sounds (as opposed to in-ear delivery), and we did not use a sleep deprivation protocol, which may explain our low success rate. Of note, another team found no difference in the number of DoA episodes after auditory stimulation combined with sleep deprivation

Table 5. Behavioral and verbal features of parasomnia episodes (Study 5)

Features	Modalities	Presence *N* (%)	Absence *N* (%)	No agreement (%)	Other reason (*N*)
Exchange	Coherent	23 (62)	8 (22)	2 (5)	Difficult to interpret (4)
	Incoherent	8 (22)	23 (62)		
Who initiated the discussion	Participants with DoA	18 (49)	19 (51)	-	-
	Partner	19 (51)	18 (49)	-	
Eye orientation during the exchange process	Partner	22 (59)	13 (35)	2 (5)	-
	Environment	5 (14)	30 (81)		
	Change	8 (22)	27 (73)		
Voice modulation	-	21 (55)	17 (45)	-	-
If yes, how	Increase	0	0	-	-
	Reduce	20 (95)	1 (5)	-	
	Fluctuate	1 (5)	20 (95)	-	
Causes	Spontaneous	13 (62)	8 (38)	-	-
	Partner's request	8 (38)	13 (62)	-	
Bed partner's "cooperation" in keeping the discussion alive	-	7 (19)	30 (81)	-	-

compared to a baseline night without any stimulation [29]. The jury is thus still out on the best conditions for experimentally triggering DoA episodes. Given our limited number of episodes, it is encouraging that we still observe one (indirect) case of discussion, but larger samples will be needed to confirm the reproducibility of this result as it remains difficult to trigger parasomnia episodes in the sleep laboratory.

Finally, home video recordings are more ecological and can be collected across multiple nights (five in Study 3), increasing the likelihood of capturing parasomnia episodes [25, 47, 48], but have practical limitations for both patients and their partners. In our specific protocol, recording an interaction between a patient and a partner required that: (1) the patient was sharing a bed with someone; (2) the patient was having an episode; (3) the partner was awake at that moment; and (4) either the patient or the partner tried to initiate a discussion. These criteria were met in only 56 of the DoA episodes, spread over 13 patients. In these cases, the discussion was successful in 66% of the episodes, with 100% of the patients engaging in a dialogue with their partner at least once. The number of exchanges was low ($N = 2.1$ on average) but could potentially have been higher if the partner encouraged the patient to interact—a behavior that was contrary to the partner's natural impulse, which was to stop the episode. Such a result needs to be confirmed in a larger cohort. Another important limitation is that sleep state was not monitored at home, so we could not formally confirm that DoA episodes emerged from NREM sleep. Furthermore, precisely determining when the episodes end can be hard to assess. To overcome the challenges of capturing and evaluating verbal interactions during parasomnia episodes, innovative strategies could be developed, for example by combining home video recordings, a portable EEG tracking device to monitor sleep states, and a "citizen science" approach [50] in which patients' partners would support the role of researchers and ask a standardized set of questions during episodes.

Of note, our cohort included only adult patients with DoA, diagnosed on the basis of clinical history and video-polysomnographic recordings of DoA episodes. Further studies are needed to determine the extent to which our findings are generalizable to children or patients selected on the basis of more stringent clinical criteria.

A mosaic of conscious states during parasomnia?

Overall, our findings underscore that DoA episodes are not a uniform condition but are associated with different levels of interaction with the external world and diverse phenomenology. These observations largely align with the results of a recent study [17]. In our studies, verbal responsiveness may be absent or present during DoA episodes, and when present, patients' responses may be simple, potentially reflexive ("I'm ok") or more elaborate, less likely to come up automatically ("I will count the stars first [before going back to bed]"). This suggests that DoA episodes may be associated with a spectrum of states of consciousness, in the same way that patients with disorders of consciousness (e.g. vegetative state vs. minimally conscious state) differ in their ability to follow instructions [51]. Similarly, our finding that patients with DoA reported a variability of mental experiences associated with DoA episodes (no content, short scene, and elaborate dream scenario) as well as different perceptions of their surroundings (realistic, distorted, or fully hallucinated) suggests differences in the content of and/or access to consciousness during DoA episodes. Thus, DoA could offer a fruitful model to test different theories of consciousness, as parasomnia affects several key aspects of consciousness, such as arousal level, conscious content, and conscious access [52, 53].

Furthermore, our team has recently shown that patients with narcolepsy and healthy individuals can respond to stimuli during most sleep stages using facial contractions [54, 55]. Here, we extend this finding by showing that patients with DoA can also interact with an experimenter upon awakening from N3 sleep, but this time, using their voice, increasing the richness of potential outputs. This finding opens up the exciting possibility of interviewing DoA participants in real time about their conscious experiences and testing how various cognitive functions (e.g. executive functions) are altered/preserved in N3 sleep.

At the clinical level, our findings highlight the limitations of the current diagnostic criteria for DoA in adults. As suggested by our team and others [12, 16, 42], we propose that the absence of dreams, the lack of interaction with others, and the amnesia of the episodes should be considered as supportive features rather than as mandatory criteria for the diagnosis of DoA. Paying more attention to patients' cognition during the episodes may be helpful to elucidate the underlying mechanisms of DoA and to adjust treatment [56]. Future studies are needed to investigate the electrophysiological changes that account for the heterogeneities we observed in parasomniac manifestations. Depending on the presence or absence of a mental experience or on the ability to respond to external stimuli during DoA episodes, one might expect distinct profiles of brain functional connectivity, brain complexity, and/or region-dependent variations in arousal levels [29, 57–59]. Future work is needed to test how behavioral and neural differences in DoA episodes are related to the type of DoA (confusional arousals, sleepwalking, and sleep terrors) and to the severity of the disorder (e.g. injury, subsequent daytime cognitive effects). For example, patients who incorporate dream elements or replace the external reality with a dream scene may be at greater risk of harming themselves or others. Clinicians may benefit from interviewing patients about such dream intrusions to anticipate these risks. Finally, it would be important to test whether DoA manifestations—including verbal responsiveness—are more homogeneous in children with DoA, as a previous study has shown that a clinical criterion of DoA (i.e. absence of mental activity associated with episodes) better matched the presentation of DoA in children than in adults [27].

In conclusion, we found that adult patients with DoA can occasionally respond to communication attempts from others, integrate dream elements into the real world during their episodes, and recall their episodes. These findings, which challenge the current diagnosis criteria for DoA, may impact the clinical approach to DoA as well as our fundamental understanding of consciousness itself.

Supplementary material

Supplementary material is available at *SLEEP* online.

Acknowledgments

We warmly thank the participants with DoA who agreed to participate in this study.

Funding

This study was funded by the Agence Nationale de la Recherche (ANR-20-CE37-0001-01, grant to DO).

Disclosure statement

Nonfinancial disclosure: The authors report no competing interests.

Data availability

All the results are presented in the main article or in Supplementary data. To protect patients' identity and in accordance with the general data protection regulation, we cannot share the videos related to this study.

References

1. Bornemann MAC, Mahowald MW, Schenck CH. Parasomnias: clinical features and forensic implications. *Chest*. 2006;**130**(2):605–610. doi:10.1378/chest.130.2.605
2. Siclari F, Khatami R, Urbaniok F, *et al*. Violence in sleep. *Brain*. 2010;**133**(Pt 12):3494–3509. doi:10.1093/brain/awq296
3. Idir Y, Oudiette D, Arnulf I. Sleepwalking, sleep terrors, sexsomnia and other disorders of arousal: the old and the new. *J Sleep Res*. 2022;**31**(4):e13596. doi:10.1111/jsr.13596
4. Lopez R, Dauvilliers Y. Challenges in diagnosing NREM parasomnias: implications for future diagnostic classifications. *Sleep Med Rev*. 2024;**73**:101888. doi:10.1016/j.smrv.2023.101888
5. Cordani R, Lopez R, Barateau L, Chenini S, Nobili L, Dauvilliers Y. Somnambulism. *Sleep Med Clin*. 2024;**19**(1):43–54. doi:10.1016/j.jsmc.2023.10.001
6. Bjorvatn B, Grønli J, Pallesen S. Prevalence of different parasomnias in the general population. *Sleep Med*. 2010;**11**(10):1031–1034. doi:10.1016/j.sleep.2010.07.011
7. Ohayon MM, Guilleminault C, Priest RG. Night terrors, sleepwalking, and confusional arousals in the general population: their frequency and relationship to other sleep and mental disorders. *J Clin Psychiatry*. 1999;**60**(4):268–76; quiz 277. doi:10.4088/jcp.v60n0413
8. Ohayon MM, Mahowald MW, Dauvilliers Y, Krystal AD, Léger D. Prevalence and comorbidity of nocturnal wandering in the U.S. adult general population. *Neurology*. 2012;**78**(20):1583–1589. doi:10.1212/WNL.0b013e3182563be5
9. Arnulf I, Zhang B, Uguccioni G, *et al*. A scale for assessing the severity of arousal disorders. *Sleep*. 2014;**37**(1):127–136. doi:10.5665/sleep.3322
10. Cartwright R. Sleepwalking violence: a sleep disorder, a legal dilemma, and a psychological challenge. *Am J Psychiatry*. 2004;**161**(7):1149–1158. doi:10.1176/appi.ajp.161.7.1149
11. Lopez R, Jaussent I, Scholz S, Bayard S, Montplaisir J, Dauvilliers Y. Functional impairment in adult sleepwalkers: a case-control study. *Sleep*. 2013;**36**(3):345–351. doi:10.5665/sleep.2446
12. Mainieri G, Loddo G, Provini F, Nobili L, Manconi M, Castelnovo A. Diagnosis and management of NREM sleep parasomnias in children and adults. *Diagn Basel Switz*. 2023;**13**(7):1261. doi:10.3390/diagnostics13071261
13. Pressman MR. Factors that predispose, prime and precipitate NREM parasomnias in adults: clinical and forensic implications. *Sleep Med Rev*. 2007;**11**(1):5–30; discussion 31. doi:10.1016/j.smrv.2006.06.003
14. Troester MM, Medicine AA of S. *The AASM Manual for the Scoring of Sleep and Associated Events, Version* 3. American Academy of Sleep Medicine; 2023.
15. American Psychiatric Association. *Diagnostic and Statistical Manual of Mental Disorders (DSM-5)*. 5th ed. American Psychiatric Publishing; 2013.
16. Zadra A, Desautels A, Petit D, Montplaisir JS. Clinical aspects and pathophysiological hypotheses. *Lancet Neurol*. 2013;**12**(3):285–294. doi:10.1016/S1474-4422(12)70322-8
17. Siclari F. Consciousness in non-REM-parasomnia episodes. *J Sleep Res*. 2024:e14275. doi:10.1111/jsr.14275
18. Broughton RJ. Sleep disorders: disorders of arousal? Enuresis, somnambulism, and nightmares occur in confusional states of arousal, not in "dreaming sleep". *Science*. 1968;**159**(3819):1070–1078. doi:10.1126/science.159.3819.1070
19. Fisher C, Kahn E, Edwards A, Davis DM, Fine J. A psychophysiological study of nightmares and night terrors. 3. Mental

content and recall of stage 4 night terrors. *J Nerv Ment Dis*. 1974;**158**(3):174–188. doi:10.1097/00005053-197403000-00002
20. Schenck CH, Milner DM, Hurwitz TD, Bundlie SR, Mahowald MW. A polysomnographic and clinical report on sleep-related injury in 100 adult patients. *Am J Psychiatry*. 1989;**146**(9):1166–1173. doi:10.1176/ajp.146.9.1166
21. Oudiette D, Leu S, Pottier M, Buzare MA, Brion A, Arnulf I. Dreamlike mentations during sleepwalking and sleep terrors in adults. *Sleep*. 2009;**32**(12):1621–1627. doi:10.1093/sleep/32.12.1621
22. Pillmann F. Complex dream-enacting behavior in sleepwalking. *Psychosom Med*. 2009;**71**(2):231–234. doi:10.1097/PSY.0b013e318190772e
23. Bhat S, Chokroverty S, Kabak B, Yang QR, Rosen D. Dream-enacting behavior in non-rapid eye movement sleep. *Sleep Med*. 2012;**13**(4):445–446. doi:10.1016/j.sleep.2011.10.029
24. Uguccioni G, Golmard JL, de Fontréaux AN, Leu-Semenescu S, Brion A, Arnulf I. Fight or flight? Dream content during sleepwalking/sleep terrors vs. rapid eye movement sleep behavior disorder. *Sleep Med*. 2013;**14**(5):391–398. doi:10.1016/j.sleep.2013.01.014
25. Mwenge B, Brion A, Uguccioni G, Arnulf I. Sleepwalking: long-term home video monitoring. *Sleep Med*. 2013;**14**(11):1226–1228. doi:10.1016/j.sleep.2013.04.027
26. Rocha AL, Arnulf I. NREM parasomnia as a dream enacting behavior. *Sleep Med*. 2020;**75**:103–105. doi:10.1016/j.sleep.2020.02.024
27. Castelnovo A, Loddo G, Provini F, Miano S, Manconi M. Mental activity during episodes of sleepwalking, night terrors or confusional arousals: differences between children and adults. *Nat Sci Sleep*. 2021;**13**:829–840. doi:10.2147/NSS.S309868
28. Longe O, Omodan A, Leschziner G, Rosenzweig I. Non-REM parasomnias: a scoping review of dreams and dreamlike mentation. *Croat Med J*. 2022;**63**(6):525–535. doi:10.3325/cmj.2022.63.525
29. Cataldi J, Stephan AM, Haba-Rubio J, Siclari F. Shared EEG correlates between non-REM parasomnia experiences and dreams. *Nat Commun*. 2024;**15**(1):3906. doi:10.1038/s41467-024-48337-7
30. Kalantari N, McDuff P, Pilon M, Desautels A, Montplaisir J, Zadra A. Self-reported developmental changes in the frequency and characteristics of somnambulistic and sleep terror episodes in chronic sleepwalkers. *Sleep Med*. 2022;**89**:147–155. doi:10.1016/j.sleep.2021.12.008
31. Schenck CH, Pareja JA, Patterson AL, Mahowald MW. Analysis of polysomnographic events surrounding 252 slow-wave sleep arousals in thirty-eight adults with injurious sleepwalking and sleep terrors. *J Clin Neurophysiol*. 1998;**15**(2):159–166. doi:10.1097/00004691-199803000-00010
32. Lopez R, Shen Y, Chenini S, *et al*. Diagnostic criteria for disorders of arousal: a video-polysomnographic assessment: disorders of arousal. *Ann Neurol*. 2018;**83**(2):341–351. doi:10.1002/ana.25153
33. Januszko P, Niemcewicz S, Gajda T, *et al*. Sleepwalking episodes are preceded by arousal-related activation in the cingulate motor area: EEG current density imaging. *Clin Neurophysiol*. 2016;**127**(1):530–536. doi:10.1016/j.clinph.2015.01.014
34. Desjardins ME, Carrier J, Lina JM, *et al*. EEG functional connectivity prior to sleepwalking: evidence of interplay between sleep and wakefulness. *Sleep*. 2017;**40**(4). doi:10.1093/sleep/zsx024
35. Cataldi J, Stephan AM, Marchi NA, Haba-Rubio J, Siclari F. Abnormal timing of slow wave synchronization processes in non-rapid eye movement sleep parasomnias. *Sleep*. 2022;**45**(7). doi:10.1093/sleep/zsac111
36. Terzaghi M, Sartori I, Tassi L, *et al*. Evidence of dissociated arousal states during NREM parasomnia from an intracerebral neurophysiological study. *Sleep*. 2009;**32**(3):409–412. doi:10.1093/sleep/32.3.409
37. Terzaghi M, Sartori I, Tassi L, *et al*. Dissociated local arousal states underlying essential clinical features of non-rapid eye movement arousal parasomnia: an intracerebral stereoelectroencephalographic study: local sleep and NREM parasomnia. *J Sleep Res*. 2012;**21**(5):502–506. doi:10.1111/j.1365-2869.2012.01003.x
38. Bassetti C, Vella S, Donati F, Wielepp P, Weder B. SPECT during sleepwalking. *Lancet (London, England)*. 2000;**356**(9228):484–485. doi:10.1016/S0140-6736(00)02561-7
39. Castelnovo A, Lopez R, Proserpio P, Nobili L, Dauvilliers Y. NREM sleep parasomnias as disorders of sleep-state dissociation. *Nat Rev Neurol*. 2018;**14**(8):470–481. doi:10.1038/s41582-018-0030-y
40. Pilon M, Montplaisir J, Zadra A. Precipitating factors of somnambulism: impact of sleep deprivation and forced arousals. *Neurology*. 2008;**70**(24):2284–2290. doi:10.1212/01.wnl.0000304082.49839.86
41. Arnulf I. Sleepwalking. *Curr Biol*. 2018;**28**(22):R1288–R1289. doi:10.1016/j.cub.2018.09.062
42. Lopez R, Micoulaud-Franchi JA, Peter-Derex L, Dauvilliers Y. Nocturnal agitation: from sleep state dissociation to sleep-related dissociative state. *Rev Neurol (Paris)*. 2023;**179**(7):675–686. doi:10.1016/j.neurol.2023.07.003
43. Arnulf I, Uguccioni G, Gay F, *et al*. What does the sleeping brain say? Syntax and semantics of sleep talking in healthy subjects and in parasomnia patients. *Sleep*. 2017;**40**(11). doi:10.1093/sleep/zsx159
44. Barros A, Uguccioni G, Salkin-Goux V, Leu-Semenescu S, Dodet P, Arnulf I. Simple behavioral criteria for the diagnosis of disorders of arousal. *J Clin Sleep Med*. 2020;**16**(1):121–128. doi:10.5664/jcsm.8136
45. Loddo G, Sessagesimi E, Mignani F, *et al*. Specific motor patterns of arousal disorders in adults: a video-polysomnographic analysis of 184 episodes. *Sleep Med*. 2018;**41**:102–109. doi:10.1016/j.sleep.2017.08.019
46. Derry CP, Harvey AS, Walker MC, Duncan JS, Berkovic SF. NREM arousal parasomnias and their distinction from nocturnal frontal lobe epilepsy: a video EEG analysis. *Sleep*. 2009;**32**(12):1637–1644. doi:10.1093/sleep/32.12.1637
47. Castelnovo A, Loddo G, Provini F, Manconi M. Frequent, complex and vivid dream-like/hallucinatory experiences during NREM sleep parasomnia episodes. *Sleep Med*. 2021;**82**:61–64. doi:10.1016/j.sleep.2021.03.032
48. Lopez R, Barateau L, Chenini S, Rassu AL, Dauvilliers Y. Home nocturnal infrared video to record non-rapid eye movement sleep parasomnias. *J Sleep Res*. 2023;**32**(2):e13732. doi:10.1111/jsr.13732
49. American Academy of Sleep Medicine. *International Classification of Sleep Disorders Third Version*. 3rd ed. American Academy of Sleep Medicine; 2014.
50. Jafarzadeh Esfahani M, Sikder N, Ter Horst R, *et al*. Citizen neuroscience: Wearable technology and open software to study the human brain in its natural habitat. *Eur J Neurosci*. 2024;**59**(5):948–965. doi: 10.1111/ejn.16227.
51. Giacino JT, Kalmar K, Whyte J. The JFK Coma Recovery Scale-Revised: Measurement characteristics and diagnostic utility11No commercial party having a direct financial interest in the results of the research supporting this article has or will confer a benefit upon the authors or upon any organization with which the authors are associated. *Archives of Physical Medicine and Rehabilitation* 2004;**85**(12):2020–2029. doi:10.1016/j.apmr.2004.02.033.
52. Seth AK, Bayne T. Theories of consciousness. *Nat Rev Neurosci*. 2022;**23**(7):439–452. doi:10.1038/s41583-022-00587-4

53. Melloni L, Mudrik L, Pitts M, *et al*. An adversarial collaboration protocol for testing contrasting predictions of global neuronal workspace and integrated information theory. *PLoS One*. 2023;**18**(2):e0268577. doi:10.1371/journal.pone.0268577
54. Konkoly KR, Appel K, Chabani E, *et al*. Real-time dialogue between experimenters and dreamers during REM sleep. *Curr Biol*. 2021;**31**(7):1417–1427.e6. doi:10.1016/j.cub.2021.01.026
55. Türker B, Musat EM, Chabani E, *et al*. Behavioral and brain responses to verbal stimuli reveal transient periods of cognitive integration of the external world during sleep. *Nat Neurosci*. 2023;**26**(11):1981–1993. doi:10.1038/s41593-023-01449-7
56. Castelnovo A, Siclari F, Spaggiari S, *et al*. Conscious experiences during non-rapid eye movement sleep parasomnias. *Neurosci Biobehav Rev*. 2024;**167**:105919. doi:10.1016/j.neubiorev.2024.105919
57. Siclari F, Bernardi G, Cataldi J, Tononi G. Dreaming in NREM Sleep: a high-density EEG study of slow waves and spindles. *J Neurosci*. 2018;**38**(43):9175–9185. doi:10.1523/JNEUROSCI.0855-18.2018
58. Siclari F, Baird B, Perogamvros L, *et al*. The neural correlates of dreaming. *Nat Neurosci*. 2017;**20**(6):872–878. doi:10.1038/nn.4545
59. Strauss M, Sitt JD, Naccache L, Raimondo F. Predicting the loss of responsiveness when falling asleep in humans. *Neuroimage*. 2022;**251**:119003. doi:10.1016/j.neuroimage.2022.119003

Fatigue is an inescapable phenomenon, arising from intense cognitive effort, prolonged wakefulness, or chronic sleep disorders. Despite its impact on attention, decision-making, and safety, it remains poorly defined and hard to measure objectively. This thesis investigates whether different manifestations of fatigue (e.g., use-dependent, time-dependent, and chronic) share a common physiological signature.

Across four studies combining laboratory, clinical, and real-life approaches, I demonstrate that fatigue reflects local intrusions of sleep into wakefulness. These episodes, indexed by the emergence of slow waves in the brain activity, capture fluctuations in cortical dynamics even when subjective reports fail to do so. Their spatial distribution predicts distinct behavioral lapses, linking neural instability to errors in real time.

In hypersomnolence disorders, altered slow-wave, as well as transient REM-like theta bursts during wakefulness, reveal pathological forms of these local intrusions. Finally, portable EEG recordings show that slow waves and spontaneous thoughts can be tracked outside the lab, paving the way for ecological monitoring of fatigue. Together, this work establishes a physiological framework for understanding fatigue and opens new avenues for mechanistic research, diagnostics, and real-world applications.

